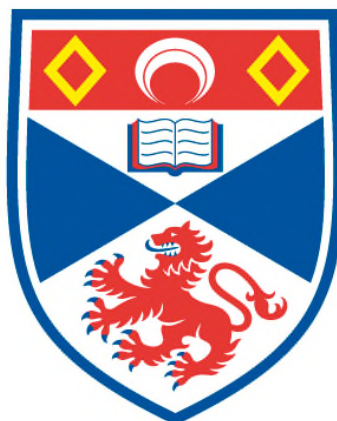


**NOVEL CATALYSTS FOR THE
HYDROXYMETHYLATION OF ALLYL ALCOHOL
A CONVENIENT SYNTHETIC ROUTE TO 1, 4-BUTANEDIOL**

Ine Ida Françoise Boogaerts

**A Thesis Submitted for the Degree of PhD
at the
University of St Andrews**



2009

**Full metadata for this item is available in
St Andrews Research Repository
at:
<http://research-repository.st-andrews.ac.uk/>**

**Please use this identifier to cite or link to this item:
<http://hdl.handle.net/10023/959>**

This item is protected by original copyright

**Novel Catalysts for the
Hydroxymethylation of Allyl Alcohol
A Convenient Synthetic Route to 1, 4-Butanediol**



Thesis presented to the University of St. Andrews in application
for the degree of Doctor of Philosophy
from the decision of the Examining Committee following
defense on 22nd October 2009 at 9 o'clock

by

Ine Ida Françoise Boogaerts

born 13th February 1983 in Turnhout

Academic promoter Prof. Dr. D. J. Cole-Hamilton
School of Chemistry, University of St. Andrews

External examiner Prof. Dr. C. Claver
Facultat de Química, Universitat Rovira i Virgili

Internal examiner Dr. C. S. J. Cazin
School of Chemistry, University of St. Andrews

The work described in this thesis was conducted at
School of Chemistry, University of St. Andrews

The work described in this thesis was financially supported by
Lyondell-Basell

Declaration

I, Ine Ida Françoise Boogaerts, hereby certify that this thesis, which is approximately 55.760 words in length, has been written by me, that it is the record of work carried out by me and that it has not been submitted in any previous application for a higher degree.

I was admitted as a research student in October, 2005 and as a candidate for the degree of Doctor of Philosophy in September, 2006; the higher study for which this is a record was carried out in the University of St Andrews between 2005 and 2009.

date: 29/10/09

signature of candidate

I hereby certify that the candidate has fulfilled the conditions of the Resolution and Regulations appropriate for the degree of Doctor of Philosophy in the University of St Andrews and that the candidate is qualified to submit this thesis in application for that degree.

date: 29/10/09

signature of supervisor

In submitting this thesis to the University of St Andrews we understand that we are giving permission for it to be made available for use in accordance with the regulations of the University Library for the time being in force, subject to any copyright vested in the work not being affected thereby. We also understand that the title and the abstract will be published, and that a copy of the work may be made and supplied to any bona fide library or research worker, that my thesis will be electronically accessible for personal or research use unless exempt by award of an embargo as requested below, and that the library has the right to migrate my thesis into new electronic forms as required to ensure continued access to the thesis. We have obtained any third-party copyright permissions that may be required in order to allow such access and migration, or have requested the appropriate embargo below.

The following is an agreed request by candidate and supervisor regarding the electronic publication of this thesis:

Embargo on both all or part of printed copy and electronic copy for the same fixed period of 5 years on the following ground:

publication would be commercially damaging to the researcher, or to the supervisor, or the University.

date: 29/10/09

signature of candidate

signature of supervisor

If I can stop one heart from breaking,

I shall not live in vain.

If I can ease one life of aching,

Or cool one pain,

Or help one fainting robin,

Unto his nest again,

I shall not live in vain.

(Emily Dickinson, 1830-1886)

In loving memory of

Frans Boogaerts

Jozef Poels

Table of Contents

Chapter 1	Hydroxymethylation Catalysis: A Conceptually Simple Alternative to Classical Hydroformylation-Reduction Sequences	1
Chapter 2	Enhanced Linear-Selective Hydroxymethylation with the Rhodium Complexes of <i>Bis</i> -(diethylphosphine) Modified Alicyclics	29
Chapter 3	Enhanced Specific Activity for the Hydroformylation of Allylic Alcohols <i>via</i> the <i>Meta</i> -Effect	67
Chapter 4	Activating Domino Hydroxymethylation <i>via</i> Multi-Component Catalysis	107
Chapter 5	Hydroxymethylation Catalysis Mediated by the Rhodium Complexes of Self-Assembling Heterodimers Based on DNA Base-Pairs	139
	Summary	173
	Appendices	177
	Acknowledgements	181

Table of Contents

Chapter 1	Hydroxymethylation Catalysis: A Conceptually Simple Alternative to Classical Hydroformylation-Reduction Sequences	1
Chapter 2	Enhanced Linear-Selective Hydroxymethylation with the Rhodium Complexes of <i>Bis</i> -(diethylphosphine) Modified Alicyclics	29
Chapter 3	Enhanced Specific Activity for the Hydroformylation of Allylic Alcohols <i>via</i> the <i>Meta</i> -Effect	67
Chapter 4	Activating Domino Hydroxymethylation <i>via</i> Multi-Component Catalysis	107
Chapter 5	Hydroxymethylation Catalysis Mediated by the Rhodium Complexes of Self-Assembling Heterodimers Based on DNA Base-Pairs	139
	Summary	173
	Appendices	177
	Acknowledgements	181

-Chapter 1-

Hydroxymethylation Catalysis:

A Conceptually Simple Alternative to Classical Hydroformylation- Reduction Sequences

Abstract. Rhodium-catalysed hydroxymethylation has been of commercial interest since the early 1970s. Much emphasis has been placed on the development of a hydroformylation-hydrogenation sequence, however capacity to optimise selectivity for both transformations has proved limited. Considerable yield loss *via* heavy-ends formation, even under modest operating conditions, is another limitation. An alternative scheme that effects all relevant bond-forming transformations in a single mechanism was therefore developed. In this chapter, the development of these hydroxymethylation pathways is reviewed. Special attention is given to their application for selective conversion of allyl alcohol to 1, 4-butanediol.

1.1 Introduction

Devising methodologies for the elaboration of relatively simple and inexpensive feedstock to valuable homologues is the underlying theme of most transition-metal catalysed processes. The hydroformylation of α -alkenes is thus established as a clean and selective method for homologation of the carbon skeleton by introducing the synthetically versatile aldehyde functionality.¹ The aldehyde is not usually the intended end-product and is typically diverted to the alcohol *via* reduction, the carboxylic acid *via* oxidation, the amine *via* hydroamination or the *N*-acetylated amino acid *via* amidocarbonylation.² However, catalyst efficiency and process efficiency are limited by the conventional focus on each catalytic reaction as a discrete event.

Converging both processes into a single reaction is thus appealing. This approach is associated with improved work-up efficiency, as only one isolation and purification phase is required, and with process efficiency, as both transformations can occur without necessity for monitoring and intervention.³ A taxonomy of coupled catalysis was proposed by Fogg and dos Santos,⁴ and their terminology allows demarcation between the different mechanisms of a catalytic transformation (Figure 1).

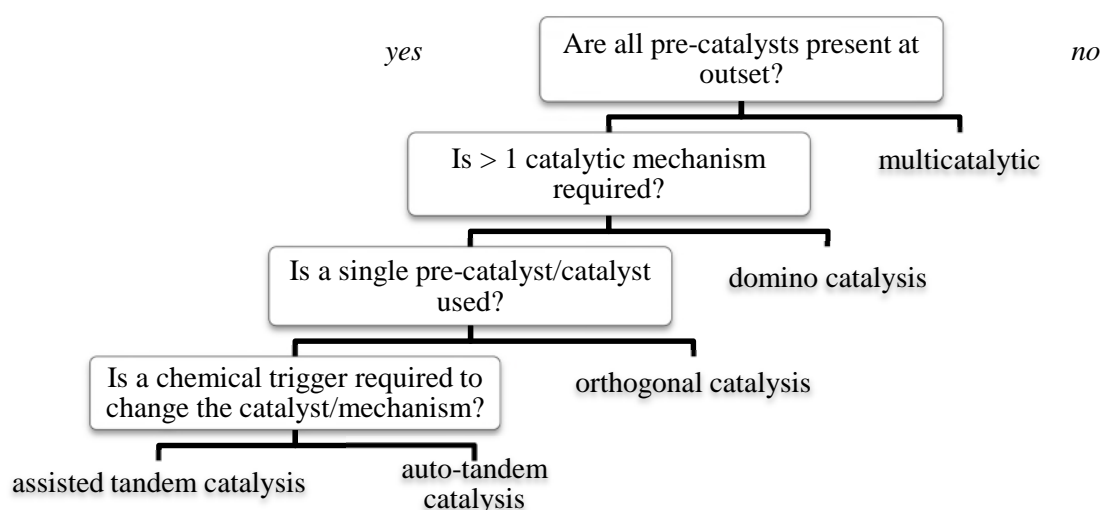


Figure 1. Criteria for the classification of coupled catalysis.⁴

The Shell Oxo Process is the most important industrial application of coupled catalytic technology.⁵ In a beautiful example, the $P^nBu_3/[Co_2(CO)_8]$ catalyst effects conversion of propene to 2-ethylhexanol *via* a hydroformylation-aldolisation-hydrogenation cascade. The production of 2-ethylhexanol, which is formulated as dioctyl phthalate plasticiser in PVC applications, accounts for ~ 70% of 1-butanal capacity.^{5b}

Hydroformylation-coupled catalysis is also an area of academic interest for which the reader is referred to reviews by Eilbracht and Breit.^{6,7}

1.2 Hydroxymethylation Catalysis

In conventional hydroformylation, the sporadic reduction of aldehyde products to alcohols is a common parallel and consecutive reaction that demotes efficiency and economy by encouraging the formation of heavy condensation products *via* acetalisation, aldolisation, Cannizzaro dismutation, esterification, oligomerisation *etc.*⁸ Conversely, optimising hydroxymethylation as the predominant catalytic pathway is of significant commercial interest as ~ 60% of aldehyde capacity is diverted to alcohols, primarily for the polymer and the detergent industries.^{5b, 8c, 9} From a fine-chemicals perspective, hydroxymethylation could be an attractive alternative to the classical syntheses *via* oxymercuration-demercuration and hydroboration-oxidation.

Hydroxymethylation is effected by *tris*(alkyl)phosphine-modified cobalt complexes, but their low specific activity requires a large volume of reaction and substantial hydrogenation of the feedstock must also be tolerated.¹⁰ The application of a cobalt system for industrial production is further limited by the need for a high-pressure and high-temperature infrastructure. It is therefore of interest to review applications that give a practical selectivity under mild operating conditions. The development of ruthenium,¹¹ platinum¹² and palladium¹³ systems as alternatives has been limited by the required presence of an acidic co-catalyst or a halide anion promoter which can form the corresponding acid under the operating conditions. Rhodium complexes are of interest as they have high reactivity, high specific activity and do not necessitate the addition of corrosive acids. Unfortunately, the need for highly efficient catalyst recovery has limited their use to date.^{8c}

1.2.1 Auto-tandem Hydroxymethylation

In auto-tandem hydroxymethylation both hydroformylation and hydrogenation are mediated by a single catalyst of essentially conserved structure.⁴ These processes are considered sequential in terms of transformation of a given molecule of α -alkene but are essentially concurrent,¹⁴ operating spontaneously by cooperative interaction. Particular merits of this scheme include efficient catalyst utility and minimal interaction of the catalytic species as these are similar. Against this must be set the potential for side reactions, where the substrate can itself enter into both catalytic cycles.¹⁵ A more fundamental difficulty lies in the limited capacity to optimise selectivity for both catalyses.^{4, 7a, 14} Fundamentally, linear-selective hydroformylation and chemoselective C=O hydrogenation are critical. Where the appropriate balance can be established, this methodology is exceptionally efficient.

Homogeneous Catalyst Systems

A first example of controlled hydroxymethylation was reported by Slauch and Mullineaux using $P^nBu_3/[RhCl_3 \cdot 3H_2O] = 2/1$ with sodium acetate as stabiliser.¹⁶ Similar complexes were previously reported to be active for reduction of a C=O functionality but significantly less for reduction of a C=C functionality.¹⁷ Application of the catalyst at 195°C and 92 bar $CO/H_2 = 1/2.1$ in ethanol effects 85% conversion of 1-pentene after 3 hours, partitioned as 5 mol% C₆-alcohol in $l/b = 5$ and 93 mol% C₆-aldehyde in $l/b = 2$, together with 2 mol% pentane from competing substrate hydrogenation. The distribution of regio-isomers in each fraction is dependent only on the sequential conversion simply because the linear aldehyde is more susceptible to hydrogenation than the branched aldehyde. Extending the reaction period to 12 hours gives an alcohol/aldehyde distribution of 25/60, with $l/b = 2$ for each fraction. It must be cautioned, however, that esters formed *via* Reppe-type chemistry could also be significant products under these operating conditions.¹⁸

The hydroxymethylation of 1-hexene with $[Rh(R)(CO)(L)_2]$ ($R = [C_2H_5COO]^-$, $[C_3H_7COO]^-$, $[C_7H_{15}COO]^-$, $[PhCH=CHCOO]^-$ and $[CF_3COO]^-$, $L = PEt_3$, P^nPr_3 , P^nBu_3 , PCy_3 and $POct_3$) was extensively researched at British Petroleum, and subsequently reported in a series of patents.¹⁹

Table 1: Hydroxymethylation of 1-hexene with $[Rh(R)(CO)(L)_2]$.^a

<i>L</i>	<i>R</i>	medium	time (h)	1-hexene-based selectivity (%)		
				C=O (<i>l/b</i>)	C-OH (<i>l/b</i>)	hyd.
PEt ₃	$[C_3H_7COO]^-$	heptanes	6	6 (0/1)	92 (2.4)	2
P ⁿ Pr ₃	$[C_3H_7COO]^-$	heptanes	5.5	3 (0/1)	95 (2.2)	2
P ⁿ Bu ₃	$[C_3H_7COO]^-$	heptanes	6	7 (0/1)	91 (2.5)	2
P ⁿ Bu ₃	$[C_2H_5COO]^-$	octanol	2	41 (0.9)	51 (7.5)	1
			4	14 (0.1)	80 (3.4)	2
P ⁿ Bu ₃	$[C_3H_7COO]^-$	octanol	0.5	73 (2.2)	20 (9.0)	trace
			4	4 (0.0)	93 (2.9)	2
P ⁿ Bu ₃	$[C_7H_{15}COO]^-$	octanol	2	31 (0.3)	61 (4.1)	1
			4	16 (0.1)	79 (2.6)	2
P ⁿ Bu ₃	$[PhCH=CHOO]^-$	octanol	1	75 (1.8)	17 (17.0)	3
			4	27 (0.3)	70 (4.4)	3
P ⁿ Bu ₃	$[HCOO]^-$	octanol	21.5	86 (1.8)	0 (-)	trace
P ⁿ Bu ₃	$[CF_3COO]^-$	octanol	4	97 (2.2)	2 (1/0)	2
PEt ₃	$[PhCH=CHOO]^-$	heptanes	8	3 (0.0)	95 (4.4)	2
P ⁿ Bu ₃	$[PhCH=CHOO]^-$	heptanes	9	47 (0.9)	51 (6.3)	2
P ⁿ Bu ₃	$[PhCH=CHOO]^-$	octanol	4	27 (0.3)	70 (2.4)	3

^aConditions: 30 mL solvent, 11 mM [Rh], Rh/1-hexene = 1/360, 88°C, 33 bar $CO/H_2 = 1/2$.

This catalyst family is able to effect the desired conversion under milder operating conditions, at temperatures below 100°C and less than 40 bar CO/H₂ = 1/2. Chemoselectivity can be optimised by varying the reaction medium and the anionic auxiliary (Table 1). Evidently, two criteria must be met in order to influence practical conversion of 1-hexene to the homologous alcohols. Firstly, a protic medium should be employed, as this significantly enhances activity for hydroxymethylation. Secondly, the rhodium catalyst must be sufficiently basic, since a trifluoroethanoate-modified catalyst gives no alcohol products.

In an extensive survey of rhodium complexes of neutral phosphorus, nitrogen, arsenic, antimony and sulphur auxiliaries as active hydroxymethylation catalysts, Foster and Lawrenson recognised that basic trialkylphosphines are the preferred modifying agents as they generate strongly nucleophilic rhodium-hydride species.²⁰ Superior catalysts can be generated when these are amalgamated with a chelating modifier, particularly a β-diketone,²¹ affording complexes of the type [Rh(*x*-acac)(CO)(*L*)] (Table 2). A protic medium is once again shown to enhance chemoselectivity at lower temperatures; specifically a monohydric alcohol with a carbon skeleton higher than C₄ is preferred as lower homologues tend to effect intermolecular acetalisation of the intermediate aldehyde products. Hydroxymethylation is only observed at a sufficiently high Rh/*S* molar ratio, typically of the order of 1/100-500, and high partial pressure of hydrogen in the gas feedstock, ideally in a ratio CO/H₂ < 1/1. The nature of the organic chelating auxiliary in the catalyst is another important consideration.

Table 2: Hydroxymethylation of 1-hexene with [Rh(*x*-acac)(CO)(*L*)].^a

<i>L</i>	(CH ₃ CO) ₂ - <i>x</i>	medium	time (h)	1-hexene-based selectivity (%)		
				C=O (<i>l/b</i>)	C-OH (<i>l/b</i>)	hyd.
P ^{<i>n</i>} Bu ₃	<i>x</i> = CH	heptanes	1	74 (2.1)	4 (1/0)	2
P ^{<i>n</i>} Bu ₃	<i>x</i> = CH	octanol	11	0 (-)	99 (2.4)	1
PPh ₃	<i>x</i> = CH	heptanes	4.5	97 (2.2)	0 (-)	2
P ^{<i>n</i>} Bu ₃	<i>x</i> = C(CH ₂ CH ₃)	heptanes	12	32 (0.1)	67 (0.8)	1

^aConditions: 30 mL solvent, 10 mM [Rh], Rh/1-hexene = 1/400, 85°C, 40 bar CO/H₂ = 1/2.

Trialkylphosphine-modified rhodium cluster complexes in aromatic media were reported by Smith for application in the hydroxymethylation of allyl alcohol.²² In this reference P^{*n*}Bu₃/[Rh₆(CO)₁₆] = 180/1 at 125°C and 63 bar CO/H₂ = 1/2 in benzene gives the C₄-diol products in *l/b* = 3, but with high concurrent selectivity to 1-propanol from competing substrate hydrogenation.

The high solubility of rhodium complexes modified with low molar volume trialkylphosphines in hydrocarbon media is successfully translated to supercritical carbon dioxide. In this transport vector chemoselectivity is apparently determined by the phase behaviour of the catalytic

system, as observed by Sellin *et al.* upon conversion of 1-hexene with $\text{PEt}_3/[\text{Rh}(\text{OAc})_2]_2$ (Figure 2).²³ Hydroxymethylation occurs when the catalyst system is below the critical point,²⁴ where the poor solvating properties of the low pressure carbon dioxide phase give rise to a biphasic system. When the solution is supercritical, however, aldehyde products are recovered almost exclusively. This suggests that hydroformylation catalysis takes place in the supercritical phase, with tandem hydrogenation in the liquid phase if this is present. Alternatively, hydroxymethylation can be instigated when the catalyst system is above the critical point by addition of a fluorinated alcohol.

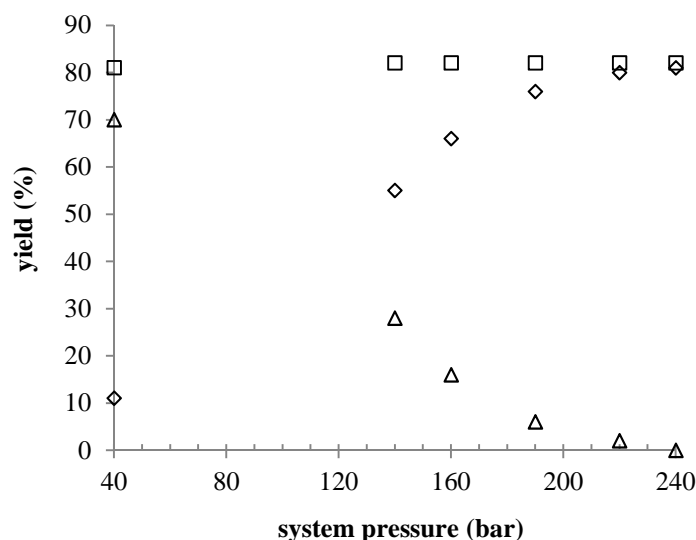


Figure 2. Course of allyl alcohol hydroxymethylation with $\text{PEt}_3/[\text{Rh}(\text{OAc})_2]_2$ in CO_2 :

(□) conversion, (◇) C_7 -aldehydes, (△) C_7 -alcohols.²³

(Conditions: 36 mL CO_2 , ~ 4.6 mM [Rh], $\text{PEt}_3/\text{Rh} = 3/1$, $\text{Rh}/1\text{-hexene} = 1/47$, 100°C , 40 bar $\text{CO}/\text{H}_2 = 1/1$)

A core frustration of hydroxymethylation catalysts modified with trialkylphosphines is low linear selectivity, typically $l/b > 2.5$. This is almost certainly due to these auxiliaries being classified low in the π -acceptor strength series and small in terms of sterics.²⁵ It is thus tempting to exploit the hydrogenation activity of these phosphines in an architecture recognised as conducive to high regioselectivity. Ichihara *et al.* synthesised a range of *bis*(dialkylphosphine)-substituted BISBI analogues as the natural bite angle of this scaffold effects *ee* chelation in trigonal bipyramidal geometry,²⁶ a mode correlated with linear-selective hydroformylation. The $L\text{-}L/[\text{Rh}(\text{acac})(\text{CO})_2]$ ($L\text{-}L = \text{Me-BISBI}$, $^n\text{Hex-BISBI}$, $^{neo}\text{Pent-BISBI}$ and $^i\text{Pr-BISBI}$) complexes were applied for the hydrohydroxymetylation of 1-decene in polar media (Table 3). Interestingly, catalyst modification with high molar volume dialkylphosphine moieties significantly reduces the chemoselectivity. This effect was associated with retarded tandem hydrogenation, so that the aldehyde products were preferentially diverted to aldols under the relatively forcing operating conditions.²⁷

Table 3: Hydroxymethylation of 1-decene with *L-L*/[Rh(acac)(CO)₂].^a

<i>L-L</i>	<i>L-L</i> /Rh	medium	T (°C)	time (h)	1-decene-based selectivity (%)	
					C=O (<i>l/b</i>)	C-OH (<i>l/b</i>)
Me-BISBI	5	ethanol	150	6	< 1 (0/1)	77 (4.1)
ⁿ Hex-BISBI	5	ethanol	150	20	22 (1.4)	53 (5.4)
^{neo} Pent-BISBI	5	ethanol	150	20	28 (0.5)	17 (0.8)
ⁱ Pr-BISBI	5	ethanol	150	30	13 (0.2)	25 (1.0)
Me-BISBI	2	ethanol	150	6	20 (0.9)	62 (3.8)
Me-BISBI	10	ethanol	150	6	7 (0.7)	64 (6.0)
Me-BISBI	5	<i>i</i> -propanol	150	6	< 1 (0/1)	83 (5.3)
Me-BISBI	5	thf	120	6	96 (1.2)	< 1 (1/0)
Me-BISBI	5	ethanol	120	6	8(1.6)	36 (9.2)
Me-BISBI	5	ethanol	170	6	< 1 (0/1)	97 (4.1)

^aConditions: 1 mL solvent, 8 mM [Rh], Rh/1-decene = 1/1000, 40 bar CO/H₂ = 1/1.

Higher reactivity of the linear aldehyde for aldol condensation is manifested in lower regioselectivity. The regioselectivity of these complexes is notably below that of the parent complex, which under analogous operating conditions affords *l/b* = 25. Slightly enhanced regiocontrol and chemocontrol are achieved in a more sterically demanding medium. This solvent effect presumably arises from its coordination to rhodium, thereby exerting hindrance in the catalyst coordination sphere and favouring formation of the less-strained linear rhodium-alkyl-carbonyl complex.²⁸

Alternatively, dialkylphosphine moieties can be introduced onto the periphery of a dendrimer. A dendritic complex typically retains the chemical properties of its small molecule complex but is modified by the steric requisite of the dendrimer architecture.²⁹ Ropartz *et al.* reported that the modification of [Rh(OAc)₂]₂ with diethylphosphine-functionalised polyhedral oligosilsesquioxane dendrimers affords excellent catalysts for the hydroxymethylation of higher alkenes and functionalised alkenes in ethanol (Table 4).³⁰ Reaction profiles confirm the presence of two kinetic regimes. Despite containing variable spacer units, these dendritic complexes afford comparable linear selectivity in the hydroxymethylation of 1-octene. This implicates similar regioselective determinants in the hydroformylation cycle. Their regioselectivity nevertheless exceeds that of the triethylphosphine-modified catalyst, which under analogous conditions affords *l/b* = 2,³¹ suggesting that some steric control is indeed exerted by the dendrimer architecture.

The reactivity of trivalent phosphorus nuclei in alkylphosphines makes their rhodium complexes susceptible to deactivation under the action of impurities in the system, particularly traces of oxygen and sulfur. Although rigorous purification of the feedstock can improve regioselectivity,³² there is an interest in developing hydroxymethylation catalysts with more chemically inert auxiliaries.

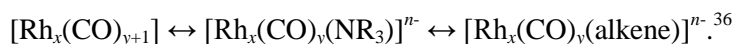
Table 4: Hydroxymethylation of α -alkenes with dendrimer-modified $[\text{Rh}(\text{OAc})_2]_2$.^a

<i>L</i>	substrate	medium	time (h)	conversion-based selectivity (%)		
				conv.	C=O (<i>l/b</i>)	C-OH (<i>l/b</i>)
G1-16ethylPEt ₂	1-octene	ethanol	8	> 99.9	nr	97.2 (3.1)
G1-24ethylPEt ₂	1-octene	ethanol	8	> 99.9	nr	96.8 (3.1)
G1-24propylPEt ₂	1-octene	ethanol	1	57.9	7.0 (nr)	50.9 (3.8)
			4	> 99.9	nr	97.9 (2.9)
G1-24ethylPEt ₂	allyl alcohol	ethanol	0.25	67.5	41 (1.6)	20 (2.6)
			2	99.9	3 (0.2)	91 (2.0)
G1-24ethylPEt ₂	allyl alcohol	thf	3	99.8	12 (0.5)	82 (2.6)
			9	99.9	1 (0.2)	94 (2.3)

^aConditions: 4 mL solvent, 8 mM [Rh], *L*/Rh = 4/1, Rh/substrate = 1/200, 120°C, 40 bar CO/H₂ = 1/1.

Trialkylamines and nitrogen-containing heterocycles have received particular attention as alternative modifying agents, since the early work of Fell and Guerts showed that their rhodium complexes effect hydroxymethylation under relatively mild operating conditions.³³ These systems were later reported to be active for selective hydrogenation of α , β -unsaturated aldehydes to the homologous alcohol products.³⁴ In an extended sequence, alkane dehydrogenation over a heterogeneous bimetallic catalyst has been integrated into the cascade reaction.³⁵

IR studies have shown that in the presence of an amine rhodium carbonyl precursors readily form anionic clusters:



The observed inhibition of tandem hydrogenation at low Rh/S molar ratios indicates competitive coordination of the amine with the alkene rather than with the aldehyde, thus it seems that $[\text{Rh}_x(\text{CO})_y(\text{alkene})]^{n-}$ and $[\text{Rh}_x(\text{CO})_y(\text{NR}_3)]^{n-}$ are independently active in the hydroformylation cycle and the hydrogenation cycle respectively. Methodological investigations have shown that monomeric amines affect the rate of tandem hydrogenation as a function of their concentration,^{33, 34, 36a} but this is not observed when polymeric amine modifiers are employed. Mizoroki *et al.* found that aminated polystyrene interacts strongly with $[\text{Rh}(\text{CO})_2\text{Cl}]_2$ to replace CO auxiliaries leading to first order dependence in carbon monoxide instead.³⁷

Imai reported that rhodium complexes of nitriles are also effective hydroxymethylation catalysts.³⁸ Full conversion of undecene is effected in 3 hours, but more forcing operating conditions are required than when amine modifiers are employed (Table 5). Typically < 3 mol% product from competing substrate hydrogenation is recovered.

It is worth noting that in instances where a cationic rhodium precursor is used, the promoting effect of these bases may simply be due to more efficient formation of the active rhodium-hydride-

dicarbonyl complex as the acid formed with the precursor counter-ion is neutralised, particularly if this is a halide or tetrafluoroborate.

Table 5: Hydroxymethylation of undecene with $L/[Rh(CO)_2Cl]_2$.^a

<i>L</i>	undecene-based selectivity (%)			Δp^b (bar)
	conv.	dodecanal	dodecanol	
-	100.0	76	20	23
succinonitrile	100.0	16	81	7
adiponitrile	100.0	15	78	19
benzonitrile	100.0	41	56	nr
diphenylacetoneitrile	> 99.5	52	44	nr
acetonitrile	> 99.2	72	25	nr

^aConditions: 6 mM [Rh], $L/Rh = 146/1$, $Rh/1\text{-undecene} = 1/1095$, 150°C , 150 bar $CO/H_2 = 1/1$, 3 hours.

^bConsumption of CO/H_2 .

The first examples of combinatorial hydroxymethylation systems were reported by Drent, juxtaposing rhodium complexes of trialkylphosphines with a carbonitrile promoter in the conversion of allyl alcohol (Table 6).³⁹ Higher linear alkyl carbonitriles appear to be preferential for this purpose. Additionally, utilising the carbonitrile as the reaction medium is advantageous for selective product recovery as the diols readily separate. Successful practice does not appear to be predicated upon the exact structure of the active rhodium species, since coordination of the carbonitrile is not precluded.

Table 6: Hydroxymethylation of allyl alcohol with $L/[Rh(R)(CO)_2]_x$ in carbonitriles.^a

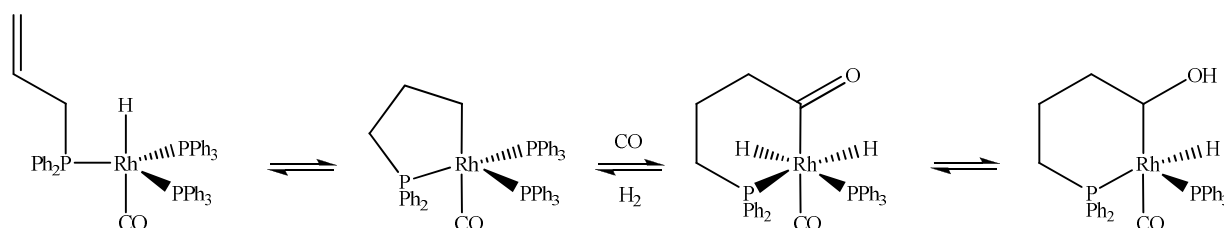
<i>L</i>	<i>R, x</i>	<i>L/Rh</i>	carbonitrile	T (°C)	conversion-based selectivity (%)
					1, 4-butanediol
$P^n\text{Oct}_3$	acac, 1	2.5	decane	75	40
$P^n\text{Oct}_3$	Cl, 2	10	heptane	85	65
$P^n\text{Bu}_3$	acac, 1	15	nonane	95	69
$P^n\text{Bu}_3$	acac, 1	5	octane	75	55 (phase separation)
$P^n\text{Bu}_3$	acac, 1	5	benzyl	75	inactive
$P(\text{benzyl})_3$	acac, 1	5	heptane	75	inactive
PEt_2Ph	acac, 1	10	tridecane	75	20 (phase separation)

^aConditions: 10 mM [Rh], $Rh/\text{allyl alcohol} = 1/345$, 60 bar $CO/H_2 = 1/2$, 5 hours.

In an extensive survey, acidic compounds were screened as promoters in combinatorial systems with the rhodium complexes of triethylphosphine or trioctylphosphine, specifically for the double hydroxymethylation of butadiene to 1, 6-hexanediol.⁴⁰ Ideally proton ionisation occurs in the pK_a range 5-20, and in this category those promoters with a capacity for hydrogen bonding such as

amines, thiols and alcohols are particularly preferred. It seems that the role of the promoter is to activate the hydrogenation catalyst, possibly by a hydride transfer.

In a different approach, the quantitative hydroxymethylation of alkenylphosphines is effected (Scheme 1).⁴¹ Due to the intramolecular chelation, regioselectivity and chemoselectivity depend upon the number of methylene spacers between the allylic functionality and the phosphine moiety. Additional stereocontrol is observed in the case of *endo*-cyclic substrates, and in a detailed study analogues of the chelating intermediates were isolated and characterised.⁴²



Scheme 1. Intramolecular hydroxymethylation of alkenylphosphines.⁴¹

It is worth mentioning from the perspective of synthetic efficiency that the hydroformylation product could also undergo stoichiometric modification prior to hydrogenation. Hydroaminomethylation is a typical example of such convergent synthesis, and the methodology has most recently been applied for the construction of complex organic amines⁴³ and azamacroheterocycles.⁴⁴ Breit and Zahn developed a hydroformylation-Wittig-hydrogenation cascade sequence for expanding the carbon skeleton of β -methylallyl *o*-diphenylphosphinobenzoate esters.⁴⁵ In an analogous methodology a piperidine-catalysed Knoevenagel condensation with malonates, β -ketoesters and β -diketones is incorporated instead.⁴⁶ Hydroxymethylation catalysis could also be coupled with homologation of the alcohol product by the introduction of CO units, resembling Fischer-Tropsch synthesis.

Heterogenised Catalyst Systems

The gas-phase hydroxymethylation of lower alkenes over heterogenised bimetallic species has been extensively explored.⁴⁷ The modification of a polysilicate-supported rhodium catalyst with molybdenum, iron, vanadium or zinc improves chemoselectivity, in that order (Table 7).⁴⁸ The hydrogen activation sites on these modified species are not inhibited by carbon monoxide adsorption and are believed to be responsible for higher C=O hydrogenation activity. Propensity for C=C hydrogenation decreases along the series of promoters, and the unmodified catalyst affords the highest yield of substrate hydrogenation product. The application of cluster-derived and zirconium oxide-supported analogues for analogous reactions has also been reported.⁴⁹

Table 7: Gas-phase hydroxymethylation of propene over M -Rh/SiO₂.^a

M -Rh/SiO ₂	M /Rh	propene-based selectivity (%)			
		conv.	C=O (<i>b/l</i>)	C-OH (<i>b/l</i>)	hyd.
Rh/SiO ₂	0	0.03	37 (0.0)	0.0 (-)	63
Mo-Rh/SiO ₂	0.5	1.27	< 1 (0.0)	32 (0.1)	68
	1	0.65	< 1 (0.0)	39 (0.2)	61
V-Rh/SiO ₂	1	0.11	2 (0.0)	68 (0.3)	30
Fe-Rh/SiO ₂	1	0.17	7 (0.6)	57 (0.1)	36
Zn-Rh/SiO ₂	1	0.07	15 (0.5)	68 (0.4)	17

^aConditions: M -Rh/SiO₂ = 0.1 g, 145°C, 34 bar propene, 68 bar CO/H₂ = 1/1, flow rate = 6 mL min⁻¹, 1 hour.

Alternatively, the catalyst-support interactions can be manipulated in order to direct hydroxymethylation. This approach was described by Sandee *et al.* using [Rh(CO)(*N*-(OMe)₃Si-propyl-Nixantphos)]⁺ immobilised on silica (Figure 2).⁵⁰

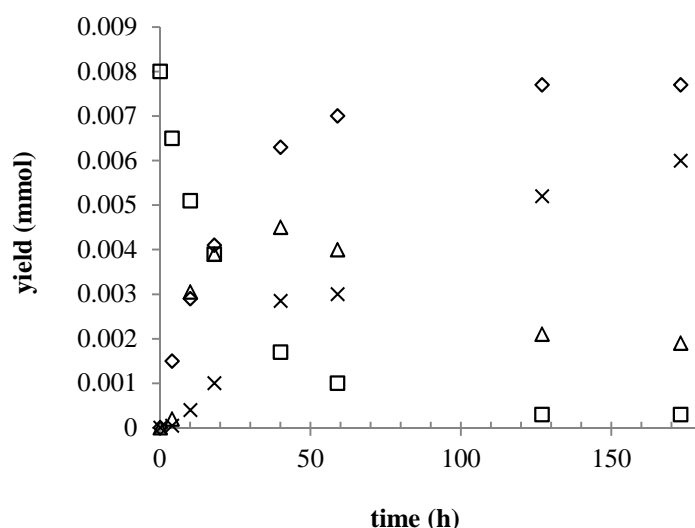


Figure 2. Course of 1-octene hydroxymethylation with silica-immobilised [Rh(CO)(*N*-(OMe)₃Si-propyl-Nixantphos)]⁺ in toluene:

(□) 1-octene, (◇) 1-nonanal + 1-nonanol, (Δ) 1-nonanal, (×) 1-nonanol.⁵⁰

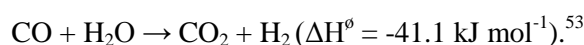
(Conditions: 10 mL toluene, 7×10^{-1} mM [Rh], L - L /Rh = 10/1, Rh/1-octene = 1/637, 80°C, 50 bar CO/H₂ = 1/1)

Under an atmosphere of *syngas*, the acidic silanols on the silica surface can convert the rhodium-hydride-dicarbonyl to the rhodium-carbonyl cation by protonation and subsequent elimination of hydrogen, and both species co-exist. Application of this system at 80°C and 50 bar *syngas* in toluene effects 20% conversion of 1-octene after 2 hours, partitioned as 96 mol% C₉-aldehyde in l/b = 65 and 4 mol% 1-nonanol, together with traces of octene isomers. Extended reaction periods increase the alcohol/aldehyde distribution, by exclusive hydrogenation of the linear aldehyde product. At 98%

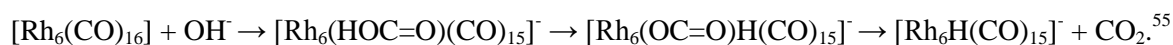
conversion of 1-octene, 1-nonanol is recovered as the predominant product. It must be noted that such a clean and selective hydroxymethylation system is quite uncommon for rhodium catalysts. Upon addition of an alcohol or an amine, hydrogenation activity is suppressed as the acidic silanols on the support are deactivated. This allows simple switching between the hydroxymethylation mode and hydroformylation mode of the system, with catalyst performance retained in each.

WGSR catalysts

The application of WGSR catalysts in hydroxymethylation can be traced to the early work of Reppe, in which basic solutions of $[\text{Fe}(\text{CO})_5]$ were used.⁵² There is considerable interest in developing this route as equilibrium thermodynamics dictate that low temperature and low pressure should favour the conversion:



Much attention has been paid to rhodium carbonyl clusters as WGSR catalysts because they can generate highly nucleophilic hydride species in basic solution.⁵⁴ IR analyses suggest the nucleophilic activation of a CO moiety on $[\text{Rh}_6(\text{CO})_{16}]$ by water or a hydroxyl ion and subsequent decarboxylation to $[\text{Rh}_6\text{HCO}]_{15}]^-$:



This anionic cluster has been acknowledged as an active catalyst for the hydrogenation of aldehydes.⁵⁶

The first examples of WGSR-based hydroxymethylation were reported for 1-pentene by Laine, using basic aqueous methanol solutions of $[\text{Rh}_6(\text{CO})_{16}]$.^{52, 57} The rate of tandem hydrogenation is reduced five-fold between pH 13 and pH 10 as the active cluster dimerises to $[\text{Rh}_{12}(\text{CO})_{32}]^{2-}$.⁵⁶ The C₆-aldehyde products are preferentially diverted to the corresponding esters under the relatively forcing operating conditions. Further complications arise as a result of catalyst decomposition below pH 10. Low regioselectivities suggests significant substrate isomerisation, a conclusion which is supported by the detection of traces of 2-ethylbutanol. Interestingly, the problematic substrate hydrogenation encountered under hydroformylation conditions does not occur here.

The addition of a strong nitrogen base to the aqueous alcoholic solution of a rhodium carbonyl cluster can enhance activity for WGSR, and Kaneda *et al.* reported the efficacy of diamine-modified and aminopyridine-modified $[\text{Rh}_6(\text{CO})_{16}]$ systems in hydroxymethylation of 1-octene (Table 8).⁵⁸ Comparable successes were later recorded using $[\text{Rh}_6(\text{CO})_{16}]$ heterogenised on an aminated polymer, with catalysis operating in a triphasic system thus allowing for a simple work-up procedure.⁵⁹

Apparently rhodium carbonyl clusters interact strongly with small tertiary amines,⁶⁰ which may be why only hydroformylation products are recovered when the triethylamine-modified $[\text{Rh}_6(\text{CO})_{16}]$ system is applied. 2-Ethoxyethanol is the preferred medium,^{54c} with the ether functionality able to solvate and stabilise the rhodium cluster anions reported to be active in aldehyde hydrogenation.

These species appear to effect highly selective C=O reduction since no nonane from competing substrate hydrogenation is recovered, however, α , β -unsaturated aldehydes undergo exclusive C=C reduction. This has been observed in catalysis under both 1 bar and 100 bar carbon monoxide.⁶¹

Table 8: WGSR-hydroxymethylation of 1-octene with $[\text{Rh}_6(\text{CO})_{16}]$ in basic aqueous ethoxyethanol.^a

amine	$\text{p}K_{\text{a}}$	1-octene-based selectivity (%)			
		conv.	C=O (<i>l/b</i>)	C-OH (<i>l/b</i>)	iso.
tetramethylpropylenediamine (TMPDA)	10.2	95	0 (-)	84 (2.8)	16
tetramethylethylenediamine (TMEDA)	8.9	88	26 (1.9)	58 (4.8)	16
4-dimethylaminopyridine (DMAP)	9.7	97	1 (0/1)	83 (1.6)	16
triethylamine	10.6	42	4 (2.0)	9 (3.5)	86

^aConditions: 3 mL methanol basified with amine solution (21 M), 16 mM [Rh], Rh/1-octene = 1/60, 80°C, 5 bar carbon monoxide, 5 hours.

In another application for organic synthesis, the TMPDA-modified system effects linear-selective hydroxymethylation of allyl alcohol under mild WGSR conditions.⁶² Catalysis under the optimised conditions of 60°C, 10 bar CO and $[\text{H}_2\text{O}] = 200 \text{ mol L}^{-1}$ gives 72% 1, 4-butanediol, 8% γ -butyrolactone and 20% isomerisation products in the recovered solution. Exchanging a diamine ligand for DMAP shifts the linear product distribution in preference of γ -butyrolactone. This is presumably formed *via* intramolecular cyclisation in a rhodium-acyl species,⁶³ in which chelation of the diamine prevents coordinating activation of the hydroxyl functionality.

1. 2. 2 Domino Hydroxymethylation

Methodological and mechanistic investigations have shown that aldehyde products do not have to be intermediaries in a hydroxymethylation scheme.^{31, 64} All the relevant bond-forming transformations can be effected in a single catalytic mechanism, in which the sequential elaboration is a consequence of the functionality generated in the preceding step.³

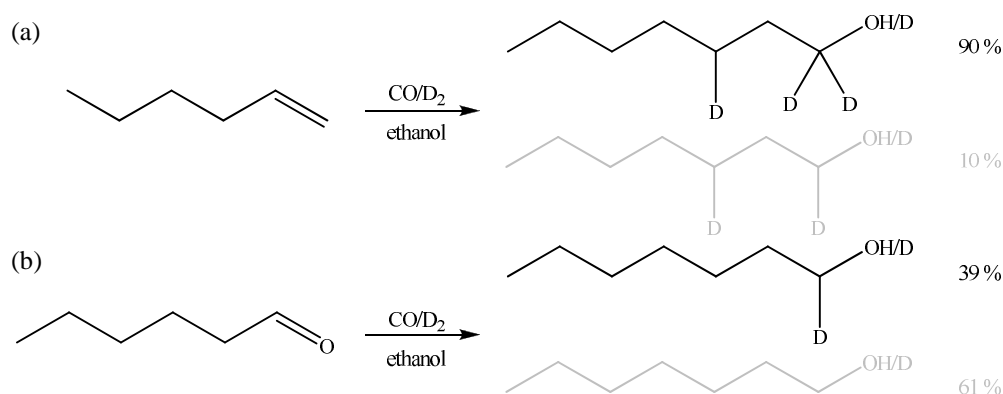
Table 9: Comparative merits of classes of coupled catalysis.

	multi-catalytic	auto-tandem	domino
work-up efficiency	negligible	high	high
process efficiency	negligible	high	high
catalyst utility	inefficient	efficient	efficient
capacity to optimise selectivity	high	limited	high
interaction of catalytic species	none	minimal	none

From a technical perspective such a pathway should overcome the limitations of the auto-tandem methodology (Table 9).⁴

Preliminary Studies

The hydroxymethylation of 1-hexene with $[\text{RhH}(\text{PEt}_3)_3]$ in ethanol was extensively studied by MacDougall and Cole-Hamilton, and reported in a series of communications.^{31, 64, 65} This catalysis superficially resembles that reported by Foster and Lawrenson,^{20, 21a} the important difference being that here $\text{PEt}_3/\text{Rh} > 2$ rather than $\text{PEt}_3/\text{Rh} < 1.5$. Solution NMR studies indicate coordination of two triethylphosphine ligands per rhodium in the relevant complexes. Deuterium labelling confirms that hydroxymethylation does not proceed by the auto-tandem pathway (Scheme 2). The predominant isotopomer of 1-heptanol recovered from 1-heptanal hydrogenation *ie.* $\text{H}/\text{DO}-\text{CH}_2-\text{CH}_2-\text{CH}_2-\text{C}_4\text{H}_9$ is only observed in 10% 1-heptanol recovered from 1-hexene hydroxymethylation *ie.* $\text{H}/\text{DO}-\text{CHD}-\text{CH}_2-\text{CHD}-\text{C}_4\text{H}_9$.



Scheme 2. Established labelling patterns in 1-heptanol:

- (a) Deuteriohydroxymethylation of 1-hexene with $[\text{RhH}(\text{PEt}_3)_3]$,
- (b) Deuteration of 1-heptanal with $[\text{RhH}(\text{PEt}_3)_3]$ in ethanol.

Strong chemoselective sensitivity to the medium is detected and a polar medium is necessary for quantitative conversion of 1-hexene to the homologous alcohols,⁶⁵ as similarly observed for the auto-tandem methodology (Table 10). Evidently, the capacity of the medium as a hydrogen donor determines which hydroxymethylation scheme is prevalent. These observations led to the proposition that protonation of a key rhodium intermediate by an alcoholic medium occurs.⁶⁷ Alcohols are similarly exploited as the proton source in catalytic generation of diethylketone from ethane, carbon monoxide and said alcohol.⁶⁸ The presence of proton sponge in an ethanolic catalyst solution inhibits activity and chemoselectivity only marginally, as the medium remains in relative excess.

Table 10: Hydroxymethylation of 1-hexene with [RhH(PEt₃)₃].^a

medium	additive (quantity)	<i>p</i> (bar)	time (h)	conversion-based selectivity (%)	
				C=O (<i>l/b</i>)	C-OH (<i>l/b</i>)
toluene		40	2	92 (2.1)	4 (1/0)
			16	92 (2.2)	1 (1/0)
thf		40	2	101 (2.4)	0 (-)
			16	4 (0/1)	115 (2.9)
thf	deio. water (2 mL)	40	2	46 (1.1)	50 (7.5)
			16	0 (-)	100 (2.4)
methanol		30	16	0 (-)	105 (2.4)
ethanol		40	2	0 (-)	101 (3.0)
			30	16	0 (-)
<i>i</i> -propanol		30	16	0 (-)	99 (2.4)
heptanol		40	2	0 (-)	100 (2.0)
heptanol			16	0 (-)	100 (1.8)
ethanol	triethylamine (1 mL)	40	3	2 (1.0)	87 (2.4)
ethanol	proton sponge (1 g)	40	2.5	4 (0.6)	78 (2.9)

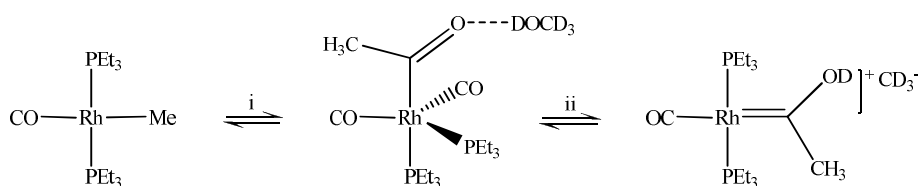
^aConditions: 4 mL solvent, 8 mM [Rh], Rh/1-hexene = 1/300, 120°C, CO/H₂ = 1/1.

The catalytic parameters are predominantly imposed by the temperature and the catalyst concentration.³¹ Practical conversion occurs at 60°C with activity then following Arrhenius behaviour up to 140°C, above which catalyst decomposition sets in. The hydroxymethylation pathway predominates at all temperatures, but some hydroformylation occurs out-with this optimum range. A relatively high catalyst concentration is necessary for significant chemocontrol, and ideally [Rh] ≥ 4 mmol L⁻¹. Hydroformylation products become progressively predominant below this limit, with a sequential hydrogenation affording the observed alcohols. Activity and selectivity are independent of the pressure condition in the range 20 to 60 bar for CO/H₂ in the range 0.5/1 to 1/1. The catalyses were performed in unstirred autoclaves,⁶⁶ so it is highly likely that mass transport effects are limiting.

Modelling Catalytic Intermediates

Faber commented that the bond-forming transformations in a domino scheme are not readily intercepted,⁶⁹ so progressive catalytic intermediates are best replicated *via* stoichiometric reactions. As an analogue of [Rh(CO-Oct)(CO)₂(PPh₃)₂], which has been spectroscopically identified during the [RhH(CO)(PPh₃)₃]-catalysed hydroformylation of 1-octene,⁷⁰ the fluxional complex [Rh(CO-Me)(CO)₂(PEt₃)₂] was synthesised and incremental addition of ethanol to its solution was monitored by ¹³C NMR spectroscopy.⁶⁴ The acyl carbon resonance at δ_C = 238 ppm shifts downfield toward

frequencies at which carbenic carbons are known to resonate as a function of ethanol concentration, with $\Delta\delta_{\text{C}} = 10.2$ ppm in neat ethanol. A hydroxycarbene carbon resonance is typically observed at $\delta_{\text{C}} \approx 300$ ppm,⁷¹ which suggests that protonation of the acyl functionality does not occur. Furthermore, the solution is found to be non-conducting. More probably, hydrogen-bonding between the acyl oxygen and ethanol creates carbenic character in the interaction between the acyl carbon and rhodium (Scheme 3).⁷² The similarity of the constants for this equilibrium with ethanol and trifluoroethanol can then be rationalised as a compensation, by which the stronger hydrogen-bonding interaction between the complex and alcohol necessitates the breakage of stronger intermolecular hydrogen-bonds between the alcohol molecules.

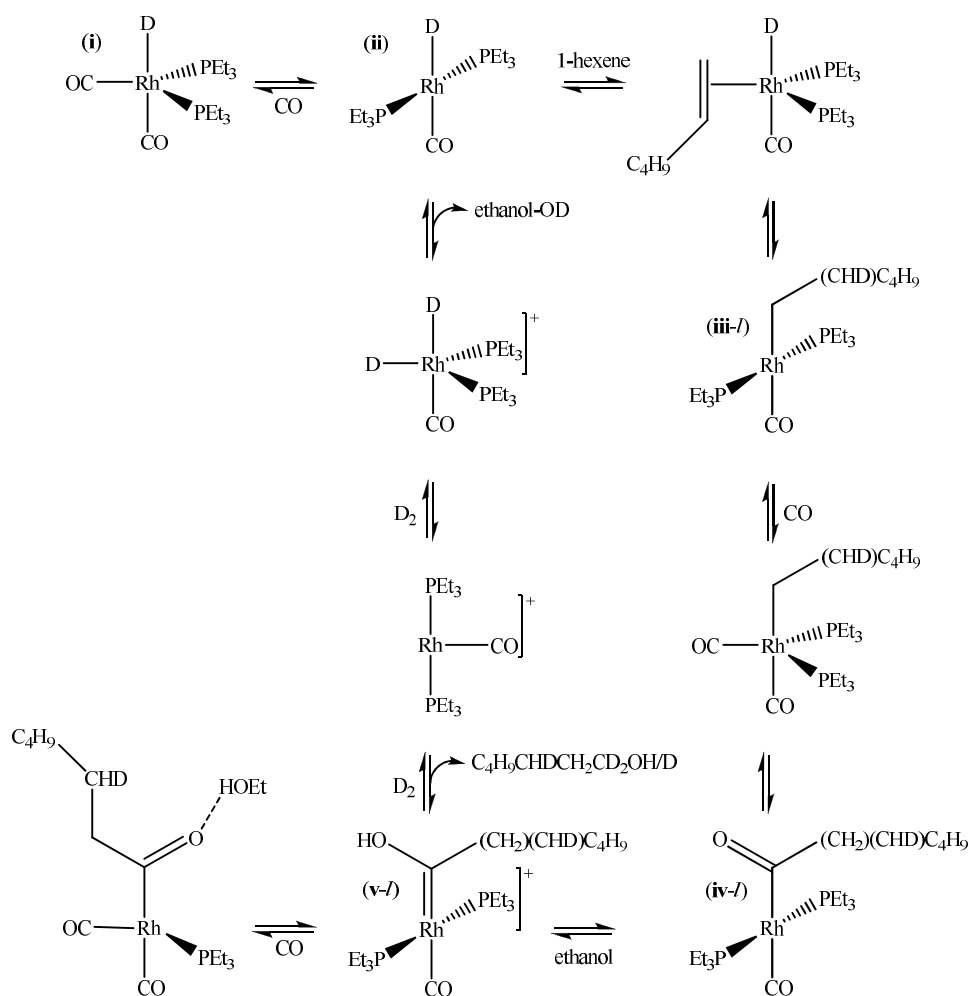


Scheme 3. Modelling catalytic intermediates of domino hydroxymethylation:

(i) carbon monoxide, CD_3OD , (ii) argon.

In the catalytic mechanism, however, the key intermediate is proposed to be square planar $[\text{Rh}(\text{CO-Me})(\text{CO})(\text{PEt}_3)]$. The removal of one CO auxiliary will localise a higher electron density on the acyl oxygen through inductive effects, thus increasing its susceptibility to protonation. Upon passing argon through a methanolic solution of $[\text{Rh}(\text{CO-Me})(\text{CO})_2(\text{PEt}_3)_2]$, the complex $[\text{Rh}(\text{C}\{\text{OH}\}\text{Me})(\text{CO})_2(\text{PEt}_3)_2]$ was generated.³¹ The acyl carbon resonance shifts downfield to $\delta_{\text{C}} = 304$ ppm, consistent with protonation of the acyl functionality and the existence of a rhodium-hydroxycarbene intermediate. Carbenic complexes were previously recognised as important in the mechanisms of alkene metathesis,⁷³ palladium-catalysed copolymerisation of propene and carbon monoxide,⁷⁴ and ruthenium-catalysed hydrogenation of carbon monoxide.^{67a}

The mechanism for domino hydroxymethylation of 1-hexene was proposed on the basis of these stoichiometric reactions, and is consistent with the deuterium labelling pattern of 1-heptanol previously observed (Scheme 4). The 18-electron rhodium-hydride-carbonyl **i** is prepared *in situ* from $[\text{RhD}(\text{PEt}_3)_3]$ under a CO atmosphere, from which the active 16-electron rhodium-hydride-carbonyl **ii** is formed *via* dissociation of triethylphosphine. Coordination of 1-hexene followed by hydride migration gives the rhodium-alkyl-carbonyl species **iii**. Coordination of carbon monoxide and subsequent migratory insertion leads to the rhodium-acyl-carbonyl complex **iv**. Protonation of acyl oxygen in **iv** by ethanol then affords the cationic rhodium-hydroxycarbene **v** counteracted by the ethoxide anion. The first oxidative addition of deuterium is followed by reductive elimination of the isomeric alcohol products, and the second by elimination of ethanol from the catalyst to recycle the active species **i**.



Scheme 4. Mechanism for domino hydroxymethylation of 1-hexene with $[\text{RhD}(\text{PEt}_3)_3]$ in ethanol.

Upon Chemoselectivity

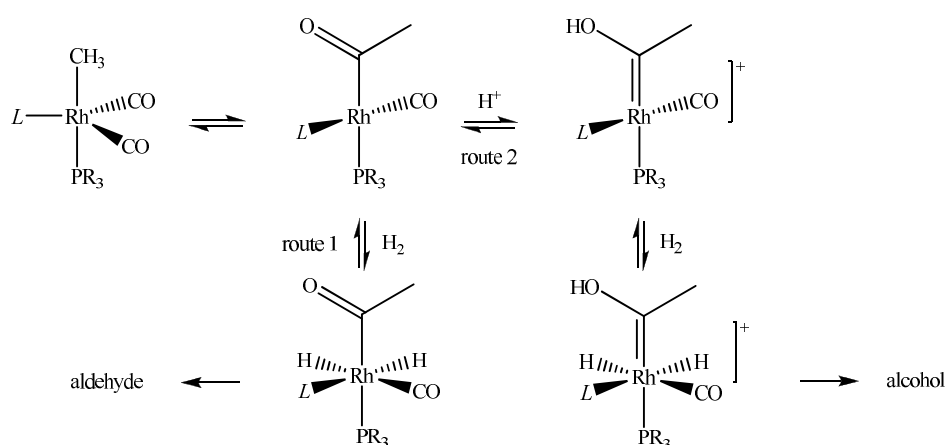
It has been demonstrated that the complexes of triarylphosphines, phosphates and phosphites are insufficiently basic to function as hydroxymethylation catalysts.^{25, 32} Conversely, a trialkylphosphine-modified catalyst does not necessarily effect the selective conversion of an α -alkene to the homologous alcohols (Table 11).^{27b, 31}

Table 11: Hydroxymethylation of with $L/[\text{Rh}(\text{OAc})_2]_2$ in ethanol.^a

<i>L</i>	<i>p</i> (bar)	conversion-based selectivity (%)		
		C=O (<i>l/b</i>)	C-OH (<i>l/b</i>)	acetals
PMe_3	48	trace	99 (2.5)	trace
PEt_3	40	0 (-)	101 (3.0)	0
P^iBu_3	44	trace	106 (2.4)	trace
P^iBu_3	40	74 (1.4)	22 (2.4)	2
P^iPr_3	52	80 (1.1)	19 (2.3)	1

^aConditions: 4 mL ethanol, 8 mM $[\text{Rh}]$, $L/\text{Rh} = 3/1$, $\text{Rh}/1\text{-hexene} = 1/300$, 120°C , $\text{CO}/\text{H}_2 = 1/1$, 16 hours.

A model study on $[\text{Rh}(\text{Me})(\text{CO})(\text{P}^i\text{Pr}_3)_2]$ has shown that under a carbon monoxide atmosphere $[\text{Rh}(\text{CO-Me})(\text{CO})_3(\text{P}^i\text{Pr}_3)]$ is exclusively formed, with the acyl functionality and the tri(*iso*-propyl)phosphine ligand mutually *trans* in the axial sites of the trigonal bipyramid.^{27a} The addition of 50% methanol to a thf solution of this complex was monitored by ^{13}C NMR spectroscopy. The acyl carbon resonance shifts only 4 ppm downfield, confirming insufficient electron density is localised on the acyl oxygen to allow interaction with the hydroxyl proton and function of the hydroxymethylation mechanism (route 2, Scheme 5). Rather, oxidative addition of hydrogen and reductive elimination of the aldehyde takes place (route 1, Scheme 5). Similar observations are reported for analogous modelling on $[\text{Rh}(\text{Me})(\text{CO})(\text{P}^i\text{Bu}_3)_2]$, although some formation of $[\text{Rh}(\text{CO-Me})(\text{CO})_2(\text{P}^i\text{Bu}_3)_2]$ is detected presumably because the secondary carbon atom is further removed from the rhodium.^{27b}



Scheme 5. Chemoselective determination in domino hydroxymethylation.

$L = \text{CO} \rightarrow \text{route 1}$, $L = \text{PR}_3 \rightarrow \text{route 2}$.

1.3 Allyl Alcohol Hydroxymethylation: A Route to 1, 4-Butanediol

It is of course of interest to extend this catalysis to more challenging substrates. Indeed, $[\text{RhH}(\text{PEt}_3)_3]$ in ethanol reportedly catalyses highly selective conversion of styrene to 2-phenylpropan-1-ol (with traces of polymeric products) and of 3, 3-dimethylbutene to 4, 4-dimethylpentan-1-ol, with similar regioselectivities noted upon their hydroformylation.^{31, 75} Analogous conversion of allyl alcohol to C_4 -diols is of particular interest as the hydroxyaldehyde products eliminated from its hydroformylation pathway are highly reactive with respect to dehydration, acetalisation and aldol condensation, and thus costly in terms of atom economy.⁷⁶ Strong selectivity for either regio-isomer is also important because the boiling points of 1, 4-butanediol and 2-methyl-propan-1, 3-diol are high and in close range, making for an intensive separation process.⁷⁷

*1. 3. 1 Constructive Commodity Products*⁷⁸

1, 4-Butanediol is a versatile intermediate in the chemical industry. It is widely used as a cross-linking agent for urethane polymers, including thermoplastic polyurethanes, cast elastomers and microcellular elastomers, and for thermoplastic polyester polymers, specifically polybutylene terephthalate and copolyester elastomers. The tough elastomeric network of these thermoplastics relies on the crystalline domains provided by 1, 4-butanediol. 1, 4-Butanediol is also used as chain extender in oxidation resistant polyester plasticers and flexible copolyester hot-melt adhesives.

Approximately 35% of 1, 4-butanediol is converted to thf as a solvent for polyvinyl chloride adhesives and as a precursor to the polyether diols poly-thf®, adipate and polycaprolactone. Poly-thf® is used in the formulation of elastomeric fibres such as Spandex and the thermoplastic elastomer Hytel.

1, 4-Butanediol may also be diverted to furanone products. Dehydration affords γ -butyrolactone, which has application as a speciality polymer solvent and as a precursor to *N*-methylpyrrolidone, a replacement for chlorinated solvents, and *N*-vinylpyrrolidone, an intermediate in the formulation of foundry resins and certain herbicides.

Smaller volume applications include formulation as 1, 4-butanediol dimethanesulfane in Myleran®, a chemotherapeutic agent to treat chronic myelocytic leukemia, and reaction with phosgene to yield chloroformates.

The applications of 2-methylpropane-1,3-diol are more limited for which the reader is referred to the hpv-review.⁷⁹

1. 3. 2 Commercial Technologies

Although 1, 4-butanediol has a relatively modest market with worldwide production in 2008 at 1 million metric tonnes,⁸⁰ several commercial technologies have been developed (Table 12).⁸¹ As relevant to this research the propylene-oxide technology for 1, 4-butanediol production, commercialised by Lyondell-Basell in 1990, is described in detail.⁸²

Propylene oxide is isomerised to allyl alcohol *via* the FMC-Progil process which employs a lithium phosphate catalyst (280°C, 10 bar). The hydroformylation catalyst is a DIOP-modified rhodium species to which a trace of DPPB is added, Rh/DIOP/DPPB = 1/75/0.2. The presence of DPPB elegantly averts catalyst poisoning by acyl intermediates or methacrolein. The high reactivity of allyl alcohol allows operating conditions to be kept mild, also effecting suppression of heavy-ends formation (60 to 65°C, 2 to 2.5 bar CO/H₂ \approx 1/4). Starvation of carbon monoxide is prevented by expeditious recycling of the gas feedstock. The reaction is monophasic, with the catalyst components suspended in toluene.

Table 12: Current technologies in the commercial production of 1, 4-butanediol.

company	precursor	technology
<ul style="list-style-type: none"> • IG Farben • Linde • Yukong 	acetylene	<i>Reppe process.</i> The condensation of 37% aqueous formaldehyde and acetylene is performed in the presence of a cuprous acetylide catalyst deposited on magnesium silicate (~ 100°C and 5 bar). The 1, 4-butanediol product is initially hydrogenated to 1, 4-butenediol with a Raney nickel catalyst (50-60°C, 7-15 bar), and so onto 1,4-butanediol using a nickel-copper-manganese catalyst on silica gel (120-140°C, 150-200 bar). A two-step hydrogenation affords purer products.
<ul style="list-style-type: none"> • Mitsubishi • BASF (for thf) 	butadiene	The initial acetoxylation of butadiene with acetic acid is performed with a heterogenous palladium-tellurium catalyst. The 1,4-diacetoxy-2-butene product is hydrogenated to 1, 4-diacetoxybutane using palladium on carbon, and saponification <i>via</i> cation exchange then affords 1, 4-butanediol and acetic acid for recycle.
<ul style="list-style-type: none"> • Kvaerner 	<i>n</i> -butane	<i>Davy process.</i> Maleic anhydride is formed via the oxidation of <i>n</i> -butane over a vanadium phosphorus oxide catalyst. This is converted to the alkyl maleate by non-catalytic esterification, and onto the dialkylmaleate by catalytic esterification with an acidic ion exchange resin. The unsaturated ester then undergoes hydrogenolysis with a copper -chromate catalyst (150-240°C, 25-75 bar), affording 1, 4-butanediol and alcohol for recycle.
<ul style="list-style-type: none"> • BASF 	<i>n</i> -butane	<i>Eurodiol process.</i> As above, but the conversion of maleic anhydride to diethylmaleate is performed <i>via</i> one esterification.
<ul style="list-style-type: none"> • BP 	<i>n</i> -butane	<i>Lurgi-Geminox process.</i> As above, but using a fluid-bed reactor to maintain a uniform temperature profile.
<ul style="list-style-type: none"> • Lyondell-Basell 	propylene oxide	<i>Kuraray process.</i>

Multi-stage extraction with water (30°C, water/toluene (v/v) = 1) allows recovery of the hydrophilic hydroxyaldehyde products in the aqueous phase and recycling of the apolar catalyst in the organic phase, typically with rhodium leaching below 10 ppb. However, some bleed of the catalyst phase is necessary in order to remove the less polar heavy-ends and also oxidised DIOP that will accumulate in the organic recycle. Raney nickel-catalysed hydrogenation of the aqueous extract of 4-hydroxybutanal and 2-methyl-3-hydroxypropanal gives the corresponding diols, together with traces of heavy-ends and nickel (60-80 °C, 9-18 bar). The nickel is precipitated by basifying the product solution to pH 8.5, and the water, together with any residual hydroxyaldehyde, is removed by distillation at 100°C. The diols are isolated from the high-boiling heavy-ends by distillation at 180°C, and a subsequent fractional distillation then separates the regio-isomers.

Lyondell-Basell operates this technology in a 55 kilo-tonne *per annum* capacity in Channelview, USA, together with a 126 kilo-tonne *per annum* capacity in Rotterdam, the Netherlands. For a description of the continuous-flow process equipment used, the reader is referred to the original patent by Matsumoto *et al.*⁷⁶

1. 3. 3 Domino Hydroxymethylation of Allyl Alcohol

In protic media, the rhodium complexes of trialkylphosphines effect the domino hydroxymethylation of allyl alcohol.⁸³ Expectedly, 1, 4-butanediol is the exclusive linear product, but surprisingly 2-methylpropanol predominates as the branched isomer. Product analysis over the course of catalysis has shown that 2-methylpropanol is formed *via* 2-methylpropanal (Figure 3).^{83b}

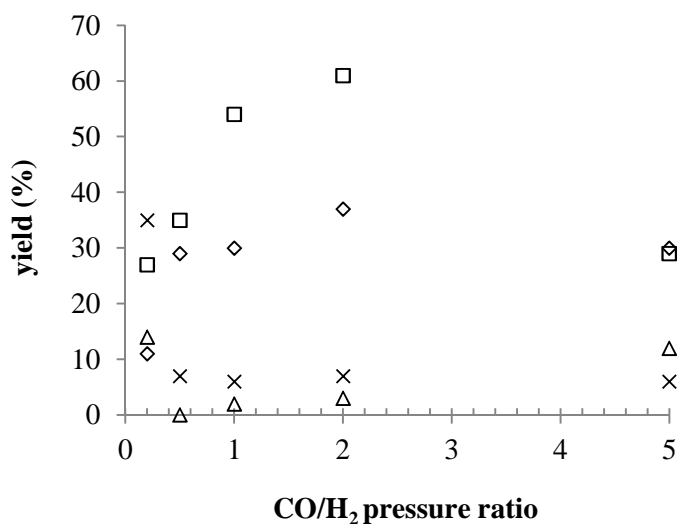


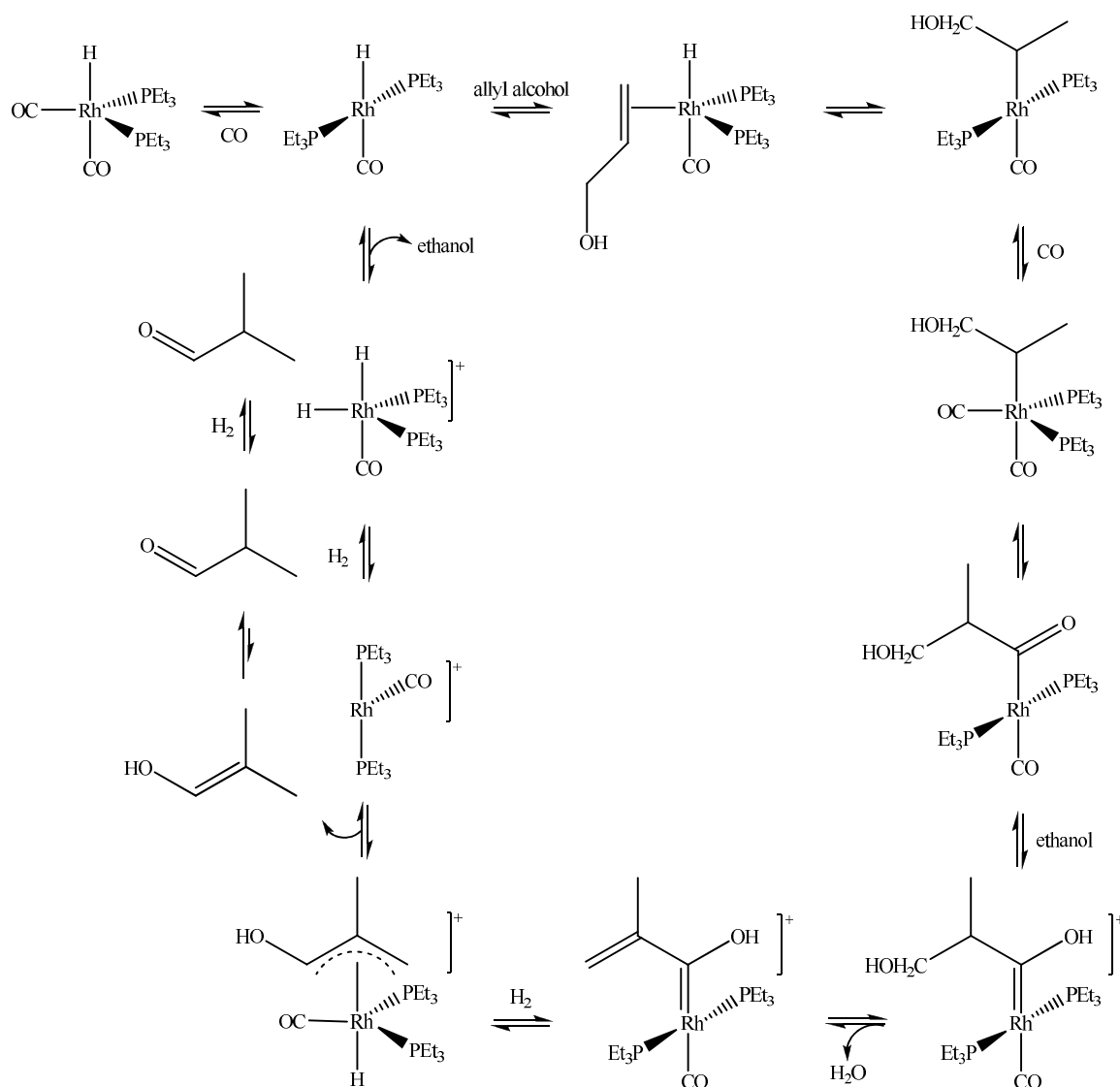
Figure 3. Course of allyl alcohol hydroxymethylation with $\text{PEt}_3/[\text{Rh}(\text{OAc})_2]_2$ in ethanol:

(□) 1, 4-butanediol, (◇) 2-methylpropanol, (Δ) 2-methylpropanal, (×) 1-propanol.

(Conditions: 4 mL ethanol, 8 mM [Rh], $\text{PEt}_3/\text{Rh} = 11/1$, $\text{Rh}/\text{allyl alcohol} = 1/300$, 120°C, 40 bar $\text{CO}/\text{H}_2 = 1/1$)

Formally this product arises from *anti*-Markovnikoff addition of methane across the C=C functionality in allyl alcohol, so that a conjugation-driven dehydration from either rhodium-(2-methylhydroxypropanoyl) or rhodium=(2-methylpropenediol) is necessary for its formation. Deuterium labelling is consistent with a mechanism in which the 2-methylpropanal is derived *via* enol-keto tautomerisation of 2-methyl-1-propenal,^{83a} and on this basis a catalytic pathway for the branched-selective domino hydroxymethylation of allyl alcohol was proposed (Scheme 6).

Formation of 1, 4-butanediol and 2-methylpropanol as the linear and branched isomers can be considered advantageous as their boiling points are apart sufficiently to facilitate fractional distillation of a mixture.⁷⁷ Nevertheless, the consideration of 2-methylpropanol as a low-value product places stronger emphasis on a linear-selective transformation, which is a prominent limitation of this current methodology.^{83b}



Scheme 6. Mechanism for branch-selective domino hydroxymethylation of allyl alcohol with PEt₃/[Rh(OAc)₂]₂ in ethanol.

The high activity for allyl alcohol isomerisation and hydrogenation, increasing at lower CO/H₂ pressure ratios, and the ease of catalyst deactivation are other core frustrations, and therefore a brief review is dedicated to each.

(1) Substrate isomerisation

The isomerisation of allyl alcohol to 1-propanal is driven by the thermodynamic gain in carbonyl formation, which renders the equilibrium effectively irreversible:



Although the double bond migration is generally accepted to proceed either *via* a metal hydride addition-elimination mechanism or *via* a π -allyl metal-hydride mechanism more extensive isomerisation than unfunctionalised alkenes has led to the postulation of a third mechanism invoking chelation of the allylic alcohol.⁸⁵ From the commercial perspective, the isomerisation of allyl alcohol represents a yield loss which can be adversely manifested in the process economics.

(2) Substrate hydrogenation

The hydroxymethylation catalysts exhibit strong capacity for hydrogenation, which under controlled conditions can be applied for the direct synthesis of alcohols.^{8, 9, 86} A sufficiently high vapour pressure for gas phase catalysis makes it difficult to suppress hydrogenation of the C=C functionality in allyl alcohol,⁶¹ which represents a yield loss.

(3) Catalyst degeneration

Under hydroformylation conditions catalyst deactivation is primarily the consequence of poisoning by α , β -unsaturated aldehydes such as methacrolein.⁸⁷ More generally, oxidative addition of the C-O bond in allyl alcohol to rhodium aggravates oxidation of the coordinated phosphine ligand.⁸⁸

1.4 Outline of Thesis

The current demands for linear alcohol products cannot be satisfied by the available hydroxymethylation methodologies. The development of novel catalytic strategies is therefore imperative. Herein are described a number of such approaches, specifically for the selective conversion of allyl alcohol to 1, 4-butanediol.

Chapter 2 describes the development of a versatile synthetic route to modular *bis*(diethylphosphine)-modified carbocyclic ligands. Their chelation modes in the rhodium-hydride-dicarbonyl complex are identified by high pressure NMR spectroscopy and compared with that of the triethylphosphine-modified complex. The application of these rhodium species for the hydroxymethylation of allyl alcohol, and their compatibility with aqueous biphasic catalyst recycling is discussed. Up to 53 mol% selectivity to 1, 4-butanediol was attained.

Recent literature reports have shown that *bis*(3, 5-dimethylphenyl)phosphine-modified chelates significantly improve the activity of their rhodium complexes for linear-selective hydroformylation of allyl alcohol. In Chapter 3, the source of this *meta*-effect and its influence on catalyst performance are assessed. The physicochemical characteristics of hybrid triarylphosphines and their coordination behaviour with rhodium(I) precursors under nitrogen are determined and compared. A semi-empirical rate model for the hydroformylation of allyl alcohol with $[\text{RhH}(\text{CO})\{(3, 5\text{-Me}_2\text{Ph})_3\text{P}\}_3]$ and recyclability of this catalyst are discussed. Selectivity to linear hydroxyaldehyde derivatives reached 96 mol%. The application of $[\text{RhH}(\text{CO})\{(3, 5\text{-Me}_2\text{Ph})_3\text{P}\}_3]$ for highly selective hydroformylation of 1, 1-*bis*(*p*-fluorophenyl)-2-propenol to 5, 5-*bis*(*p*-fluorophenyl)tetrahydrofuranol is described in context of a new synthetic route to the neuroleptic *Fluspirelen*.

The application of mixed-ligand catalysis is presented in Chapter 4, using systems based on a *bis*(diarylphosphine) chelate/triethylphosphine composition. The coordination behaviour of the mixed ligands with rhodium(I) precursors under nitrogen and *syngas* and the performance of the mixed-ligand system in allyl alcohol hydroxymethylation are discussed. The highest observed selectivity to 1, 4-butanediol is 66 mol%. The influence of triethylphosphine on selectivity is investigated by selective additive experiments and deuterium labelling, giving some insight into the catalytic pathway.

The extension of a supramolecular methodology based on adenine-thymine base pairing is presented in Chapter 5. Hetero-combinatorial assembly of the platforms and the rhodium chemistry of the heterodimers is investigated by a range of NMR spectroscopic methods. The performance of the heteroleptic rhodium catalysts in allyl alcohol hydroxymethylation is discussed. Although selectivity to 1, 4-butanediol can reach 73 mol%, these species are sensitive to the operating conditions.

References and Notes

- (1) (a) *The Chemistry of the Carbonyl Group*. Patai, S. (Ed). Wiley-Interscience: New York, 1970. (b) *Methoden der Organischen Chemie*, vol. E3. Falbe, J. (Ed). Thieme: Stuttgart, 1983.
- (2) Schulte, M. M.; Herwig, J.; Fischer, R. W.; Kohlpaintner, C. W. *J. Mol. Catal. A* **1999**, *150*, 147.
- (3) Tietze, L. F. *Chem. Rev.* **1996**, *96*, 115.
- (4) Fogg, D. E.; dos Santos, E. N. *Coord. Chem. Rev.* **2004**, *248*, 2365.
- (5) (a) Crabtree, R. H. *The Organometallic Chemistry of the Transition Metals*. Wiley: Toronto, 1994. (b) Cornils, B. *Catalysis from A to Z: A Concise Encyclopedia*. Cornils, B.; Herrmann, W. A.; Schlögl, R.; Wong, C. -H. (Eds). Wiley: Toronto, 2000. (c) Bohnen, H.; Cornils, B. *Advances in Catalysis* **2002**, *47*, 1.

- (6) Tandem and domino catalysis under hydroformylation conditions. Eilbracht, P.; Bärfacker, L.; Buss, C.; Hollmann, C.; Kitsos-Rzychon, B.E.; Kranemann, C. L.; Rische, T.; Roggenbuck, R.; Schmidt, A. *Chem. Rev.* **1999**, *99*, 3329.
- (7) Reaction sequences to complex organics incorporating hydroformylation. Breit, B. *Acc. Chem. Res.* **2003**, *36*, 264.
- (8) (a) Wender, I.; Pino, P. *Organic Synthesis via Metal Carbonyls*, vol. 2. Wiley: New York, 1977. (b) Falbe, J. *Carbon Monoxide in Organic Synthesis*. Springer: Berlin, 1970. (c) Cornils, B. *New Syntheses with Carbon Monoxide*. Falbe, J. (Ed) Springer: Berlin, 1980. (d) Parshall, G. W.; Ittel, S. D. *Homogeneous Catalysis: The Applications and Chemistry by Soluble Transition Metal Complexes*. Wiley: New York, 1992.
- (9) Beller, M.; Cornils, B.; Frohning, C. D.; Kohlpaintner, C. W. *J. Mol. Catal.* **1995**, *104*, 17.
- (10) (a) Wender, I.; Levine, R.; Orchin, M. *J. Am. Chem. Soc.* **1950**, *72*, 4375. (b) Goetz, R. W.; Orchin, M. *J. Org. Chem.* **1962**, *27*, 3698. (c) Slaugh, L. H.; Mullineaux, R. D. *J. Organomet. Chem.* **1968**, *13*, 469.
- (11) (a) Tominaga, K.; Sasaki, Y. *J. Mol. Catal. A* **2004**, *220*, 159. (b) Cesarotti, E.; Fusi, A.; Ugo, R.; Zanderighi, G. M. *J. Mol. Catal.* **1978**, *4*, 205. (c) Sanchez-Delgado, R. A.; Bradley, J. S.; Wilkinson, G. *J. Chem. Soc., Dalton Trans.* **1976**, 399. (d) Knifton, J. F. *J. Mol. Catal.* **1988**, *47*, 99.
- (12) Botteghi, C.; Paganelli, S.; Matteoli, U.; Scrivanti, A.; Rocco, C.; Venanzi, L. *Helv. Chim. Acta* **1990**, *73*, 284.
- (13) (a) Drent, E.; Budzelaar, P. H. M. *J. Organomet. Chem.* **2000**, *594*, 211. (b) Konya, D.; Almeida-Leñero, K. Q.; Drent, E. *Organometallics*, **2006**, *25*, 3166.
- (14) *Tandem Organic Reactions*. Ho, T. -L. (Ed). Wiley: New York, 1992.
- (15) Best exemplified in the tandem aldol-hydrogenation catalysis of acetone. Pittman Jr., C. U.; Liang, Y. F. *J. Org. Chem.* **1980**, *45*, 5048.
- (16) Slaugh, L. Mullineaux, R. D. *US Pat.* 3.239.566, 1966.
- (17) [1, 2, 3-(PPh₃)₃RhCl₃]. (a) Osborn, J. A.; Wilkinson, G.; Young, J. F. *J. Chem. Soc., Chem. Commun.* **1965**, 17. (b) Wilkinson, G. *Fr. Dem.* 1.459.643.
- (18) Knifton, J. F. *J. Org. Chem.* **1976**, *41*, 2885 and references therein.
- (19) (a) Johnson, P.; Lawrenson, M. J. *Fr. Dem.* 1.549.414, 1968. (b) Lawrenson, M. J. *Fr. Dem.* 1.558.222, 1969.
- (20) Foster, G.; Lawrenson, M. J. *Ger. Pat.* 1.901.145, 1969.
- (21) (a) Lawrenson, M. J.; Foster, G. *Ger. Pat.* 1.819.504, 1969. (b) Lawrenson, M. J. *Br. Pat.* 1.254.222, 1971. (d) Lawrenson, M. J. *Br. Pat.* 1.284.615, 1972.
- (22) Smith, W. E. *Ger. Pat.* 2.758.473, 1978.
- (23) Sellin, M. F.; Bach, I.; Webster, J. M.; Montilla, F.; Rosa, V.; Avilés, T.; Poliakoff, M.; Cole-Hamilton, D. J. *J. Chem. Soc., Dalton Trans.* **2002**, 4569.
- (24) $T_c = 31.1^\circ\text{C}$ and $P_c = 72.9$ bar. *Reactions in Supercritical Carbon Dioxide*. Jessop P. G., Leitner, W. (Eds.). Springer-Verlag: Berlin, 1999.
- (25) van Leeuwen, P. W. N. M.; Claver, C. *Rhodium Catalysed Hydroformylation*. James, B. R.; Ugo, R. (Eds). Kluwer Academic: Dordrecht, 2000.

- (26) Ichihara, T.; Nakano, K.; Katayama, M.; Nozaki, K. *Chem. Asian J.* **2008**, *3*, 1722.
- (27) Reduced hydrogenation activity could also be due to η^1 -coordination of the chelate. (a) Cheliatsidou, P.; White, D. F. S.; Cole-Hamilton, D. J. *Dalton Trans.* **2004**, 2425. (b) Cheliatsidou, P.; White, D. F. S.; Slawin, A. M. Z.; Cole-Hamilton, D. J. *Dalton Trans.* **2008**, 2389.
- (28) Desphande, R. M.; Divekar, S. S.; Gholap, R. V.; Chaudhari, R. V. *Ind. Eng. Chem. Res.* **1991**, *30*, 1389.
- (29) Newcome, G. R.; He, E. F.; Morefield, C. N. *Chem. Rev.* **1999**, *99*, 1689.
- (30) Ropartz, L.; Foster, D. F.; Morris, R. E.; Slawin, A. M.; Cole-Hamilton, D. J. *J. Chem. Soc., Dalton Trans.* **2002**, 1997.
- (31) MacDougall, J. K.; Simpson, M. C.; Green, M. J.; Cole-Hamilton, D. J. *J. Chem. Soc., Dalton Trans.* **1996**, 1161.
- (32) Frohning, C. D.; Kohlpaintner, C. W. *Applied Homogeneous Catalysis with Organometallic Compounds*, vol. 1. Cornils, B.; Herrmann, W. A. (Eds). VCH: Weinheim, 1996.
- (33) Fell, B.; Guerts, A. *Chem. Ing. Techn.* **1972**, *44*, 708.
- (34) (a) Meguro, S.; Mizoroki, T.; Ozaki, A. *Chem. Lett.* **1975**, 943. (b) Mizoroki, T.; Seki, K.; Meguro, S.; Ozaki, A. *Bull. Chem. Soc. Jpn.* **1977**, *50*, 2148.
- (35) Imai, T. *US Pat.* 4.438.287, 1984.
- (36) (a) Jurewicz, A. T.; Rollmann, L. D.; Whitehurst, D. D. *Homogeneous Catalysis*, vol. 2. Forster, D.; Roth, J. F. (Eds). ACS: Washington D. C., 1974. (b) Martinengo, S.; Chini, P. *Gazz. Chim. Ital.* **1972**, *102*, 344. (c) Rollmann, L. D. *Inorg. Chim. Acta* **1972**, *6*, 137.
- (37) (a) Mizoroki, T.; Kioka, M.; Suzuki, M.; Sakatani, S.; Okumura, A.; Maruya, K. –I. *Bull. Chem. Soc. Jpn.* **1984**, *57*, 577. (b) Haag, W. O.; Whitehurst, D. D. *Int. Congr. Catal.* *V*, 29. Palm Beach, FL, 1972.
- (38) Imai, T. *US Pat.* 4.219.684, 1979.
- (39) Drent, E. *US Pat.* 4.590.311, 1986.
- (40) Guram, A. S.; Briggs, J. R.; Packett, D. L.; Olson, K. D.; Eisenschmid, T. C.; Tjaden, E. B. *US Pat.* 6.172.269, 2001.
- (41) (a) Jackson, W. R.; Perlmutter, P.; Suh, G. –H. *J. Chem. Soc., Chem. Commun.* **1987**, *40*, 129. (b) Jackson, W. R.; Perlmutter, P.; Suh, G. –H.; Tasdelen, E. E. *Aust. J. Chem.* **1991**, *44*, 951. (c) van der Slot, S. C.; Kamer, P. C. J.; van Leeuwen, P. W. N. M. *Organometallics* **2001**, *20*, 1079.
- (42) Couthino, K. J.; Dickson, R. S.; Fallon, G. D.; Jackson, W. R.; Simone, T. D.; Skelton, B. W. *J. Chem. Soc., Dalton Trans.* **1997**, 3193.
- (43) For review see: (a) Reference 7a. (b) Ungvary, F. *Coord. Chem. Rev.* **2001**, *213*, 1.
- (44) (a) Kranemann, C. L.; Costisella, B.; Eilbracht, P. *Tet. Lett.* **1999**, 7773. (b) Kranemann, C. L.; Eilbracht, P. *Eur. J. Org. Chem.* **2000**, 2367.
- (45) Breit, B.; Zahn, S. K. *Angew. Chem. Int. Ed.* **1999**, 969.
- (46) Breit, B.; Zahn, S. K. *Angew. Chem. Int. Ed.* **2001**, 1910.
- (47) Iron, vanadium and zinc. (a) Ichikawa, M. *Polyhedron* **1988**, *7*, 2351. (b) Sachtler, W. M. H.; Ichikawa, M. *J. Phys. Chem.* **1986**, 4752.
- (48) Tomishige, K.; Furikado, I.; Yamagishi, T.; Ito, S. –I.; Kunimori, K. *Catal. Lett.* **2005**, *103*, 15.

- (49) (a) Cluster derived catalyst. Trunschke, A.; Böttcher, H. -C.; Fukuoka, A.; Ichikawa, M.; Miessner, H. *Catal. Lett.* **1991**, *8*, 221. (b) ZrO₂-supported catalyst. Marengo, S.; Miessner, H.; Trunschke, A.; Martinengo, S.; Zanderighi, L. *Collect. Czech. Chem. Commun.* **1992**, *57*, 2565.
- (50) Sandee, A. J.; Reek, J. N. H.; Kamer, P. C. J.; van Leeuwen, P. W. N. M. *J. Am. Chem. Soc.* **2001**, *123*, 8468.
- (51) For reference examples see: (a) References 19-22, 31, 33-35, 38, 39. (b) Anderson, J. -A. M.; Currie, A. W. S. *Chem. Commun.* **1996**, 1543. (c) Zhous, J. -Q.; Alper, H. *J. Chem. Soc., Chem. Commun.* **1991**, 233.
- (52) Laine, R. *J. Am. Chem. Soc.* **1978**, *100*, 6451 and references therein.
- (53) *J. Phys. and Chem. Reference Data*, 11, supplement 2, 1982.
- (54) (a) *Metal Clusters in Catalysis*. Gates, B. C.; Gucci, L.; Knozinger, H. (Eds). Elsevier: Amsterdam, 1986. (b) Kaneda, K.; Mizugaki, T. *Organometallics* **1996**, *15*, 3247. (c) Kaneda, K.; Yasumura, M.; Imanaka, T.; Teranishi, S. *J. Chem. Soc., Chem. Commun.* **1982**, 935.
- (55) (a) Kaneda, K., Takemoto, T.; Kitaoka, K.; Imanaka, T. *Organometallics* **1991**, *10*, 846. (b) Heaton, B. T.; Strona, L.; Martinengo, S.; Strumolo, D.; Goodfellow, R. J.; Sadler, I. H. *J. Chem. Soc., Dalton Trans.* **1982**, 1499.
- (56) Mizugaki, T.; Ebitani, K.; Kaneda, K. *Appl. Surf. Sci.* **1997**, *121/122*, 360.
- (57) Laine, R. *US Pat.* 4. 226.845, 1980.
- (58) Kaneda, K.; Yasumura, M.; HIRaki, M.; Imanaka, T.; Teranishi, S. *Chem. Lett.* **1981**, 1763.
- (59) (a) Kaneda, K.; Kuwahara, H.; Imanaka, T. *J. Mol. Catal.* **1992**, *72*, 27. (b) Kaneda, K.; Kuwahara, H.; Imanaka, T. *J. Mol. Catal.* **1994**, *88*, 267.
- (60) Pardey, A. J.; Fernández, M.; Moreno, M. A.; Alvarez, J.; Rivas, A. B.; Ortega, M. C.; Mendez, B.; Baricelli, P. J.; Longo, C. *React. Kinet. Catal. Lett.* **2000**, *70*, 293.
- (61) Vannice, M. A.; Sen, B. *J. Catal.* **1989**, *115*, 65.
- (62) Kaneda, K.; Imanaka, T.; Teranishi, S. *Chem. Lett.* **1983**, 1465.
- (63) Taqui-Khan, M. M.; Halligudi, S. B.; Abdi, S. H. R. *J. Mol. Catal.* **1988**, *45*, 215.
- (64) MacDougall, J. K.; Simpson, M. C.; Cole-Hamilton, D. J. *Polyhedron* **1993**, *12*, 2877.
- (65) (a) MacDougall, J. K.; Cole-Hamilton, D. J. *Polyhedron* **1990**, *9*, 1235. (b) MacDougall, J. K.; Cole-Hamilton, D. J. *J. Chem. Soc., Chem. Commun.* **1990**, 165.
- (66) MacDougall, J. K. *PhD Thesis*, University of St. Andrews, 1991. Chapter 5.
- (67) Protonation of a formyl/acyl complex is recognised in several catalytic systems. (a) carbon monoxide hydrogenation by [Ru(CHOMe)(CO)(DPPE)₂][SbF₆]. Barrat, D. S.; Glidewell, C.; Cole-Hamilton, D. J. *J. Chem. Soc., Dalton Trans.* **1988**, 1079. (b) carbon monoxide activation by [Ir(CO)(DPPE)₂Cl]₂⁺. Lilger, M. A.; Ibers, J. A. *Organometallics* **1985**, *4*, 590. (c) C-H activation of 3, 3-diphenylpropene by [Os(CO)₂(PPh₃)₃]. Grundy, K. R.; Roper, W. R. *J. Organomet. Chem.* **1981**, *216*, 255.
- (68) Isnard, P.; Denise, B.; Sneed, R. P. A.; Cognion, J. M.; Durnal, P. *J. Organomet. Chem.* **1982**, *240*, 169.
- (69) Mayer, S. F.; Kroutil, W.; Faber, K. *Chem. Soc. Rev.* **2001**, *30*, 33.

- (70) (a) Brown, J. M.; Kent, A. G. *J. Chem. Soc., Chem. Commun.* **1982**, 723. (b) Brown, J. M.; Kent, A. G. *J. Chem. Soc., Perkins Trans. II* **1987**, 1597.
- (71) Mann, B. E.; Taylor, B. F. *¹³C NMR Data for Organometallic Compounds*. Academic Press: London, 1981.
- (72) An oxycarbene resonance form effects short M-C bonds and long C-O bonds in many metal formyl complexes. Gladysz, J. A. *Adv. Organomet. Chem.* **1982**, *20*, 1 and references therein.
- (73) Grubbs, R. H. *Prog. Inorg. Chem.* **1978**, *24*, 1.
- (74) Batistini, A.; Consiglio, G. *Organometallics* **1992**, *11*, 1767.
- (75) Simpson, M. C. *PhD Thesis*, University of St. Andrews, 1994. Chapter 5.
- (76) Matsumoto, K.; Miura, N.; Koichi, T.; Masuhiko, K.; Hedetaka, K.; Kamashita, Kunio, K.; Yamashita, S. *US Pat.* 4.567.305, 1986.
- (77) (a) 1, 4-Butanediol bpt. = 230°C. (b) 2-methyl-1, 3-propanediol bpt. = 210°C. (c) 2-methylpropanol bpt. = 108°C. Pedley, J. B.; Naylor, J. D.; Kirby, S. P. *Thermochemical Data of Organic Compounds*. Chapman & Hall: London, 1986.
- (78) For compilation source see: (a) Karas, L.; Piel, W. J. *Kirk-Othmer Encyclopedia of Chemical Technologies*. Wiley: New York, 2004.
- (79) *MPDiol® Glycol: High Production Volume Chemical Challenge Program*. CAS RN 2163-42-0. Lyondell-Basell, 2004.
- (80) *1, 4-Butanediol: Price and Demand in Chemical Markets*. Chem. Week, April 2008.
- (81) *1, 4-Butanediol Technologies - PERP Report*. Nexant Chemical Systems, 2008.
- (82) Provided by Lyondell-Basell, Newtown Square Technology Centre, 3801 West Chester Pike, Newtown Square, PA 19073, USA.
- (83) (a) Simpson, M. C.; Porteous, K.; MacDougall, J. K.; Cole-Hamilton, D. J. *Polyhedron* **1993**, *12*, 2883. (b) Simpson, M. C.; Currie, A. W. S.; Andersen, J. A. M.; Cole-Hamilton, D. J.; Green, M. J. *J. Chem. Soc., Dalton Trans.* **1996**, 1793.
- (84) Carey, F. A.; Sundberg, R. J. *Advanced Organic Chemistry*, vol. 1. Plenum Press: New York, 1991.
- (85) For review see: van der Drift, R. C.; Bouwman, E.; Drent, E. *J. Organomet. Chem.* **2002**, *650*, 1.
- (86) Pruet, R. L. *Adv. Organomet. Chem.* **1979**, *17*, 1.
- (87) (a) Harano, Y. *US Pat.* 4.465.873, 1984. (b) Budge, J. R.; Pedersen, S. E. *US Pat.* 4.810.807, 1989. (c) Kojima, H.; Horikawa, T.; Kagotani, M. *US Pat.* 4.537.997, 1985.
- (88) Desphande, R. M.; Chaudhari, R. V. *J. Catal.* **1989**, *115*, 326.

-Chapter 2-

Enhanced Linear-Selective Hydroxymethylation with the Rhodium Complexes of *Bis*-(diethylphosphine) Modified Alicyclics

Abstract. Complexes of the type $[\text{RhH}(\text{CO})_2(\text{L-L})]$ ($\text{L-L} = \textit{trans}$ -1, 2-*bis* (diethylphosphinomethyl) cyclohexane (**7a**), *trans*-1, 2-*bis*-(diethylphosphinomethyl) cyclopentane (**7b**) and *trans*-1, 2-*bis*-(diethylphosphinomethyl) cyclobutane (**7c**)) adopt predominantly *ea* geometry, which effects domino hydroxymethylation as the primary catalytic scheme. An increasingly flexible chelate ring in the order **7c** < **7b** < **7a** led to simultaneously enhanced activity and inhibited regioselectivity. These catalysts could be recycled *via* biphasic separation with high efficiency, the small loss ascribed to catalyst poisoning by methacrolein.

2.1 Introduction

The DIOP ligand has been of interest for applications that require the generation and stabilisation of an asymmetric catalyst since its preparation was first reported by Dang and Kagan in 1971 (Figure 1).¹ Previous reports on asymmetric hydroformylation quoted the use of chiral heterogeneous catalysts² or homogeneous precursors modified with chiral monophosphines,³ but relatively low optical inductions were observed. DIOP-modified rhodium and platinum-tin chloride complexes have been applied with comparative success in the asymmetric hydroformylation of prototypical alkenes.^{1a, 4, 5} This chelate is of keen interest as it can be easily tuned for enhanced selectivity or catalyst recovery by modifications in the phosphorus moiety and in the dioxolan ring.⁶

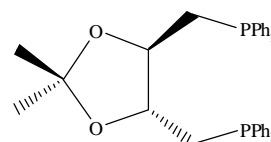


Figure 1. DIOP ligand.

Maki *et al.* first explored the application of DIOP-modified rhodium as a catalyst for the hydroformylation of allyl alcohol, and reported excellent regioselectivity.⁷ In subsequent research by Lyondell-Basell significant suppression of C₃-product formation was observed,⁸ presumably because the C₂-symmetry element of the ligand minimises the number of potential substrate-catalyst arrangements thereby eliminating competing pathways. Improved linear-selective hydroformylation appears to be substrate specific however, and only minor enhancements have been observed upon hydroformylation of 1-hexene and 1-octene.^{9, 10}

This intimate lock-and-key relationship between DIOP and allyl alcohol stimulated our exploration of chiral diphosphines based on alternative alicyclic scaffolds, as related catalysts frequently display a continuum with respect to activity and selectivity. Thus, rhodium modified with *trans*-2, 3-*bis*-(diphenylphosphinomethyl)bicyclo-[2, 2, 1] heptane or with *trans*-2, 3-*bis*-(diphenylphosphinomethyl)-bicyclo-[2, 2, 1] hept-5-ene catalyses the hydroformylation of allyl alcohol with comparable regioselectivity and chemoselectivity.^{7c}

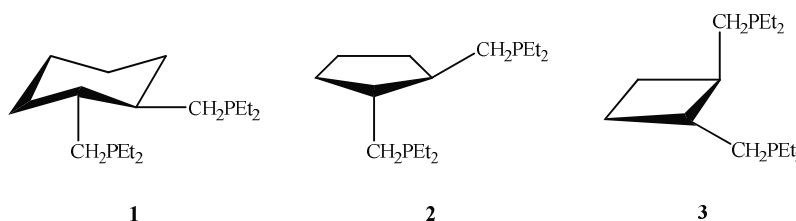


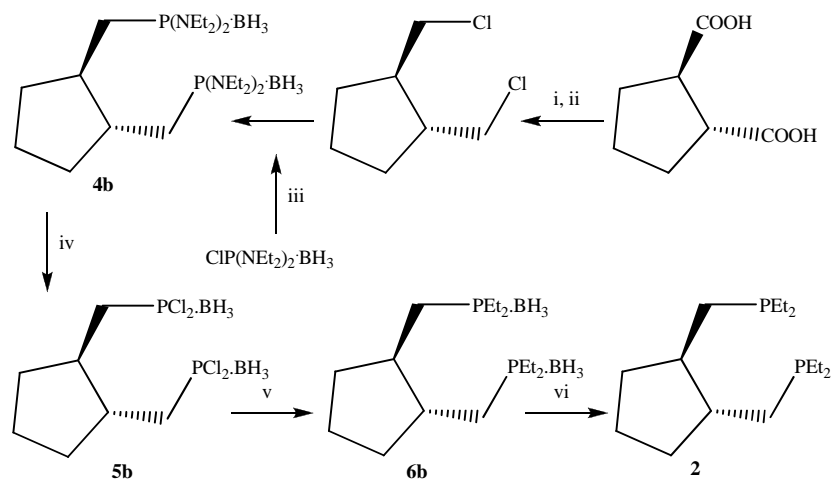
Figure 2. Chiral carbocyclic-based diphosphines **1-3**.

In this chapter we report the synthesis of **1-3**, which have a modular scaffold configuration but are essentially isoelectronic (Figure 2). The considerations were initially examined by molecular modelling, and then confirmed by high pressure NMR spectroscopy of their chelated rhodium(I)

species. The application of these complexes in hydroxymethylation catalysis was investigated, and their recovery and recyclability is described. Mechanistic inferences are made on the basis of deuterium labelling studies.

2.2 Synthesis

All three ligands are synthesised by the same synthetic route (Scheme 1).



Scheme 1. Retrosynthesis of **2**:

- (i) LiAlH_4 , $-10^\circ\text{C} \rightarrow 80^\circ\text{C}$, thf, (ii) SOCl_2 , 90°C , neat, (iii) Li/naphthalene, $-75^\circ\text{C} \rightarrow \text{ambient T}$, thf, (iv) gaseous HCl, ambient T, Et_2O , (v) EtMgBr , $0^\circ\text{C} \rightarrow 70^\circ\text{C}$, (vi) $\text{HBF}_4 \cdot \text{O}(\text{CH}_3)_2$, ambient T, CH_2Cl_2 .

The reduction of commercially available *trans*-1, 2-cycloalkane dicarboxylic acid to *trans*-1, 2-cycloalkanedimethanol is achieved with 2.3 equivalents lithium aluminium hydride, and subsequent reaction with excess thionyl chloride gives the *trans*-1, 2-bis-(chloromethyl)cycloalkane in 74-82% yield after bulb-to-bulb distillation. Subsequent nucleophilic substitution of the dichloro-derivatives was found to proceed more cleanly than that of the difluoro and *bis*(toluenesulfonyl) analogues.

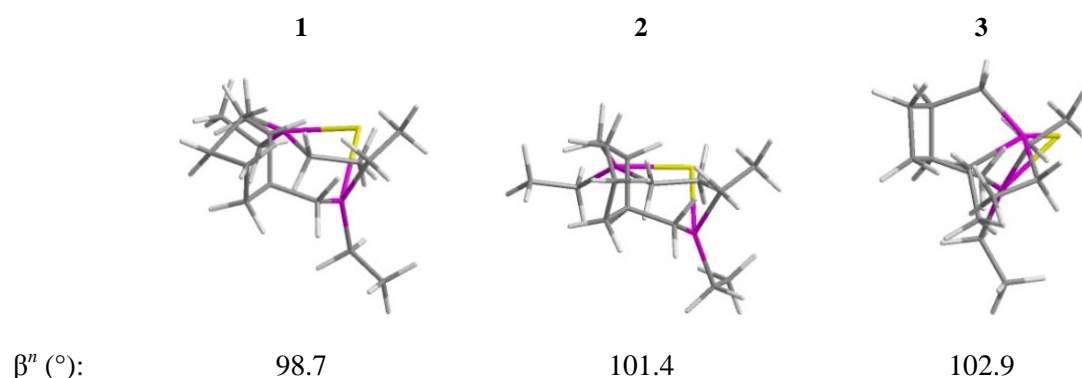
Treatment of *bis*-(diethylamino)chlorophosphine with 1.2 equivalents $\text{BH}_3 \cdot \text{thf}$ furnishes *bis*-(diethylamino)chlorophosphine borane as a viscous oil. Purification is effected by eluting through a short column of silica gel to give 84% yield, as all attempts at column chromatography were met with decomposition. Effective lithium/chloride exchange is accomplished by the addition of 2 equivalents lithium naphthalenide, generated from metallic lithium and a stoichiometric amount of naphthalene. The orange solution of lithiated *bis*-(diethylamino)phosphine borane is found to be ~ 96% pure by $^{31}\text{P}\{^1\text{H}\}$ NMR spectroscopy.¹¹

Lithiated *bis*-(diethylamino)phosphine borane is quenched with 0.5 equivalents *trans*- 1, 2-*bis*-(dichloromethyl) cycloalkane. Nucleophilic substitution with lithium *bis*-(diethylamino)phosphide led to intramolecular ring closure,^{12a} and the phosphonium chloride thus formed was found to be resistant to reduction by sodium acetate. Attempted ring opening by addition of excess lithiated phosphide furnished the heterocyclic ylid,^{12b} probably by proton abstraction from a bridging methylene. The C_2 -symmetrical *trans*-1, 2-*bis*-{(diethylamino)phosphinomethyl} cycloalkane borane complex (**4a-c**) is obtained as white crystals in 71-75% yield following column chromatography. Saturation of an ethereal solution with hydrochloric acid furnishes the *trans*- 1, 2-*bis*-(dichlorophosphinomethyl) cycloalkane borane (**5a-c**), characterised *in situ*, which is treated directly with 4 equivalents ethyl magnesium bromide to give the *trans*-1, 2-*bis*-(diethylphosphinomethyl) cycloalkane borane (**6a-c**). The residue is then purified by flash chromatography affording 57-69% of the compound as white solid.

Surprisingly, the adducts were found to be resistant to aminolysis by excess diethylamine, triethylamine, morpholine and 1, 4-diazabicyclo[2.2.2]octane.¹³ However, deprotection could be achieved by stirring with a 15-fold excess fluoroboric acid dimethyl ether complex. All attempts at traditional purification were unsuccessful. The oxide impurities were found to be insoluble in pentane and spectroscopically pure samples are obtained by washing the crude product with pentane, then decanting from the impurity sludge. **1-3** are thus recovered as viscous colourless oils in 44-51% yield.

2.3 Theoretical Considerations

In order to approximate the influence of carbocyclic ring structure on natural bite angle,¹⁴ Rh-**1**, Rh-**2** and Rh-**3** fragments were modelled. Initial conformations were calculated from the crystallographic structure of [Rh(acac)(DIOP)]¹⁵ using the PM3(tm) method as implemented in SPARTAN SGI,¹⁶ and geometry optimisations were finalised by eigenvector following as implemented in GAUSSIAN 98.¹⁷



The molecular model indicates that the natural bite angle is less than 103° in all cases, therefore a preference for *ea* chelation in trigonal bipyramidal geometry is expected. An *ea* rhodium-acyl-dicarbonyl complex endows the acyl moiety with the full σ -donor capacity of a *trans* phosphorus and should therefore promote its susceptibility to protonation by the solvent, effecting domino hydroxymethylation. In the *ee* geometry the *trans* site is occupied by a strong π -acceptor CO auxiliary and the electronic effect might be diluted.

2.4 Rhodium(I) Chemistry Under Syngas

The influence of carbocyclic ring structure on the formation of rhodium(I) complexes was investigated by high pressure NMR spectroscopy, using triethylphosphine as a non-chelating reference (Table 2). The species were generated *in situ* from $[\text{Rh}(\text{acac})(\text{CO})_2]$.

Table 2: HP-NMR data for the rhodium(I) complexes of **1**, **3** and PEt_3 under syngas in d_8 -toluene.^a

complex	<i>L-L</i>	³¹ P{ ¹ H}		¹ H (hydride region)			
		δ (ppm)	¹ J _{Rh-P} (Hz)	δ (ppm)	¹ J _{Rh-H} (Hz)	² J _{P-H} (Hz)	² J _{P-H} (Hz)
$[\text{RhH}(\text{CO})_2(\text{L-L})]$	1	d. 22.7	114	dt. -9.2	11.8	52.6	2.1, 105.2
	3	d. 12.4	117	dt. -9.6	8.7	39.2	
	PEt_3	d. 22.1	122	td. -10.1	5.8	14.8	
$[\text{Rh}(\text{CO})_2(\text{L-L})]_2$	1	d. 7.3	157				
	3	d. -0.41	158				
$[\text{Rh}(\text{CO})(\text{L})_3]_2$	PEt_3	d. 18.2	95				

^aConditions: 1.5 mL d_8 -toluene, 12.9 mM [Rh], *L-L*/Rh = 2/1, 40°C, 40 bar CO/H₂ = 1/1.

1. The formation of $[\text{RhH}(\text{CO})_2(\mathbf{1})]$, a resting state under hydroformylation conditions, is confirmed after 15 minutes at 40°C. The hydride signal is observed as a doublet of triplets at $\delta_{\text{H}} = -9.4$ ppm in the ¹H NMR spectrum, with ¹J_{Rh-H} = 11.8 Hz and ²J_{P-H} = 52.6 Hz (Figure 3a). Small *cis* phosphorus-hydride couplings, usually in the range 1-16 Hz, are reported for rhodium-hydride-dicarbonyl complexes with *ee* geometry.^{11, 18} Species with an *ea* configuration display a large *trans* phosphorus-hydride coupling in the slow exchange limit, usually in the range 90-120 Hz.^{11, 19} The intermediate triplet coupling observed in the present case therefore suggests a time-averaged *cis/trans* relationship between the two phosphorus nuclei. De-resolution of the *cis* coupling at -40°C is manifested in the broadening of the central resonance. The slow exchange limit is reached at -80°C, with the discrete *trans* coupling resolved as ²J_{P-H} = 105.2 Hz and the discrete *cis* coupling is ²J_{P-H} = 2.1 Hz. The *ee/ea* equilibrium ratio is thus calculated to be 5/95 (Equation 1).²

$${}^2J_{P-H} = \chi_{ee}J_{ee} + \chi_{ea}J_{ea} = \chi_{ee}J_{ee} + (1 - \chi_{ee})J_{ea} \quad (\text{Equation 1})$$

The ${}^{31}\text{P}\{^1\text{H}\}$ NMR spectrum exhibits a characteristic doublet at $\delta_{\text{P}} = 22.7$ ppm, with ${}^1J_{\text{Rh-P}} = 114$ Hz (Figure 3b). Broadening of this signal is observed at -80°C and attributed to a time-averaged C_2 -symmetry of the chelate ring. This assignment is consistent with NMR analyses of similar compounds.²¹ The two equatorial CO auxiliaries give rise to a sharp singlet at $\delta_{\text{C}} = 190.9$ ppm in the ${}^{13}\text{C}\{^1\text{H}\}$ NMR spectrum (Figure 4).

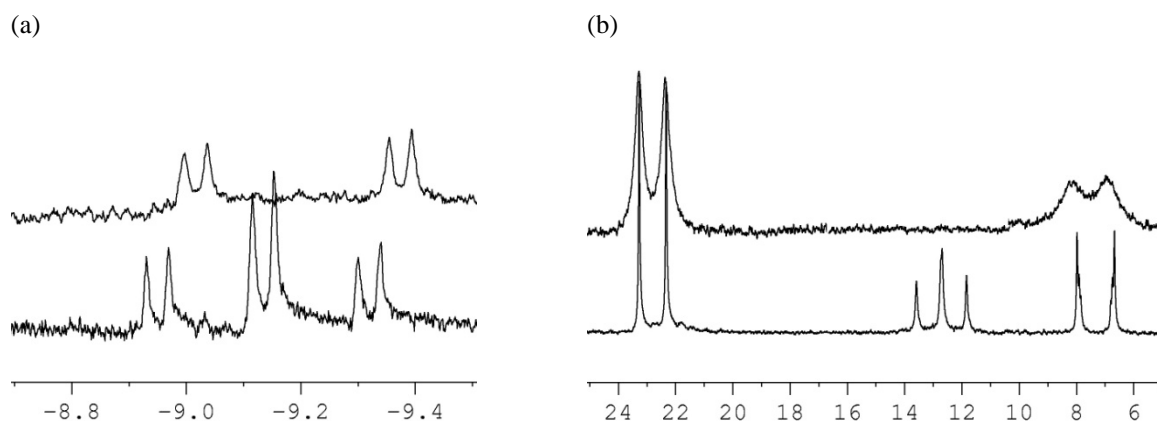


Figure 3. HP-NMR spectra of $[\text{RhH}(\text{CO})_2(\mathbf{1})]$:

- (a) ${}^1\text{H}$ NMR spectrum of hydride region at 40°C (lower), -60°C (centre) and -80°C (upper),
 (b) ${}^{31}\text{P}\{^1\text{H}\}$ NMR spectrum at 40°C (lower) and -80°C (upper).

The doublet resonating at $\delta_{\text{P}} = 7.3$ ppm in the ${}^{31}\text{P}\{^1\text{H}\}$ NMR spectrum displays a complex pattern consistent with an $\text{AA}'\text{A}''\text{A}'''\text{XX}'$ spin system, which is ascribed to the formation of the $[\text{Rh}(\text{CO})(\mathbf{1})(\mu\text{-CO})_2]$ dimer.²² Fast site exchange between the bridging and terminal carbonyls is manifested as a single broad resonance at $\delta_{\text{C}} = 225.7$ ppm in the ${}^{13}\text{C}\{^1\text{H}\}$ NMR spectrum, between the usual positions for a terminal CO (180-200 ppm) and a bridging CO (230-240 ppm) auxiliary. At temperatures below 25°C it is no longer possible to observe the fine structure.

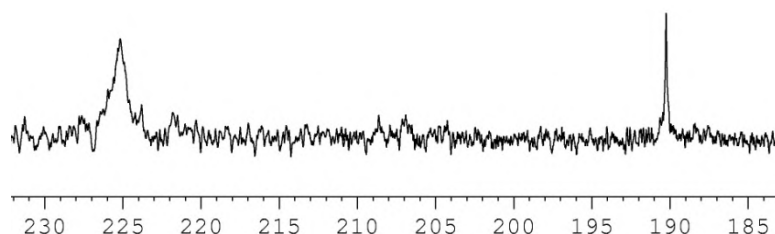


Figure 4. HP- ${}^{13}\text{C}\{^1\text{H}\}$ NMR spectrum of rhodium(I) complexes based on $\mathbf{1}$ at 40°C .

The formation of $[\text{RhH}(\text{CO})(\mathbf{1})(\eta\text{-}1)]$ is evidenced by a doublet of triplets at $\delta_{\text{P}} = 78.6$ ppm, with $^1J_{\text{Rh-P}} = 109$ Hz and $^2J_{\text{P-P}} = 67$ Hz, a doublet of doublets at $\delta_{\text{P}} = 12.7$ ppm, with $^1J_{\text{Rh-P}} = 103$ Hz and $^2J_{\text{P-P}} = 67$ Hz, and a singlet at $\delta_{\text{P}} = -23.4$ ppm in the $^{31}\text{P}\{^1\text{H}\}$ NMR spectrum. A $^1\text{H}/^{31}\text{P}$ -HMQC NMR sequence correlates these signals with the broad resonance at $\delta_{\text{H}} = -10.5$ ppm in ^1H NMR spectrum. Irreversible dissociation of this complex is noted below 8°C , which could be responsible for the observed colour change of the solution from orange to red on cooling. It is surprising that an AMTX spin system is observed, but the AB_2X spin system reported for analogous systems is not detected.²³

3. The $[\text{RhH}(\text{CO})_2(\mathbf{3})]$ complex is characterised by a doublet of triplets at $\delta_{\text{H}} = -9.7$ ppm in the ^1H NMR spectrum, with $^1J_{\text{Rh-H}} = 8.7$ Hz and $^2J_{\text{P-H}} = 39$ Hz, after 20 minutes at 40°C (Figure 5a). The dynamic equilibration between the *ee* and *ea* geometries could not be frozen at -60°C , which suggests that the energy difference between these isomers is as low as 8.38 kJ mol^{-1} .²⁰ The discrete phosphorus-hydride coupling constants cannot be determined, so it is most accurate to define a maximum and a minimum *ee/ea* equilibrium ratio at each temperature using -2 and $+2$ Hz as limits of the *cis* coupling and assuming *trans* $^2J_{\text{P-H}} = 105$ Hz: at -60°C $(ee/ea)_{\text{max}} = 78/22$ and $(ee/ea)_{\text{min}} = 76/24$, at 25°C $(ee/ea)_{\text{max}} = 77/23$ and $(ee/ea)_{\text{min}} = 75/25$ and at 80°C $(ee/ea)_{\text{max}} = 75/25$ and $(ee/ea)_{\text{min}} = 73/27$. The doublet at $\delta_{\text{P}} = 12.4$ ppm, with $^1J_{\text{Rh-P}} = 117$ Hz, is assigned as the corresponding signal in the $^{31}\text{P}\{^1\text{H}\}$ NMR spectrum (Figure 5b). Broadening of this signal is noted at -60°C .

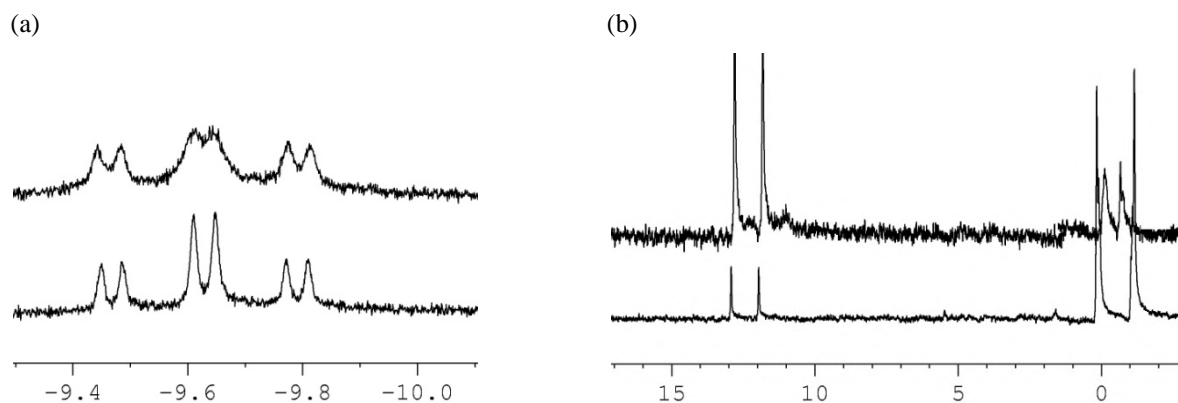


Figure 5. HP-NMR spectra of $[\text{RhH}(\text{CO})_2(\mathbf{3})]$:

(a) ^1H NMR spectrum of hydride region at 40°C (lower) and -60°C (upper),

(b) $^{31}\text{P}\{^1\text{H}\}$ NMR spectrum at 40°C (lower) and -60°C (upper).

Formation of the carbonyl-bridged rhodium dimer is confirmed by the apparent doublet at $\delta_{\text{P}} = -0.41$ ppm in the $^{31}\text{P}\{^1\text{H}\}$ NMR spectrum, with $^1J_{\text{R-P}} = 158$ Hz (Figure 6). The discrete coupling constants are obtained from the simulated NMR spectrum as $^1J_{\text{Rh-P}} = 157$ Hz, $^3J_{\text{Rh-P}} = 8$ Hz, $^2J_{\text{P-P}} = 46$

Hz, ${}^4J_{\text{P-P}} = 5$ Hz. It is demonstrated that higher temperatures promote formation of the mononuclear complex at the expense of $[\text{Rh}(\text{CO})(\mathbf{3})(\mu\text{-CO})]_2$. This corresponds with the reported formation of the dimer by exothermal loss of hydrogen.²⁴

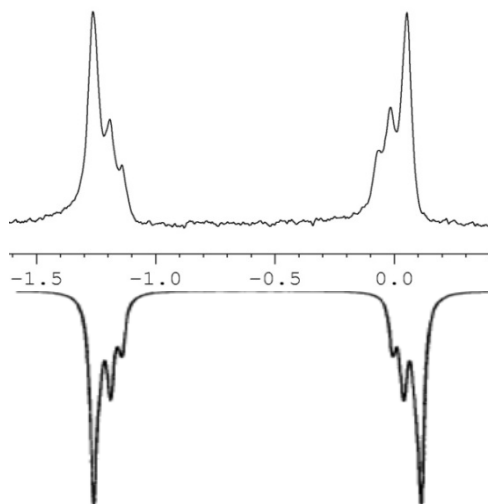


Figure 6. HP- ${}^{31}\text{P}\{^1\text{H}\}$ NMR spectrum of $[\text{Rh}(\text{CO})(\mathbf{3})(\mu\text{-CO})]_2$ at 40°C: observed, simulated (reverse).

Triethylphosphine. By reference to earlier reports,²⁵ the presence of $[\text{RhH}(\text{CO})_2(\text{PET}_3)_2]$ is confirmed by the triplet of doublets at $\delta_{\text{H}} = -10.1$ ppm in the ${}^1\text{H}$ NMR spectrum, with ${}^1J_{\text{Rh-H}} = 5.8$ Hz and ${}^2J_{\text{P-H}} = 15$ Hz, and the doublet at $\delta_{\text{P}} = 22.1$ ppm in the ${}^{31}\text{P}\{^1\text{H}\}$ NMR spectrum, with ${}^1J_{\text{Rh-P}} = 122$ Hz (Figure 7).

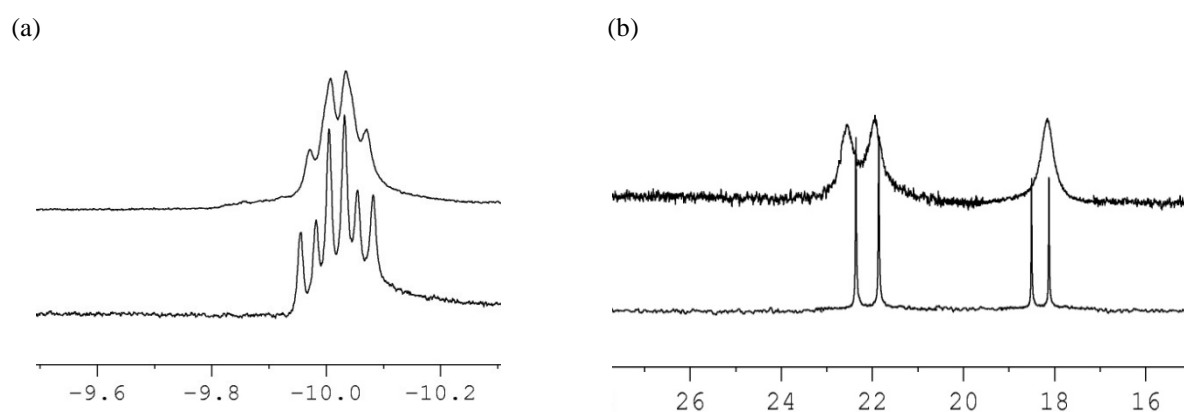


Figure 7. HP-NMR spectra of the rhodium(I) complexes based on triethylphosphine:

(a) ${}^1\text{H}$ NMR spectrum of hydride region at 40°C (lower) and 80°C (upper),

(b) ${}^{31}\text{P}\{^1\text{H}\}$ NMR spectrum at 40°C (lower) and 80°C (upper).

The ${}^{31}\text{P}\{^1\text{H}\}$ NMR spectrum establishes $[\text{Rh}(\text{CO})(\text{PET}_3)_3]_2$ as the main competing species from the strong doublet at $\delta_{\text{P}} = 18.2$ ppm, with ${}^1J_{\text{Rh-P}} = 95$ Hz.²⁵ The dimer is presumably formed by loss of

hydrogen from $[\text{RhH}(\text{CO})(\text{PEt}_3)_3]$. Extensive line broadening indicates exchange between $[\text{RhH}(\text{CO})_2(\text{PEt}_3)_2]$, $[\text{Rh}(\text{CO})(\text{PEt}_3)_3]$ and free triethylphosphine at higher temperatures.

Fluxional processes in $[\text{RhH}(\text{CO})_2(\mathbf{1})]$. A simultaneous bending motion of the hydride and CO auxiliaries in $[\text{RhH}(\text{CO})_2(\mathbf{1})]$ can effectively interconvert the equatorial and axial phosphorus nuclei without need for the two successive interconversions *via* the high-energy intermediate prescribed by Berry-type rotation (Figure 8).²⁶ This rearrangement is also more credible in consideration of the favoured *ea* chelation and inflexible nature of $\mathbf{1}$.²⁷

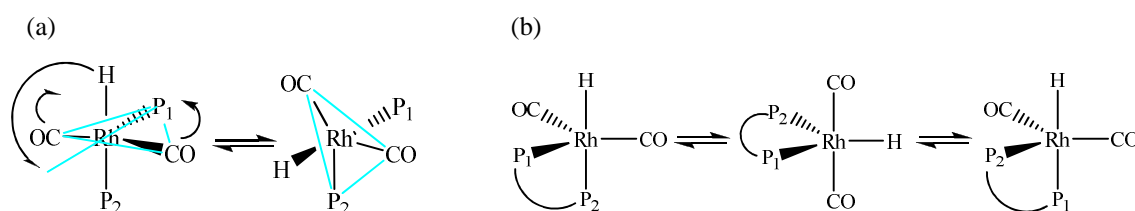


Figure 8. Phosphorus exchange processes in an *ea* geometry: (a) *e-a* phosphorus exchange, (b) Berry rotation.

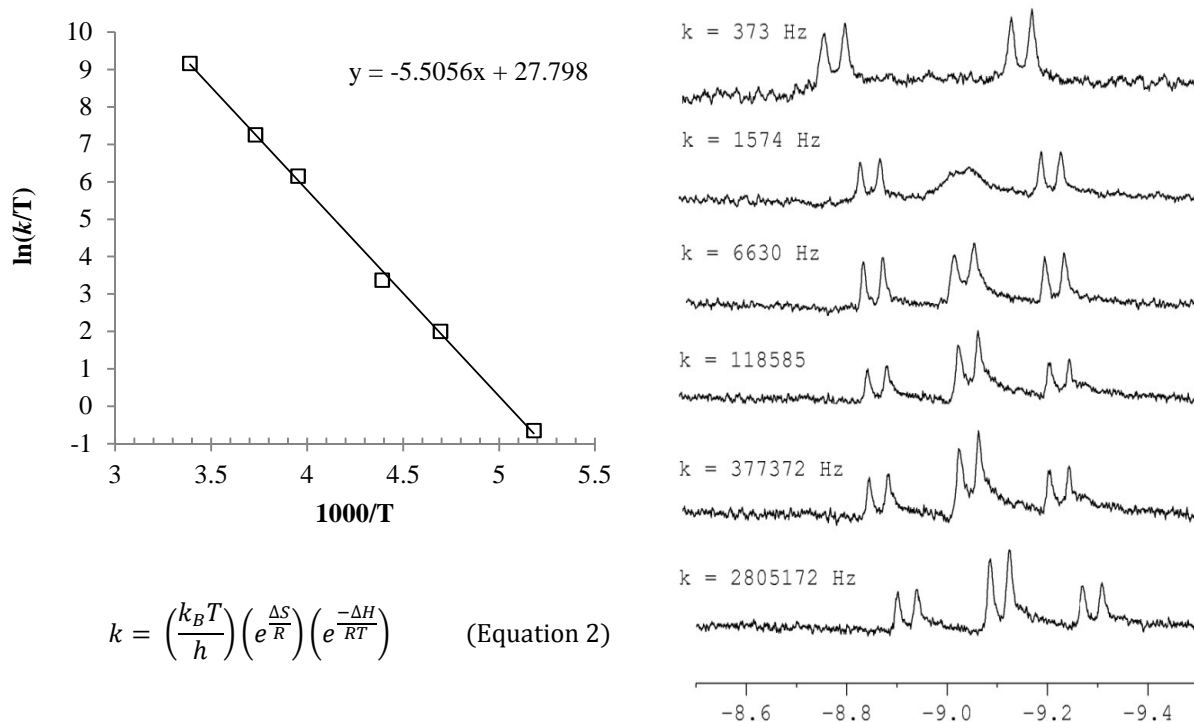


Figure 9. Intramolecular phosphorus exchange in $[\text{RhH}(\text{CO})_2(\mathbf{1})]$

(a) Eyring plot, (b) ^1H NMR spectra (-80 to 22°C) and calculated exchange rates.

Rate constants for the exchange process were determined by dynamic line-shape analyses of the ^1H NMR and simulated ^1H NMR spectra over the temperature range -80 to 22°C,²⁸ and are

constructed as an Eyring plot (Figure 9). The enthalpy of activation and entropy of activation are thus calculated to be $\Delta H^\ddagger = 45.78 \text{ kJ mol}^{-1}$ and $\Delta S^\ddagger = 0.45 \text{ J K}^{-1} \text{ mol}^{-1}$ (Equation 2). The small entropy of activation is characteristic of an intramolecular rearrangement.^{27, 29} This renders the activation barrier relatively insensitive to the temperature condition, for example $\Delta G_{293\text{K}}^\ddagger = 45.65 \text{ kJ mol}^{-1}$ and $\Delta G_{333\text{K}}^\ddagger = 45.63 \text{ kJ mol}^{-1}$.

The exchange process in $[\text{RhH}(\text{CO})_2(\mathbf{3})]$ cannot be analysed in such detail because the extensive line-broadening at lower temperatures, 11.6 Hz relative to 2 Hz, introduces a significant error into rate constant determination.

The complex $[\text{RhH}(\text{CO})_2(\mathbf{1})]$ provides an example of the *trans* fusion of cyclohexane to cycloheptane. The symmetrical doublet at $\delta_{\text{P}} = 22.7 \text{ ppm}$ in the $^{31}\text{P}\{^1\text{H}\}$ NMR spectra corresponds to a dynamic equilibrium between different conformers of the seven-membered chelate ring, a phenomenon first highlighted in research by Brown and Chaloner.³⁰ One of the ring conformations can be described as a C_4 -chair and the other as a distorted B_5 -boat (Figure 10).³¹ Coalescence of the signal is noted in the range -20 to -80°C , indicating that the barrier to chair \leftrightarrow boat interconversion is approached in this temperature range. The inversion barrier in cycloheptane is $\Delta G_{184\text{K}}^\ddagger = 8.5 \text{ kJ mol}^{-1}$,³¹ but cyclic fusion creates strain energy in the ground state so a lower activation barrier is expected for $[\text{RhH}(\text{CO})_2(\mathbf{1})]$.³³

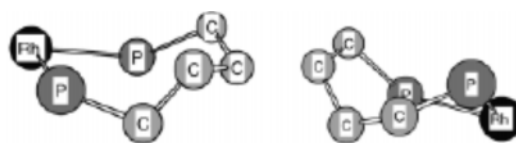


Figure 10. View of the C_4 (left) and distorted B_5 (right) chelate ring conformations in $[\text{RhH}(\text{CO})_2(\mathbf{1})]$.^{21b}

2.5 Catalysis

In order to investigate the extended influence of carbocyclic ring structure, the complexes $[\text{RhH}(\text{CO})_2(L-L)]$ ($L-L = \textit{trans}$ -1, 2-*bis*-(diethylphosphinomethyl) cyclohexane (**7a**), *trans*-1, 2-*bis*-(diethylphosphinomethyl) cyclopentane (**7b**) and *trans*-1, 2-*bis*-(diethylphosphinomethyl) cyclobutane (**7c**)) were applied for the hydroxymethylation of allyl alcohol (Table 3). These were prepared *in situ* from $[\text{Rh}(\text{acac})(\text{CO})_2]$, and the solutions were incubated at the requisite temperature and 30 bar $\text{CO}/\text{H}_2 = 1$ for 40 minutes in order to maximise the rhodium-hydride-dicarbonyl/carbonyl-bridged rhodium dimer ratio.

A product mixture of linear aldehyde, branched aldehyde, linear alcohol (1, 4-butanediol) and branched alcohol (2-methylpropanol) is recovered. The linear aldehyde and branched aldehyde are obtained as statistical mixtures of crotonaldehyde and 2-ethoxyfuran and methacrolein, 2-methylpropanal and 1, 1-diethoxy-2-methylpropane respectively. Substrate isomerisation leads to the

formation of 1-propanal and 2-methylpentanal, and 1-propanol is recovered as the substrate hydrogenation product.³⁴

Table 3: Hydroxymethylation of allyl alcohol with **7a-7c** in ethanol.^a

catalyst	<i>L-L</i> /Rh	T (°C)	allyl alcohol-based selectivity (mol%)				k^d	TOF ^e (h ⁻¹)
			C=O ^b (<i>l/b</i>)	-OH ^c (<i>l/b</i>)	iso.	hyd.		
7a	1	120	19 (3.1)	47 (3.3)	30	4	10.31	126.4
7a	2	60	36 (2.7)	52 (2.8)	6	6	10.59	130.2
7a	2	120	25 (2.5)	60 (2.5)	10	5	11.07	135.6
7a	5	60	26 (2.6)	68 (2.7)	2	4	11.34	137.8
7a	5	90	20 (2.5)	73 (2.6)	2	5	11.38	140.3
7a	5	120	22 (2.3)	66 (2.3)	5	6	11.61	141.9
7a	10	90	25 (2.4)	70 (2.5)	1	4	9.82	120.2
7a	10	120	25 (2.3)	66 (2.3)	3	6	10.09	124.5
7b	1	120	35 (3.2)	37 (3.4)	24	4	3.49	43.7
7b	2	90	42 (3.6)	45 (3.7)	8	5	3.72	45.6
7b	2	120	39 (3.4)	49 (3.4)	9	3	4.03	49.3
7b	5	60	40 (3.8)	51 (3.9)	4	5	4.17	51.1
7b	5	90	37 (3.7)	56 (3.8)	1	6	4.51	55.2
7b	10	90	42 (3.7)	52 (3.6)	1	5	2.98	36.5
7b	10	140	35 (3.2)	47 (3.4)	1	17	2.74	33.6
7c	1	120	37 (5.0)	38 (5.2)	21	4	3.26	39.9
7c	2	120	43 (5.6)	47 (5.6)	6	4	3.70	45.3
7c	2	140	35 (5.3)	45 (5.3)	1	19	2.47	30.2
7c	5	90	41 (6.4)	54 (6.6)	1	4	4.22	51.7
7c	5	120	44 (6.2)	51 (6.3)	1	4	4.48	54.9
7c	10	90	46 (6.4)	50 (6.7)	0	4	3.44	42.1
-	-	120	82 (0.8)	1 (1.1)	15	2	4.75	58.2

^aConditions: 4 mL ethanol, 8 mM [Rh], Rh/allyl alcohol = 1/370, 40 bar CO/H₂ = 1. ^bHydroxyaldehyde derivatives. ^cDiol derivatives. ^dFirst order rate constant ($\times 10^{-5} \text{ s}^{-1}$) calculated as the gradient of a plot of $\ln(P_t/P_{t=0})$ in time. ^eTurnover frequency at 1 mol L⁻¹ allyl alcohol.

Activity. Initial reaction rates were determined from reaction profile plots of $\ln(P_t/P_{t=0})$ in time. Previously it was shown that catalyst modification with DMPE inhibits the reaction markedly,^{25a} but this does not appear to be a general trend for *cis*-chelating diphosphines. Activity of the complexes **7a-7c** varies non-linearly as a function of the *L-L*/Rh molar ratio. Type I kinetics (Equation 3) is assumed from the observed first order dependence on allyl alcohol concentration,³⁵ so the inverse

dependency beyond $L-L/Rh = 5$ is most probably due to competition between the diphosphine and allyl alcohol for coordination sites on the rhodium.

$$\text{Rate (type I)} = \frac{C[\text{allyl alcohol}][Rh]}{D + [L]} \quad (\text{Equation 3})$$

The catalysts are shown to be active in the temperature range 60 to 120°C. The enhancement at elevated temperatures is typical Arrhenius behaviour, but some contribution from thermodynamic instability of the dimeric resting state at higher temperature cannot be not precluded.

Complexes **7b** and **7c** display comparable activity, which suggests that diphosphines based on smaller carbocyclic scaffolds impart comparable stability upon chelation. Interestingly, complex **7a** is found to be more than twice as active. This difference can be correlated with the relative position of the monomer↔dimer equilibrium, as the latter is known to be inactive for hydroformylation.^{19,36} At a given temperature, the concentration of each rhodium can be determined from the high pressure ³¹P{¹H} NMR spectrum and the Henry coefficient can be used to determine the concentration of hydrogen in solution (Table 4).³⁷

Table 4: Thermodynamic data for $H_2 + [Rh(CO)(L-L)(\mu-CO)]_2 \leftrightarrow 2 [RhH(CO)_2(L-L)]$ equilibria of **7a** and **7c** in d_8 -toluene.^a

	7a	7c	BDPP ^b
$[H_2] = \sqrt{(p/K_H)} \text{ (M)}$	0.021	0.021	0.014-0.033
$[RhH(CO)_2(L-L)] \text{ (mM)}$	10.56	2.74	
$[Rh(CO)(L-L)(\mu-CO)]_2 \text{ (mM)}$	2.74	3.42	
$K = \frac{[RhH(CO)_2(L-L)]^2}{[Rh(CO)(L-L)(\mu-CO)]_2[H_2]}$	1.93	1.36	1.82

^aConditions: 1.5 mL d_8 -toluene, 12.9 mM [Rh], 70°C, 40 bar $CO/H_2 = 1$.^b19 in References and Notes.

Of course, higher flexibility of the chelate ring in **1** is also a consideration because this should lower the relevant transition state energies during catalysis.

Regioselectivity. It is demonstrated for **7a** that increasing the $L-L/Rh$ molar ratio from 2 to 5 suppresses allyl alcohol isomerisation by 4.8 mol%, with a corresponding improvement in selectivity to branched products. Under analogous conditions with **7b** and **7c** isomerisation is almost eliminated as the $L-L/Rh$ molar ratio approaches 5, but in these cases enhanced selectivity to linear products is observed. Regioselectivity is not sensitive to higher $L-L/Rh$ molar ratios presumably due to a saturation effect. Upon increasing temperature, selectivity to linear products drops as the activation energy difference between rhodium-hydroxypropyl-carbonyl and rhodium-methylhydroxyethyl-

carbonyl formation is reduced. Furthermore, allyl alcohol isomerisation becomes progressively competitive.

Regioselectivity is found to correlate with the torsional angle $\text{PCH}_2\text{-}\angle\text{-CH}_2\text{P}$ of the *trans*-fused carbocyclic scaffold, $r^2 = 0.98$, which is affiliated with the configurational rigidity of the cycloheptane ring formed upon chelation (Figure 11).³⁸ The $\text{O}=\text{CC}\text{-}\angle\text{-CC}=\text{O}$ torsional angles of the corresponding dicarboxylic acids have been used here as a first approximation.³⁹ Upon coordination of allyl alcohol to the square-planar rhodium-hydride-carbonyl species the other auxiliaries bend away in response to electronic orbital rehybridisation on the rhodium, approaching a less congested trigonal bipyramidal geometry. The observations suggest that attainment of a rigid chiral chelate ring configuration arranges the geometrical orientation of the ethyl chains on the phosphorus nuclei for *anti*-Markovnikoff hydride migration.

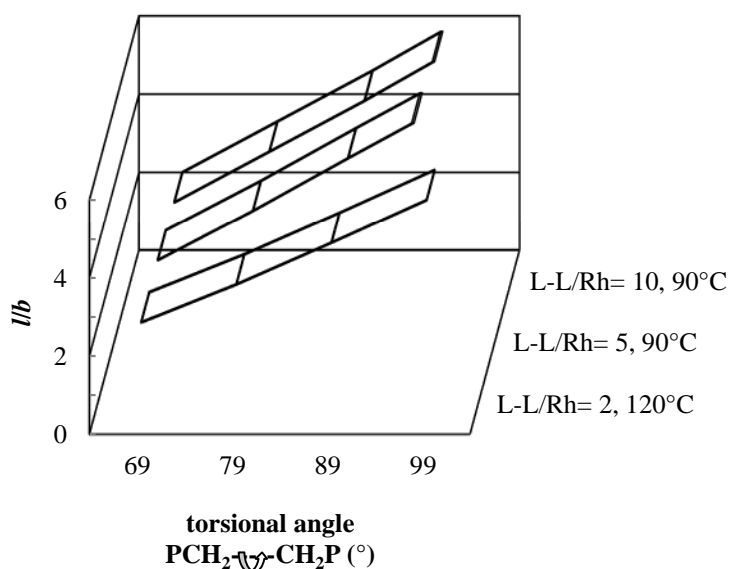


Figure 11. Regioselectivity of **7a-7c** in hydroxymethylation of allyl alcohol as a function of the carbocyclic scaffold torsional angle $\text{PCH}_2\text{-}\angle\text{-CH}_2\text{P}$.

Chemoselectivity. In all cases using $L\text{-}L/\text{Rh} = 1$ gives excessive activity for the isomerisation of allyl alcohol because coordinatively unsaturated rhodium species are available to accommodate the intermediate hydrido η^3 -allyl configuration, although surprisingly this transformation is not catalysed by the unmodified rhodium precursor. It is presumed the isomerisation catalysts are deactivated by the incorporation of their rhodium into *bis*-phosphine or *tris*-carbonyl complexes.

Complexes **7a-7c** are found to be moderately active for the hydrogenation of allyl alcohol. The strong σ -donor character of the diphosphines concurrently promotes oxidative addition of hydrogen to the rhodium-alkyl-dicarbonyl complex and impedes CO insertion into the rhodium-alkyl bond. Blackening of the autoclave is observed at 140°C and taken as evidence for catalyst

decomposition. High selectivity to hydrogenation product at this temperature is therefore tentatively ascribed to heterogeneous hydrogenation by metallic rhodium.

A mixture of diols and hydroxyaldehydes is recovered from catalysis with **7a-7c**, despite favourable *ea* geometry relative to triethylphosphine. Since a domino hydroxymethylation scheme is implicated, it is suggested that enforced *ea* geometry in the rhodium-butyldiol-hydride-carbonyl cation can induce adverse chemoselectivity (Figure 12). The placement of a strong σ -donor phosphine *trans* to the functionalised moiety enhances negative fractional charge on its coordinated carbon, impeding nucleophilic interaction with the hydride and making β -hydride abstraction by rhodium or the ethoxide anion more favourable. Consequently reductive elimination of the hydroxyaldehyde is observed. For complexes **7b** and **7c**, which exist in a higher *ee/ea* equilibrium ratio, aldehyde products can also be formed *via* the conventional hydroformylation pathway.

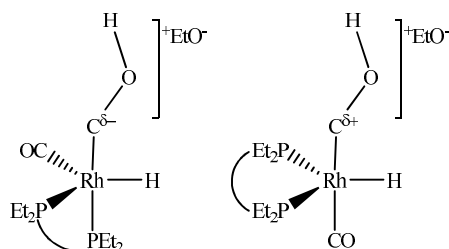


Figure 12. The *ea* and *ee* geometry of the rhodium-hydroxypropanol-hydride-carbonyl cation.

Relatively harsh temperature conditions are required to attain moderate chemoselectivity at low *L-L/Rh* molar ratios. The highest selectivity to diols is consistently obtained at *L-L/Rh* = 5 and 90°C. When the molar ratio exceeds this limit, temperature ceases to be an important parameter. Heterogeneous hydrogenation can account for the relatively high percentage of diol derivatives recovered when catalysis is performed at 140°C.

Recycling. Complexes **7a** and **7c** are expected to be resilient to the rhodium-induced fragmentation suffered by the diphenylphosphine-substituted analogues,⁴⁰ so their potential recyclability was studied under reaction conditions approximating the process parameters used by Lyondell-Basell (Table 5).⁴¹ After each cycle the reaction mixture was carefully transferred from the autoclave with a small overpressure. The catalyst was recycled efficiently following aqueous extraction of the products (Figure 13).

The conversion is slightly reduced upon catalyst recycling. In order to gain insight into the origin of this, the consumption of CO/H₂ = 1 in time was monitored for two consecutive cycles using **12a** (Figure 14). The protracted initial rate observed for the second cycle is associated with lower overall conversion. Analysis of the aqueous phase after the first cycle by ICP-MS establishes that this

is not due to rhodium leaching. Furthermore, second cycle aqueous extracts are found to be catalytically inactive.

Table 5: Recyclability of **7a** and **7c** in the hydroformylation of allyl alcohol by toluene/water extraction.^a

catalyst	cycle	conversion ^b (mol%)		
		toluene	H ₂ O	<i>l/b</i>
7a	1	89.2		3.2
		[Rh] _{aq} = 3.1 ppm (0.4% leaching)		
	2	86.8	0.0	3.3
	3	83.5	3.42	3.1
7c	1	81.3		5.9
		[Rh] _{aq} = 2.7 ppm (0.3% leaching)		
	2	80.4	0.0	5.7
	3	79.7		5.7

^aConditions: 4 mL toluene, 8 mM [Rh], *L-L*/Rh = 5, Rh/allyl alcohol = 1/250, 60°C, 10 bar CO/H₂=1. ^bTotal conversion of allyl alcohol after 1 hour.

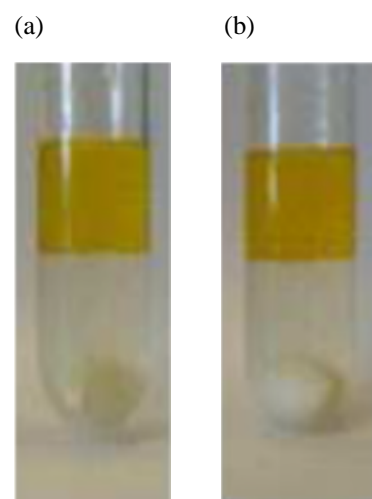


Figure 13. Phase separation: (a) cycle 1, (b) cycle 3.

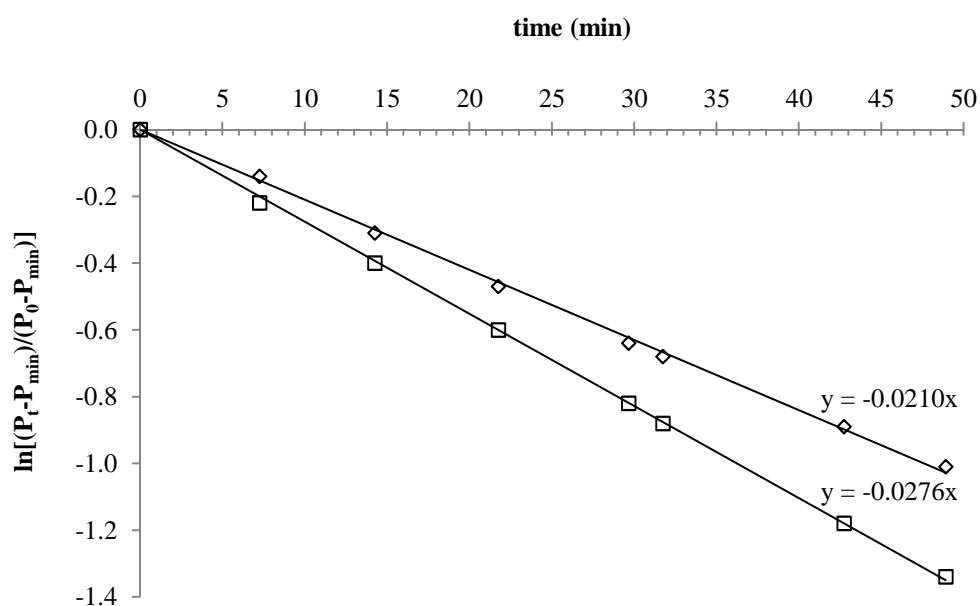


Figure 14. Plot of $\ln[(P_t - P_{\min})/(P_0 - P_{\min})]$ in time for allyl alcohol hydroformylation with **7a** over two consecutive cycles: (□) cycle 1, (◇) cycle 2.

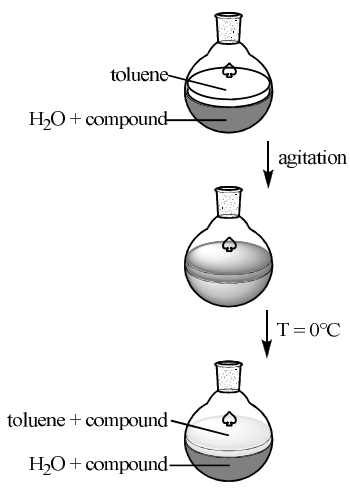
The partitioning of crotonaldehyde, 2-ethoxyfuran, γ -butyrolactone, methacrolein, 2-methylpropanal, 1, 1-diethoxy-2-methylpropane, 1-propanal, 2-methylpentanal and 1-propanol in the biphasic toluene/water system was examined (Table 6). A majority of these reaction products exhibit

substantial affinity for the aqueous phase. The moderate partitioning of 2-methylpentanal and 1, 1-diethoxy-2-methylpropane can be explained by their relatively developed aliphatic character. Surprisingly, methacrolein has an approximately equal distribution over the two phases. Significantly reduced conversion is observed upon enriching a first cycle solution of **12a** with methacrolein, implicating a role as catalyst poison.⁴²

³¹P{¹H} NMR spectroscopy of the organic extracts of **12c** shows that only 3% of the phosphorus donor sites are lost through oxidation per cycle, despite the oxygen-sensitive nature of these diphosphines. Observed retention of linear selectivity upon catalyst recycling corroborates this. However, the oxidised species do not display sufficient affinity for the aqueous phase on extraction to eliminate them as another source of catalyst deactivation.

Table 6: Partitioning of allyl alcohol hydroformylation products in H₂O/toluene

compound	<i>P</i> ^a H ₂ O/toluene
crotonaldehyde	62
2-ethoxyfuran	64
γ-butyrolactone	58
methacrolein	0.8
2-methylpropanal	59
1, 1-diethoxy-2-methylpropane	9.3
1-propanal	65
2-methylpentanal	17
1-propanol	66



^aPartition coefficients in a 1:1 (v/v) mixture of H₂O and toluene at 0°C determined by gravimetric methods ($P = c_{\text{aqueous}}/c_{\text{organic}}$). The average measurement is given with estimated error ± 1 in the last digit.

2.6 Deuterium Labelling Studies

Deuterium isotope effects in ¹³C{¹H} NMR spectroscopy. ¹³C{¹H} NMR spectroscopy has been widely used to monitor the position of deuterium labels in organic compounds.⁴³ A deuterium nucleus has spin $I = 1$ giving rise to distinctive splitting patterns depending on the extent of incorporation (Figure 15). Splitting by a directly bound deuterium nucleus is approximately one-sixth that of the corresponding proton-carbon coupling, due to the smaller gyromagnetic ratio of deuterium. Deuterium incorporation also induces carbon isotope shifts upfield. Measurable effects are principally observed on carbon resonances from directly bonded deuterium atoms (α) and deuterium on vicinal carbons (β). The α -shift is of the order of 0.4 ppm per deuterium, while β -shifts are ~ 0.05 -0.12 ppm per deuterium depending on the environment of the carbon nucleus. It is generally accepted

that these arise from slight changes of averaged molecular geometry caused by rovibrational perturbations on isotopic substitution.

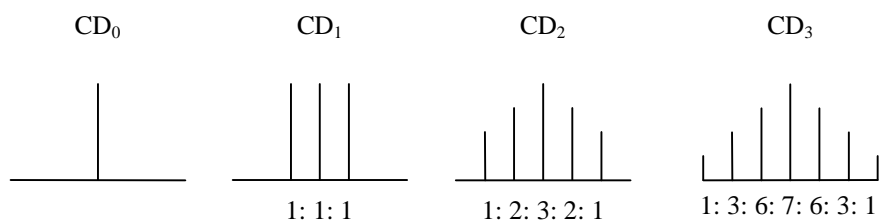


Figure 15. ^{13}C nucleus splitting for noted deuterium incorporation.

Quantitative measurement of deuterium enrichment is complicated by the slow relaxation of carbon nuclei when bound to deuterium relative to hydrogen. Therefore the NOE on signals due to CH_2 , CHD and CD_2 is different, preventing direct comparison. This problem is typically overcome by using different pulse sequences or relaxation agents, but a simpler approach is to use the β -shifted resonance as reporter. The nuclear Overhauser effect of carbon nuclei β to hydrogen or deuterium are similar since deuterium coupling over two bonds is negligible (< 1 Hz). The level of enrichment at any position can therefore be reliably determined from the relative intensity of these shifted signals.

Mechanism of 1-hexene deuteriohydroxymethylation. Trialkylphosphine-modified rhodium catalysts can encourage the selective formation of alcohols from terminal alkenes *via* the auto-tandem hydroxymethylation mechanism.^{44a} In the case of 1-hexene, 1-heptanal and 2-methylhexanal are reductively eliminated from the hydroformylation cycle and undergo a sequential hydrogenation. Thus, the deuterium labelling pattern in the C_1 -position of 1-heptanol should approximate the deuterium labelling pattern in the C_1 -position of the deuteration product of 1-heptanal. Domino hydroxymethylation allows formation of the alcohols as primary reaction products,^{44b} and in this case the deuterium labelling pattern in 1-heptanol is expected to deviate from the deuterium labelling pattern in the deuteration product of 1-heptanal.

In order to distinguish between these mechanisms, **7a**-deuteride was concurrently applied for the deuteriohydroxymethylation of 1-hexene and for the deuteration of 1-heptanal. This catalyst was selected for these labelling reactions because **7a**-hydride exists almost exclusively in *ea* geometry (*vide supra*), and it was felt that a dynamic equilibrium of the geometric isomers might lead to a more complex interplay of catalytic pathways. The C_7 -aldehyde and C_7 -alcohol product fractions were isolated by fractional distillation of the product solution and examined by $^{13}\text{C}\{^1\text{H}\}$ NMR spectroscopy (Table 7).

Table 7a: Deuteriohydroxymethylation of 1-hexene with **12a**-deuteride in ethanol^a – ¹³C{¹H} NMR C₇-OH product analysis.^a

	1/ppm	2/ppm	3/ppm	4/ppm	5/ppm	6/ppm	7/ppm				
heptanol - calculated	62.80	32.20	25.60	29.30	31.80	22.70	14.10				
heptanol - sample	62.72	32.80	25.92	29.32	31.84	22.61	14.08				
heptanol/OD - D ₂ O exchange	62.45	32.83	25.98	29.31	31.83	22.61	14.07				
2-methylhexanol - calculated	69.90	35.62	17.00	34.30	29.30	23.00	14.10				
2-methylhexanol - sample	68.16	35.85	16.73	34.24	29.12	21.97	13.07				

	1/ppm	J _{C-D} /Hz	2/ppm	I	3/ppm	J _{C-D} /Hz	4/ppm	5/ppm	6/ppm	7/ppm
1-hexene +CO/D ₂										
H/DO-CD ₂ -CH ₂ -CHD-C ₄ H ₉	61.84	m. 21.4	32.52	79	25.51	t. 19.3	29.24	32.01	22.77	14.13
H/DO-CD ₂ -CH(CH ₂ D)-C ₄ H ₉	67.25	m. 20.9	35.57	21	16.38	t. 19.3	33.05	29.41	23.15	14.13
1-heptanal +CO/D ₂										
H/DO-CH ₂ -CH ₂ -CH ₂ -C ₄ H ₉	62.39		32.82	62	25.91		29.40	31.99	22.86	14.12
H/DO-CHD-CH ₂ -CH ₂ -C ₄ H ₉	62.02	t. 21.1	32.73	38	25.91		29.40	31.99	22.86	14.12

^aConditions: 4 mL ethanol, 8 mM [Rh], **1**/Rh = 2, Rh/1-hexene = 1/200, 120°C, 40 bar CO/(D₂ or H₂) = 1, 3 hours.

Table 7b: Deuteriohydroxymethylation of 1-hexene with **12a**-deuteride in ethanol^a – ¹³C{¹H} NMR C₇-C=O product analysis.^a

	1/ppm	2/ppm	3/ppm	4/ppm	5/ppm	6/ppm	7/ppm				
heptanal - calculated	202.20	43.50	28.20	28.80	31.50	22.70	14.10				
heptanal- sample	202.73	43.97	28.53	28.94	31.64	22.14	14.03				
2-methylhexanal - calculated	204.10	46.40	14.00	29.60	28.80	22.70	14.10				
	1/ppm	J _{C-D} /Hz	2/ppm	3/ppm	J _{C-D} /Hz	4/ppm	I	5/ppm	6/ppm	7/ppm	
1-hexene +CO/H ₂											
O=CH-CH ₂ -CH ₂ -C ₄ H ₉	203.27		44.04	22.25		29.10		31.80	22.68	14.07	
O=CH-CH(CH ₃)-C ₄ H ₉	205.66		46.47	13.42		30.44		29.37	22.82	13.98	
1-hexene +CO/D ₂											
O=CD-CH ₂ -CHD-C ₄ H ₉	202.85	t. 25.9	43.83	21.90	t. 19.6	29.01	68	31.81	22.71	14.06	
O=CD-CH ₂ -CH ₂ -C ₄ H ₉	202.85	t. 25.9	43.97	22.26		29.09	10	31.81	22.71	14.06	
O=CD-CH(CH ₂ D)-C ₄ H ₉	205.21	t. 25.3	46.28	13.09	t. 19.6	30.45	22	29.39	22.94	13.97	

^aConditions: 4 mL ethanol, 8 mM [Rh], 1/Rh = 2, Rh/1-hexene = 1/200, 120°C, 40 bar CO/(D₂ or H₂) = 1, 3 hours.

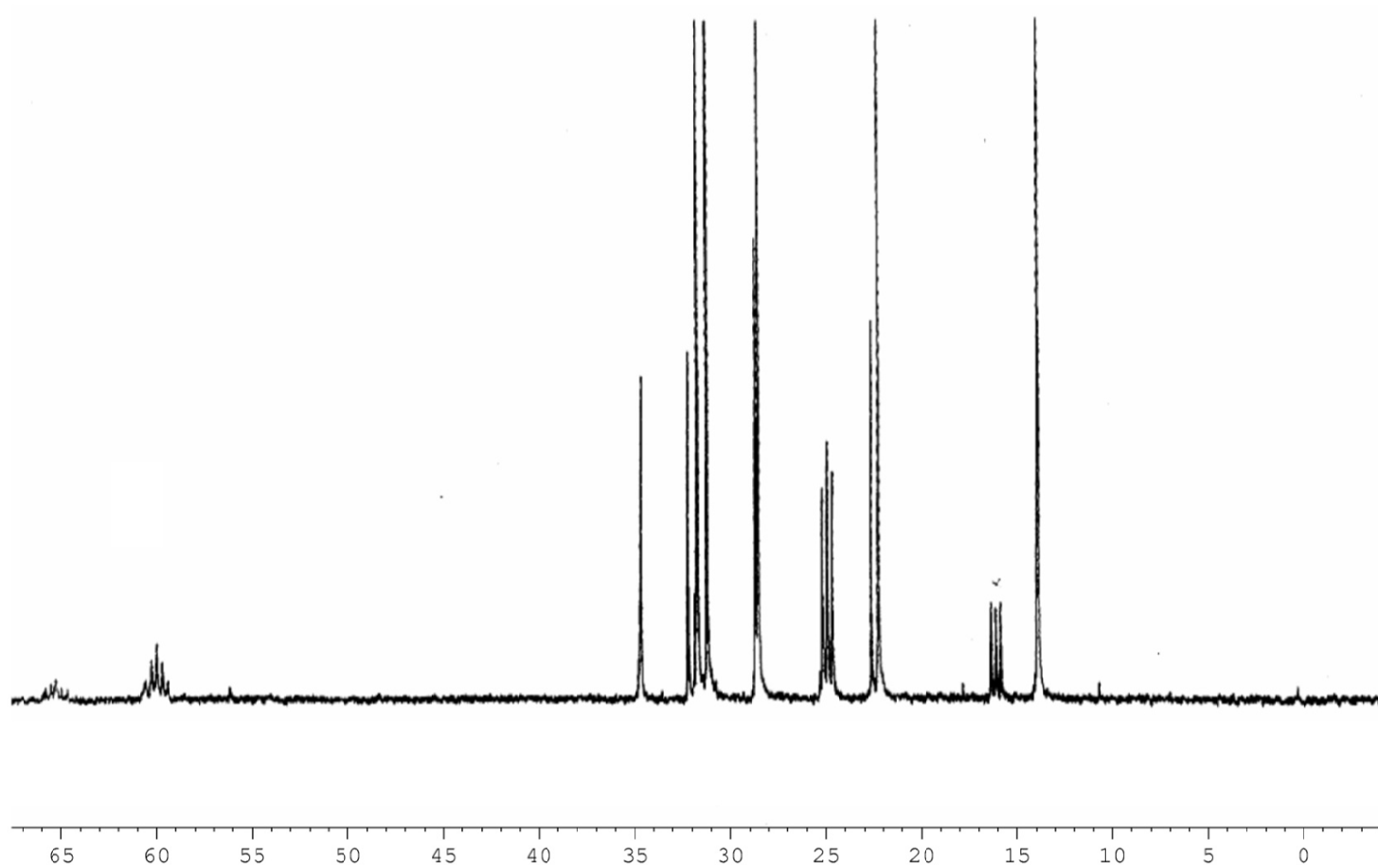


Figure 16. Deuteriohydroxylation of 1-hexene in ethanol- $^{13}\text{C}\{^1\text{H}\}$ NMR spectrum of $-\text{OH}$ product fraction.

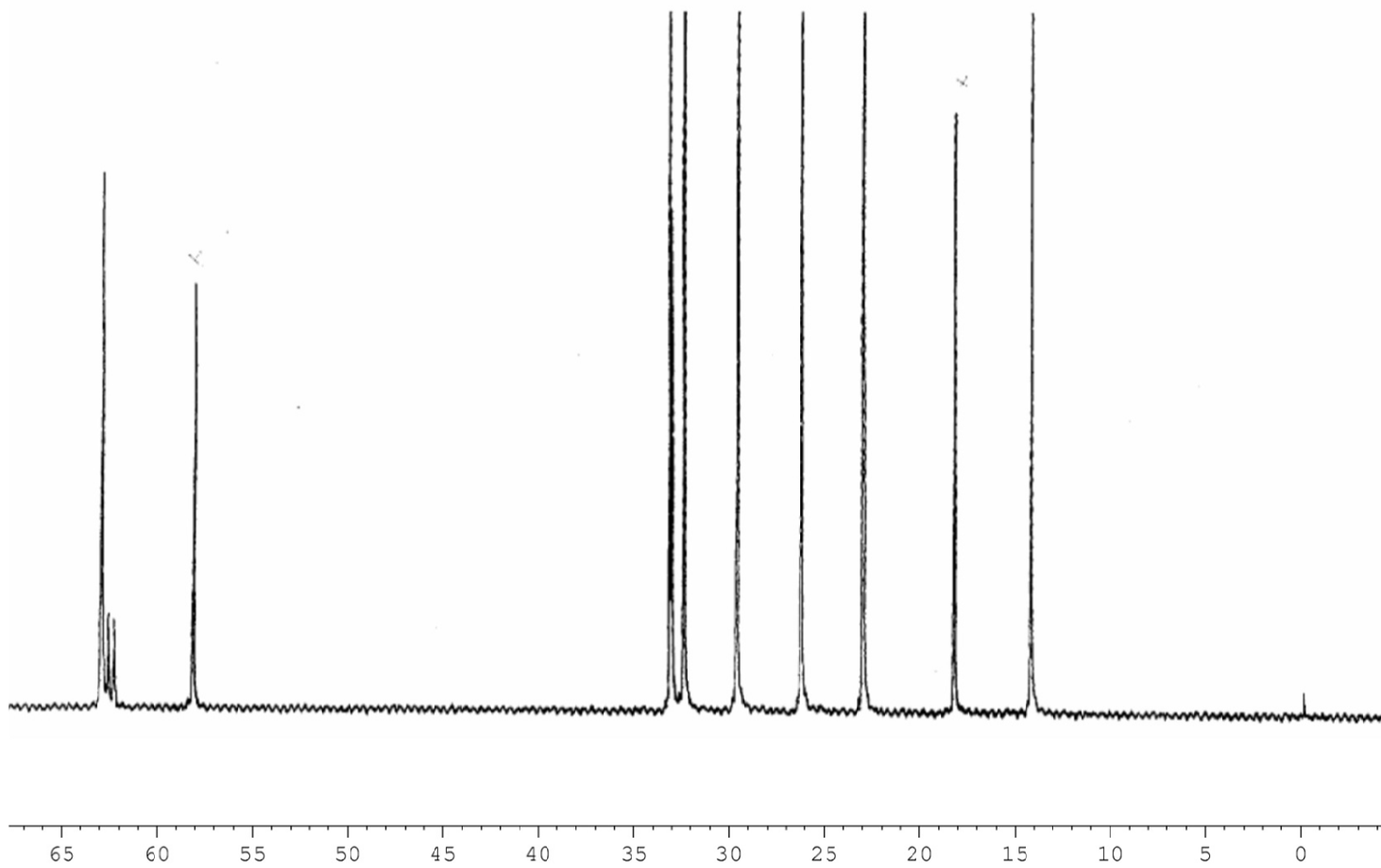


Figure 17. Deuteration of 1-heptanal in ethanol- $^{13}\text{C}\{^1\text{H}\}$ NMR spectrum of product fraction.

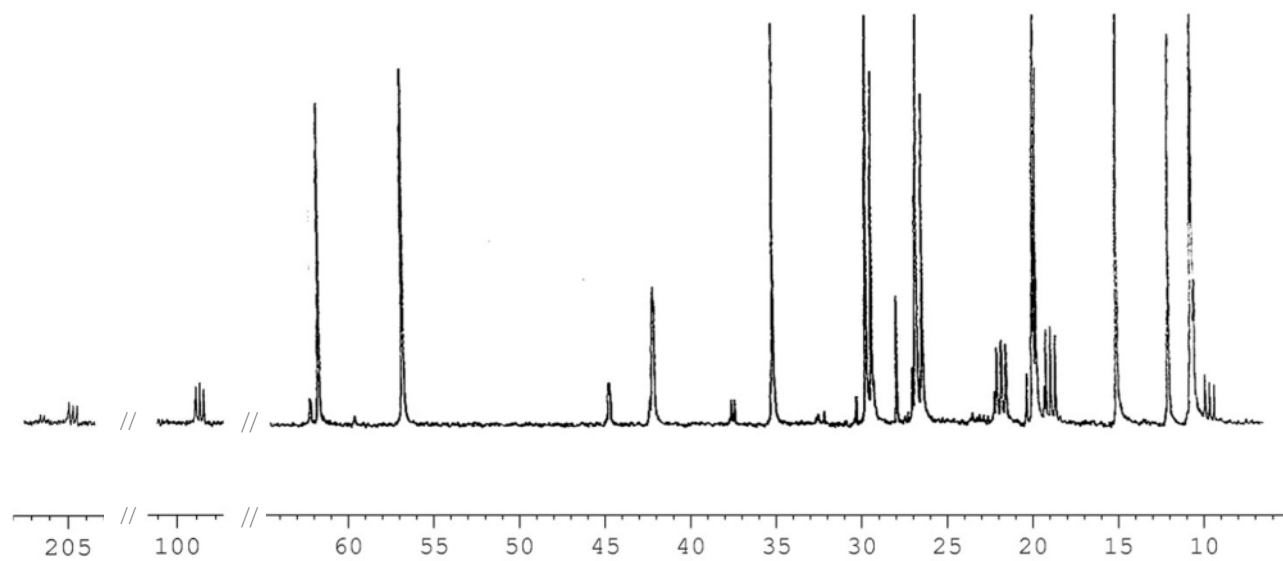


Figure 18. Deuteriohydroxylation of 1-hexene in ethanol- $^{13}\text{C}\{^1\text{H}\}$ NMR spectrum of C=O product fraction.

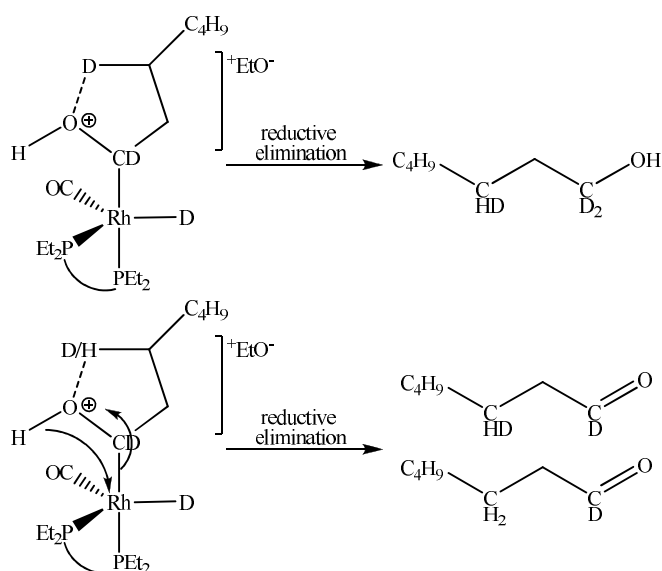
H/DO-CD₂-CH₂-CHD-C₄H₉ and H/DO-CD₂-CH(CH₂D)-C₄H₉ are identified as the linear and branched alcohol products from the deuteriohydroxymethylation of 1-hexene (Figure 16). The C₁ signal is resolved as a quintet for both 1-heptanol, $J_{C-D} = 21.4$ Hz, and 2-methylhexanol, $J_{C-D} = 20.9$ Hz. The α -shifts are ~ 0.40 ppm per deuterium, allowing for some β -shift from partial deuteration of the hydroxyl site. The expected C₁ and β -shifted C₁ resonances are resolved as a time-averaged signal due to rapid hydrogen-deuterium exchange in the hydroxyl site, thus it is not possible to establish which isotope is incorporated in the hydroxyl position of the initially formed product. Replacing the hydroxyl hydrogen with deuterium by exchange with D₂O causes C₁ to shift 0.27 ppm upfield. The C₃ signal of both products is split into a triplet by coupling to a single deuterium nucleus, $J_{C-D} = 19.3$ Hz. α -shifts of 0.47 ppm and 0.35 ppm are observed for 1-heptanol and 2-methylhexanol respectively. The C₂ resonances experience an upfield shift of ~ 0.30 ppm, equivalent to three β -shifts, due to the deuterium nuclei on vicinal carbons. A β -shift of 0.08 ppm is also noted for the C₄-signal of 1-heptanol.

1-Heptanol is recovered as H/DO-CH₂-CH₂-CH₂-C₄H₉ and H/DO-CHD-CH₂-CH₂-C₄H₉ from the deuteration of 1-heptanal (Figure 17). The signals from the non-deuterated isotopomer appear at the expected frequencies, while monodeuteration in the C₁ position causes splitting of this signal into a triplet, $J_{C-D} = 21.1$ Hz, with an α -shift of 0.37 ppm. A β -shift of 0.10 ppm is observed for the corresponding C₂ resonance. By integration of the C₂ signals it is established that only 36% of 1-heptanol has deuterium incorporated in the C₁ position. It can thus be concluded that 1-heptanal is not an intermediate in this hydroxymethylation, since a auto-tandem scheme should yield primarily H/DO-CHD-CH₂-CHD-C₄H₉ but only H/DO-CD₂-CH₂-CHD-C₄H₉ is observed. Even if all 1-heptanal is eliminated in the form O=CD-CH₂-CHD-C₄H₉, a mixture of monodeuterated and dideuterated C₁ is expected in the sequential product.

By comparison with the products from the corresponding hydroformylation reaction, it is shown that the aldehydes are recovered primarily as O=CD-CH₂-CHD-C₄H₉ and O=CD-CH(CH₂D)-C₄H₉ (Figure 18). The C₁ signal is split into a triplet for both 1-heptanal, $J_{C-D} = 25.9$ Hz, and 2-methylhexanal, $J_{C-D} = 25.3$ Hz, with α -shifts of 0.42 ppm and 0.45 ppm respectively. The C₃ resonances are also resolved as strong triplets, $J_{C-D} = 19.6$ Hz. α -shifts of 0.35 ppm and 0.33 ppm are observed for the 1-heptanal and 2-methylhexanal signals respectively. The C₂ signals of 1-heptanal and 2-methylhexanal are subject to a β -shift of ~ 0.20 ppm, due to two deuterium nuclei on vicinal carbons. Fine splitting of these signals, ${}^2J_{C-D} = 3.2$ Hz for 1-heptanal and ${}^2J_{C-D} = 2.8$ Hz for 2-methylhexanal, is the result of two-bond coupling to the deuterium incorporated in the C₁ position. The enhanced coupling is probably due to the enlarged bond angle imposed by the sp² hybridised state of C₁. A β -shift of 0.09 ppm is observed for the C₄ resonance of 1-heptanal. A small percentage of 1-heptanal is shown to be present as O=CD-CH₂-CH₂-C₄H₉. A weak C₂ signal is noted downfield of the main triplet, with a β -shift of 0.07 ppm induced by the deuterium nucleus on C₁. Fine splitting is not observed however, presumably due to partial eclipse by the main C₂ signal. Weak singlets due to the

C_3 and C_4 nuclei are observed 0.36 ppm and 0.08 ppm downfield from their main resonances respectively. By integration of the C_4 signals it is shown that 87% of 1-heptanal is deuterated in the C_3 position.

The fact that 1-hexene deuteriohydroxymethylation gives 1-heptanol exclusively monodeuterated in the C_3 -position together with 1-heptanal partially non-deuterated in the C_3 -position shows that 1-heptanal cannot be an intermediate in the production of 1-heptanol. Either different modes of C_3 -D/H bond formation are possible, the C_3 position is modified later in the catalytic pathway or the isotopic pattern on C_3 determines chemoselective outcome. Since the C_3 -D/H bond formation precedes chemoselective determination in the catalytic scheme, it seems very unlikely that the hydroxymethylation products have a different C_3 labelling pattern as a result of possible different modes. Instead, an agostic association between the hydroxyl-oxygen and the isotopic nucleus incorporated in the C_3 position *via* a transient 5-membered intermediate is proposed to occur in the rhodium-hydroxyheptyl-deuteride-carbonyl complex (Scheme 2).

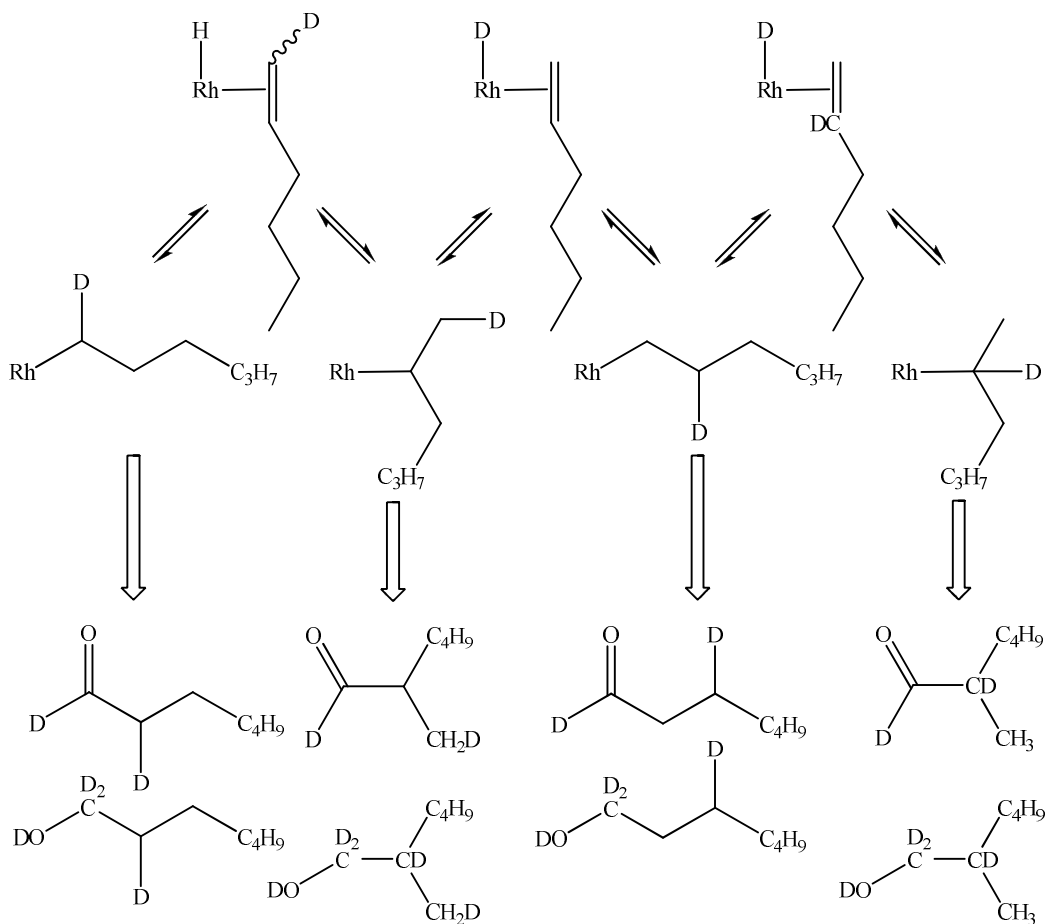


Scheme 2. Proposed sequences for aldehyde and alcohol formation.

This is expected to be more severe with the protium analogue because a carbon-deuterium bond has smaller vibrational frequencies relative to a carbon-hydrogen bond, which can be regarded as the deuterium nucleus having a smaller effective van der Waals radius.⁴⁵ The association can enforce migration of the hydroxyl hydrogen onto rhodium and reductive elimination of 1-heptanol. The elimination of concurrently coordinating ethoxide as ethanol-OD then generates a rhodium-hydride-carbonyl species, which can account for the small percentage of hydrogen incorporated in the C_3 site of 1-heptanal. If this is correct, all rhodium-hydroxyheptyl-deuteride-carbonyl species with a non-deuterated C_3 -site must undergo the β -hydride abstraction, suggesting a remarkably high secondary isotope effect. The steric considerations of the isotopic nuclei are also manifested in regioselective

control, since hydride migration apparently favours formation of the less hindered rhodium-hexyl-carbonyl complex.

Regiocontrol. Deuteriohydroxymethylation provides a sensitive probe to distinguish between irreversible and reversible formation of the rhodium-alkyl-dicarbonyl species.⁴⁶ Irreversible formation will result in deuterium incorporation in the C₃ position while reversibility provides a competing mechanism for deuterating the C₂ site instead (Scheme 3). In this case all the C₇ reaction products were recovered with deuterium incorporated exclusively in C₁ and C₃ positions. It can thus be stated that for these systems, regioselectivity is determined by irreversible hydride migration onto coordinated 1-hexene, forming the rhodium-hexyl/methylpentyl-dicarbonyl intermediate committed to carbonylation.

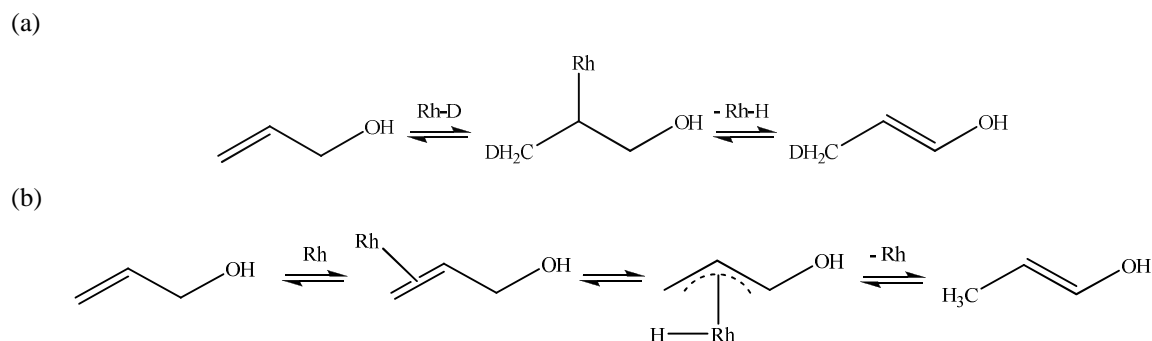


Scheme 3. Deuteriohydroxymethylation prove for the reversibility of rhodium-alkyl-dicarbonyl formation.

Mechanism of allyl alcohol isomerisation/hydrogenation. C₃-product formation from allyl alcohol is deleterious to process economics, so the formation mechanisms have been explored in detail by applying the complex **7a**-deuteride for the deuteriohydroxymethylation of allyl alcohol.

Following fractional distillation off the catalyst, the C₃-product and solvent fractions were examined by ¹³C{¹H} NMR spectroscopy (Table 8).

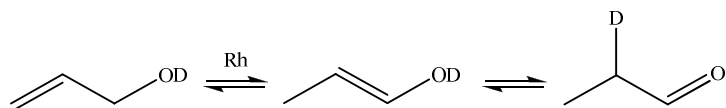
1-Propanal is obtained as the final product of allyl alcohol isomerisation. The double bond migration can proceed either by metal hydride addition-elimination or by an intramolecular hydrogen 1, 3-shift *via* a π -allyl complex (Scheme 4).⁴⁷ A third possibility could be isomerisation by an internal redox mechanism, involving bidentate coordination of the substrate, although this has only been reported for ruthenium complexes.⁴⁸ Tautomerisation of prop-1-en-1-ol then generates the aldehyde.



Scheme 4. Rhodium-catalysed allyl alcohol isomerisation mechanisms:

(a) metal hydride addition-elimination (b) *via* π -allyl complex.

1-Propanal is recovered exclusively as O=CH-CH₂-CH₃ (Figure 19). This is consistent with the π -allyl-rhodium mechanism, but the enol was not intercepted during catalysis. The kinetic stability of prop-1-en-1-ol under atmospheric pressure CO/H₂ = 1 was therefore monitored by ¹H NMR spectroscopy, according to procedure of Bergens and Bosnich (Table 9).⁴⁹ Although some catalytic tautomerisation is observed, a thermal pathway seems predominant. At room temperature all prop-1-en-1-ol solutions took ~ 45 minutes to completely dissipate, but at 100°C tautomerisation was found to be complete within 3 minutes.



Scheme 5. Rhodium-catalysed isomerisation of allyl alcohol-OD.

A thermal tautomerisation pathway is further implicated by the observation that deuterium is transferred exclusively to the C₂ position of 1-propanal upon the deuteriohydroxymethylation of allyl alcohol-OD;⁵⁰ a catalytic process would probably have led to some scrambling (Scheme 5).

Table 8: Deuteriohydroxymethylation of allyl alcohol with **12a**-deuteride in ethanol – $^{13}\text{C}\{^1\text{H}\}$ NMR C_3 - product analysis.^a

	1/ppm	2/ppm	3/ppm				
propanal - calculated	202.20	37.30	6.50				
propanal - sample	203.21	37.19	6.04				
propanol - calculated	65.00	25.20	10.10				
propanol - sample	64.45	24.29	10.18				
propanol/OD – D ₂ O exchange	65.28	24.11	10.26				

	1/ppm	$J_{\text{C-D}}/\text{Hz}$	I	2/ppm	$J_{\text{C-D}}/\text{Hz}$	3/ppm	$J_{\text{C-D}}/\text{Hz}$
allyl alcohol-OH + CO/D ₂							
O=CH-CH ₂ -CH ₃	203.40			37.17		5.98	
H/DO-CH ₂ -CHD-CH ₂ D	64.23		63	22.91	t. 20.1	9.70	t. 19.8
H/DO-CH ₂ -CH ₂ -CH ₃	64.31		37	23.43		10.21	
allyl alcohol-OD + CO/H ₂							
O=CH-CHD-CH ₃	203.31		36.81	t. 20.1	5.87		
1-propanal + CO/D ₂							
H/DO-CH ₂ -CH ₂ -CH ₃	64.37		86	25.70	36.6	10.03	
H/DO-CHD-CH ₂ -CH ₃	63.98	t. 21.6	14	25.60	33.7	10.03	

^aConditions: 4 mL ethanol, 8 mM [Rh], 1/Rh = 1, Rh/allyl alcohol = 1/200, 120°C, 40 bar CO/(D₂ or H₂) = 1.

Table 9: Kinetic stability of prop-1-en-1-ol in d_8 -toluene solution.^a

[Rh]	T (°C)	TOF ₉₈ ^b	primary spectrum ^c	
			prop-1-en-1-ol ^{d(i)}	1-propanal ^{d(ii)}
0	25	1.81	97	3
5	25	2.33	95	3
8	25	2.75	97	4
8	80	13.62	77	22
0	100	27.84	56	45

^aConditions: 0.5 mL d_8 -toluene, atmospheric pressure CO/H₂=1, 0.1 M [prop-1-en-1-ol]. ^bTurn over frequency ($\times 10^{-8}$ mol s⁻¹) determined at ~ 98% tautomerisation. ^cPrimary spectrum ran after 1.34 min. ^dCH₃-⁽ⁱ⁾dd. $\delta = 1.58$, ¹J = 6.6 Hz, ²J = 1.8 Hz, ⁽ⁱⁱ⁾t. $\delta = 1.09$, ¹J = 7.1 Hz.

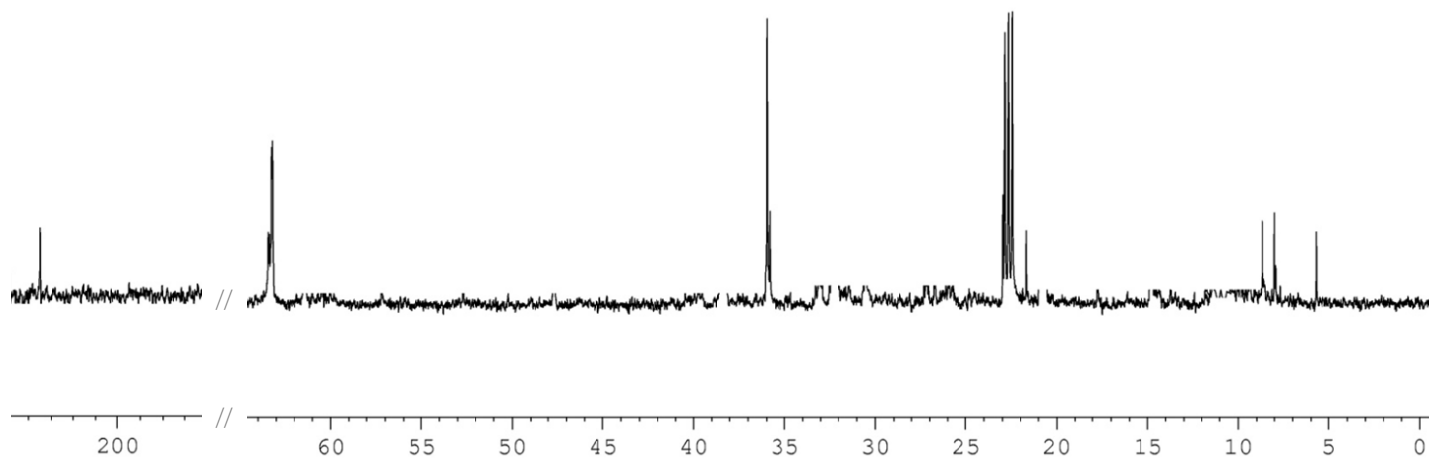


Figure 19. Deuteriohydroxylation of allyl alcohol in ethanol- $^{13}\text{C}\{^1\text{H}\}$ NMR spectrum of C_3 -product fraction.

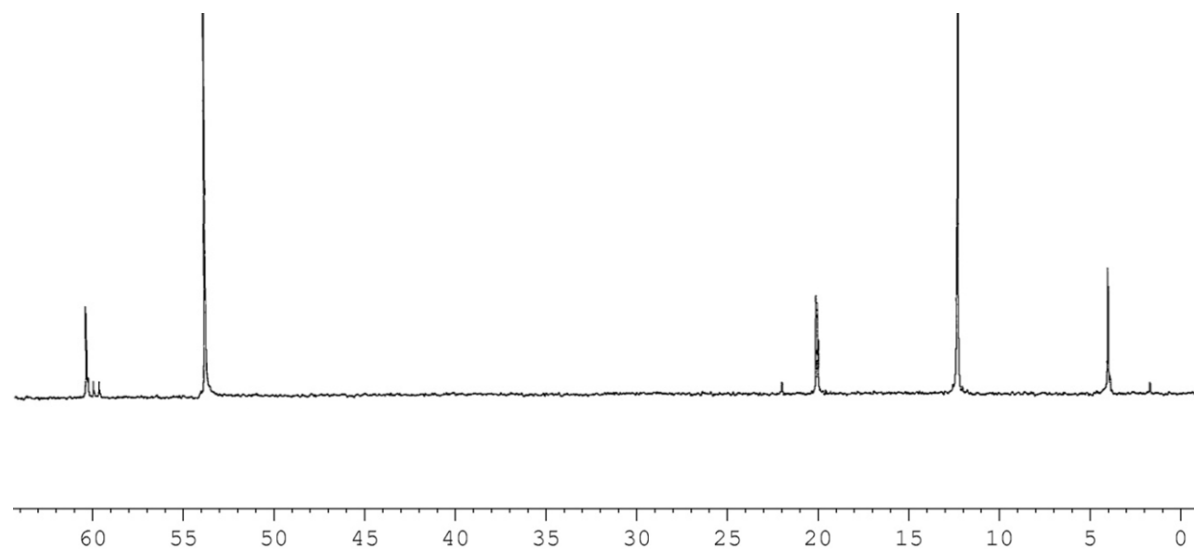


Figure 20. Deuteration of 1-propanal in ethanol- $^{13}\text{C}\{^1\text{H}\}$ NMR spectrum of product fraction.

1-Propanol is recovered as a mixture of H/DO-CH₂-CH₂-CH₂ and H/DO-CH₂-CHD-CH₂D (Figure 19). The C₂ signal of the dideuterated product is split into a triplet by coupling to a single deuterium nucleus, $J_{C-D} = 20.1$ Hz. The C₃ resonance is similarly resolved as a triplet, $J_{C-D} = 19.8$ Hz. For these signals the α -shift is compounded with a β -shift due to the deuterium nucleus on the vicinal carbon, to give observed upfield shifts of ~ 0.50 ppm. A β -shift of 0.13 ppm is observed for the C₁-resonance, taking into account some β -shift resulting from partial deuterium incorporation into the hydroxyl position. Exchange of the hydroxyl hydrogen in 1-propanol with deuterium is shown to induce a β -shift of 0.22 ppm in the C₁ signal. It can be inferred that catalytic deuteration of allyl alcohol is responsible for the formation of this isotopomer, since deuteration of 1-propanal can only place deuterium in the C₂ site. The resonances from non-deuterated 1-propanol appear at the expected frequencies. By integration of the C₁ signals it is shown that 63% of 1-propanol is deuterated in the C₂ position. Derivation of this isotopomer by deuteration of the isomerisation product is confirmed by the deuteration of 1-propanal, which gives 86% H/DO-CH₂-CH₂-CH₂ and 14% H/DO-CHD-CH₂-CH₂ (Figure 20) as determined by integration of the C₂ signals.

2.7 Conclusions

Strong σ -donor diphosphines based on a carbocyclic scaffold have been prepared in four steps *via* the borane adducts. High oxophilicity of the phosphorus nuclei makes the synthesis and purification of these *bis*phosphines quite challenging. Their rhodium(I) species were characterised by high pressure NMR spectroscopy. The rhodium-hydride dicarbonyl complexes exist preferentially as the *ea* isomer, and the activation barrier for phosphorus exchange was calculated to be ~ 46 kJ mol⁻¹. The carbonyl-bridged rhodium dimer was identified as the main competing species.

Minor modification of the structural nature of the carbocyclic scaffold had significant impact on catalyst activity and selectivity. A more flexible chelate ring enhanced activity by favouring a higher rhodium-hydride-dicarbonyl/ rhodium dimer ratio, but inhibited regioselectivity by not being able to rigidify the configuration of the substituents on phosphorus. Regiocontrol was shown to be manifested in irreversible formation of the rhodium-alkyl-dicarbonyl complex. The chelate rings were stable at elevated temperatures allowing activity to be increased to a synthetically useful level, but decomposition of the catalysts was noted at 140°C. Under replicated conditions of the Lyondell-Basell process the catalysts could be recycled *via* biphasic separation without excessive loss of rhodium to the product extraction phase. However, a slight loss in activity was observed, probably due to catalyst poisoning by methacrolein.

Deuterium labelling studies implicated domino hydroxymethylation as the primary catalytic scheme. It is proposed that diol derivatives are recovered as primary products by reductive elimination from the rhodium-hydroxyalkyl-hydride-carbonyl cation whereas β -hydride abstraction or reversion

of the protonation equilibrium leads to elimination of hydroxyaldehyde products. It was also shown by deuterium labelling that allyl alcohol isomerisation proceeds by intramolecular hydrogen 1, 3-shift via a π -allyl complex.

2.8 Experimental Section

Materials. Chemicals were purchased from Acros Organics, Sigma-Aldrich and Strem. All operations were performed under N_2 (passed through column of dichromate adsorbed on silica) in a glove box or using standard Schlenk and catheter tubing techniques. All glassware was flame-dried under vacuum. Diethyl ether, hexane and thf were distilled from sodium benzophenone ketyl, dichloromethane was distilled from calcium hydride and absolute ethanol was distilled from magnesium ethoxide. HPLC-grade toluene and pentane were dispensed from argon-flushed La Roche A-2/Engelhard Q-5 drying columns. All solvents were degassed prior to use by fpt cycles. Celite and Kieselgel (60 SiO_2) were activated in a tube furnace at 250°C for 3 hours. The *trans*- 1, 2-*bis*-(chloromethyl) cycloalkanes⁵¹ and lithiated *bis*-(diethylamino)phosphine borane¹² were prepared according to the literature procedures.

Analytical techniques. NMR spectra were recorded on Bruker Avance 300 and Bruker Avance II 400 spectrometers with tetramethylsilane (1H , ^{13}C) and 85% H_3PO_4 (^{31}P) as external references. IR spectra were recorded on a Perkin-Elmer 1710 FT-IR spectrometer. Gas chromatography was performed on a Hewlett-Packard 6890 chromatograph fitted with a 30 m BP10™ column (carrier gas 3.2 mL min^{-1} He, flame-ionisation detector). Elemental analyses were done using a Perkin-Elmer 240C CHNS/O microanalyser. ICP-MS analyses were performed on an Iris Advantage analyser.

***Trans*- 1, 2-*bis*-(diethylamino)phosphinomethyl) cyclohexane borane (4a).** A solution of 1.0431 g *trans*-1, 2-*bis*-(chloromethyl) cyclohexane (5.76 mmol) in thf (15 mL) was added dropwise to 35 mL of a 0.33 M solution of lithiated *bis*-(diethylamino)phosphine borane (11.52 mmol) in thf at -78°C. The reaction mixture was slowly warmed to 25°C and stirred for 10 hours. Solvent was removed *in vacuo*, then chloroform (25 mL) was added and the resulting suspension was filtered successively over Celite and $MgSO_4$. The filtrate was concentrated *in vacuo* and the off-white solid purified by column chromatography (Kieselgel, toluene) yielding 1.5861 g (74 %) of white crystals. $R_f = 0.52$ (toluene). 1H NMR ($CDCl_3$, 300.1 MHz): δ 3.08 (m, 8H), 2.77 (m, 4H), 1.96 (m, 2H), 1.58-1.34 (m, 8H), 1.11 (t, $J = 6.9$ Hz, 12H), 1.09-0.33 (br, 3H). $^{13}C\{^1H\}$ NMR ($CDCl_3$, 75.5 MHz): δ 43.9 (d, $^2J_{P-C} = 14.5$ Hz), 35.6 (s), 33.4 (s), 32.1 (d, $^1J_{P-C} = 26.8$ Hz), 27.1 (s), 14.9 (d, $^3J_{P-C} = 2.4$ Hz). $^{31}P\{^1H\}$ NMR (C_6D_6 , 121.4 MHz): δ 36.2 (q, $^1J_{P-B} = 64.3$ Hz). *Anal.* Calculated for $C_{16}H_{40}B_2N_4P_2$: C,

51.65; H, 10.84; N, 15.06. Found: C, 51.61; H, 10.69; N, 15.05. Ir (KBr, cm^{-1}): 2355 (s, $\nu_{\text{B-H}}$), 2339 (w, $\nu_{\text{B-H}}$), 651 (m, $\nu_{\text{P-B}}$).

Trans- 1, 2-bis-((diethylamino)phosphinomethyl) cyclopentane borane (4b). Preparation of **4b** was performed by a similar procedure to that employed for the preparation of **4a**. Starting from 0.9323 g *trans*-1, 2-bis-(chloromethyl) cyclopentane (5.58 mmol) and 35 mL of a 0.32 M solution of lithiated *bis*-(diethylamino)phosphine borane (11.16 mmol) in thf yielded 1.4985g (75%) of white crystals. $R_f = 0.55$ (toluene). ^1H NMR (CDCl_3 , 300.1 MHz): δ 3.04 (m, 8H), 2.69 (m, 4H), 1.87 (m, 2H), 1.49-1.37 (m, 5H), 1.11 (t, $J = 6.9$ Hz, 12H), 1.05-0.41 (br, 3H). $^{13}\text{C}\{^1\text{H}\}$ NMR (CDCl_3 , 75.5 MHz): δ 37.2 (d, $^2J_{\text{P-C}} = 14.5$ Hz), 34.7 (s), 33.8 (d, $^1J_{\text{P-C}} = 27.1$ Hz), 30.4 (s), 25.1 (s), 16.3 (d, $^3J_{\text{P-C}} = 2.4$ Hz). $^{31}\text{P}\{^1\text{H}\}$ NMR (C_6D_6 , 121.4 MHz): δ 36.8 (q, $^1J_{\text{P-B}} = 64.4$ Hz). *Anal.* Calculated for $\text{C}_{15}\text{H}_{38}\text{B}_2\text{N}_4\text{P}_2$: C, 50.32; H, 10.70; N, 15.65. Found: C, 50.41; H, 10.63; N, 15.62. Ir (KBr, cm^{-1}): 2357 (s, $\nu_{\text{B-H}}$), 2344 (w, $\nu_{\text{B-H}}$), 655 (m, $\nu_{\text{P-B}}$).

Trans- 1, 2-bis-((diethylamino)phosphinomethyl) cyclobutane borane (4c). Preparation of **4c** was performed by a similar procedure to that employed for the preparation of **4a**. Starting from 0.8999 g *trans*-1, 2-bis-(chloromethyl) cyclobutane (5.88 mmol) and 35 mL of a 0.34 M solution of lithiated *bis*-(diethylamino)phosphine borane (11.76 mmol) in thf yielded 1.4362 g (71%) of white crystals. $R_f = 0.57$ (toluene). ^1H NMR (CDCl_3 , 300.1 MHz): δ 3.05 (m, 8H), 2.63 (m, 4H), 2.26 (m, 2H), 1.93-1.79 (m, 4H), 1.11 (t, $J = 6.9$ Hz, 12H), 1.01-0.37 (br, 3H). $^{13}\text{C}\{^1\text{H}\}$ NMR (CDCl_3 , 75.5 MHz): δ 40.7 (d, $^1J_{\text{P-C}} = 27.1$ Hz), 36.3 (d, $^2J_{\text{P-C}} = 14.5$ Hz), 31.1 (s), 27.2 (s), 17.1 (d, $^3J_{\text{P-C}} = 2.4$ Hz). $^{31}\text{P}\{^1\text{H}\}$ NMR (C_6D_6 , 121.4 MHz): δ 37.1 (q, $^1J_{\text{P-B}} = 64.4$ Hz). *Anal.* Calculated for $\text{C}_{14}\text{H}_{36}\text{B}_2\text{N}_4\text{P}_2$: C, 48.88; H, 10.55; N, 16.29. Found: C, 49.01; H, 10.59; N, 16.19. Ir (KBr, cm^{-1}): 2358 (s, $\nu_{\text{B-H}}$), 2341 (w, $\nu_{\text{B-H}}$), 658 (m, $\nu_{\text{P-B}}$).

Trans- 1, 2-bis-(dichlorophosphinomethyl) cyclohexane borane (5a). Excess anhydrous HCl was bubbled through a solution of 1.3000 g **4a** (3.49 mmol) in diethyl ether (50 mL) at -78°C for 10 minutes. The ammonium salt was removed by filtering the reaction mixture through a glass frit, and washed with diethyl ether (3×15 mL). The combined extracts were reduced under pressure to ~ 25 mL, and the product was characterised *in situ*. The solutions were then made up with diethyl ether to 35 mL. ^1H NMR (d_4 -methanol, 300.1 MHz): δ 2.82 (m, 4H), 1.77 (m, 2H), 1.54-1.37 (m, 8H), 1.42-0.77 (br, 3H). $^{13}\text{C}\{^1\text{H}\}$ NMR (d_4 -methanol, 75.5 MHz): δ 55.1 (d, $^1J_{\text{P-C}} = 28.5$ Hz), 25.4 (s), 31.5 (s), 26.2 (s). $^{31}\text{P}\{^1\text{H}\}$ NMR (d_4 -methanol, 121.4 MHz): δ 96.4 (q, $^1J_{\text{P-B}} = 46.6$ Hz).

Trans- 1, 2-bis-(dichlorophosphinomethyl) cyclopentane borane (5b). Preparation of **5b** was performed by a similar procedure to that employed for the preparation of **5a**, starting from 1.2000 g **4b** (3.49 mmol). The product was characterised *in situ*. ^1H NMR (d_4 -methanol, 300.1 MHz): δ 2.75

(m, 4H), 1.64-1.44 (m, 8H), 1.45-0.82 (br, 3H). $^{13}\text{C}\{^1\text{H}\}$ NMR (d_4 -methanol, 75.5 MHz): δ 54.8 (d, $^1J_{\text{P-C}} = 28.8$ Hz), 28.3 (s), 34.1 (s), 24.6 (s). $^{31}\text{P}\{^1\text{H}\}$ NMR (d_4 -methanol, 121.4 MHz): δ 96.9 (q, $^1J_{\text{P-B}} = 46.8$ Hz).

Trans- 1, 2-bis-(dichlorophosphinomethyl) cyclobutane borane (5c). Preparation of **5c** was performed by a similar procedure to that employed for the preparation of **5a**, starting from 1.2000 g **4c** (3.49 mmol). The product was characterised *in situ*. ^1H NMR (d_4 -methanol, 300.1 MHz): δ 2.73 (m, 4H), 1.92 (m, 2H), 1.99-1.79 (m, 4H), 1.38-0.79 (br, 3H). $^{13}\text{C}\{^1\text{H}\}$ NMR (d_4 -methanol, 75.5 MHz): δ 54.7 (d, $^1J_{\text{P-C}} = 28.9$ Hz), 32.9 (s), 26.4 (s). $^{31}\text{P}\{^1\text{H}\}$ NMR (d_4 -methanol, 121.4 MHz): δ 97.2 (q, $^1J_{\text{P-B}} = 46.6$ Hz).

Trans- 1, 2-bis-(diethylphosphinomethyl) cyclohexane borane (6a). The solution of **5a** (3.49 mmol) in diethyl ether was added dropwise to 4.6 mL of a 1.5 M solution of ethyl magnesium bromide (6.98 mmol) in diethyl ether at -20°C . The reaction mixture was heated to 85°C under gentle reflux, and maintained for 16 hours. After cooling to 15°C , the precipitated magnesium salts were filtered over Celite and washed with hexane (2×10 mL). The solvents were removed *in vacuo* and the viscous white resin was purified by column chromatography (Kieselgel, hexane/dichloromethane = 7/3) yielding 0.7611 g (69%) of white solid. $R_f = 0.64$ (hexane/dichloromethane = 7/3). $[\alpha]_{\text{D}}^{20} = +49.8^\circ$ (c 2.58, toluene). ^1H NMR (CDCl_3 , 300.1 MHz): δ 2.81 (m, 4H), 1.87 (m, 2H), 1.66 (dq, $J = 7.1$ Hz, $^2J_{\text{P-H}} = 9.6$ Hz, 8H), 1.53-1.27 (m, 8H), 1.01 (dt, $J = 7.1$ Hz, $^3J_{\text{P-H}} = 2.9$, 12H), 1.06-0.42 (br, 3H). $^{13}\text{C}\{^1\text{H}\}$ NMR (CDCl_3 , 75.5 MHz): δ 34.4 (s), 33.7 (s), 32.9 (d, $^1J_{\text{P-C}} = 27.3$ Hz), 27.3 (d, $^1J_{\text{P-C}} = 27.2$ Hz), 26.2 (s), 11.7 (d, $^2J_{\text{P-C}} = 12.4$ Hz). $^{31}\text{P}\{^1\text{H}\}$ NMR (C_6D_6 , 121.4 MHz): δ 19.1 (q, $^1J_{\text{P-B}} = 67.8$ Hz). *Anal.* Calculated for $\text{C}_{16}\text{H}_{40}\text{B}_2\text{P}_2$: C, 60.80; H, 12.76. Found: C, 61.01; H, 12.81. Ir (KBr, cm^{-1}): 2367 (s, $\nu_{\text{B-H}}$), 2344 (w, $\nu_{\text{B-H}}$), 678 (m, $\nu_{\text{P-B}}$).

Trans- 1, 2-bis-(diethylphosphinomethyl) cyclopentane borane (6b). Preparation of **6b** was performed by a similar procedure to that employed for the preparation of **6a**. Starting from the solution of **5b** (3.49 mmol, 35 mL) and 4.6 mL of a 1.5 M solution of ethyl magnesium bromide (6.98 mmol) in diethyl ether yielded 0.6013 g (57%) of white solid. $R_f = 0.66$ (hexane/dichloromethane = 7/3). $[\alpha]_{\text{D}}^{20} = -12.6^\circ$ (c 1.48, toluene). ^1H NMR (CDCl_3 , 300.1 MHz): δ 2.72 (m, 4H), 1.83 (m, 2H), 1.68 (dq, $J = 7.1$ Hz, $^2J_{\text{P-H}} = 9.8$ Hz, 8H), 1.61-1.33 (m, 5H), 1.01 (dt, $J = 7.1$ Hz, $^3J_{\text{P-H}} = 3.1$, 12H), 1.08-0.39 (br, 3H). $^{13}\text{C}\{^1\text{H}\}$ NMR (CDCl_3 , 75.5 MHz): δ 35.7 (s), 34.1 (d, $^1J_{\text{P-C}} = 27.5$ Hz), 31.2 (s), 27.8 (d, $^1J_{\text{P-C}} = 27.2$ Hz), 24.9 (s), 10.3 (d, $^2J_{\text{P-C}} = 12.4$ Hz). $^{31}\text{P}\{^1\text{H}\}$ NMR (C_6D_6 , 121.4 MHz): δ 19.9 (q, $^1J_{\text{P-B}} = 67.8$ Hz). *Anal.* Calculated for $\text{C}_{15}\text{H}_{38}\text{B}_2\text{P}_2$: C, 59.65; H, 12.68. Found: C, 59.71; H, 12.64. Ir (KBr, cm^{-1}): 2367 (s, $\nu_{\text{B-H}}$), 2347 (w, $\nu_{\text{B-H}}$), 684 (m, $\nu_{\text{P-B}}$).

Trans- 1, 2-bis-(diethylphosphinomethyl) cyclobutane borane (6c). Preparation of **6c** was performed by a similar procedure to that employed for the preparation of **6a**. Starting from the solution of **5c** (3.49 mmol, 35 mL) and 4.6 mL of a 1.5 M solution of ethyl magnesium bromide (6.98 mmol, 4.6 mL) in diethyl ether yielded 0.6237 g (62%) of white solid. $R_f = 0.74$ (hexane/dichloromethane = 7/3). $[\alpha]_D^{20} = -15.7^\circ$ (c 1.22, toluene). $^1\text{H NMR}$ (CDCl_3 , 300.1 MHz): δ 2.69 (m, 4H), 2.05 (m, 2H), 2.02-1.87 (m, 4H), 1.68 (dq, $J = 7.1$ Hz, $^2J_{\text{P-H}} = 9.9$ Hz, 8H), 1.01 (dt, $J = 7.1$ Hz, $^3J_{\text{P-H}} = 3.2$, 12H), 1.11-0.60 (br. q, $^1J_{\text{B-H}} = 95.6$ Hz, 3H). $^3\text{C}\{^1\text{H}\}$ NMR (CDCl_3 , 75.5 MHz): δ 38.4 (d, $^1J_{\text{P-C}} = 27.5$ Hz), 35.7 (s), 27.9 (s), 27.2 (d, $^1J_{\text{P-C}} = 27.2$ Hz), 10.0 (d, $^2J_{\text{P-C}} = 12.4$ Hz). $^{31}\text{P}\{^1\text{H}\}$ NMR (C_6D_6 , 121.4 MHz): δ 20.3 (q, $^1J_{\text{P-B}} = 67.8$ Hz). *Anal.* Calculated for $\text{C}_{14}\text{H}_{36}\text{B}_2\text{P}_2$: C, 58.38; H, 12.60. Found: C, 58.23; H, 12.62. Ir (KBr, cm^{-1}): 2372 (s, $\nu_{\text{B-H}}$), 2351 (w, $\nu_{\text{B-H}}$), 688 (m, $\nu_{\text{P-B}}$).

Trans- 1, 2-bis-(diethylphosphinomethyl) cyclohexane (1). Deprotection of the borane complex was accomplished *via* a modified literature procedure. 4.2 mL of fluoroboric acid dimethyl ether complex (34.75 mmol) was added dropwise to 0.7322 g **6a** (2.32 mmol) in dichloromethane (30 mL) at -15°C . The reaction mixture was allowed to warm to room temperature and stirred overnight. After diluting with dichloromethane (15 mL) and saturated NaHCO_3 solution (35 mL) the reaction mixture was stirred a further 20 minutes, then the aqueous phase was extracted with dichloromethane (3×15 mL). The combined extracts were washed successively with brine (15 mL) and water (2×10 mL) and dried over MgSO_4 . The solvents were removed *in vacuo*, and pentane was added to the residue. The mixture was sonicated over 5-10 minutes, and the solution transferred from the insoluble paste by syringe. Concentrating *in vacuo* afforded 0.2975 g (44%) of viscous colourless oil. $^1\text{H NMR}$ (C_6D_6 , 300.1 MHz): δ 2.73 (dd, $J = 5.6$ Hz, $^2J_{\text{P-H}} = 10.1$ Hz), 1.91 (m, 2H), 1.64 (dq, $J = 7.0$ Hz, $^2J_{\text{P-H}} = 9.9$ Hz, 8H), 1.63-1.27 (m, 8H), 0.98 (dt, $J = 7.0$ Hz, $^3J_{\text{P-H}} = 3.1$, 12H). $^{13}\text{C}\{^1\text{H}\}$ NMR (C_6D_6 , 75.5 MHz): δ 35.1 (s), 33.6 (s), 33.2 (d, $^1J_{\text{P-C}} = 28.2$ Hz), 27.2 (s), 19.3 (d, $^1J_{\text{P-C}} = 27.9$ Hz), 9.9 (d, $^2J_{\text{P-C}} = 12.1$ Hz). $^{31}\text{P}\{^1\text{H}\}$ NMR (C_6D_6 , 121.4 MHz): $\delta - 27.4$. *Anal.* Calculated for $\text{C}_{16}\text{H}_{34}\text{P}_2\text{S}_2$: C, 54.52; H, 9.72; S, 18.19. Found: C, 54.39; H, 9.65; S, 17.97.

Trans- 1, 2-bis-(diethylphosphinomethyl) cyclopentane (2). Preparation of **2** was performed by a similar procedure to that employed for the preparation of **1**. Starting from 0.5921 g **6b** (1.96 mmol) and 3.5 mL of fluoroboric acid dimethyl ether complex (29.41 mmol) yielded 0.2555 g (47%) of viscous colourless oil. $^1\text{H NMR}$ (CDCl_3 , 300.1 MHz): δ 2.65 (m, 4H), 1.87 (m, 2H), 1.65 (dq, $J = 7.0$ Hz, $^2J_{\text{P-H}} = 9.9$ Hz, 8H), 1.61-1.33 (m, 5H), 1.01 (dt, $J = 7.0$ Hz, $^3J_{\text{P-H}} = 3.1$, 12H). $^{13}\text{C}\{^1\text{H}\}$ NMR (CDCl_3 , 75.5 MHz): δ 36.2 (s), 35.4 (d, $^1J_{\text{P-C}} = 28.3$ Hz), 35.1 (s), 25.8 (s), 19.6 (d, $^1J_{\text{P-C}} = 27.9$ Hz), 10.0 (d, $^2J_{\text{P-C}} = 12.1$ Hz). $^{31}\text{P}\{^1\text{H}\}$ NMR (C_6D_6 , 121.4 MHz): $\delta - 26.8$. *Anal.* Calculated for $\text{C}_{15}\text{H}_{32}\text{P}_2\text{S}_2$: C, 53.39; H, 9.56; S, 19.00. Found: C, 53.52; H, 9.44; S, 18.97.

Trans- 1, 2-bis-(diethylphosphinomethyl) cyclobutane (3). Preparation of **3** was performed by a similar procedure to that employed for the preparation of **1**. Starting from 0.6172 g **6c** (2.14 mmol) and 3.8 mL of fluoroboric acid dimethyl ether complex (32.15 mmol) yielded 0.2874 g (51%) of viscous colourless oil. ^1H NMR (CDCl_3 , 300.1 MHz): δ 2.59 (m, 4H), 2.04-1.88 (m, 4H), 1.65 (dq, $J = 7.0$ Hz, $^2J_{\text{P-H}} = 9.9$ Hz, 8H), 1.01 (dt, $J = 7.0$ Hz, $^3J_{\text{P-H}} = 3.1$, 12H). $^{13}\text{C}\{^1\text{H}\}$ NMR (CDCl_3 , 75.5 MHz): δ 38.3 (d, $^1J_{\text{P-C}} = 28.5$ Hz), 35.7 (s), 27.6 (s), 20.1 (d, $^1J_{\text{P-C}} = 27.9$ Hz), 9.9 (d, $^2J_{\text{P-C}} = 12.1$ Hz). $^{31}\text{P}\{^1\text{H}\}$ NMR (C_6D_6 , 121.4 MHz): δ -26.1. *Anal.* Calculated for $\text{C}_{14}\text{H}_{30}\text{P}_2\text{S}_2$: C, 52.15; H, 9.38; S, 19.89. Found: C, 52.31; H, 9.36; S, 19.76.

Theoretical studies. The natural bite angles of **1-3** were determined by semi-empirical calculations. Initial conformations of Rh-**1**, Rh-**2** and Rh-**3** were determined by the PM3(tm) method as implemented in the SPARTAN SGI software, using the crystallographic data for $[\text{Rh}(\text{acac})(\text{DIOP})]$ as the starting point. The geometries thus obtained were further optimised by eigenvector following as implemented in the GAUSSIAN 98 program, with a termination criterion of rms gradient < 0.001 kJ $\text{mol}^{-1} \text{ \AA}^{-1}$.

High pressure NMR. In a typical experiment the 10 mm sapphire NMR cell was primed with a solution of 5.0 mg $[\text{Rh}(\text{acac})(\text{CO})_2]$ (0.02 mmol) and **1**, **3** or PEt_3 (0.04 mmol) in d_8 -toluene (1.5 mL) under N_2 . The cell was purged thrice with $\text{CO}/\text{H}_2 = 1$ and then pressurised to 40 bar. NMR spectra at different temperatures were recorded. Line-shape analyses and simulations were performed using the *d*NMR and daisy spectrum simulation options in the TOPSPIN™ software provided by Bruker BioSpin.

Catalysis. Syngas was purchased from BOC (**Caution!** Carbon monoxide is extremely poisonous and accidents may be lethal. A sensitive personal detector was carried and all experiments were performed in a well ventilated fume-hood fitted with a detector, maintaining the concentration of carbon monoxide below the mac value at all times). Hydroxymethylation reactions were carried out on the CAT rig with stirrer speed set at 800 rpm. In a typical experiment a solution of **1-3** (0.04-0.40 mmol) in ethanol (3 mL) was added to 10.4 mg $[\text{Rh}(\text{acac})(\text{CO})_2]$ (0.04 mmol). The resulting solution was sonicated over 10 minutes and transferred into the autoclave under $\text{CO}/\text{H}_2 = 1$; any residues were transferred with a further aliquot of ethanol (1 mL). The solution was incubated for 40 minutes at the appointed temperature and 30 bar $\text{CO}/\text{H}_2 = 1$. After 1 mL allyl alcohol (14.70 mmol, azeotropically dried with toluene and distilled) was injected the pressure was adjusted to 40 bar, and the reaction was run to completion. The autoclave was then cooled and depressurised. 50 μL diglyme was added as internal standard to a 1 mL aliquot of the product solution, and the sample was analysed by GC. The experiments were performed at least in duplo.

For catalyst recycling experiments, a solution of **1** or **3** (0.08 mmol) in toluene (3 mL) was added to 10.4 mg [Rh(acac)(CO)₂] (0.04 mmol). The resulting solution was sonicated over 10 minutes and transferred into the autoclave under CO/H₂ = 1; any residues were transferred with a further aliquot of toluene (1 mL). The solution was incubated for 20 minutes at 60°C and 10 bar CO/H₂=1. 1 mL allyl alcohol (14.70 mmol) was injected and the reaction was run to completion. The autoclave was cooled, depressurised to 1 bar and the product solution thus transferred *via* cannula to a Schlenk vessel equipped with a magnetic stirrer. The addition of water (2.5 mL) gave immediate phase separation and the biphasic system was stirred 5 minutes at 20°C. The organic phase was carefully transferred to a volumetrically graduated Schlenk tube *via* syringe; fresh toluene was added to make up 4 mL volume. This solution was re-applied in catalysis.

Determination of partition coefficients. A known amount of product (2.3 mmol) was solvated in water (2 mL). A biphasic system was created by the addition of toluene (2 mL). The mixture was sonicated over 5-10 minutes and then allowed to equilibrate at 0°C. Once two clear phases were obtained, a 0.5 mL aliquot was withdrawn from each and its weight determined (\pm 0.5 mg).

Deuterium labelling. Carbon monoxide was purchased from BOC and D₂ was purchased from Cambridge Isotope Laboratories. Labelling reactions were performed in a hastelloy autoclave. In a typical experiment a solution of **1** and 10.4 mg [Rh(acac)(CO)₂] (0.04 mmol) in ethanol (4 mL) was sonicated over 10 minutes and transferred into the autoclave under carbon monoxide, together with 1 mL substrate. The autoclave was pressurised with 20 bar D₂ and 20 bar carbon monoxide, and then heated to 120°C. After 3 hours the autoclave was cooled and depressurised. The product mixture was fractionated by spinning-band distillation. The fractions were analysed qualitatively by ¹³C{¹H} NMR spectroscopy and quantitatively by ¹³C{¹H, ²H} NMR spectroscopy.

References and Notes

- (1) (a) Kagan, H. B. *Comprehensive Asymmetric Catalysis*. Jacobsen, E. N.; Pfaltz, A.; Yamamoto, H. (Eds). Springer: Berlin, 1999. (b) Kagan, H. B.; Dang, T. P. *J. Am. Chem. Soc.* **1972**, *94*, 6429.
- (2) (a) Klabunovski, E. I.; Levitina, E. S. *Russ. Chem. Rev.* **1970**, *39*, 1035. (b) Izumi, Y. *Bull. Chem. Soc. Jap.* **1963**, *36*, 155.
- (3) (a) Horner, L.; Siegel, H.; Buthe, H. *Angew. Chem. Int. Ed.* **1968**, *7*, 232. (b) Knowles, W. S.; Sabacky, M. J. *J. Chem. Soc., Chem. Commun.* **1968**, 1445. (c) Morrison, J. D.; Burnett, R. E.; Agniar, A. M.; Morrow, C. J.; Phillips, C. *J. Am. Chem. Soc.* **1971**, *93*, 1301.
- (4) Hayashi, T.; Tanaka, M.; Ikeda, Y.; Ogata, I. *Bull. Chem. Soc. Jap.* **1979**, *52*, 2605.

- (5) (a) Consiglio, G.; Nefkens, S. C. A.; Borer, A. *Organometallics* **1991**, *10*, 2046. (b) Serivanti, A.; Paganelli, S.; Matteoli U. *J. Organomet. Chem.* **1990**, *397*, 119.
- (6) (a) Yan, Y. -Y.; RajanBabu, T. V. *J. Org. Chem.* **2000**, *65*, 900. (b) Yan, Y. -Y.; RajanBabu, T. V. *Org. Lett.* **2000**, *2*, 4137. (c) Aghmiz, A.; Masdeu-Bultó, A. M.; Claver, C.; Sinou, D. *J. Molec. Catal. A* **2002**, *184*, 111.
- (7) Maki, K.; Kujita, T.; Marumo, K. *JP Kokai*. 6.279.344, 1996. (b) Maki, K.; Kujita, T.; Marumo, K. *JP Kokai*. 6.279.345, 1996. (c) Maki, K.; Kujita, T.; Marumo, K. *US Pat.* 5.693.832, 1997.
- (8) (a) Dubner, W. S.; Shum, W. P. *US Pat.* 6.225.509, 2001. (b) Dubner, W. S.; Shum, W. P. *Eur. Pat.* 1.244.608, 2001.
- (9) Hughes O. R.; Unruh, J. D. *J. Mol. Catal.* **1981**, *12*, 71.
- (10) Casey, C. P.; Whiteker, G. T.; Melville, M. G.; Petrovich, L. M.; Gavney, J. A.; Powell, D. R. *J. Am. Chem. Soc.* **1992**, *114*, 5535.
- (11) $^{31}\text{P}\{^1\text{H}\}$ NMR (CDCl_3 , 81.0 MHz): δ 72.5 ($^1J_{\text{P-B}} = 95$ Hz). Cowley, A. H.; Damasco, M. C. *J. Am. Chem. Soc.* **1971**, *93*, 6815.
- (12) (a) $^{31}\text{P}\{^1\text{H}\}$ NMR (CDCl_3 , 121.4 MHz): δ 22.5. (b) $^{31}\text{P}\{^1\text{H}\}$ NMR (CDCl_3 , 121.4 MHz): δ 65.3.
- (13) Decomplexation is most commonly performed *via* aminolysis. Brunel, J. M.; Faure, B.; Maffei, M. *Coord. Chem. Rev.* **1998**, *178/180*, 665.
- (14) Defined as the preferred chelation angle determined only by scaffold constraints and not by metal valence angles. van Leeuwen, P. W. N. M.; Kamer, P. C. J.; Reek, J. N. H.; Dierkes, P. *Chem. Rev.* **2000**, *100*, 2741.
- (15) Chapter 4, p. 111.
- (16) SPARTAN 5.1.1 SGI. Wavefunction Inc., Irvine CA, 2005.
- (17) GAUSSIAN 98, Revision A.9. Gaussian Inc., Pittsburg PA, 1998.
- (18) Damoense, L.; Datt, M.; Green, M.; Steenkamp, C. *Coord. Chem. Rev.* **2004**, *248*, 2393.
- (19) Castellanos-Páez, A.; Castillón, S.; Claver, C.; van Leeuwen, P. W. N. M.; de Lange, W. G. J. *Organometallics* **1998**, *17*, 2543.
- (20) van Leeuwen, P. W. N. M.; van der Veen, L. A.; Boele, M. D. K.; Breman, F. R.; Kamer, P. C. J.; Goubitz, K.; Fraanje, J.; Schenk, H.; Bo, C. *J. Am. Chem. Soc.* **1998**, *120*, 11616.
- (21) (a) Toth, I.; Hanson, B. *Organometallics* **1993**, *12*, 1506 and references therein. (b) Kadyrov, R.; Börner, A.; Selke, R. *Eur. J. Inorg. Chem.* **1999**, 705.
- (22) Similar signals assigned to $[\text{Rh}(\text{CO})(\text{DPPE})(\mu\text{-CO})_2]$, $[\text{Rh}(\text{CO})(\text{DPPP})(\mu\text{-CO})_2]$, $[\text{Rh}(\text{CO})(\text{DIOP})(\mu\text{-CO})_2]$. James, B. R.; Mahajan, D.; Rettig, S. J.; Williams, G. M. *Organometallics* **1983**, *2*, 1452.
- (23) 16-Line multiplets assigned to $[\text{RhH}(\text{CO})(\text{DIOP})(\eta_1\text{-DIOP})(\eta_1\text{-DIOP})\text{-}(\text{RhH}(\text{CO})(\text{DIOP}))]$, $[\text{RhH}(\text{CO})(t\text{-BDCB})(\eta_1\text{-}t\text{-BDCB})(\eta_1\text{-}t\text{-BDCB})\text{-}\text{RhH}(\text{CO})(t\text{-BDCB})]$, $[\text{RhH}(\text{CO})(\text{BDPP})(\eta_1\text{-BDPP})(\eta_1\text{-BDPP})\text{-}\text{RhH}(\text{CO})(\text{BDPP})]$. (a) Reference 10. (b) Reference 19. (c) White, D. F. S. *PhD Thesis*, University of St. Andrews, 2001. Chapter 2.
- (24) (a) Evans, D.; Yagupsky, G.; Wilkinson, G. *J. Chem. Soc. A* **1968**, 2660. (b) Brown, C. K.; Wilkinson, G. *Tetrahedron Lett.* **1969**, *22*, 1725. (c) Brown, C. K.; Wilkinson, G. *J. Chem. Soc. A* **1970**, 2753.

- (25) (a) MacDougall, J. K.; Simpson, M. C.; Green, M. J.; Cole-Hamilton, D. J. *J. Chem. Soc., Dalton Trans.* **1996**, 1161. (b) MacDougall, J. K. *PhD Thesis*, University of St. Andrews, 1991. Chapter 5.
- (26) Berry, R. S. *J. Chem. Phys.* **1960**, *32*, 933.
- (27) Meakin P.; Muetterties, E. L. *J. Am. Chem. Soc.* **1972**, *94*, 5271.
- (28) Bain, A. D.; Duns, G. J. *J. Magn. Reson.* **1995**, *112*, 258.
- (29) (a) Meakin, P.; Jesson, J. P.; Tebbe, F. N.; Muttetities, E. L. *J. Am. Chem. Soc.* **1971**, *93*, 1797. (b) Hyde, E. M.; Swain, J. R.; Verkade, J. G.; Meakin, P. *J. Chem. Soc., Dalton Trans.* **1976**, 1169. (c) Veldman, N.; Spek, A. L. *Organometallics* **1996**, *15*, 835.
- (30) Brown, J. M.; Chaloner, P. A. *J. Am. Chem. Soc.* **1978**, *100*, 4307.
- (31) Heller, D.; Holz, J.; Borns, S.; Spannenberg, A.; Kempe, R.; Schmidt, U.; Börner, A. *Tetrahedron: Asymmetry* **1997**, *8*, 213.
- (32) (a) Bocian, D. F.; Strauss, H. L. *J. Am. Chem. Soc.* **1977**, *99*, 2876. (b) Elser, V.; Strauss, H. *Chem. Phys. Lett.* **1983**, *96*, 276.
- (33) Chair \leftrightarrow boat interconversion for [Rh(DIOP)(cod)][BF₄]: $\Delta G_{184K}^\ddagger = 8.0 \text{ kJ mol}^{-1}$. Reference 21b.
- (34) A2.2, p. 180.
- (35) van Leeuwen, P. W. N. M.; Claver, C. *Rhodium Catalysed Hydroformylation*. James, B. R.; Ugo, R. (Eds). Kluwer Academic: Dordrecht, 2000.
- (36) van der Veen, L. A.; Kamer, P. C. J.; van Leeuwen, P. W. N. M. *Organometallics* **1999**, *18*, 4765.
- (37) *Solubilities of Inorganic and Organic Compounds*, vol. 1. Stephen, H.; Stephen, T. (Eds). Pergamon Press: Oxford, 1963.
- (38) Glaser, R.; Twaiq, M.; Geresh, S.; Blumenfeld, J. *Tetrahedron Lett.* **1977**, *52*, 4635.
- (39) (a) *Trans*-1, 2-cyclohexane dicarboxylic acid. Benedetti, E.; Corradini, P.; Pedone, C. *J. Am. Chem. Soc.* **1969**, *91*, 4075. (b) *trans*-1, 2-cyclopentane dicarboxylic acid mono *N*-methyl amide. Allen, F. H.; Kennard, O. *Cryst. Structure Commun.* **1973**, *2*, 149. (c) *trans*-1, 2-cyclobutane dicarboxylic acid. Benedetti, E.; Corradini, P.; Pedone, C. *Acta Cryst. B* **1970**, *26*, 493.
- (40) Frohning, C. D.; Kohlpaintner, C. W. *Applied Homogeneous Catalysis with Organometallic Compounds*, vol. 1. Cornils, B.; Herrmann, W. A. (Eds). VCH: Weinheim, 1996.
- (41) Provided by Lyondell-Basell, Newtown Square Technology Centre, 3801 West Chester Pike, Newtown Square, PA 19073, USA.
- (42) Conversion is then less affected upon recycling **12c** as this effects a more linear-selective hydroformylation.
- (43) (a) Bain, A. D. *Prog. Nucl. Magn. Reson. Spectro.* **2003**, *43*, 63. (b) MacDougall, J. K.; Simpson, M. C.; Cole-Hamilton, D. J. *J. Chem. Soc. Dalton Trans.* **1994**, 3061.
- (44) (a) Chapter 1, p. 3. (b) Chapter 1, p. 13.
- (45) The difference is 0.03 ppm. (a) Mislow, K.; Graeve, R.; Gordon, A. J.; Wahl, G. H. *J. Am. Chem. Soc.* **1963**, *85*, 1199. (b) Ibrom, K.; Kohn, G; Boeckmann, K. -U.; Kraft, R.; Holba-Schulz, P.; Ernst, L. *Org. Lett.* **2000**, *2*, 4111.
- (46) Casey, C. P.; Petrovich, L. M. *J. Am. Chem. Soc.* **1995**, *117*, 6007.

- (47) For comprehensive mechanistic discourse see: McGrath, D. V.; Grubbs, R. H. *Organometallics* **1994**, *13*, 224.
- (48) For review see: van der Drift, R. C.; Bouwman, E.; Drent, E. *J. Organomet. Chem.* **2002**, *650*, 1.
- (49) Bergens, S. H.; Bosnich, B. *J. Am. Chem. Soc.* **1991**, *113*, 958.
- (50) Schuetz, R. D.; Millard, F. W. *J. Org. Chem.* **1959**, *24*, 297.
- (51) Birch, S. F.; Dean, R. A.; Whitehead, E. V. *J. Inst. Petroleum* **1954**, 1449.

-Chapter 3-

Enhanced Specific Activity in the Hydroformylation of Allylic Alcohols *via* the *Meta*-Effect

Abstract. Hybrid phosphines of the form PArAr'_2 ($\text{Ar} = \text{Ph}, \text{C}_6\text{H}_4\text{-3-Me}, \text{C}_6\text{H}_3\text{-3, 5-Me}_2$ and $\text{Ar}' = \text{Ph}, \text{C}_6\text{H}_4\text{-3-Me}, \text{C}_6\text{H}_3\text{-3, 5-Me}_2$) were prepared, and their physicochemical properties assessed as a function of systematic *meta*-substitution. Although the structural requisite of the triarylphosphine was not significantly affected, variable temperature ^1H NMR spectroscopy has shown that the steric exertions of *meta*-methyl substituents increase the activation barrier to phosphorus-(*ipso*)carbon rotation. The consequential formation of a rigid and well-defined coordination sphere in $[\text{RhH}(\text{CO})\{(3, 5\text{-Me}_2\text{Ph})_3\text{P}\}]$ effects dramatically enhanced linear-selective hydroformylation of allylic alcohols. This catalyst was recycled *via* biphasic separation twelve times with 94 % average retention of activity. The kinetics of allyl alcohol hydroformylation with $[\text{RhH}(\text{CO})\{(3, 5\text{-Me}_2\text{Ph})_3\text{P}\}_3]$ were investigated in the temperature range 333-353 K, from which the activation energy was found to be $E_A = 32.62 \text{ kJ mol}^{-1}$.

3.1 Introduction

The most rudimentary approach to ligand development involves simple modification of an existing motif. In the case of triphenylphosphine, this strategy has been implemented by introducing substitution patterns onto the phenyl moieties. The screening of these triarylphosphines in asymmetric catalysis has led to the identification of a *meta*-effect,¹ effectively an enantiomeric enhancement when a phenyl ring is substituted with a 3, 5-dialkylphenyl ring. Transition metal complexes modified with a *bis*(3, 5-dialkylphenyl)phosphine chelate have also been applied successfully for a variety of catalytic transformations (Table 1). The intricacies of the *meta*-effect have so far only been investigated with high specificity for particular complexes.

Table 1: Examples of enantioselective enhancement in current literature.

transformation	catalyst	substrate	<i>ee</i> (%)	
Heck arylation	[Pd(3, 5-Me ₂ - MeO-BIPHEP)Cl ₂]	dihydrofuran	86-90	^{1a}
allylic alkylation	[Pd(3, 5- ^t Bu ₂ - MeO-BIPHEP)Cl ₂]	oxobenzonorbornadiene	97-98	^{1b}
hydrogenation	[Rh(3, 5-Me ₂ - GLUPhos)(COD)]SbF ₆	dehydroamino acid	97-99	²
	[Ru(C ₆ H ₆)(3, 5-Me ₂ -BINAP)Cl ₂]/ diamine (jst-class catalysts)	acetophenones	80-99	³
	[Ru(C ₆ H ₆)(3, 5-Me ₂ -BINAP)Cl ₂]	β-keto esters	88-95	⁴
hydrocyanation	[Ni(COD) ₂]/3, 5-(CF ₃) ₂ C ₆ H ₃	vinyl arenes	75-91	⁵
hydrosilylation	[Pd(π-C ₃ H ₅)Cl] ₂ /3, 5-(CF ₃) ₂ -H-MOP	styrenes	95-98	⁶
fluorination	[Pd(<i>m</i> -OH)(3, 5-Me ₂ -BINAP)] ₂ ⁺	cyclic β-keto esters	88-92	⁷

Unfortunately the application of such catalysts for non-asymmetric transformations has been relatively overlooked. Recently, White *et al.* applied rhodium complexes of *bis*(3, 5-dimethylphenyl)phosphine-DIOP and *bis*(3, 5-dimethylphenyl)phosphine-CBM for the hydroformylation of allyl alcohol,⁸ reporting significantly enhanced linear selectivity and suppression of C₃-product formation. Yields of 94.1 kg 4-hydroxybutanal per gram rhodium have been achieved with these species under optimised conditions. The corresponding activities are equally intriguing, but have not been explored further.

In this chapter we report the first systematic evaluation of how *meta*-methyl substitution in triarylphosphines affects their physicochemical requisites, both in isolated state and in their rhodium(I) complexes. The performance of [RhH(CO){(3, 5-Me₂Ph)₃P}₃] in allyl alcohol hydroformylation is presented from the perspectives of catalyst recycling and macrokinetics. Application of the aforementioned species in an alternative preparation of the neuroleptic *Fluspirelen* is also described.

3.2 Indexation of Ligand Characteristics

Hybrid triarylphosphines are of increasing interest as ligands, however systematic reports of their characteristics remain scarce in the literature. Specifically, the physicochemical exertions of a *meta*-methyl substituent on the aryl ring are of theoretical and experimental interest.⁹

Electronic parameters. Experimental determination of the electronic properties of a series of phosphines requires a responsive and sensitive probe. Relative scales have been constructed on the basis of collections and estimates of their acidity constants, calorimetric data and spectroscopic measurements of their transition metal carbonyl complexes,¹⁰ however the Tolman electronic parameter (χ) remains the preferred characterisation. Monodentate phosphines are related by the A_1 stretching frequency of their $[\text{Ni}(\text{CO})_3(\text{A})]$ complexes (Equation 1).¹¹

$$\nu_{\text{CO}} = \nu_{\text{CO}}[\text{Ni}(\text{CO})_3(\text{P}^t\text{Bu}_3)] + \chi \quad (\text{Equation 1})$$

Strong σ -donor phosphines decrease the formal charge on nickel, which increases nickel-CO π -back-bonding and shifts the relevant band to a lower frequency. The complexes $[\text{Ni}(\text{CO})_3(\text{L})]$ ($\text{L} = \text{PPh}_3$, $\text{P}(\text{C}_6\text{H}_4\text{-3-Me})_3$, $\text{P}(\text{C}_6\text{H}_3\text{-3, 5-Me}_2)\text{Ph}_2$, $\text{P}(\text{C}_6\text{H}_3\text{-3, 5-Me}_2)_2\text{Ph}$ and $\text{P}(\text{C}_6\text{H}_3\text{-3, 5-Me}_2)_3$) were prepared *in situ* from $[\text{Ni}(\text{CO})_4]$ in dichloromethane (Table 2). Tolman defined these conditions of measurement in order to eliminate the dependence of ν_{CO} on solvent choice and on packing effects and polymorphism in the solid state sample.^{11, 12}

Table 2: Spectral data for $[\text{Ni}(\text{CO})_3(\text{L})]$ in dichloromethane.^a

L	$A_1 \nu_{\text{CO}}$ (cm^{-1})	χ	$^{13}\text{C}\{^1\text{H}\} \delta^b$ (ppm)	C_B/E_B
PPh_3	2069.1	13.0	4.2	4.4
$\text{P}(\text{C}_6\text{H}_4\text{-3-Me})_3$	2067.0	10.9	4.4	5.2
$\text{P}(\text{C}_6\text{H}_3\text{-3, 5-Me}_2)\text{Ph}_2$	2067.8	11.7	4.3	4.8
$\text{P}(\text{C}_6\text{H}_3\text{-3, 5-Me}_2)_2\text{Ph}$	2066.8	10.7	4.4	5.2
$\text{P}(\text{C}_6\text{H}_3\text{-3, 5-Me}_2)_3$	2065.7	9.6	4.5	5.7

^aConditions: 2 mL dichloromethane, ~ 50 mM $[\text{Ni}(\text{CO})_3(\text{L})]$, 25°C, atmospheric pressure of nitrogen. ^b Reported downfield from $[\text{Ni}(\text{CO})_4]$.

Replacements of triphenylphosphine in $[\text{Ni}(\text{CO})_3(\text{L})]$ with tri(*meta*-methylphenyl)phosphine and *tris*-(3, 5-dimethylphenyl)phosphine shift the ν_{CO} band of the complex to lower frequency by 2.1 cm^{-1} and 3.4 cm^{-1} respectively. Similarly, each substitution of a phenyl-substituent in triphenylphosphine with a (3, 5-dimethylphenyl)-substituent shifts this to a lower frequency by ~ 1.0

cm^{-1} . The IR data confirm that a *meta*-methyl substituent exerts positive inductive and mesomeric effects on the conjugated system, with a corresponding shift of $\sim -0.6 \text{ cm}^{-1}$.

The data displays good proportionality for the sum of the Hammett parameter, $\sigma(m\text{-Me}) = -0.069$.¹³ The correlation is fitted by $r^2 = 0.98$, which demonstrates that the accuracy of the measurements made by this method. Moreover, insignificant deviation from this electronic correlation intimates effective isostericity of these triarylphosphines.

The IR data is advantageous because it can be reliably compared with that calculated from the electrostatic-covalent (ECW) model (Equation 2).¹⁴ In effect, E_B and C_B provide a dual-parameter, enthalpy-based σ -donor scale that is used to correlate the physicochemical measurement (x) and the donor-acceptor bond strength.

$$x = E_A E_B + C_A C_B + W \quad (\text{Equation 2})$$

In order to incorporate these hybrid triarylphosphines into the model, *in situ* formation of the $[\text{Ni}(\text{CO})_3(L)]$ adducts in d_2 -dichloromethane was additionally monitored by $^{13}\text{C}\{^1\text{H}\}$ NMR spectroscopy. Stronger nickel-CO π -back-bonding shields the carbon nucleus as separation between the ground state and the lowest energy excited states is reduced.¹⁵ The C_B/E_B ratio for each donor can then be calculated from the simultaneous equations, one for each physicochemical measurement. The relevant input values are $E_A = -52.4$, $C_A = -12.2$ and $W = 2143$ for $\nu\text{-}[\text{Ni}(\text{CO})_3(L)]$, and $E_A = 8.27$, $C_A = 1.95$ and $W = -7.47$ for $^{13}\text{C}\text{-}[\text{Ni}(\text{CO})_3(L)]$.^{14c}

Electrochemical behaviour. Most triarylphosphines are relatively easy to oxidise to the corresponding phosphoniumyl radical.¹⁶ It is well-established that the kinetic stability of such species is almost exclusively determined by the steric embrace of the phosphorus nucleus,¹⁷ so the anodic oxidations of triphenylphosphine, tri(*meta*-methylphenyl)phosphine and *tris*-(3, 5-dimethylphenyl)phosphine in *n*-butyronitrile were investigated (Table 3).

Table 3: Anodic oxidation data for triarylphosphines.^a

	pulse voltammetry		cyclic voltammetry	
	mV s^{-1}	E_p (V)	V s^{-1}	I^c/I^a
PPh ₃ (···)	10	1.41	0.25	0
			5	0
P(C ₆ H ₄ -3-Me) ₃ (---)	10	1.33	0.25	0
P(C ₆ H ₃ -3, 5-Me ₂) ₃ (—)	10	1.19	0.25	0
			5	0

^aConditions: 3.5 mL *n*-butyronitrile, 10 mM [*tris*(aryl)-phosphine], 0.1M [N^nBu_4][PF₆].

The life-time of a phosphoniumyl radical can be estimated from the ratio of cathodic peak current (I^c) to anodic peak current (I^a) in the cyclic voltammogram.¹⁸ The shapes of these did not change significantly upon increasing *meta*-substitution in the triarylphosphine, and non-detection of a cathodic peak current upon reversion of the potential sweep intimates that fundamentally transient phosphoniumyl radicals are generated (Figure 1). Even at a scanning rate of 5 V s^{-1} , the oxidations are virtually irreversible. This confirms a comparable kinetic stabilisation of the phosphoniumyl radical, and thus a comparable steric embrace of the phosphorus nucleus..

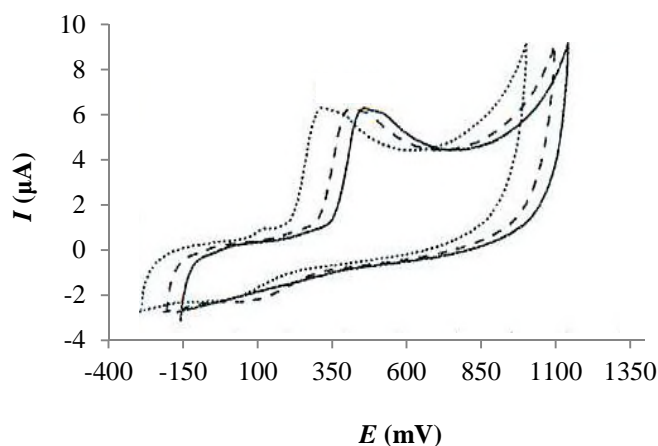


Figure 1. Cyclic voltammograms of systematic *meta*-substituted triarylphosphines.

The anodic oxidations of triphenylphosphine, *tris(meta-methylphenyl)phosphine* and *tris(3,5-dimethylphenyl)phosphine* in *n*-butyronitrile were also modulated by normal pulse voltammetry with reference to the saturated calomel electrode,¹⁹ which gave reproducible oxidation potentials (E_p). Defined diffusion-controlled anodic waves are evident from the voltammograms, and single electron oxidations are implicated (Figure 2).^{18b}

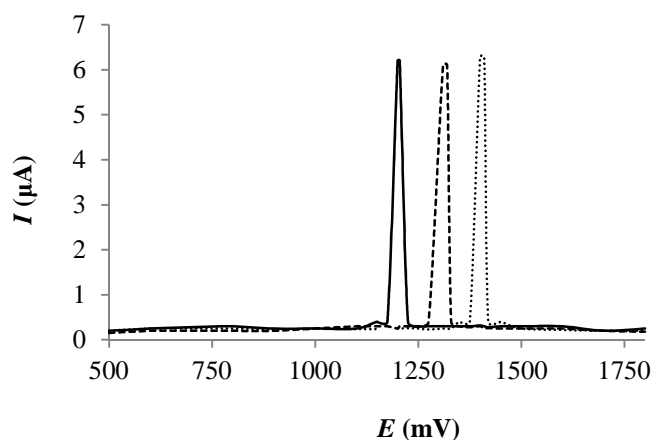


Figure 2. Normal pulse voltammograms of systematic *meta*-substituted triarylphosphines.

Changing from triphenylphosphine to tri(*meta*-methylphenyl)phosphine and *tris*-(3, 5-dimethylphenyl)phosphine reduces the oxidation potential by 0.08 V and 0.22 V respectively, reflecting a change in the energy of the HOMO. The systematic introduction of *meta*-methyl substituents increases the relative contribution of the 3*p* atomic orbital of the phosphorus nucleus to this molecular orbital, thereby increasing its energy and facilitating the expulsion of an electron.

Molecular structures. A structural comparison of hybrid *meta*-methyl substituted triarylphosphines is necessarily limited because a search of the Cambridge Crystallography Data Centre database led to the location of only three reported molecular structures of relevance; triphenylphosphine,²⁰ tri(3-methylphenyl)phosphine²⁰ and *tris*(3, 5-dimethyl-4-methoxyphenyl)phosphine.^{9b} White crystals of *tris*(3,5-dimethylphenyl)phosphine suitable for single crystal X-ray diffraction analysis were obtained by slow diffusion of *n*-pentane into a concentrated chloroform solution. The molecular structure is presented (Figure 3). Selected bond angles and distances for several of these geometries are presented in a comparative compilation (Table 4).

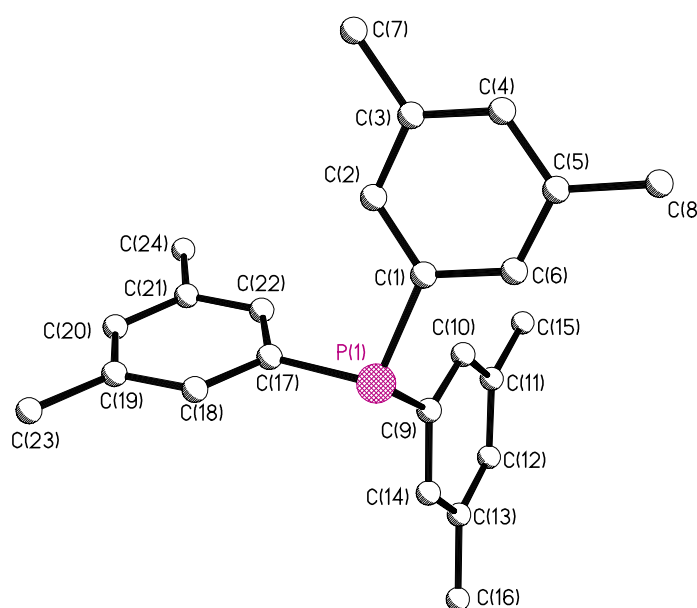


Figure 3. ORTEP drawing of *tris*(3, 5-dimethylphenyl)phosphine with ellipsoids at 50 % probability level. Hydrogen atoms are omitted for clarity.

The isomorphs adopt a paddle-like configuration in which the aryl rings extend from an axis of rotation and twist to impart a helical conformation to the molecule. The carbon-phosphorus-carbon bond angles in triphenylphosphine (*e.g.* C(1)-P(1)-C(9) = 102.0°), tri(3-methylphenyl)phosphine (*e.g.* C(1)-P(1)-C(9) = 102.2 °) and *tris*(3, 5-dimethylphenyl)phosphine (*e.g.* C(1)-P(1)-C(9) = 102.46°) correspond well with one another, suggesting that *meta*-methyl substituents do not significantly alter the steric configuration at the donor site. The phosphorus-carbon bond distances in

triphenylphosphine (e.g. P(1)-C(17) = 1.840 Å), tri(3-methylphenyl)phosphine (e.g. P(1)-C(17) = 1.838 Å) and tris(3, 5-dimethylphenyl)phosphine (e.g. P(1)-C(17) = 1.840 Å) are similarly convergent. The sp^2 - sp^2 and sp^2 - sp^3 carbon-carbon bond distances average 1.387 Å and 1.533 Å respectively.

Table 4: Selected bond lengths (Å) and bond angles (°) for triarylphosphines, (ESD).

bond distance		bond angle	
triphenylphosphine			
P(1)-C(1)	1.844 (6)	C(1)-P(1)-C(9)	102.0 (27)
P(1)-C(9)	1.820 (6)	C(1)-P(1)-C(17)	103.8 (28)
P(1)-C(17)	1.840 (5)	C(9)-P(1)-C(17)	101.7 (28)
C(17)-C(18)	1.406 (7)		
C(21)-C(24)	1.526 (7)		
tris(3-methylphenyl)phosphine			
P(1)-C(1)	1.838 (8)	C(1)-P(1)-C(9)	102.2 (3)
P(1)-C(9)	1.829 (7)	C(1)-P(1)-C(17)	102.2 (3)
P(1)-C(17)	1.838 (7)	C(9)-P(1)-C(17)	100.6 (3)
C(17)-C(18)	1.402 (12)		
C(21)-C(24)	1.532 (11)		
tris(3, 5-dimethylphenyl)phosphine			
P(1)-C(1)	1.838 (3)	C(1)-P(1)-C(9)	102.46 (12)
P(1)-C(9)	1.830 (3)	C(1)-P(1)-C(17)	103.22 (12)
P(1)-C(17)	1.840 (3)	C(9)-P(1)-C(17)	99.85 (11)
C(17)-C(18)	1.385 (4)		
C(21)-C(24)	1.517 (4)		

The torsional angles measured from the centroid of the three *ipso* carbons through the phosphorus nucleus back to the *ipso* carbons can be used to quantitatively describe the rotation of the aryl rings from vertical positions (Figure 4).²¹ By this technique, the zero-torsion angle occurs when the aryl ring eclipses the corresponding phosphorus-(*ipso*)carbon bond. An increase in the torsional angle is then proportional to the rotational freedom of the aryl ring. The average torsional angles for triphenylphosphine, tri(3-methylphenyl)phosphine and tris(3, 5-dimethylphenyl)phosphine are determined as 144°, 136° and 133° respectively. Although these differences are relatively minor, some restricted rotation is almost certainly imposed by short contacts between the methyl substituents on one aryl ring and the

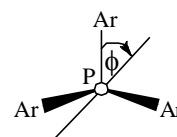


Figure 4. Torsional angle (ϕ) in triarylphosphines.

conjugated skeleton of another aryl ring. Pregosin *et al.* identified such contacts *via* intramolecular NOEs in the 2-dimensional NMR spectra of palladium and ruthenium complexes of *tris*(3, 5-di-*tert*-butylphenyl)phosphine.^{1a}

3.3 Rhodium(I) Chemistry Under Nitrogen

A solid state model of triarylphosphines intimates some restricted rotational freedom of *meta*-methyl substituted aryl rings around their phosphorus-(*ipso*)carbon bonds, and it is of interest to define how this is manifested in their rhodium(I) chemistry.

Isolated complexes. $[\text{Rh}(\text{CO})_2\text{Cl}]_2$ and the triarylphosphine reacted smoothly in cold toluene, with yellow prisms of the *trans*- $[\text{Rh}(\text{CO})(L)_2\text{Cl}]$ complex obtained upon ethanolic crystallisation of the crude residue (Table 5). The ^{31}P NMR spectra show a sharp doublet at $\delta_{\text{P}} = 29.8\text{--}31.7$ ppm, consistent with a *trans* square planar configuration of the phosphorus nuclei. Each substitution of a phenyl-substituent in triphenylphosphine with a (3, 5-dimethylphenyl)-substituent reduces the rhodium-phosphorus coupling, reflecting decreasing electronegativity of the triarylphosphines. In the IR spectra, the intense ν_{CO} band observed at $1974\text{--}1979\text{ cm}^{-1}$ is characteristic of a terminal CO auxiliary *trans* to chloride.²² The spectral data is in excellent agreement with that previously reported for *trans*- $[\text{Rh}(\text{CO})(\text{PPh}_3)_2\text{Cl}]$.^{22c}

Table 5: Spectroscopic and analytical data for *trans*- $[\text{Rh}(\text{CO})(L)_2\text{Cl}]$.

<i>L</i>	$^{31}\text{P}\{^1\text{H}\}$ NMR ^a		IR (cm ⁻¹) ^b	CHN found (calc.)	
	δ (ppm)	$^1J_{\text{Rh-P}}$ (Hz)	ν_{CO}	C	H
PPh ₃	31.7	132	1979 (s)	64.19 (64.32)	4.30 (4.38)
P(3, 5-Me ₂ Ph)Ph ₂	31.0	129	1977 (s)	65.85 (65.92)	4.99 (5.13)
P(3, 5-Me ₂ Ph) ₂ Ph	30.3	128	1976 (s)	67.47 (67.30)	5.84 (5.77)
P(3, 5-Me ₂ Ph) ₃	29.8	126	1974 (s)	68.48 (68.49)	6.41 (6.33)

^a1 mL *d*₃-chloroform, 7 mM [Rh], ambient temperature, atmospheric pressure of nitrogen. ^bKBr disc.

The solid state structure of *trans*- $[\text{Rh}(\text{CO})\{(3, 5\text{-Me}_2\text{Ph})_3\text{P}\}_2\text{Cl}]$ was determined. Yellow prisms suitable for single crystal X-ray diffraction analysis were obtained by slow diffusion of acetonitrile into a concentrated dichloromethane solution. The molecular structure and selected bond angles and distances are presented (Figure 5, Table 6). The complex has crystallographically imposed mirror symmetry, with a slightly distorted square planar rhodium geometry shown in the immediate bond angles ($\text{P}(1)\text{-Rh}(1)\text{-P}(2) = 172.7^\circ$, $\text{Cl}\text{-Rh}\text{-C} = 186.8^\circ$, $\text{Cl}(1)\text{-Rh}(1)\text{-P} < 90^\circ$ and $\text{C}(51)\text{-Rh}(1)\text{-P} > 90^\circ$). The bond distances in the nearest surrounding of rhodium ($\text{Rh}(1)\text{-P}(1) = 2.335\text{ \AA}$, $\text{Rh}(1)\text{-P}(2) = 2.326\text{ \AA}$, $\text{Rh}(1)\text{-C}(51) = 1.813\text{ \AA}$ and $\text{Rh}(1)\text{-Cl}(1) = 2.361\text{ \AA}$) correspond well with those of *trans*-

[Rh(CO)(PPh₃)₂Cl].²³ The bond distance in CO (C-O = 2.14 Å) is considered fairly standard for complexes of this type.²⁴ With relevance to the hydroformylation scheme [Rh(CO){(3, 5-Me₂Ph)₃P}₂Cl] can be considered a structural model of [RhH(CO){(3, 5-Me₂Ph)₃P}₂],²⁵ formed by CO dissociation from the catalyst resting state. Square planar hydride complexes of nickel, molybdenum and tungsten have previously been generated by substitution of halide auxiliaries using SuperHydride®.²⁶ Unfortunately, attempts to convert [Rh(CO){(3, 5-Me₂Ph)₃P}₂Cl] to its hydride analogue by this method failed. Square planar [RhH(CO)(L)₂] species are rarely observed.²⁷

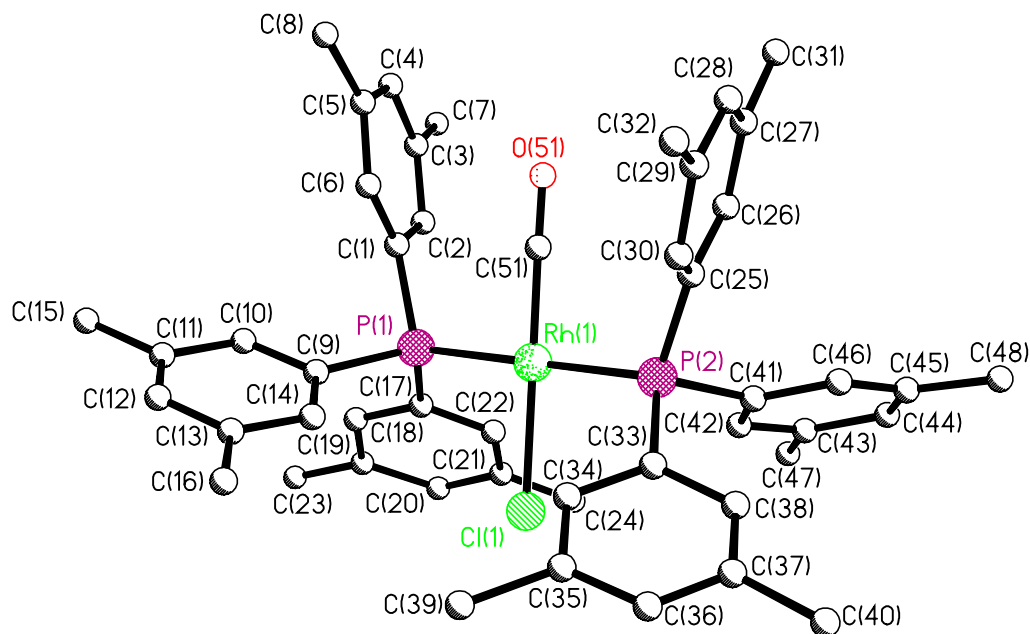


Figure 5. ORTEP drawing of *trans*-[Rh(CO){(3, 5-Me₂Ph)₃P}₂Cl] with ellipsoids at 50 % probability level.

Hydrogen atoms are omitted for clarity.

Table 6: Selected bond distances (Å) and bond angles (°) for *trans*-[Rh(CO){(3, 5-Me₂Ph)₃P}₂(CO)], (ESD).

bond distance		bond angle	
Rh(1)-P(1)	2.335(19)	P(1)-Rh(1)-P(2)	172.7(3)
Rh(1)-P(2)	2.326(2)	C(51)-Rh(1)-Cl(1)	186.8(3)
Rh(1)-C(51)	1.813(3)	P(1)-Rh(1)-Cl(1)	87.11(8)
Rh(1)-Cl(1)	2.361(7)	P(2)-Rh(1)-Cl(1)	87.11(8)
		P(1)-Rh(1)-C(51)	93.0(3)
		P(2)-Rh(1)-C(51)	92.8(3)
C(51)-O(51)	1.126(4)		
P(1)-C(1)	1.818(7)	Rh-P(1)-C(1)	114.9(2)
P(1)-C(17)	1.833(8)	Rh-P(1)-C(17)	115.6(2)

Solution dynamics under nitrogen. To complement the measurements of the isolated structures, the solution dynamics of $[\text{Rh}(\text{CO})\{(3, 5\text{-Me}_2\text{Ph})\text{Ph}_2\text{P}\}_2\text{Cl}]$ and $[\text{Rh}(\text{CO})\{(3, 5\text{-Me}_2\text{Ph})_2\text{PhP}\}_2\text{Cl}]$ were probed by variable temperature ^1H NMR spectroscopy (Figure 6).

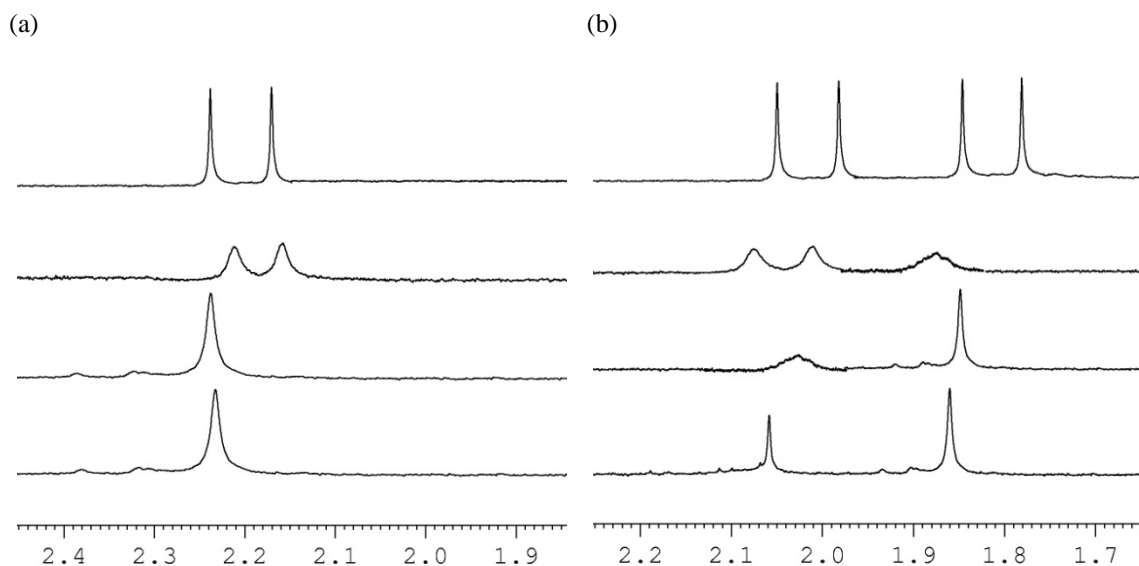


Figure 6. Variable temperature ^1H NMR spectra of $[\text{Rh}(\text{PAr}_3)_2(\text{CO})\text{Cl}]$ (methyl region):

- (a) $\text{PAr}_3 = \text{P}(3, 5\text{-Me}_2\text{Ph})\text{Ph}_2$ at 25°C, -10°C, -30°C, -60°C (ascending),
 (b) $\text{PAr}_3 = \text{P}(3, 5\text{-Me}_2\text{Ph})_2\text{Ph}$ at 25°C, -10°C, -30°C, -60°C (ascending).

The methyl protons in $[\text{Rh}(\text{CO})\{(3, 5\text{-Me}_2\text{Ph})\text{Ph}_2\text{P}\}_2\text{Cl}]$ are resolved as a sharp singlet at ambient temperature, but at -30°C rotation of the *meta*-substituted ring around its phosphorus-(*ipso*)carbon bond begins to become restricted. This rotation is frozen at -60°C. The ^1H NMR spectrum of $[\text{Rh}(\text{CO})\{(3, 5\text{-Me}_2\text{Ph})_2\text{PhP}\}_2\text{Cl}]$ is marked by two spin systems, due to a configuration with one *meta*-substituted ring in an equatorial site and the other in a *pseudo*-axial site (Figure 7).

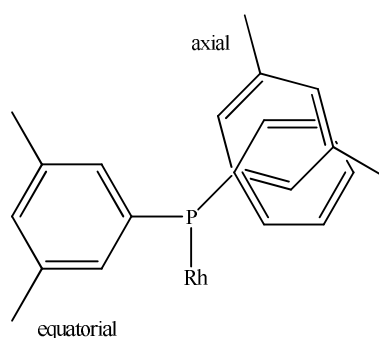


Figure 7. Aryl ring positions in a rhodium-coordinated fragment of $\text{P}(3, 5\text{-Me}_2\text{Ph})_2\text{Ph}$.

Restricted phosphorus-(*ipso*)carbon rotation begins to affect one of these at -10°C, the low barrier to rotation implicating the equatorial analogue.^{1b} The two inequivalent methyl signals are resolved at -

30°C, and at this temperature slower dynamic of the second *meta*-substituted is also noted. The four methyl signals are resolved at -40°C.

Rate constants for the phosphorus-(*ipso*)carbon rotation of the 3, 5-dimethylphenyl moieties in $[\text{Rh}(\text{CO})\{(3, 5\text{-Me}_2\text{Ph})\text{Ph}_2\text{P}\}_2\text{Cl}]$ and $[\text{Rh}(\text{CO})\{(3, 5\text{-Me}_2\text{Ph})_2\text{PhP}\}_2\text{Cl}]$ were determined by dynamic line-shape analyses of the ^1H NMR and simulated ^1H NMR spectra at -30°C, and the corresponding activation barriers were calculated from the Eyring equation (Equation 3) (Table 7).

Table 7: Phosphorus-(*ipso*)carbon rotation in $[\text{Rh}(\text{CO})(\text{L})_2\text{Cl}]$.^a

<i>L</i>	<i>k</i> (Hz)	$\Delta^\ddagger G_{243\text{K}}$ (kJ mol ⁻¹)
(3, 5-Me ₂ Ph)Ph ₂ P	8630	40.79
(3, 5-Me ₂ Ph) ₂ PhP (<i>e</i>)	3192	42.23
(3, 5-Me ₂ Ph) ₂ PhP (<i>pseudo-a</i>)	2966	42.27

$$k = \left(\frac{k_B T}{h}\right) e^{\frac{-\Delta G}{RT}} \quad (\text{Equation 3})$$

^a1 mL *d*₈-toluene, 7 mM [Rh], -30°C, atmospheric pressure of nitrogen.

These calculations suggest that substitution of a phenyl substituent in a hybrid triarylphosphine with a (3, 5-dimethylphenyl) substituent increases the rotational activation barrier by ~1.5 kJ mol⁻¹,²⁸ almost certainly because the motion of *meta*-substituted aryl rings past each other is more strained. Stabilisation of the *pseudo*-axial aryl by π -stacking with the conjugated skeleton in *trans*- $[\text{Rh}(\text{CO})\{(3, 5\text{-Me}_2\text{Ph})_2\text{PhP}\}_2\text{Cl}]$ presumably accounts for the slightly higher barrier to rotation relative to the equatorial aryl. It is worth noting that this steric effect should be more significant in the five-coordinate transition states of the hydroformylation scheme.

Solubility. *Trans*- $[\text{Rh}(\text{CO})(\text{L})_2\text{Cl}]$ is smoothly converted to the $[\text{RhH}(\text{CO})(\text{L})_3]$ complex by sequential reduction with sodium propoxide and hydrogen,²⁹ for which solubility behaviour was then examined (Table 8). NMR analyses highlight a similarity between these species, indicating that the introduction of two *meta*-methyl substituents does not significantly affect structural and electronic properties of the parent complex.

Table 8: Selected NMR data and solubility data for $[\text{RhH}(\text{CO})(\text{L})_3]$ in various organic media.

<i>L</i>	NMR ^a		solubility (g L ⁻¹) ^b			
	δ_P (ppm)	$^1J_{\text{Rh-H}}$ (Hz)	toluene	diethyl ether	acetone	methanol
PPh ₃	19.2	9.4	83	76	65	33
P(C ₆ H ₃ -3, 5-Me ₂)Ph ₂	19.2	9.6	96	70	59	32
P(C ₆ H ₃ -3, 5-Me ₂) ₂ Ph	19.5	9.7	110	65	52	24
P(C ₆ H ₃ -3, 5-Me ₂) ₃	19.7	9.9	120	62	44	19

^aIn *d*₃-chloroform. ^bSolubility in HPLC-grade solvent at 25°C.

Upon changing from acetone to diethyl ether to toluene, solubilities of the $[\text{RhH}(\text{CO})(\text{L})_3]$ complexes improve with decreasing polarity of the medium. The magnitude of the change corresponds to the *meta*-methyl substitution pattern in the triarylphosphine, which expands the lipophilic domain of its complex making it relatively more apolar. Relatively low solubilities in methanol are no doubt due to the poor hydrogen bonding character of these species.

3.4 Catalysis

To evaluate the *meta*-effect as a control element for catalyst performance, the complex $[\text{RhH}(\text{CO})\{(3, 5\text{-Me}_2\text{Ph})_3\text{P}\}_3]$ was prepared. Using the hydroformylation of allyl alcohol in toluene as a model reaction, the effects of the operating conditions on the performance of the catalyst were assessed.³⁰ The catalyst solutions were incubated at the requisite temperature and CO/H_2 pressure for 10 minutes to allow milieu stabilisation. The specific activity of the catalyst is best described by a conversion-time profile, from which mass balance and reaction stoichiometry can also be estimated.

In the experimental range of operating conditions a product mixture of typically > 93% linear aldehyde (2-hydroxyfuran) and < 7% branched aldehyde (2-methylpropanal) is recovered.³¹ This high regioselectivity is ascribed specifically to the steric exertions of the *meta*-methyl substituents on the rings of the triarylphosphine. The restricted rotation of the (3, 5-dimethylphenyl) moieties around their phosphorus-(*ipso*)carbon bond in addition to steric crowding, which makes this ligand more intrusive with respect to other auxiliaries, should create a rigid and well-defined coordination sphere around rhodium.

Catalyst concentration. The dependence of conversion and selectivity on the catalyst concentration is presented (Figure 8). Complete conversion is achieved in all cases in < 14 minutes. Catalyst productivity increases five-fold along the experimental range, making catalyst concentration a limiting factor for the activity. The catalyst gives little activity for the isomerisation of allyl alcohol, typically < 0.25 mol %, which suggests that an intermediate hydrido η^3 -allyl rhodium configuration required cannot be accommodated.³¹ Unusually, no activity for the hydrogenation of allyl alcohol is observed.

Calculated at complete conversion, linear selectivity increases from $l/b = 14.7$ at $[\text{Rh}] = 4.27$ mM to $l/b = 18.2$ at $[\text{Rh}] = 6.83$ mM. These are exceptionally high ratios for allyl alcohol and particularly impressive in consideration of the modest L/Rh molar ratio used. Similar patterns have been reported for $[\text{RhH}(\text{CO})(\text{Ph}_3\text{P})_3]$ ³² and $[\text{RhH}(\text{CO})\{(p\text{-CF}_3\text{-C}_6\text{H}_4)_3\text{P}\}_3]$.³² It is assumed that high catalyst loadings minimise dissociation of the active species, in the *tris*-carbonyl end-product is active for branch-selective hydroformylation:

$[\text{RhH}(\text{CO})\{(3, 5\text{-Me}_2\text{Ph})_3\text{P}\}_3] \leftrightarrow [\text{RhH}(\text{CO})_2\{(3, 5\text{-Me}_2\text{Ph})_3\text{P}\}_2] \leftrightarrow [\text{RhH}(\text{CO})_3\{(3, 5\text{-Me}_2\text{Ph})_3\text{P}\}_2]$.³³
 The distribution of the regio-isomers in time changes more significantly at higher catalyst concentrations, which suggests that the rate of branch-selective hydroformylation becomes increasingly competitive. Kinetic selectivity studies have previously shown that the rate of linear-selective hydroformylation and the rate of branch-selective hydroformylation are most accurately expressed by different models.³⁴

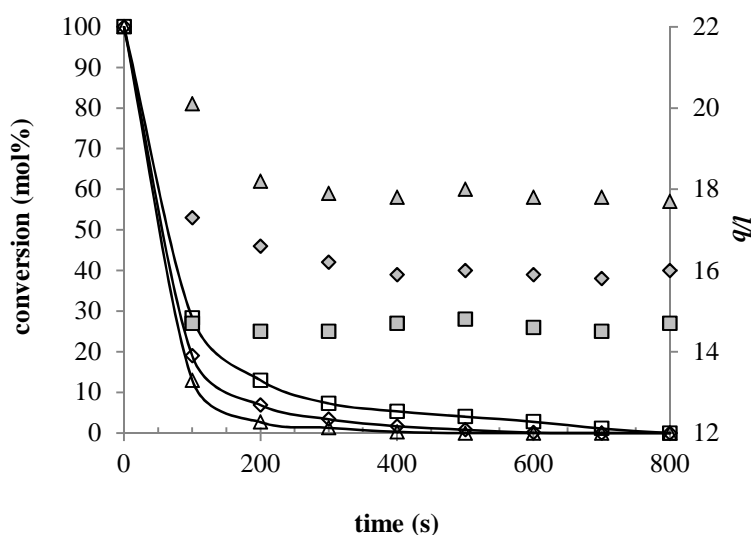


Figure 8. Conversion-time profiles for allyl alcohol hydroformylation with $[\text{RhH}(\text{CO})\{(3, 5\text{-Me}_2\text{Ph})_3\text{P}\}_3]$ at variable catalyst concentration: (\square) 4.27 mM [Rh], (\diamond) 5.12 mM [Rh], (\triangle) 6.83 mM [Rh], $(\square - \diamond - \triangle)$ l/b ratio. (Conditions: 4 mL toluene, 2.94 M [allyl alcohol], 353 K, 30 bar $\text{CO}/\text{H}_2 = 1$)

Allyl alcohol concentration. The demonstration of consistently high specific activity at a high substrate/catalyst molar ratio is an important measure of the commercial feasibility of a catalytic reaction. The effect of the allyl alcohol concentration on conversion and selectivity is presented (Figure 9).

Calculated at 5 minutes, conversion drops from 100 mol% at $\text{Rh}/\text{S} = 1/257$ to 89 mol% at $\text{Rh}/\text{S} = 1/861$. This is correlated with a higher activity for the isomerisation of allyl alcohol which ties up the catalyst in an alternative pathway. Furthermore, Strohmeier and Michel have shown that hydroformylation catalyses at high substrate concentrations proceed with negligible conversion due to formation of the inactive carbonyl-bridged rhodium dimer.³⁵

The regioselectivity is found to be adversely affected by increasing allyl alcohol concentration, suggesting that the branch-selective scheme is higher order with respect to this parameter than the linear-selective pathway. Similar behaviour has been recognised in selectivity

studies on the cobalt-catalysed hydroformylation of propene and the rhodium-catalysed hydroformylation of vinyl acetate.^{34b, 36}

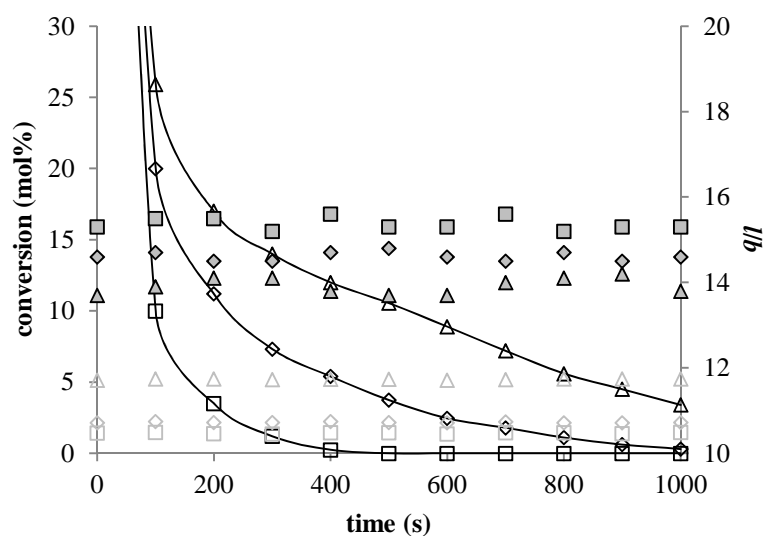


Figure 9. Conversion-time profiles for allyl alcohol hydroformylation with $[\text{RhH}(\text{CO})\{(3, 5\text{-Me}_2\text{Ph})_3\text{P}\}_3]$ at variable substrate concentration: (\square) 1.76 M [allyl alcohol], (\diamond) 2.94 M [allyl alcohol], (\triangle) 5.88 M [allyl alcohol], (\square - \diamond - \triangle) 1-propanal, (\blacksquare - \blacklozenge - \blacktriangle) l/b ratio. (Conditions: $(5-V_{\text{substrate}})$ mL toluene, 6.83 mM [Rh], 333 K, 40 bar $\text{CO}/\text{H}_2=1$)

Recycling. The solution stability of $[\text{RhH}(\text{CO})\{(3, 5\text{-Me}_2\text{Ph})_3\text{P}\}_3]$ was assessed by recycling experiments under reaction conditions approximating the process parameters used by Lyondell-Basell (Table 9).³⁷ After each cycle the reaction mixture was carefully transferred from the autoclave with a small overpressure and the catalyst was recycled efficiently following aqueous extraction of the products.

Table 9: Recyclability of $[\text{RhH}(\text{CO})\{(3, 5\text{-Me}_2\text{Ph})_3\text{P}\}_3]$ in the hydroformylation of allyl alcohol by toluene/water extraction.^a

cycle	TOF ^b (h^{-1})	ar ^c	$[\text{Rh}]_{\text{aq}}$	$[\text{P}]_{\text{aq}}$
1	13.95×10^2			
2	13.74×10^2	0.98	2.1 ppm	7.7 ppm
6	13.35×10^2	$\langle 0.99 \rangle^{ci}$		
7	11.72×10^2	0.88		
12	7.33×10^2	$\langle 0.92 \rangle^{cii}$	208.9 ppm	691.2 ppm

^aConditions: 4 mL toluene, 5.12 mM [Rh], Rh/allyl alcohol = 1/574, 343 K, 10 bar $\text{CO}/\text{H}_2=1$. ^bTurnover frequency defined as mol conversion per mol initial Rh per hour. ^cActivity retention ($ar = a_{\text{cycle}(n)}/a_{\text{cycle}(n-1)}$), ⁱaverage per cycle for cycles 3-6, ⁱⁱaverage per cycle for cycles 8-12.

Conversion is only significantly reduced after six or more consecutive cycles. The product layers from cycles 6-12 are observed to be of a pale orange colour, suggesting some leaching of the catalyst. Analysis of the collective aqueous extract by ICP-MS confirmed this view. Both rhodium (208.9 ppm) and phosphorus (691.2 ppm) were detected, corresponding to a loss of 3.4% of initial rhodium and 3.75% of initial phosphorus per cycle.³⁸ It seems that an initial catalyst leaching enhances this effect through subsequent cycles.

Despite a decrease in the turnover frequency, the total turnover number achieved after multiple cycles make a strong case for the use of $[\text{RhH}(\text{CO})\{(3, 5\text{-Me}_2\text{Ph})_3\text{P}\}_3]$ in continuous flow mode (Figure 10). The catalyst aliquot can be recycled twelve times, with $\sim 94\%$ catalyst activity retention per cycle giving a cumulative turnover number of 14.66×10^4 mol per mol of catalyst. This is significantly higher than the cumulative turnover number achieved with $[\text{RhH}(\text{CO})(\text{PPh}_3)_3]$.

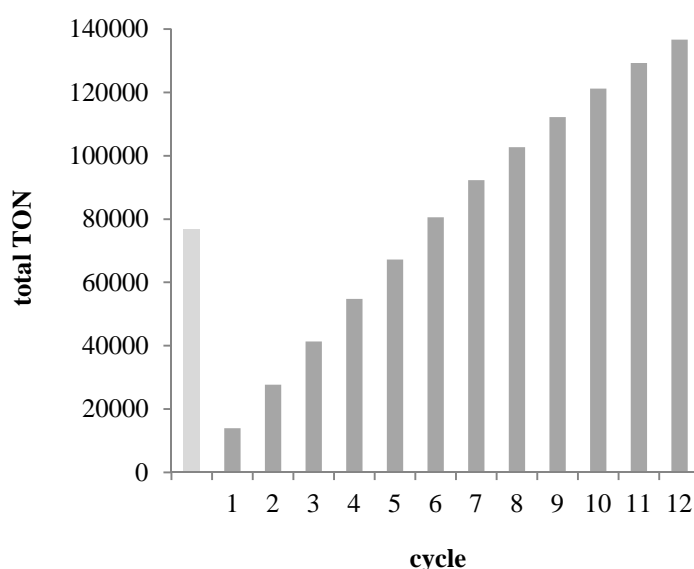


Figure 10. Cumulative turnover number achieved in the hydroformylation of allyl alcohol:

(■) $[\text{RhH}(\text{CO})\{(3, 5\text{-Me}_2\text{Ph})_3\text{P}\}_3]$, (□) $[\text{RhH}(\text{CO})(\text{Ph}_3\text{P})_3]$ in cycle 12.

(Conditions: 4 mL toluene, 5.12 mM [Rh], Rh/allyl alcohol = 1/574, 343 K, 10 bar CO/H₂= 1)

3.5 Macrokinetics

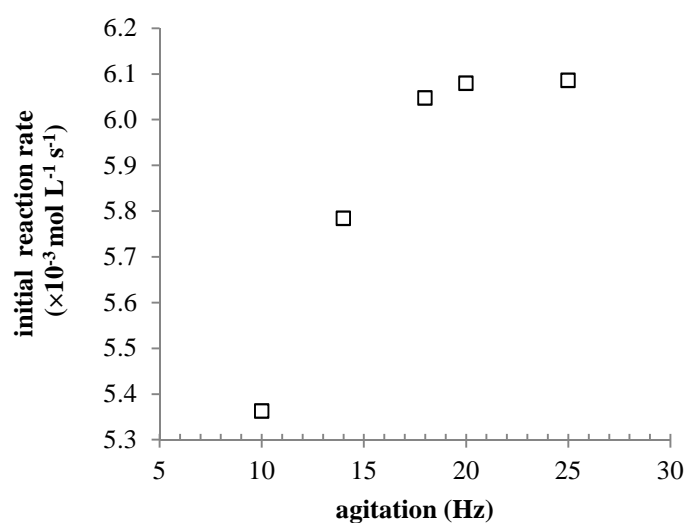
Ideally, the rate equation of a catalytic reaction allows recognition of mechanistic aspects over a broad range of operating conditions and application for engineering designs.³⁹ The kinetics of allyl alcohol hydroformylation with $[\text{RhH}(\text{CO})\{(3, 5\text{-Me}_2\text{Ph})_3\text{P}\}_3]$ in toluene was therefore systematically investigated (Table 10).

Table 10: Experimental range for macrokinetic study on hydroformylation of allyl alcohol with $[\text{RhH}(\text{CO})\{(3, 5\text{-Me}_2\text{Ph})_3\text{P}\}_3]$.

catalyst concentration (mM)	4.27-8.54
allyl alcohol concentration (M)	0.59-5.88
carbon monoxide partial pressure (MPa)	0.20-2.03
hydrogen partial pressure (MPa)	0.51-2.03
temperature (K)	333-353
medium	toluene
reaction volume (mL)	5

Material balance. For accurate kinetic analysis it was necessary to first illustrate mass balance and gas balance (Table 11). Measured at three-minute intervals, the observed molar consumptions of carbon monoxide and hydrogen correspond well with the requisite consumption calculated from the molar formation of hydroxyaldehyde products. The calculated composition of CO/H_2 in the autoclave at each interval confirms that supply of $\text{CO}/\text{H}_2 = 1$ is adequate to maintain the initial stoichiometry of the gaseous reagents. The calculated amount of hydrogen correlates with that determined by gas analysis of the sample within a 4% error range.

Kinetic regime. Since hydroformylation involves gaseous reagents in a liquid medium, kinetic analysis must be performed with no possibility for mass-transfer limitations.⁴⁰ By evaluating the reaction rate as a function of agitation, kinetic regime is identified above 18 Hz (Figure 11). Therefore consecutive rate data has been collected at an agitation speed of 20 Hz.

**Figure 11.** Activity of $[\text{Rh}\{(3, 5\text{-Me}_2\text{Ph})_3\text{P}\}_3(\text{CO})\text{H}]$ in the hydroformylation of allyl alcohol as a function of agitation.

(Conditions: 4 mL toluene, 6.83 mM $[\text{Rh}]$, $\text{Rh}/\text{allyl alcohol} = 1/690$, 353 K, 40 bar $\text{CO}/\text{H}_2 = 1$)

Table 11: Mass balance in the hydroformylation of allyl alcohol with [RhH(CO){(3, 5-Me₂Ph)₃P}₃] in toluene.^a

	0 min	3 min	6 min	9 min
2-hydroxyfuran (mmol)	0.00	7.06	16.36	20.99
2-methylpropanal (mmol)	0.00	0.42	0.91	1.23
1-propanal (mmol)	0.00	0.11	0.17	0.17
allyl alcohol conversion (mmol)	-	7.59	17.44	22.39
carbon monoxide requirement (mmol)	0.00	7.48	17.27	22.22
hydrogen requirement (mmol)	0.00	7.90	18.18	23.45
CO/H ₂ requirement (mmol)	-	15.38	35.45	45.67
CO/H ₂ requirement (MPa)	-	1.07	2.46	3.17
CO/H ₂ consumed	-	18/19	19/20	18/19
CO/H ₂ consumed (MPa)	0.00	1.12	2.52	3.26
CO/H ₂ consumed (mmol)	-	16.14	36.31	46.25
material balance error (%)	-	< 4.7	< 2.5	< 2.8
CO/H ₂ restocked (MPa)	0.00	0.56	1.23	1.59
CO/H ₂ restocked (mmol)	-	0.56	1.23	1.59
		8.07	17.72	22.91
		8.07	17.72	22.91
autoclave carbon monoxide content (mmol)	29.20	29.42	29.23	29.61
autoclave hydrogen content (mmol)	29.20	28.99	28.30	28.36
autoclave carbon monoxide content (%)	50.00	50.37	50.81	51.08
autoclave hydrogen content (%)	50.00	49.63	49.19	48.92

^aConditions: 4.4 mL toluene, 1.71 mM [Rh], Rh/allyl alcohol = 1/1029, 343 K, 4.05 MPa CO/H₂ = 1.

The presence of kinetic regime can be confirmed upon evaluating the ratio of observed rate to maximum mass transport rate, as proposed by Chaudhari and Doraiswamy (Equation 3).⁴² The maximum mass transport rate for a gas is defined as the product of its concentration in the liquid and the mass transport coefficient.

$$\alpha = \frac{k_{obs}}{c(k_1 a)} \quad (\text{Equation 3})$$

The solubility of the gas at the interface was calculated from the relevant Henry constant (Table 13). The volumetric mass transport coefficient was determined as 0.3039 s⁻¹ from the proposed correlation (Equation 4). For catalysis described herein, α_{CO} is in the range 0.11-0.46 and α_{H_2} is in the range 0.08-0.34 confirming that the rate of hydroformylation is generally lower than the prevailing rate of mass transfer.

$$k_1 a = (1.48 \times 10^{-3})(s)^{2.18} \left(\frac{v_g}{v_l}\right)^{1.88} \left(\frac{d_1}{d_2}\right)^{2.1} \left(\frac{h_1}{h_2}\right)^{1.16} \quad (\text{Equation 4})$$

s	agitation (Hz)	20.0
v_g	gas volume (m^3)	10.2×10^{-5}
v_l	liquid volume (m^3)	5.0×10^{-5}
d_1	rotor diameter (m)	2.0×10^{-2}
d_2	autoclave diameter (m)	3.7×10^{-2}
h_1	rotor height (m)	0.4×10^{-2}
h_2	liquid height (m)	1.4×10^{-5}

Gas solubilities. Solubility data for carbon monoxide and for hydrogen in the liquid medium are necessary for interpreting hydroformylation kinetics, and are also of practical interest for calculating vapour-liquid equilibria in systems with commercial potential. A large volume of solubility data for these gases in neat liquids is available,⁴³ but a literature search has shown that for liquid mixtures this information is limited.⁴⁴

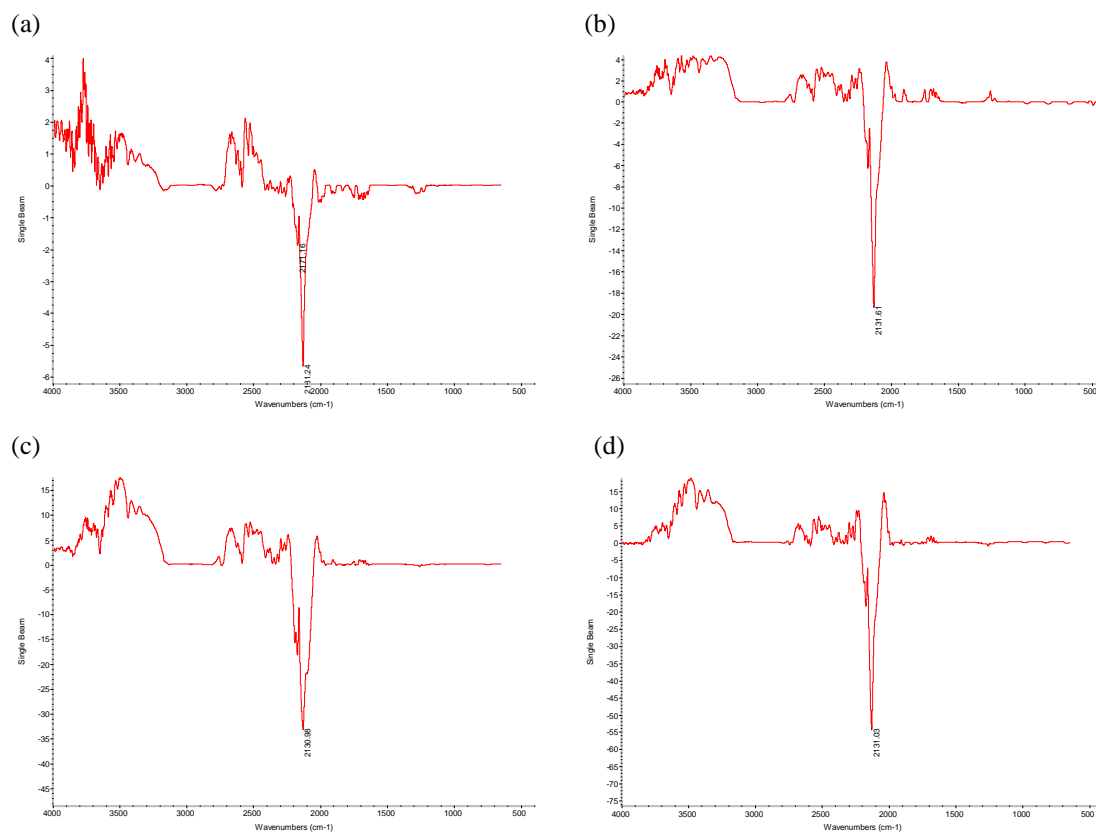


Figure 12. HP-IR spectra of carbon monoxide in toluene at 333K:

(a) 0.71 MPa, (b) 2.33 MPa, (c) 4.05 MPa, (d) 6.79 MPa.

The concentration of carbon monoxide in mixtures of toluene and allyl alcohol was determined experimentally at 333 K, 343 K and 353 K in the pressure range 0.71-6.79 MPa, using beam depth measured by high-pressure IR spectroscopy. A worked example is presented (Figures 12-13, Table 12).

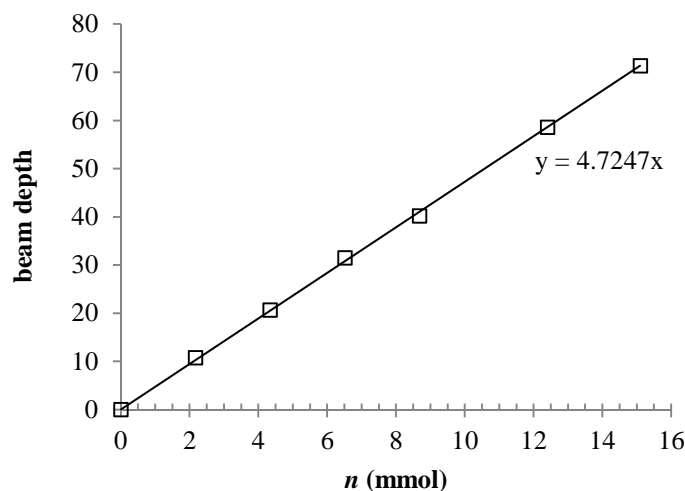


Figure 13. Beam-depth calibration for carbon monoxide solubility in toluene.

Table 12: HP-IR data for carbon monoxide solubility in toluene at 333 K.^a

	0.71 MPa	2.33 MPa	4.05 MPa	6.79 MPa
spectral quality				
allowed range	5.6-9.8	5.6-9.8	5.6-9.8	5.6-9.8
peak value	8.92	9.06	8.77	9.44
analysis				
ν_{CO} (cm ⁻¹)	2131	2132	2131	2131
beam depth	4.04	18.92	33.01	54.18
n (mmol)	0.84	4.00	6.98	11.45
[CO] (mol L ⁻¹)	0.04	0.20	0.35	0.57

^aConditions: 20 mL toluene, 333 K, mixing period of 15 minutes at 15 Hz.

In accordance with Henry's law (Equation 5) the concentration increases linearly with pressure; this correlation is fitted by $r^2 > 0.99$. The solubility is therefore best defined as the Henry constant (K_H) (Table 13). Good agreement with the literature data demonstrates the validity of this methodology.

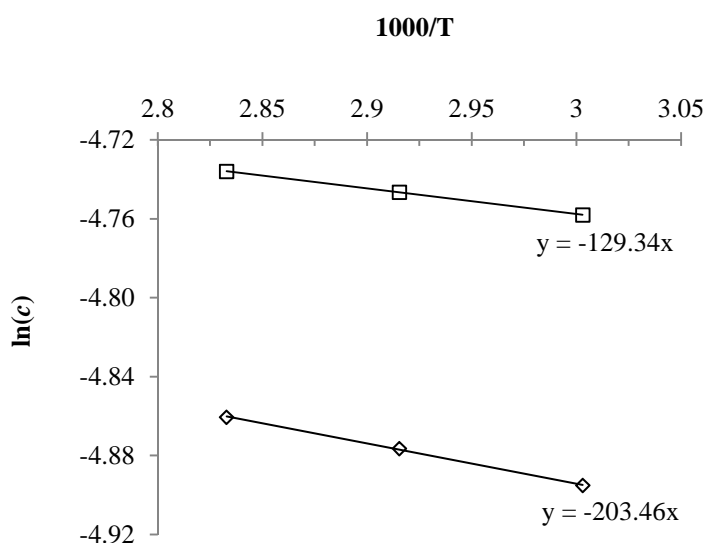
$$K_H = \frac{p}{c} \quad (\text{Equation 5})$$

Table 13: Henry constants (MPa L mol⁻¹) for carbon monoxide and hydrogen in mixtures of toluene and allyl alcohol.

liquid mixture	solute gas	333 K	343 K	353 K
toluene	carbon monoxide	11.81 (11.90 ^a)	11.67 (11.70 ^a)	11.55 (11.53 ^b)
toluene	hydrogen	29.30 ^c	28.10 ^c	26.80 ^b
10% allyl alcohol/toluene	carbon monoxide	12.01	11.86	11.68
20% allyl alcohol/toluene	carbon monoxide	12.22	12.04	11.89
40% allyl alcohol/toluene	carbon monoxide	12.47	12.41	12.33
80% allyl alcohol/toluene	carbon monoxide	13.12	13.07	12.65
allyl alcohol	carbon monoxide	13.54	13.29	13.08

^a44c in References and Notes. ^b45 in References and Notes. ^c43a in References and Notes.

The solubility of carbon monoxide increases with temperature, but this effect is relatively small. It has previously been shown that the solubility of carbon monoxide is reduced in polar liquids,^{44b, 45} and this trend is observed as the concentration of allyl alcohol in toluene increases. The enthalpy of carbon monoxide dissolution is estimated to be $\Delta^{abs}H = 1.07 \text{ kJ mol}^{-1}$ in toluene and $\Delta^{abs}H = 1.69 \text{ kJ mol}^{-1}$ in allyl alcohol (Figure 14).

**Figure 14.** Eyring plot for carbon monoxide concentration in organic liquids at 0.101 MPa:

(□) toluene, (◇) allyl alcohol.

The solubility of carbon monoxide in neat toluene has been additionally calculated using a semi-empirical correlation based on the theory of regular solution (Equation 6).⁴⁶

$$-\ln(c_2) = \ln\left(\frac{f_2^l}{f_2^0}\right) + \frac{\Phi_1 v_2 (\delta_1 - \delta_2)^2}{RT} \quad (\text{Equation 6})$$

$\ln(f_2^l)$	fugacity of hypothetical liquid solute (atm)	Equation 7
$\ln(f_2^0)$	fugacity of pure gas (atm)	Equation 8
Φ_1	volume fraction of solvent	unity
v_2	molar liquid volume of solute ($\text{m}^3 \text{mol}^{-1}$)	3.210×10^{-5}
δ_1	solvent solubility parameter ($\text{J}^{0.5} \text{m}^{-1.5}$)	18.203×10^{-3}
δ_2	gas solubility parameter ($\text{J}^{0.5} \text{m}^{-1.5}$)	6.403×10^{-3}

The fugacity of the hypothetical liquid solute is determined by the critical temperature and critical pressure of carbon monoxide, and may be calculated from the correlation between fugacity and temperature in the range 273-373 K (Equation 7).^{46b}

$$\ln(f_2^l) = 4.7475 + 588.52T^{-1} - (1.3151 \times 10^5)T^{-2} \quad (\text{Equation 7})$$

The fugacity of pure carbon monoxide is defined as the pressure quotient needed at a given temperature to satisfy the ideal gas equation, and can be calculated from its fugacity coefficient (Equation 8).^{46c}

$$\ln(f_2^0) = \left(\frac{37.59 - 155.15 \left(\frac{133}{T}\right)^{1.5}}{RT} \right) \quad (\text{Equation 8})$$

The theory of regular solution postulates that activity coefficients are inversely proportional to temperature, so that the term $(\Phi_1 v_2 (\delta_1 - \delta_2)^2)$ is constant with temperature. The solubility parameter for carbon monoxide and its molar volume were therefore taken from the literature.⁴⁷ The solubility parameter for toluene was determined from its heat of vapourisation at 298 K and molar volume (Equation 9).⁴⁸ This approach is only valid for non-polar liquids; a correction factor must be introduced to determine the solubility parameter for polar liquids.⁴⁹

$$\delta_1 = \left(\frac{\Delta H_v - RT}{v_2} \right) \quad (\text{Equation 9})$$

From the concentration of solute gas in the liquid phase thus calculated, the Henry constant is determined. The comparison between theoretical and experimental solubilities is fitted by $r^2 > 0.97$ (Figure 15).

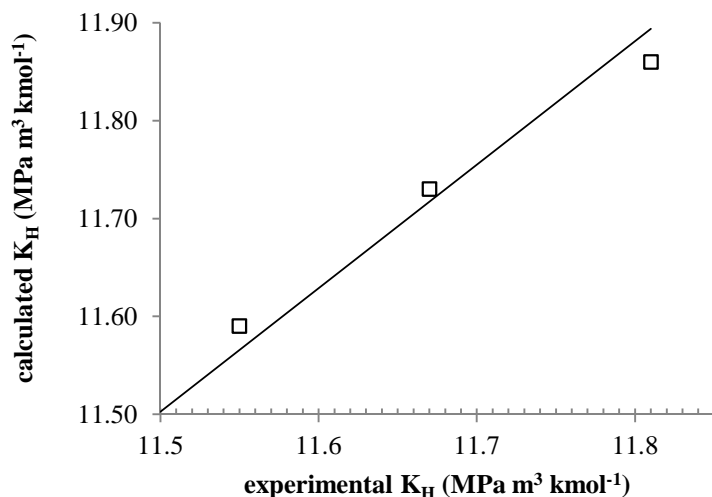


Figure 15. Correlation of calculated and experimental solubility of carbon monoxide in toluene.

The solubility data for hydrogen in toluene was taken directly from the literature (Table 13). Liquid mixtures should affect carbon monoxide solubility more significantly than hydrogen solubility due to the presence of a dipole moment and higher polarisability.⁵⁰

Initial rate data. Initial rates of hydroformylation were determined from reaction profile plots of CO/H₂ uptake in time using IGOR PRO.⁵¹

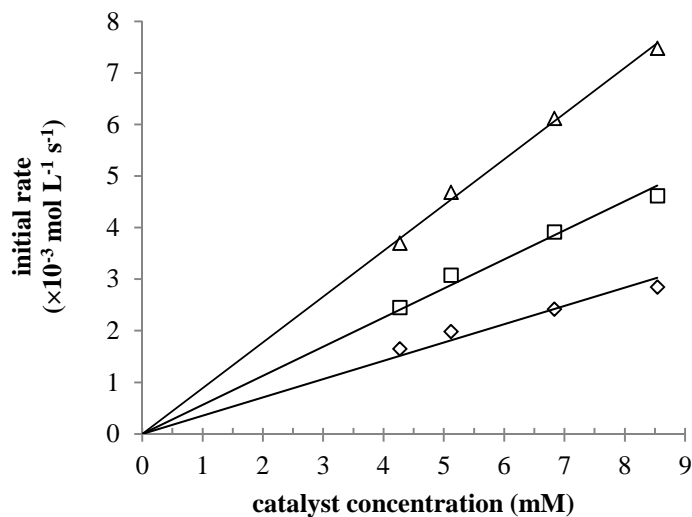


Figure 16. Activity of $[\text{RhH}(\text{CO})\{(3, 5\text{-Me}_2\text{Ph})_3\text{P}\}_3]$ in the hydroformylation of allyl alcohol as a function of catalyst concentration: (\square) 333 K, (\diamond) 343 K, (Δ) 353 K, (-) predicted.

(Conditions: 4 mL toluene, 2.94 M [allyl alcohol], 40 bar CO/H₂ = 1)

The rate of hydroformylation of allyl alcohol increases linearly with catalyst concentration at all range temperatures (Figure 16). This fractional-order dependence is consistent with a higher effective concentration of the active rhodium species, in concurrence with previous reports.⁵¹

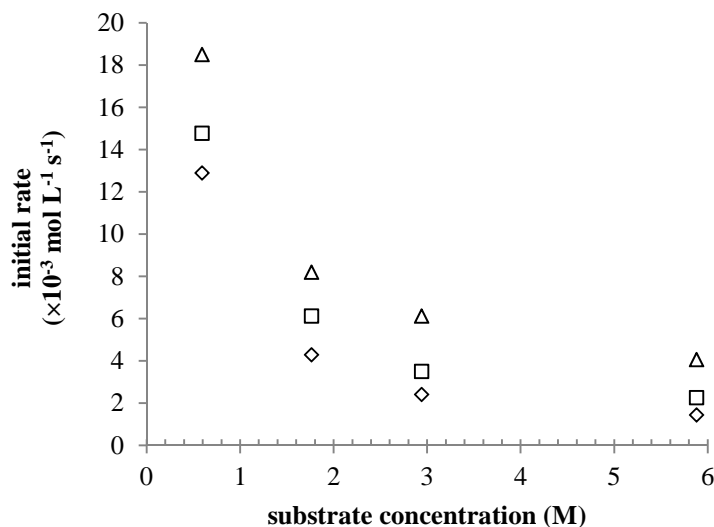


Figure 17. Activity of $[\text{RhH}(\text{CO})\{(3, 5\text{-Me}_2\text{Ph})_3\text{P}\}_3]$ in the hydroformylation of allyl alcohol as a function of substrate concentration: (□) 333 K, (◇) 343 K, (Δ) 353 K. (Conditions: $(5 - V_{\text{substrate}})$ mL toluene, 6.83 mM [Rh], 40 bar $\text{CO}/\text{H}_2 = 1$)

The rate of hydroformylation is found to be of a negative order with respect to allyl alcohol concentration at all range temperatures, and the individual reaction profile plots indicate that rate increases in time (Figure 17). This case of substrate inhibited kinetics is almost certainly attributable to a amalgamation of increasingly competitive isomerisation of allyl alcohol which traps the catalyst in an alternative scheme, and formation of the carbonyl-bridged rhodium dimer, which is inactive for hydroformylation.⁵³ Disintegration of the catalyst by ligand oxidation under the action of the allyl alcohol hydroxyl functionality may also contribute.⁵⁴ Desphande and Chaudhari previously reported substrate inhibited kinetics in the hydroformylation of 1-hexene with $[\text{RhH}(\text{CO})(\text{PPh}_3)_3]$ beyond a critical concentration.^{52b}

The rate of hydroformylation of allyl alcohol at all range temperatures indicates first-order kinetics with respect to the partial pressure of hydrogen (Figure 18). This is a common feature in rhodium-catalysed hydroformylation catalysis and suggests that oxidative addition of hydrogen to the rhodium-acyl-carbonyl intermediate is the rate limiting process.⁵² In order to ensure that the rhodium is not primarily incorporated into the carbonyl-bridged dimer under rapid equilibration, as this is also expected to effect a positive order with respect to this parameter,⁵⁵ the partial pressure of hydrogen was kept below 0.51 MPa with a modest Rh/S molar ratio.

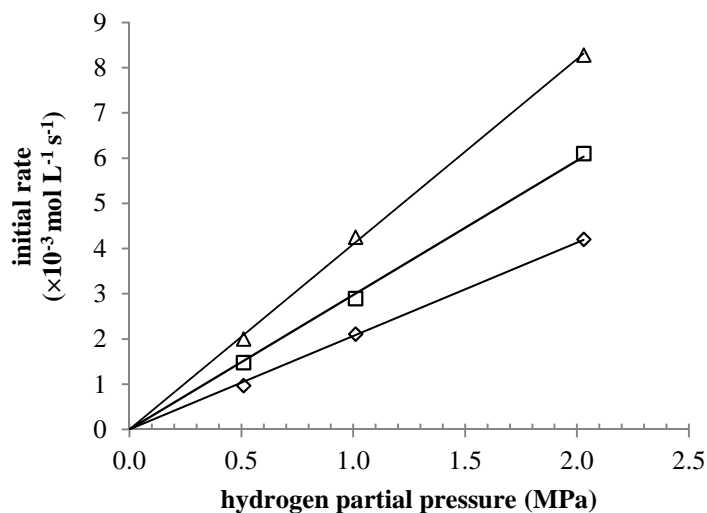


Figure 18. Activity of $[\text{RhH}(\text{CO})\{(3, 5\text{-Me}_2\text{Ph})_3\text{P}\}_3]$ in the hydroformylation of allyl alcohol as a function of hydrogen partial pressure: (□) 333 K, (◇) 343 K, (△) 353 K, (-) predicted. (Conditions: 4.4 mL toluene, 6.83 mM [Rh], Rh/allyl alcohol = 1/258, 40 bar $\text{CO}/\text{H}_2/\text{Ar} = 20/x/(20-x)$)

The rate of hydroformylation of allyl alcohol is more complexly dependent upon the partial pressure of carbon monoxide (Figure 19). In the region of substrate inhibited kinetics the effective concentration of the active rhodium species is reduced by association equilibria, where the *bis*-carbonyl and *tris*-carbonyl species cannot activate hydrogen:

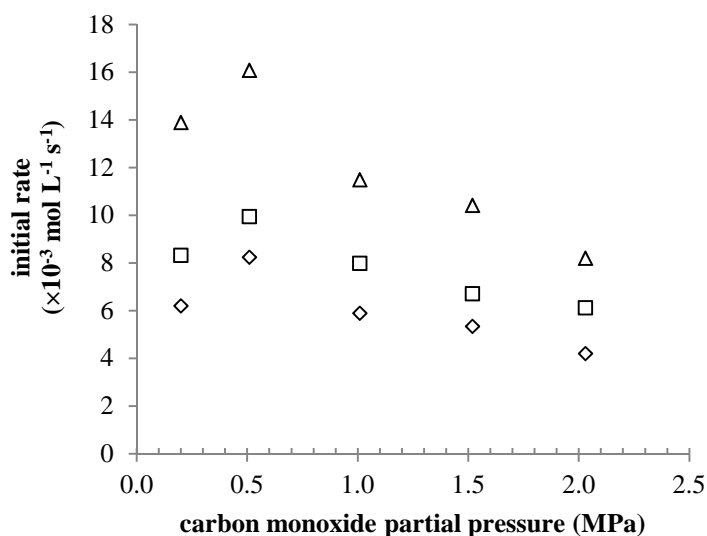


Figure 19. Activity of $[\text{RhH}(\text{CO})\{(3, 5\text{-Me}_2\text{Ph})_3\text{P}\}_3]$ in the hydroformylation of allyl alcohol as a function of carbon monoxide partial pressure: (□) 333 K, (◇) 343 K, (△) 353 K. (Conditions: 4.4 mL toluene, 6.83 mM [Rh], Rh/allyl alcohol = 1/258, 40 bar $\text{CO}/\text{H}_2/\text{Ar} = x/20/(20-x)$)

At a lower partial pressure of carbon monoxide formation of these saturated complexes is expected to be negligible, and the rate is found to be of a positive order.

The temperature dependence of the reaction is constructed as an Arrhenius plot (Figure 20) from which the activation energy is calculated to be $E_A = 32.62 \text{ kJ mol}^{-1}$ (Equation 10).

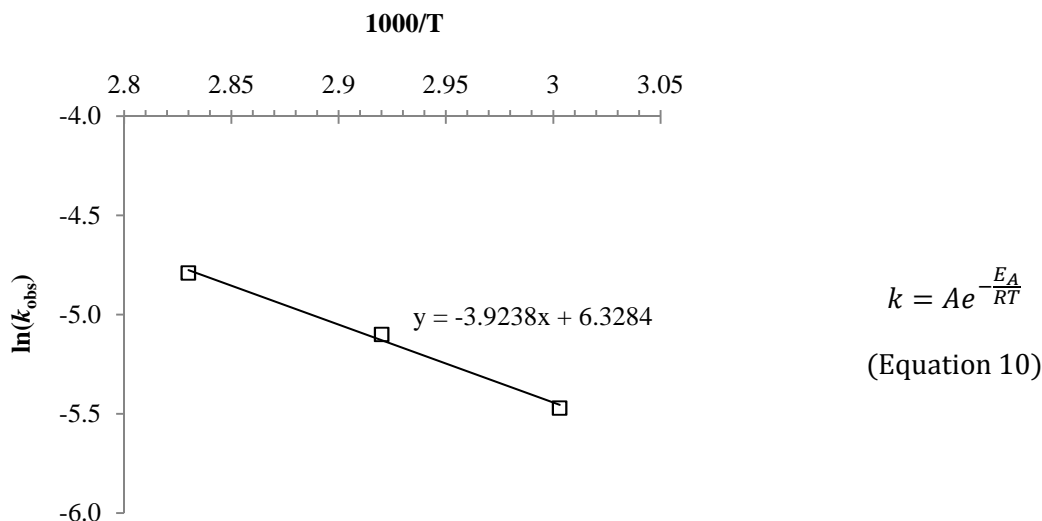


Figure 20. Arrhenius plot for hydroformylation of allyl alcohol with $[\text{RhH}(\text{CO})\{(3, 5\text{-Me}_2\text{Ph})_3\text{P}\}_3]$.

Deshpande and Chaudhari previously established the activation energy for the hydroformylation of allyl alcohol with $[\text{RhH}(\text{CO})(\text{PPh}_3)_3]$ as $E_A = 94.00 \text{ kJ mol}^{-1}$,⁵⁴ which is significantly higher. One explanation may be that ground state excitation effects greater change in the rotation dynamic around the rhodium-phosphorus bond in $[\text{RhH}(\text{CO})\{(3, 5\text{-Me}_2\text{Ph})_3\text{P}\}_3]$. Assuming an associative rate limiting step, which produces a more ordered transition state, this entropic contribution should then accelerate the reaction.

Kinetic model. As the experimental data was collected under relatively mild temperature conditions, it would be inaccurate to reduce rate limitation to one single step of the hydroformylation mechanism.⁴⁰ By the method of initial rates, the data is found to be well represented by the expression

$$\text{rate} = \frac{k[\text{CO}][\text{H}_2]^{1.5}[\text{Rh}]^{1.4}[\text{allyl alcohol}]}{(1 + K_1[\text{CO}])(1 + K_2[\text{allyl alcohol}])} \quad (\text{Equation 11})$$

$[\text{CO}]$	$P_{\text{CO}} \times H_{\text{CO}} (\text{mol L}^{-1})$
$[\text{H}_2]$	$P_{\text{H}_2} \times H_{\text{H}_2} (\text{mol L}^{-1})$
$[\text{Rh}]$	(mol L^{-1})
$[\text{allyl alcohol}]$	(mol L^{-1})
k	rate parameter ($\text{L}^3 \text{mol}^{-4.6} \text{s}^{-1}$)
K_1, K_2	equilibrium parameters (L mol^{-1})

The experimental data at 353 K was fitted to the model using the nonlinear least-squares regression analysis option in ORIGIN,⁵⁶ which is based on the Marquardt method. The parameters were then estimated as $k = 6.22 \times 10^6 \text{ L}^3 \text{ mol}^{-4.6} \text{ s}^{-1}$, $K_1 = 1.31 \times 10^4 \text{ L mol}^{-1}$, $K_2 = 7.29 \times 10^3 \text{ L mol}^{-1}$. The standard deviation between experimental and predicted data is determined as $\phi_{\min} = 2.05 \times 10^{-11}$. This objective function is within the acceptable range.⁵⁷ The data derived from the rate expression demonstrates good comparability with that determined experimentally (Figures 16 and 18).

3.6 Integrated Catalysis

The molecular configuration of a 4, 4-*bis*(*para*-fluorophenyl)butyl moiety bound to a nitrogen heterocycle represents a class of therapeutically active compounds,⁵⁸ including the neuroleptics *Fluspirilen* (**1**), *Penfluridol* and *Pimozide*, the Parkinsons relief drug *PR-608*, the vasodilator *Lidoflazine* and a number of hypolipaeamic agents. A key synthon for this structural framework, 4, 4-*bis*(*para*-fluorophenyl)butylbromide (**6**) is commercially prepared from cyclopropane carboxylic acid methyl ester and *para*-fluorophenyl magnesium bromide,⁵⁹ but the procedure is frustrated by low overall yield, typically > 50%.

The hydroformylation of tertiary allylic alcohols provides a construction strategy to substituted furanols, which are valuable and versatile units in fine-chemical synthesis (Figure 21).⁶⁰

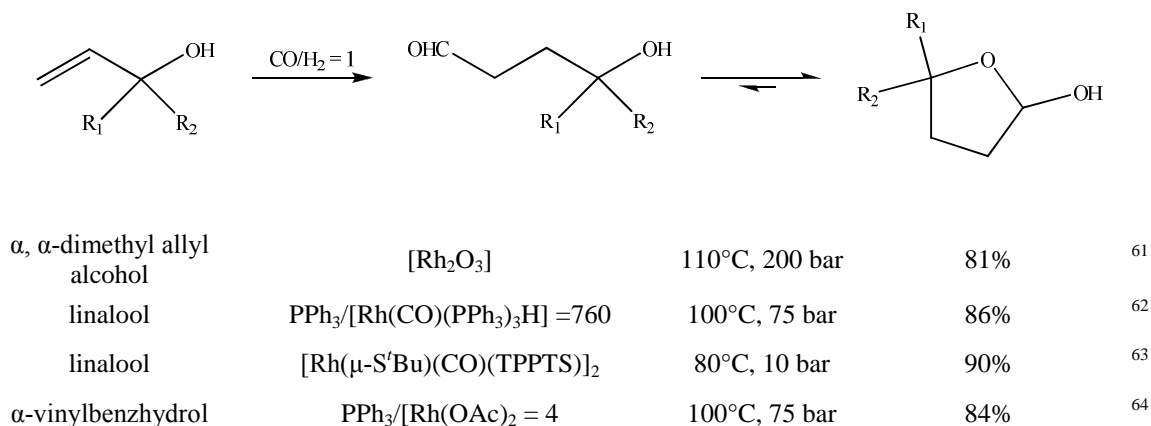
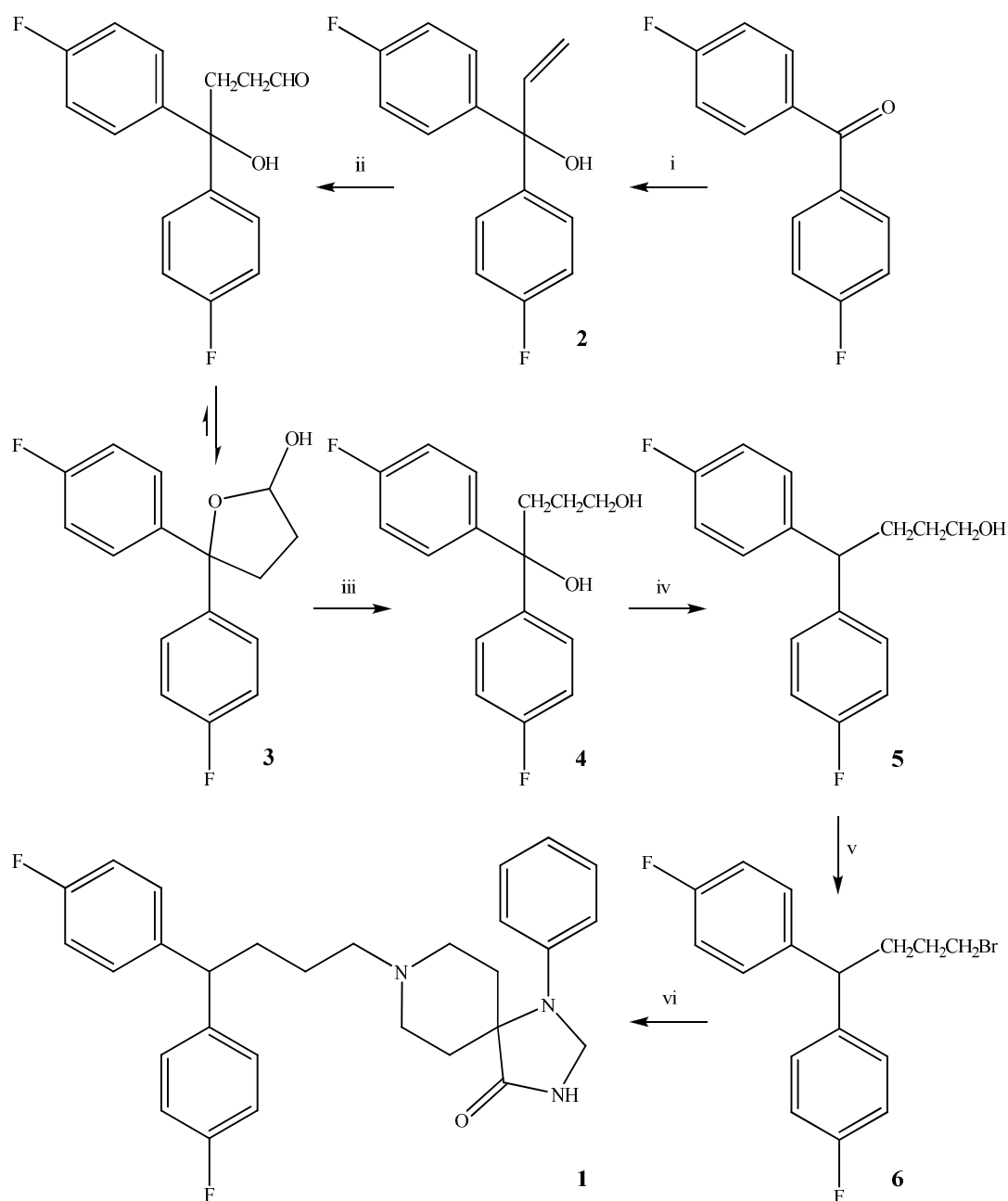


Figure 21. Examples of hydroformylation of tertiary allylic alcohols.

In particular, the 5, 5-diaryltetrahydrofuranols are easily reduced to the corresponding 4, 4-*bis*(aryl)butanediols.⁶⁵ Subsequent hydrogenolysis of the tertiary carbon-oxygen bond should yield the 4, 4-*bis*(aryl)butanol,⁶⁶ which is a convenient precursor to the bromide. This new preparative approach to 4, 4-*bis*(*para*-fluorophenyl)butylbromide has been incorporated into the total synthesis of *Fluspirilen* (**1**) (Scheme 1).



Scheme 1. Synthesis of **1**:

- (i) $\text{CH}_2=\text{CHMgBr}$, $5^\circ\text{C} \rightarrow \text{aT}$, Et_2O , (ii) $[\text{RhH}(\text{CO})\{(3, 5\text{-Me}_2\text{Ph})_3\text{P}\}_3]/30 \text{ bar CO}/\text{H}_2 = 1$, 70°C , toluene, (iii) $\text{NaBH}_4/\text{NaOH}$, aT, MeOH, (iv) 10% Pd/C/1 bar H_2 , 80°C , EtOH, (v) Br_2/PPh_3 , $< 5^\circ\text{C} \rightarrow \text{aT}$, MeCN, (vi) 1-phenyl-1, 3-8-triazaspiro[4, 5]decan-4-one/ $\text{Na}_2\text{CO}_3/\text{KI}$, 120°C , toluene.

The reaction of commercially available 4, 4-*bis*(*para*-fluorophenyl)benzophenone with 1.1 equivalents vinyl magnesium bromide gives 1, 1-*bis*(*para*-fluorophenyl)-2-propenol (**2**) as colourless oil in 82% yield after bulb-to-bulb distillation. Following optimisation, the hydroformylation of **2** is performed using 2×10^{-3} equivalents $[\text{RhH}(\text{CO})\{(3, 5\text{-Me}_2\text{Ph})_3\text{P}\}_3]$ in toluene at 70°C and 30 bar $\text{CO}/\text{H}_2 = 1$ (Table 14). The GC-FID spectra at 3 hour time intervals are presented (Figure 22). In

accordance with previous reports it is assumed that 4, 4-*bis*(fluorophenyl)benzophenone and 1-propanal are primarily formed *via* thermal retro-aldolisation of the branched hydroformylation product.^{58b}

Table 14: Hydroformylation of **2** with [RhH(CO){(3, 5-Me₂Ph)₃P}₃] in organic media.^a

T (°C)	<i>p</i> (bar)	medium	conv. (%)	substrate-based selectivity (mol%) ^b		
				3	4, 4'- <i>bis</i> (<i>p</i> -fluorophenyl) benzophenone	1-propanal
50	30	toluene	93	88	2	3
50	50	toluene	96	94	1	1
70	30	toluene	98	96	1	1
70	30	thf	89	83	3	3
70	50	toluene	99	94	2	3
70	50	hexanes	90	86	2	2
110	30	toluene	100	95	2	3
110	30	thf	99	90	4	5
110	50	toluene	100	96	2	2

^aConditions: 5 mL medium, 8 mM [Rh], Rh/allyl alcohol = 1/102, CO/H₂ = 1, 9 hours. ^bA2. 2 for GC parameters for this substrate.

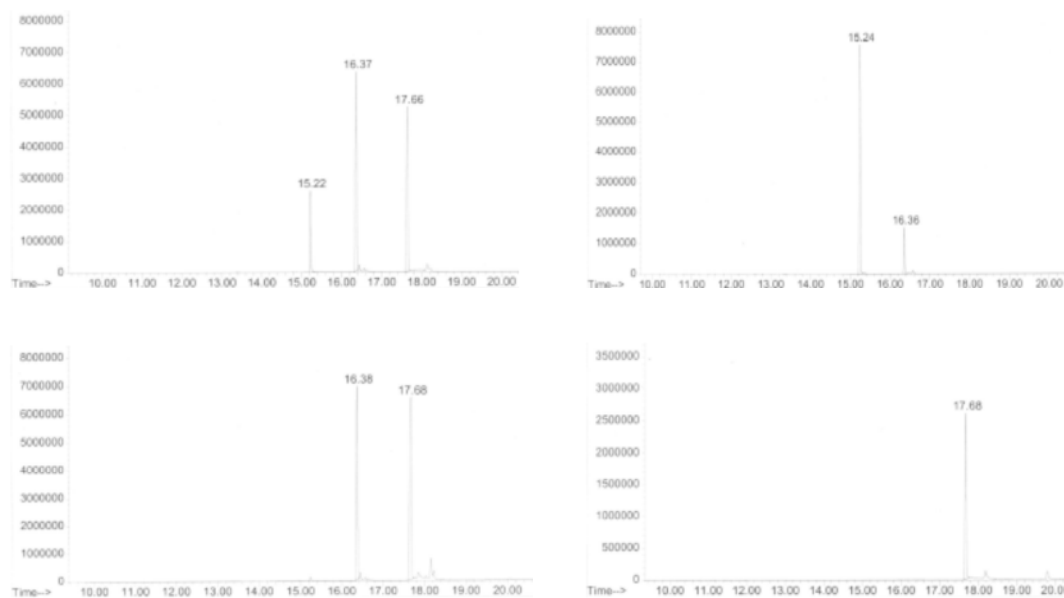


Figure 22. Sequential GC-FID spectra for hydroformylation of **2** with [RhH(CO){(3, 5-Me₂Ph)₃P}₃] in time.^a

^a $R_t = 15.22$ (**2**), $R_t = 16.38$ (**3**-hydroxyaldehyde), $R_t = 17.68$ (**3**-furanol).

5, 5-*Bis*(*para*-fluorophenyl)tetrahydrofuranol (**3**) is crystallised from the crude product residue with *n*-pentane as white powder in 93% yield. A simple reduction with 0.4 equivalents sodium borohydride

in 2 M sodium hydroxide furnishes 4, 4-*bis*(*para*-fluorophenyl)-1, 4-butanediol (**4**), recovered as white solid in 91% yield following flash chromatography. Regioselective hydrogenolysis of **4** with 10% palladium on carbon in toluene at 80°C and 1 bar hydrogen gives 4, 4-*bis*(*para*-fluorophenyl)-butanol (**5**) as white solid in 84% yield after flash chromatography. The bromine functionality is introduced upon reaction of **5** with 1.6 equivalents bromine in the presence of triphenylphosphine. Purification is effected by flash chromatography to give 84% of **6** as pale yellow oil. *N*-alkylation of 1-phenyl-1, 3,8-triazaspiro[4, 5]decan-4-one with 1.1 equivalents **6** in the presence of puratronic sodium carbonate and potassium iodide provides **1**.⁶⁷ The crude residue is crystallised from *n*-hexane and purified by flash chromatography to give the pure product as white powder in 71% yield. The overall yield based on 4, 4-*bis*(*para*-fluorophenyl)benzophenone is 48%.

3.7 Conclusions

The concept of selectivity enhancement *via meta*-effect has been successfully applied for several catalytic transformation, but studies that seek to establish a thorough understanding of how *meta*-substitution in triarylphosphines affects their physicochemical properties and transition metal chemistry are scarce. In this chapter, the relevant effects of systematic *meta*-methyl substitution in triphenylphosphine are reported. It was shown that *meta*-methyl substituents do not have a significant structural impact on the uncoordinated ligand, but variable temperature ¹H NMR studies indicated a significant change to the solution dynamics of its Vaska complex. As rotation of the 3, 5-disubstituted aryl rings past each other is more strained, the activation barrier to phosphorus-(*ipso*)carbon rotation in the *bis*(3, 5-dimethylphenyl)phenylphosphine-modified species was calculated to be ~ 0.45 kJ mol⁻¹ higher than that in the (3, 5-dimethylphenyl)diphenylphosphine-modified species. Rhodium complexes of the highly *meta*-substituted triarylphosphines displayed more defined solubility as a consequence of their lipophilic methyl domains.

The performance of [RhH(CO){(3, 5-Me₂Ph)₃P}₃] in allyl alcohol hydroformylation confirmed a significant *meta*-effect on regioselectivity, as restricted phosphorus-(*ipso*)carbon rotation effects a well-defined coordination sphere around rhodium. Linear-selective hydroformylation was found to be most favoured at high catalyst concentration and low substrate concentration. Under replicated conditions of the Lyondell-Basell process, this catalyst could be recycled with ~94% efficiency *via* biphasic separation. The kinetics of this reaction in toluene was found to be satisfactorily represented by the model

$$\text{rate} = \frac{k[\text{CO}][\text{H}_2]^{1.5}[\text{Rh}]^{1.4}[\text{allyl alcohol}]}{(1 + K_1[\text{CO}])(1 + K_2[\text{allyl alcohol}])}$$

The parameters k , K_1 and K_2 were determined in the temperature range 333-353 K, and the activation energy was calculated to be ~ 33 kJ mol⁻¹. A novel methodology for determination of carbon monoxide concentration in solution mixtures has also been described.

The complex [RhH(CO){(3, 5-Me₂Ph)₃P₃}] also catalysed highly linear-selective hydroformylation of 1, 1-*bis*(*p*-fluorophenyl)-2-propenol, which can be exploited as a key step in a new preparative route to *Fluspirelen*.

Although advantageous in this instance, it is worth noting that restricted phosphorus- (*ipso*)carbon rotation in the transition metal complexes of a *meta*-methyl substituted triarylphosphine could induce a change in transition state structures of the catalytic scheme, thereby reducing selectivities. Further, the catalytic transformation of a sterically exerting substrate could well lead to an insignificant *meta*-effect. It is of interest to identify the extent to which selectivity enhancement is substrate specific.

3.8 Experimental Section

Materials. Chemicals were purchased from Lancaster Synthesis, Alfa Aesar, Sigma-Aldrich, Matheson and Strem. Unless stated otherwise, all operations were performed under N₂ (passed through column of dichromate adsorbed on silica) in a glove box or using standard Schlenk and catheter tubing techniques. All glassware was flame-dried under vacuum. Diethyl ether, hexane and thf were distilled from sodium benzophenone ketyl, dichloromethane, acetonitrile and *n*-butyronitrile were distilled from calcium hydride, absolute ethanol was distilled from magnesium ethoxide methanol was distilled from calcium methoxide, all under N₂ onto activated Linde 4 Å molecular sieves. HPLC-grade toluene, and pentane were dispensed from argon-flushed La Roche A-2/Engelhard Q-5 drying columns. All solvents were degassed prior to use by fpt cycles. MgSO₄, Na₂SO₄, Celite and Kieselgel (60 SiO₂) were activated in a tube furnace at 250°C for 3 hours.

Analytical techniques. NMR spectra were recorded on Bruker Avance 300 and Bruker Avance II 400 spectrometers with tetramethylsilane (¹H, ¹³C) and 85% H₃PO₄ (³¹P) as external references. Solution IR spectra were recorded on a Nicolet Avatar 360 FT-IR spectrometer. Gas chromatography was performed on a Hewlett-Packard 6890 chromatograph fitted with a 30 m BP10™ column (carrier gas 3.2 psi He, flame-ionisation detector). Gas phase analyses were done on an SRI Multiple gas analyser. Elemental analyses were done using a Perkin-Elmer 240C CHNS/O microanalyser. ICP-MS analyses were performed on an Iris Advantage analyser. Melting point ranges were determined using an MPA1000 OptiMelt analyser. Cyclic voltammograms were recorded using an IPC-Pro 7.56 potentiostat in three-electrode mode with a 3 mm pyrographite electrode as working electrode, a commercial sce as reference electrode and a platinum electrode as auxiliary. Normal pulse voltammograms were recorded on a Tacussel PRG 5 potentiostat in three-electrode mode with a

platinum disk electrode as working electrode, a commercial sce as reference electrode and a platinum electrode as auxiliary.

(3, 5-Dimethylphenyl)diphenylphosphine. Over 30 min, 4.6 mL of a 2.5 M solution of *n*-BuLi (11.50 mmol) in hexanes was added to a solution of 2.1550 g 5-bromo-*m*-xylene (11.65 mmol) in thf (125 mL) at -40°C. After stirring at constant temperature for 75 min 2.0 mL diphenylchlorophosphine (11.50 mmol) was introduced dropwise, and the yellow solution was slowly warmed to 35°C. After diluting with 0.02 M HCl (15 mL), thf was removed *in vacuo* and the remaining mixture was extracted with dichloromethane (2×25mL). The combined extracts were percolated through a column of MgSO₄-zsm-5, and filtrate was concentrated *in vacuo*. The oily residue was crystallised from ethanol, yielding 1.9851 g (59 %) of white crystals. Mpr. 62-64°C. ¹H NMR (CDCl₃, 300.1 MHz): δ 7.42-7.33 (m, 10H), 6.94 (s, 1H), 6.91 (d, *J* = 8.7 Hz, 2H), 2.31 (s, 6H). ³¹P{¹H} NMR (CDCl₃, 121.4 MHz): δ - 4.6. *Anal.* Calculated for C₁₇H₁₅N₂P: C, 82.74; H, 6.60. Found: C, 82.59; H, 6.69.

Bis(3, 5-dimethylphenyl)phenylphosphine. Preparation of *bis*(3, 5-dimethylphenyl)phenylphosphine was performed by a similar procedure to that employed for the preparation of (3, 5-dimethylphenyl)diphenylphosphine. Starting from 2.1550 g 5-bromo-*m*-xylene (11.65 mmol), 4.6 mL of a 2.5 M solution of *n*-BuLi (11.50 mmol) in hexanes and 0.9850 g dimethylphenylphosphonite (11.50 mmol) yielded 0.8642 g (46 %) of white crystals. Mpr. 91-92°C. ¹H NMR (CDCl₃, 300.1 MHz): δ 7.45-7.34 (m, 5H), 6.89 (s, 2H), 6.85 (d, *J* = 8.7 Hz, 4H), 2.28 (s, 12H). ³¹P{¹H} NMR (CDCl₃, 121.4 MHz): δ - 4.4. *Anal.* Calculated for C₁₇H₁₅N₂P: C, 82.99; H, 7.28. Found: C, 82.81; H, 7.35.

Tris(3, 5-dimethylphenyl)phosphine. Preparation of *tris*(3, 5-dimethylphenyl)phosphine was performed by a similar procedure to that employed for the preparation of (3, 5-dimethylphenyl)diphenylphosphine. Starting from 2.1550 g 5-bromo-*m*-xylene (11.65 mmol), 4.6 mL of a 2.5 M solution of *n*-BuLi (11.50 mmol) in hexanes and 1.200 g triphenylphosphite (11.50 mmol) yielded 0.8296 g (62 %) of white crystals. Mpr. 158-159°C. ¹H NMR (CDCl₃, 300.1 MHz): δ 6.93 (s, 3H), 6.89 (d, *J* = 8.8 Hz, 6H), 2.25 (s, 18H). ³¹P{¹H} NMR (CDCl₃, 121.4 MHz): δ - 4.0. *Anal.* Calculated for C₁₇H₁₅N₂P: C, 83.20; H, 7.86. Found: C, 83.07; H, 7.85.

Synthesis of complexes from [Ni(CO)₄]. A solution of 1.7 mg [Ni(CO)₄] (0.01 mmol) in dichloromethane (1 mL) was added to the triarylphosphine (0.1 mmol) at 15°C under N₂. The solution was sonicated over 10 minutes, and allowed to warm to 25°C. Any unreacted precursor was carefully removed *in vacuo*. The stock solution was diluted with dichloromethane (1 mL) for analysis by solution IR spectroscopy, calibrated with solutions of [Ni(CO)₃(PPh₃)] (*A*₁ *v*_{CO} = 2069.1 cm⁻¹). The

stock solution was also diluted with d_2 -dichloromethane (1 mL) for analysis by $^{13}\text{C}\{^1\text{H}\}$ NMR spectroscopy, calibrated with a solution of $[\text{Ni}(\text{CO})_4]$ ($\delta_{\text{C}} = 396$).

Electrochemical studies. A solution of the triarylphosphine (4.65×10^{-3} mmol) in *n*-butyronitrile (1 mL) was prepared with a solution of 58.1 mg tetra-*n*-butylammonium hexafluorophosphate (0.15 mmol) in *n*-butyronitrile (1 mL), which had been percolated through a column of activated alumina. This was transferred to the cell and purged with N_2 for 20 minutes. For cyclic voltammetry, the working electrode was cleaned with aluminium powder for 3 minutes before analysis. Voltammograms were recorded at scanning rates in the range 250–5000 mV s^{-1} . For normal pulse voltammetry, the platinum disk electrode was cleaned by cathodic pretreatment in the test solution for 60 s at -1800 mV before analysis. Voltammograms were recorded using pulse duration of 28 ms, cycle duration of 1 s and scanning rate of 10 mV s^{-1} .

Crystal structure determination of *tris*(3, 5-dimethylphenyl)phosphine. Suitable crystals were grown by method of slow-diffusion of *n*-pentane into a concentrated chloroform solution. $[\text{C}_{24}\text{H}_{27}\text{P}]$, $M_r = 346.43$. A white plate-shaped crystal ($0.24 \text{ mm} \times 0.24 \text{ mm} \times 0.24 \text{ mm}$) was fixed to a glass capillary and transferred into the N_2 stream on a Rigaku Mercury/MM007 RA diffractometer with rotating anode. The measure crystal was monoclinic, space group $P2_1$ with $a = 14.406(4) \text{ \AA}$, $b = 9.033(2) \text{ \AA}$, $c = 17.313(5) \text{ \AA}$, $\alpha = 90.000^\circ$, $\beta = 112.665(7)^\circ$, $\gamma = 90.000^\circ$, $V = 2078.9(10) \text{ \AA}^3$, $Z = 4$, $D_x = 1.107 \text{ g cm}^{-3}$, $F(000) = 744$, $\mu(\text{MoK}\alpha) = 0.135 \text{ mm}^{-1}$. 12833 reflections were measured, 3800 of which were independent, $R_{\text{int}} = 0.0676$ ($3.06^\circ < \theta < 25.36^\circ$), $T = 93(2) \text{ K}$, MoK α radiation, graphite monochromator, $\lambda = 0.71073 \text{ \AA}$, ϕ scan and ω scans with κ offset, distance crystal to detector 50 mm, absorption correction by multiscan. The structure was solved by the heavy atom method and refined by the full-matrix least-squares against F^2 method in SHELLXTL.⁶⁸ Refinement converged at $wR2 = 0.1539$, GooF = 1.046 and $-0.296 < \Delta\rho < 0.301 \text{ e \AA}^{-3}$.

Synthesis of complexes from $[\text{Rh}(\text{CO})_2\text{Cl}]_2$. A solution of the triarylphosphine (0.03 mmol) in toluene (3 mL) was added to 11.7 mg $[\text{Rh}(\text{CO})_2\text{Cl}]_2$ (0.03 mmol) at 30°C under N_2 . When carbon monoxide evolution was no longer discernable, the yellow solution reduced *in vacuo*. The crude residue was crystallised from boiling ethanol. Evaporating the solvent afforded yellow prisms which were washed with cold methanol ($2 \times 1.2 \text{ mL}$).

Crystal structure determination of *trans*- $[\text{Rh}\{(\text{3, 5-Me}_2\text{Ph})_3\text{P}\}_2(\text{CO})\text{Cl}]$. Suitable crystals were grown by method of slow-diffusion of acetonitrile into a concentrated dichloromethane solution. $[\text{C}_{49}\text{H}_{54}\text{ClOP}_2\text{Rh}]$, $M_r = 859.22$. A yellow prism-shaped crystal ($0.20 \text{ mm} \times 0.20 \text{ mm} \times 0.06 \text{ mm}$) was fixed to a glass capillary and transferred into the N_2 stream on a Rigaku Mercury/MM007 RA diffractometer with rotating anode. The measure crystal was monoclinic, space group Cc with $a =$

17.8670(14) Å, $b = 17.6180(13)$ Å, $c = 14.4793(12)$ Å, $\alpha = 90.000^\circ$, $\beta = 110.752(4)^\circ$, $\gamma = 90.000^\circ$, $V = 4262.1(6)$ Å³, $Z = 4$, $D_x = 1.339$ g cm⁻³, $F(000) = 1792$, $\mu(\text{MoK}\alpha) = 0.574$ mm⁻¹. 18377 reflections were measured, 7212 of which were independent, $R_{int} = 0.0586$ ($1.68^\circ < \theta < 25.35^\circ$, $T = 93(2)$ K, MoK α radiation, graphite monochromator, $\lambda = 0.71073$ Å, ϕ scan and ω scans with κ offset, distance crystal to detector 50 mm, absorption correction by multiscan. The structure was solved by the heavy atom method and refined by the full-matrix least-squares against F^2 method in SHELLXTL.⁶⁸ Refinement converged at $wR2 = 0.1180$, $\text{Goof} = 1.185$ and $-0.974 < \Delta\rho < 0.623$ e Å⁻³.

Variable temperature NMR spectroscopy. An NMR tube was primed with a solution of the complex *trans*-[Rh(CO)(PAr₃)₂Cl] (0.02 mmol) in *d*₃-chloroform under N₂, and sonicated over 5 minutes. ¹H NMR spectra were recorded in the temperature range -60 to 25°C. Line-shape analyses was performed using the *d*NMR option in the TOPSPINTM software provided by Bruker BioSpin.⁶⁹

Synthesis of complexes from *trans*-[Rh(CO)(PAr₃)₂Cl]. To a solution of the *trans*-[Rh(CO)(PAr₃)₂Cl] (1 mmol) and the triarylphosphine (2 mmol) in toluene (25 mL) under CO, was added 0.1642 g sodium propoxide (2 mmol, freshly prepared)⁶⁹ in one portion. The reaction mixture was maintained at 55°C for 3 hours. The orange suspension was cooled to ambient temperature and the sodium chloride was removed by filtering through a Celite pad. The filtrate was reduced under pressure to ~ 6 mL. H₂ was bubbled through the red solution until no further colour change to yellow was observed. The solution was reduced under pressure to ~ 0.5 mL, from which the product crystallised upon treatment with *n*-hexane.

Catalysis. Carbon monoxide and hydrogen were purchased from BOC (**Caution!** Carbon monoxide is extremely poisonous and accidents may be lethal. A sensitive personal detector was carried and all experiments were performed in a well ventilated fume-hood fitted with a detector, maintaining the concentration of carbon monoxide below the mac value at all times). Hydroformylation reactions were carried out on the CAT rig with stirrer speed set at 1200 rpm. In a typical experiment a solution of [RhH(CO){(3, 5-Me₂Ph)₃P}₃] (0.021-0.043 mmol) in toluene (1.6-3.8 mL) was sonicated over 10 minutes and transferred into the autoclave under N₂; any residues were transferred with a further aliquot of toluene (1 mL). The solution was incubated for 20 minutes at the requisite temperature and 30 bar CO/H₂. After allyl alcohol (2.94-29.41 mmol, azeotropically dried with toluene and distilled) was injected the pressure was adjusted to 40 bar, and the reaction was run to completion. The autoclave was then cooled and depressurised. Intermittently, gas samples were withdrawn from the void space in the autoclave using a stainless steel gas pipette and analysed for H₂ content. 50 µL diglyme was added as internal standard to a 1 mL aliquot of the product solution, and the sample was analysed by GC. The experiments were performed at least in duplo.

For catalyst recycling experiments, a solution of $[\text{RhH}(\text{CO})\{(3, 5\text{-Me}_2\text{Ph})_3\text{P}\}_3]$ (0.0026 mmol) in toluene (3 mL) was sonicated over 10 minutes and transferred into the autoclave under $\text{CO}/\text{H}_2 = 1$; any residues were transferred with a further aliquot of toluene (1 mL). The solution was incubated for 20 minutes at 60°C and 10 bar $\text{CO}/\text{H}_2 = 1$. 1 mL allyl alcohol (14.70 mmol) was injected and the reaction was run to completion. The autoclave was cooled, depressurised to 1 bar and the product solution thus transferred *via* cannula to a Schlenk vessel equipped with a magnetic stirrer. The addition of water (2.5 mL) gave immediate phase separation and the biphasic system was stirred 5 minutes at 20°C . The organic phase was carefully transferred to a volumetrically graduated Schlenk tube *via* syringe; fresh toluene was added to make up 4 mL volume. This solution was re-applied in catalysis.

Gas solubility. The HP-IR autoclave was primed with 20 mL of the appointed liquid under N_2 . The cell was purged twice with 4 bar CO and heated to the desired temperature. Following thermal equilibration, the void space in the cell was carefully flushed with CO and pressurised as appointed. Equilibrium between the liquid phase and the gas phase was initiated by agitating at 15 Hz for 10 minutes. The IR spectrum was then recorded. The reference spectrum of the liquid under 1 bar N_2 at the appointed temperature was subtracted from the experimental spectrum.

1, 1-Bis(*p*-fluorophenyl)-2-propen-1-ol (2). 12.6 mL of a 1 M solution of vinyl magnesium bromide (12.600 mmol) was added dropwise to a solution of 2.5000 g 4, 4'-difluorobenzophenone (11.450 mmol) in diethyl ether (25 mL) at 0°C . The reaction mixture was heated to 80°C , and maintained under gentle reflux for 5 hours. After cooling to ambient temperature the reaction was quenched by addition of saturated NH_4Cl solution (15 mL), and the aqueous phase was extracted with diethyl ether (3×15 mL). The combined extracts were dried over MgSO_4 and concentrated *in vacuo*. The residual pale yellow liquid was purified by bulb-to-bulb distillation (93°C , 0.05 mmHg), yielding 2.3121 g (82 %) of clear oil. ^1H NMR (CDCl_3 , 300.1 MHz): δ 7.43-7.29 (m, 4H), 7.14-6.95 (m, 4H), 6.46 (dd, $J = 10.8, 16.9$ Hz, 2H), 2.41 (s, 1H). MS (70 eV) m/z (relative intensity): 246 (M^+ , 2). *Anal.* Calculated for $\text{C}_{15}\text{H}_{12}\text{OF}_2$: C, 73.16; H, 4.91. Found: C, 72.98; H, 4.97.

5, 5-Bis(*p*-fluorophenyl)tetrahydrofuranol (3). A Hastelloy autoclave was primed with a solution of 9.37 mg $[\text{RhH}(\text{CO})\{(3, 5\text{-Me}_2\text{Ph})_3\text{P}\}_3]$ (0.008 mmol) and 1.000 g **2** (4.060 mmol) in toluene (5 mL) under N_2 , and pressurised with 30 bar $\text{CO}/\text{H}_2 = 1$. After 9 hours at 70°C the autoclave was cooled and depressurised. GC analysis of the product mixture confirms 98% conversion, partitioned as 96% **3**, 1% 4, 4'-bis(*para*-fluorophenyl)benzophenone and 1% 1-propanal. The recovered solution was concentrated *in vacuo* and the white residue was crystallised from *n*-hexane, yielding 0.9828 g (93 %) of white flakes. Mpr. $110\text{-}113^\circ\text{C}$. ^1H NMR (CDCl_3 , 300.1 MHz): δ 7.52-7.30 (m, 4H), 7.05-6.89 (m, 4H), 5.74 (q, $J = 3.6$ Hz, 1H), 2.68-2.53 (m, 2H), 2.06 (m, 2H). MS (70

eV) m/z (relative intensity): 276 (M^+ , 10). *Anal.* Calculated for $C_{16}H_{14}OF_2$: C, 69.56; H, 5.11. Found: C, 69.62; H, 4.20.

1, 1-Bis(*p*-fluorophenyl)-1, 4-butanediol (4). A suspension of 53.4 mg sodium borohydride (0.008 mmol) and 80 μ L of a 2 M NaOH solution in H_2O (0.75 mL) was added dropwise to a solution of 1.0000 g **3** (3.600 mmol) in methanol (10 mL). The reaction mixture was stirred at ambient temperature, the conversion being monitored by gc-ms. Methanol was removed under reduced pressure, and after diluting (3 mL) the aqueous mixture was extracted with diethyl ether (3×10 mL). The combined extracts were percolated through a column of $MgSO_4$ -zsm-5 and concentrated *in vacuo*. The off-white residue was purified by flash chromatography (Kieselgel, hexane/diethyl ether = 3/2), yielding 0.9117 g (91 %) of white solid. R_f = 0.52 (hexane/diethyl ether = 3/2). Mpr. 93-94°C. 1H NMR ($CDCl_3$, 300.1 MHz): δ 7.50-7.33 (m, 4H), 7.07-6.91 (m, 4H), 3.73 (t, J = 7.2 Hz, 2H), 3.48 (br s, 1H), 2.44 (t, J = 7.2 Hz, 2H), 1.91 (br s, 1H), 1.72-1.55 (m, 2H). MS (70 eV) m/z (relative intensity): 278 (M^+ , 1). *Anal.* Calculated for $C_{16}H_{16}O_2F_2$: C, 69.05; H, 5.79. Found: C, 69.24; H, 5.91.

1, 1-Bis(*p*-fluorophenyl)-butanol (5). A suspension of 0.500 g **4** (1.800 mmol) and 0.2250 g 10 % Pd/C in ethanol (10 mL) was treated with H_2 . The reaction mixture was maintained at 95°C under reflux for 16 hours. After cooling to ambient temperature the suspension was filtered through a pad of Celite, and the filtrate was reduced *in vacuo*. The opaque liquid residue was purified by flash chromatography (Kieselgel, hexane/diethyl ether = 7/3), yielding 0.3966 g (84%) of clear oil. R_f = 0.46 (hexane/diethyl ether = 7/3). 1H NMR (CD_2Cl_2 , 300.1 MHz): δ 7.22-7.07 (m, 4H), 7.02-6.92 (m, 4H), 3.90 (t, J = 0.6 Hz, 1H), 3.41 (t, J = 7.2 Hz, 2H), 2.25-2.12 (m, 2H), 1.89-1.76 (m, 2H). MS (70 eV) m/z (relative intensity): 262 (M^+ , 7). *Anal.* Calculated for $C_{16}H_{16}OF_2$: C, 73.27; H, 6.15. Found: C, 73.54; H, 6.17.

1, 1-Bis(*p*-fluorophenyl)butylbromide (6). A solution of 0.7500 g triphenylphosphine (2.850 mmol) in acetonitrile (4 mL) was cooled to 0°C and added dropwise to 0.4550 g bromine, maintaining temperature at < 5°C. The mixture was slowly warmed to ambient temperature and a solution of 0.5000 g **5** (1.800 mmol) in acetonitrile (1.5 mL) was added dropwise. The resulting solution was stirred for 4 hours and then concentrated under reduced pressure. The residue was taken up with *n*-pentane, and the resulting suspension filtered through a pad of Celite. The filtrate was reduced *in vacuo* and the yellow liquid residue was purified by flash chromatography (Kieselgel, hexane/diethyl ether = 7/3), yielding 0.5159 g (84 %) of pale yellow oil. R_f = 0.57 (hexane/diethyl ether = 7/3). 1H NMR ($CDCl_3$, 300.1 MHz): δ 7.20-7.09 (m, 4H), 7.05-6.92 (m, 4H), 3.90 (t, J = 0.6 Hz, 1H), 3.44 (t, J = 7.2 Hz, 2H), 2.21-2.10 (m, 2H), 1.94-1.72 (m, 2H). MS (70 eV) m/z (relative intensity): 325 (M^+ , 3). *Anal.* Calculated for $C_{16}H_{15}OF_2Br$: C, 73.30; H, 6.10. Found: C, 73.44; H, 6.22.

Fluspirelen (1). A solution of 0.7500 g **6** (2.325 mmol), 0.4689 g 1-phenyl-1, 3, 8-triazaspiro[4, 5]decan-4-one (2.025 mmol) 0.3728 g puratronic Na₂CO₃ (3.525 mmol) and three crystals of KI in toluene (10 mL) was maintained at 125°C under reflux, the conversion being monitored by gc-ms. The reaction mixture was cooled to ambient temperature and diluted with toluene (5 mL) and H₂O (9 mL). The organic phase was removed, dried over Na₂SO₄ and concentrated *in vacuo*. The pale yellow residue was crystallised from *n*-pentane and purified by flash chromatography (Kieselgel, chloroform), yielding 0.6838 g (71 %) of white powder. ¹H NMR (CD₂Cl₂, 300.1 MHz): δ 7.25-6.88 (m, 13H), 4.69 (s, 2H), 3.90 (t, *J* = 0.6 Hz, 1H), 2.77-2.55 (m, 6H), 2.43 (t, *J* = 7.2 Hz, 2H), 2.06 (q, *J* = 7.2 Hz, 2H), 1.73 (d, *J* = 7.2 Hz, 2H), 1.54-1.34 (m, 2H). MS (70 eV) *m/z* (relative intensity): 475 (M⁺, 6). *Anal.* Calculated for C₂₉H₃₁N₃OF₂: C, 73.24; H, 6.57; N, 8.84. Found: C, 73.13; H, 6.62; N, 8.86.

References and Notes

- (1) (a) Trabesinger, G.; Albinati, A.; Feiken, N.; Kunz, R.; Pregosin, P. S.; Tschoerner, M. *J. Am. Chem. Soc.* **1997**, *119*, 6315. (b) Dotta, P.; Kumar, P. G. A.; Pregosin, P. S. *Organometallics* **2004**, *23*, 2295.
- (2) (a) RajanBabu, T. V.; Ayers, T. A.; Casalnuovo, A. L. *J. Am. Chem. Soc.* **1994**, *116*, 4101. (b) RajanBabu, T. V.; Ayers, T. A.; Halliday, G. A.; You, K. K.; Calabrese, J. C. *J. Org. Chem.* **1997**, *62*, 6012.
- (3) (a) Ohkuma, T.; Ooka, H.; Hashiguchi, S.; Ikariya, T.; Noyori, N. *J. Am. Chem. Soc.* **1995**, *117*, 2675. (b) Doucet, H.; Ohkuma, T.; Murata, K.; Yokozawa, T.; Kozawa, M.; Katayama, E.; England, A. F.; Ikariya, T.; Noyori, R. *Angew. Chem. Int. Ed.* **1998**, *37*, 1703.
- (4) Ager, D. J.; Laneman, S. A. *Tetrahedron: Asymmetry* **1997**, *8*, 3327.
- (5) (a) RajanBabu, T. V.; Casalnuovo, A. L. *J. Am. Chem. Soc.* **1992**, *114*, 6265. (b) Casalnuovo, A. L. *J. Am. Chem. Soc.* **1994**, *116*, 9869.
- (6) (a) Hayashi, T.; Hirate, S.; Kitayama, K.; Tsuji, H.; Torii, A.; Uozumi, Y. *Chem. Lett.* **2000**, 1272. (b) Hayashi, T.; Hirate, S.; Kitayama, K.; Tsuji, H.; Torii, A.; Uozumi, Y. *J. Org. Chem.* **2001**, *66*, 1441.
- (7) (a) Hamashima, Y.; Yagi, K.; Takano, H.; Tamas, L.; Sodeoka, M. *J. Am. Chem. Soc.* **2002**, *124*, 14530. (b) Hamashima, Y.; Suzuki, t.; Shimura, Y.; Shimizu, T.; Umebayashi, N.; Tamura, T.; Sasamoto, N.; Sodeoka, M. *Tetrahedron Lett.* **2005**, *127*, 10164.
- (8) (a) White, D. F. S.; Dubner, W. S. *US Pat.* 7.271.295, 2007. (b) White, D. F. S. *US Pat.* 7.279.606, 2007.
- (9) (a) Barg, L. A.; Byrn, R. W.; Carr, M. D.; Nolan, D. H.; Storhoff, B. N.; Huffman, J. C. *Organometallics* **1998**, *17*, 1340. (b) Romain, J. K.; Ribblett, J. W.; Byrn, R. W.; Snyder, R. D.; Storhoff, B. N.; Huffman, J. C. *Organometallics* **2000**, *19*, 2047.
- (10) For review see: Kühl, O. *Coord. Chem. Rev.* **2005**, *249*, 693.
- (11) ν_{CO} [Ni(CO)₃(P^tBu₃)] = 2056.1 cm⁻¹. Tolman, C. A. *Chem. Rev.* **1977**, *77*, 313.

- (12) (a) v_{CO} dependence on packing defects in solid state. Otto, S.; Roodt, A. *Inorg. Chim. Acta* **2004**, *357*, 1. (b) v_{CO} dependence on polymorphism in solid state. Kemp, G.; Roodt, A.; Purcell, W. *Rhodium Express* **1995**, *12*, 21.
- (13) March, J. *Advanced Organic Chemistry*. Wiley: New York, 1992.
- (14) (a) Drago, R. S. *Organometallics* **1995**, *14*, 3408. (b) Drago, R. S.; Joerg, S. *J. Am. Chem. Soc.* **1996**, *118*, 2654. (c) Joerg, S.; Drago, R. S.; Sales, J. *Organometallics* **1998**, *17*, 589.
- (15) (a) Bodner, G. M. *Inorg. Chem.* 1975, *14*, 1932. (b) Cotton, F. A.; Edwards, W. T.; Rauch, F. C.; Graham, M. A.; Perutz, R. N.; Turner, J. J. *Coord. Chem.* **1973**, *2*, 247.
- (16) For examples see: (a) Alberti, A.; Hudson, A.; Pedulli, G. F. *Tetrahedron* **1984**, *40*, 4955. (b) Emoto, T.; Okazaki, R.; Inamoto, N. *Bull. Chem. Soc. Jpn.* **1973**, *46*, 898. (c) Ohmori, H.; Takanami, T.; Masui, M. *Tetrahedron Lett.* **1985**, 2199. (d) Effenberger, F.; Kottmann, H. *Tetrahedron* **1985**, *41*, 4171.
- (17) (a) Griller, D.; Ingold, K. U. *Acc. Chem. Res.* **1980**, *13*, 193 and references therein. (b) Il'Yasov, A. V.; Kargin, Y. M.; Nikitin, E. V.; Vafina, A. A.; Romanov, G. V.; Parakin, O. V.; Kazakova, A. A.; Pudovik, A. N. *Phosphorus Sulfur Relat. Elem.* **1980**, *8*, 259. (c) Culcasi, M.; Gronchi, G.; Tordo, P. *Phosphorus Sulfur Relat. Elem.* **1987**, *30*, 511.
- (18) (a) Kissinger, P. T.; Heineman, W. R. *J. Chem. Ed.* **1983**, *60*, 702. (b) Brett, C. M. A.; Bret, A. M. O. *Electrochemistry: Principles, Methods and Applications*. Oxford University Press: Oxford, 1993.
- (19) E_p (SCE) = +0.242 V. Bard, A. J.; Faulkner, L. R. *Electrochemical Methods*. Wiley: New York, 1980.
- (20) Cameron, T. S.; Howlett, K. D.; Miller, K. *Acta Crystallogr.* **1978**, *B34*, 1639.
- (21) Bye, E.; Schweizer, B.; Dunitz, J. D. *J. Am. Chem. Soc.* **1982**, *104*, 5893.
- (22) For examples see: (a) Lagally, H. *Zeit. Anorg. Allg. Chem.* **1943**, *251*, 96. (b) Vallarino, L. *J. Chem. Soc.* **1957**, 2287. (c) Chatt, J.; Shaw, B. L. *J. Chem. Soc. A, Inorg. Phys. Theor.* **1966**, 1437.
- (23) Potekin, K. A.; Batsanov, A. S.; Struchov, Y. T. *Rhodium Express* **1993**, *1*, 3.
- (24) For examples see: (a) Reference 23. (b) van der Vlugt, J. I.; Sablong, R.; Magusin, P. C. M. M.; Mills, A. M.; Spek, A. L.; Vogt, D. *Organometallics* **2004**, *23*, 3177. (c) Rankin, J.; Poole, A. D.; Benyei, A. C.; Cole-Hamilton, D. J. *Chem. Commun.* **1997**, 1835. (d) Cheliatsidou, P.; White, D. F. S.; Slawin, A. M. Z.; Cole-Hamilton, D. J. *Dalton Trans.* **2008**, 2389. (e) Clarke, M. L.; Ellis, D.; Mason, K. L.; Orpen, G. A.; Pringle, P. G.; Wingad, R. L.; Zaher, D. A.; Baker, T. R. *Dalton Trans.* **2005**, 1294.
- (25) Freeman, M. A.; Young, D. A. *Inorg. Chem.* **1986**, *25*, 1556.
- (26) (LiB(Et₃)H). (a) [NiCl₂(DIPPE)] → [Ni(μ-H)₂(DIPPE)]. Vicic, D. A.; Jones, W. D. *J. Am. Chem. Soc.* **1997**, *119*, 10855. (b) [M(CO)₂(PMe₃)₃Cl₂] (M = W, Mo) → [MH(CO)₂(PMe₃)₃Cl]. Contreras, L.; Monge, A.; Pizzano, A.; Ruiz, C.; Sánchez, L.; Carmona, E. *Organometallics* **1993**, *12*, 4228.
- (27) Engeldinger, E.; Armspach, D.; Matt, D. *Chem. Eur. J.* **2003**, *9*, 3091 and references therein.
- (28) MM3* calculations on triarylphosphine fragments suggest the rotational barrier increases by ~5 kJ mol⁻¹ upon substituting a phenyl group with a 3, 5-di-*tert*-butylphenyl group. Reference 1a.
- (29) Gregorio, G.; Pregaglia, G.; Ugo, R. *Inorg. Chim. Acta* **1969**, *3*, 89.

- (30) A non-nucleophilic medium should avoid the complications of tandem hydroformylation sequences.
- (31) A. 2. 2, p. 180.
- (32) Chapter 2, p. 53.
- (33) (a) [RhH(CO)(PPh₃)₃] in organic media. Brown, C. K.; Wilkinson, G. *J. Chem. Soc. A* **1970**, 2753. (b) [RhH(CO){(*p*-CF₃-C₆H₄)₃P}₃] in supercritical carbon dioxide. Palo, D. R.; Erkey, C. *Ind. Eng. Chem. Res.* **1999**, 38, 2163.
- (34) For review see: Kamer, P. C. J.; van Rooy, A.; Schoemaker, G. C.; van Leeuwen, P. W. N. M. *Coord. Chem. Rev.* **2004**, 248, 2409.
- (35) (a) Gholap, R. V.; Kut, O. M.; Bourne, J. R. *Ind. Eng. Chem. Res.* **1992**, 31, 1597. (b) Gholap, R. V.; Kut, O. M.; Bourne, J. R. *Ind. Eng. Chem. Res.* **1992**, 31, 2446. (c) Cornils, B. *New Synthesis with Carbon Monoxide*. Falbe, J. (Ed). Springer-Verlag: New York, 1980. (d) Pino, P.; Piacenti, F.; Binchi, M. *Organic Synthesis via Metal Carbonyls*. Wender, I.; Pino, P. (Eds). Wiley: New York, 1977.
- (36) Strohmeier, W.; Michel, M. Z. *Phys. Chem.* **1981**, 124, 23.
- (37) Barole, Y. L. *PhD Thesis*, University of Mumbai, 2004. Chapter 4.
- (38) Provided by Lyondell-Basell, Newtown Square Technology Centre, 3801 West Chester Pike, Newtown Square, PA 19073, USA.
- (39) The relatively lower leaching of rhodium can be explained by ligand oxidation, which degenerates the catalyst to rhodium particles and phosphine oxides. The latter will have a higher affinity for the aqueous phase.
- (40) Connors, K. A. *Chemical Kinetics: The Study of Reaction Rates in Solution*. VCH: Weinheim, 1990.
- (41) Frohning, C. D.; Kohlpaintner, C. W. *Applied Homogeneous Catalysis with Organometallic Compounds*, vol. 1. Cornils, B.; Herrmann, W. A. (Eds). VCH: Weinheim, 1996.
- (42) Chaudhari, R. V.; Doraiswamy, L. K. *Chem. Eng. Sci.* **1974**, 29, 349.
- (43) For comprehensive coverage see: (a) hydrogen solubility in organic media. Young, C. L. *IUPAC Solubility Series*, vol. 5/6 Hydrogen and Deuterium. Pergamon Press: Oxford, 1981. (b) carbon monoxide solubility in organic media. Cargill, R. W. *IUPAC Solubility Series*, vol. 43 Carbon Monoxide. Pergamon Press: Oxford, 1990. (c) hydrogen solubility in ionic liquids. Anthony, J. L.; Maginn, E. J.; Brennecke, J. F. *J. Phys. Chem. B* **2002**, 106, 7315. (d) Ohlin, C. A. Dyson, P. J.; Laurenczy, G. *Chem. Commun.* **2004**, 1070.
- (44) Only three examples found: (a) Dake, S. B.; Chaudhari, R. V. *J. Chem. Eng. Data* **1985**, 30, 400. (b) Purwanto, P.; Desphande, R. M.; Chaudhari, R. V.; Delmas, H. *J. Chem. Eng. Data* **1996**, 41, 1414. (c) Nair, V. S.; Mathew, S. P.; Chaudhari, R. V. *J. Mol. Catal. A* **1999**, 143, 99.
- (45) Jáuregui-Haza, U. J.; Pardillo-Fontdevila, E. J.; Wilhelm, A. M.; Delmas, H. *Latin American Appl. Res.* **2004**, 34, 71.
- (46) (a) Barton, A. F. M. *CRC Handbook of Solubility Parameters and Other Cohesion Parameters*. CRC Press: Boca Raton, 1991. (b) Yen, C. L.; McKetta, J. J. *AIChE J.* **1962**, 8, 501. (c) Kumelan, J.; Kamps, A. P.; Tuma, D.; Maurer, G. *Fluid Phase Equil.* **2005**, 228/229, 207.
- (47) Katayama, T.; Nitta, T. *J. Chem. Eng. Data* **1976**, 21, 194.
- (48) Hildebrand, J. H.; Scott, R. L. *Am. Chem. Soc.* **1948**, 424, 9.

- (49) (a) Lemcoff, N. O. *J. Catal.* **1977**, *46*, 356. (b) Radhakrishnathna, K.; Ramachandran, P. A.; Brahme, P. H.; Chaudhari, R. V. *J. Chem. Eng. Data* **1983**, *28*, 1.
- (50) (a) Prausnitz, J. M.; Lichtenhaler, R. N.; de Azevedo, E. G. *Molecular Thermodynamics of Fluid-Phase Equilibria*. Prentice Hall: New Jersey, 1999. (b) Stogryn, D. E.; Stogryn, A. P. *Mol. Phys.* **1966**, *11*, 371.
- (51) IGOR PRO, Version 6.1. WaveMetrics Inc., Lake Oswego OR, 2007.
- (52) For examples with similar catalysts see: (a) styrene hydroformylation with [RhH(CO)(PPh₃)₃]. Reference 44c. (b) 1-hexene hydroformylation with [RhH(CO)(PPh₃)₃]. Deshpande, R. M.; Chaudhari, R. V. *Ind. Eng. Chem. Res.* **1988**, *27*, 1996. (c) 1-octene hydroformylation with [RhH(CO)(PPh(NR-RN)₃)]. Reference 34.
- (53) van Leeuwen, P. W. N. M.; Claver, C. *Rhodium Catalysed Hydroformylation*. James, B. R.; Ugo, R. (Eds). Kluwer Academic: Dordrecht, 2000.
- (54) Deshpande, R. M.; Chaudhari, R. V. *J. Catal.* **1989**, *115*, 326.
- (55) Castellanos-Páez, A.; Castellón, S.; Claver, C. *Organometallics* **1998**, *17*, 2543.
- (56) ORIGIN-08. OriginLab, Northampton MA, 2006.
- (57) For kinetic analysis lowest limit $\phi_{\min} = 5 \times 10^{-7}$.
- (58) (a) Botteghi, C.; Paganelli, S.; Marchetti, M.; Pannocchia, P. *J. Mol. Catal. A* **1999**, *143*, 233. (b) Botteghi, C.; Marchetti, M.; Paganelli, S.; Persi-Paoli, F. *Tetrahedron* **2001**, *57*, 1631.
- (59) Janssen, P. A. J. *Fr. M3059*, 1965.
- (60) Botteghi, C.; Paganelli, S.; Schionato, A.; Marchetti, M. *Chirality* **1991**, *3*, 355.
- (61) Fell, B.; Barl, M. *Chem. Ztg.* **1977**, *101*, 343.
- (62) Chalk, A. J. *Catalysis of Organic Reactions*. Rylander, P. N.; Greenfield, H.; Augustine, R. L. (Eds). Dekker: New York, 1985.
- (63) da Silva, J. G.; Barros, H. J. V.; dos Santos, E. N.; Gusevskaya, E. V. *Appl. Catal. A* **2006**, *309*, 169.
- (64) Anastasiou, D.; Jackson, W. R.; McCubbin, Q. J.; Trnzcek, A. E. *Aust. J. Chem.* **1993**, *46*, 1623.
- (65) Walker, E. R. H. *Chem. Soc. Rev.* **1976**, *5*, 23.
- (66) Heathcock, C. H.; Ratcliffe, R. *J. Am. Chem. Soc.* **1971**, *97*, 1746.
- (67) Hermans, H. K. F.; Niemegeers, C. J. E. *J. US Pat.* 3.575.990, 1971.
- (68) SHELLXTL, Version 6.10. Sheldrick, G. M. Bruker AXS, Madison WI, 2004.
- (69) Chandran, K.; Nithya, R.; Sankaran, K.; Gopalan, A.; Ganesan, V. *Bull. Mater. Sci.* **2006**, *29*, 173.

-Chapter 4-

Activating Domino Hydroxymethylation *via* Multi-Component Catalysis

Abstract. The specific activity of a diphosphine-modified rhodium catalyst for hydroformylation was successfully translated for hydroxymethylation by incorporating into the system a modest molar ratio of triethylphosphine. Experimental observations have implicated the presence of a *tris*-phosphine rhodium species at the instant chemoselectivity is determined, but an analogous complex could not be synthesised. It was ascertained that a sequential hydrogenation, homogenous or heterogeneous, was not responsible. At higher molar ratios of triethylphosphine, the activity of its complexes frustrated catalysis.

4.1 Introduction

The domino hydroxymethylation scheme involves two critical selectivity determinations, each optimised by a rhodium catalyst of specific structure. The complexes of those diarylphosphine-substituted chelates with a natural bite angle in the range 115 to 145° confer high regioselectivity,¹ while the complexes of primary trialkylphosphines confer high chemoselectivity.² In a conventional approach to overall selectivity improvement, a new ligand is configured from the appropriate features of the individuals, often *via* a laborious synthetic route. A mixed-ligand methodology then becomes an interesting alternative.

At a low diphosphine to transition metal molar ratio the inclusion of a monophosphine may effect equilibria between *bis*-phosphine and *tris*-phosphine catalytic intermediates, which should exert a significant influence upon activity and selectivity. Inclusion of triphenylphosphine and diarylalkylphosphines in a solution of DIOP-modified rhodium is of reported benefit to regioselectivity in hydroformylation catalysis.³ ³¹P{¹H} NMR spectroscopy of the catalyst solution confirms the formation of a *tris*-phosphine-modified rhodium-hydride-dicarbonyl species (Figure 1).^{3a}

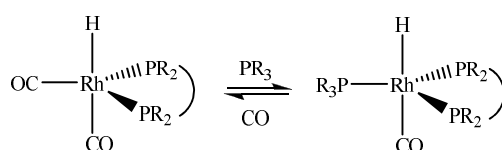


Figure 1. Equilibration of $[\text{Rh}(\text{CO})_{2-x}(\text{L-L})(\text{L})_x\text{H}]$ ($x = 0$ or 1) in mixed-ligand systems.

Although the dissociation of a CO auxiliary from such a species is quite improbable, the presence of *tris*-phosphine complex during alkene coordination and subsequent hydride migration was proposed to account for the observed improvement. A similar mixed-ligand system gave enhanced regioselectivity and enhanced enantioselectivity in the hydroformylation of styrene with both rhodium⁴ and platinum-tin chloride^{5a} catalysts. In the latter case, the species $[\text{Pt}(\text{DPPP})(\text{PPh}_2\text{Py})\text{Cl}]^+$ has been characterised spectroscopically.^{5b}

At high mixed-ligand to rhodium molar ratios, systems comprised of a diphosphine and a trialkylphosphine reportedly effect highly selective hydroxymethylation of 1-octene to 1-nonanol⁶ and 5-penten-1-ol to 1, 6-hexanediol.⁷ In the simplest case such a mixture will afford three rapidly inter-converting catalysts: two non-mixed *bis*-phosphine species and one mixed *tris*-phosphine species. In a more realistic spectrum some or all of two non-mixed *mono*-phosphine species, a mixed *bis*-phosphine species and two non-mixed *tris*-phosphine species are formed alongside,⁸ in addition to active complexes of higher nuclearity. The conglomeration of catalytic profiles then frustrates discussion of a mechanistic discourse.

With these considerations in mind, we report the utility of *bis*(diarylphosphine) chelate/triethylphosphine systems in the hydroxymethylation of allyl alcohol at relatively low mixed-ligand to rhodium molar ratios. The choice of diphosphine was made with a view to evaluating a representative range of natural bite angles and rigidity, these structural considerations borne out by molecular modelling (Figure 2). The complexation behaviour in these multi-component systems was investigated by NMR spectroscopy and IR spectroscopy, under both atmospheric and catalytic conditions. Mechanistic inferences are made on the basis of catalytic studies and deuterium labelling studies.

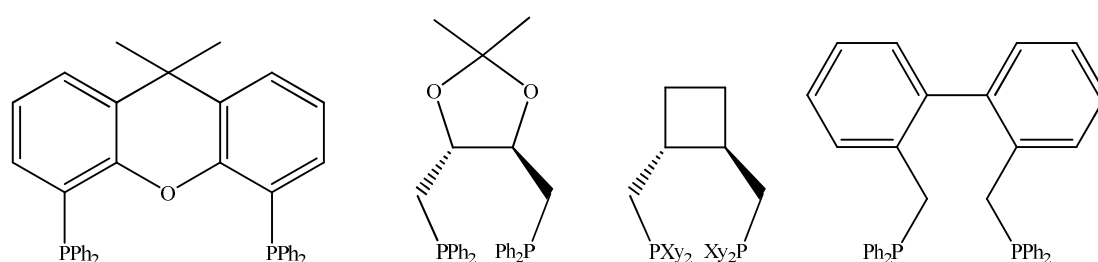


Figure 2. Diphosphine range (l→r): XANTPHOS, DIOP, CBM-DXP, BISBI.

4.2 Theoretical considerations

Computer modelled geometries were used to estimate the natural bite angle and the flexibility range of the diphosphines.⁹ Initial calculations were performed using the PM3(tm) method as implemented in SPARTAN SGI¹⁰ with high energy constraints fixing the rhodium-phosphorus bond length at 2.315 Å, a typical distance observed in crystal structures.¹¹ The natural bite angle was determined from the minimised conformation, accessed by eigenvector following as implemented in GAUSSIAN 98.¹² The flexibility range was estimated from a computed plot of potential energy as a function of the bite angle.

Table 1: Natural bite angles from molecular modelling, (corresponding flexibility range).^a

	XANTPHOS	DIOP	CBM-DXP	BISBI
PM3(tm) ^b	112.1 (96-133)	102.8 (94-117)	103.2 (93-122)	112.6 (104-142)
Tripos force field ^{ci}	111.7 (97-135)	102.3 (90-120)		112.6 (101-148)
Amber force field ^{cii}		102.3 (90-120)		113.0 (92-155)

^a $r_{\text{Rh-P}} = 2.315 \text{ \AA}$. ^bSPARTAN SGI. ^{ci}SYBYL, 13 in References and Notes, ^{cii}MACROMODEL, 14 in References and Notes.

4.3 Rhodium(I) Chemistry

Complexes under nitrogen. The influence of a competitive triethylphosphine concentration on diphosphine coordination behaviour was investigated, monitoring *in situ* complexation reactions in ethanol by NMR and solution IR spectroscopy. Addition of a solution of the mixed ligands gives exclusive formation of the [Rh(acac)(*L-L*)] complex (Table 2).

Table 2: Spectroscopic and analytical data for [Rh(acac)(*L-L*)].

<i>L-L</i>		³¹ P{ ¹ H} NMR			CHN found (calc.)	
		δ (ppm)	¹ J _{Rh-P} (Hz)	Δδ ^c (ppm)	C	H
XANTPHOS	<i>in situ</i> ^a	d. 42.2	179	56.4		
	isolated ^b	d. 42.9	178	57.1	42.82 (42.76)	3.31 (3.47)
DIOP	<i>in situ</i>	d. 39.1	188	62.4		
	isolated	d. 41.5	186	64.8	37.68 (37.80)	3.79 (3.83)
CBM-DXP	<i>in situ</i>	d. 36.8	185	62.7		
	isolated	d. 35.9	183	61.8	40.47 (40.66)	4.15 (4.23)
BISBI	<i>in situ</i>	d. 48.7	174	60.6		
	isolated	d. 48.0	174	59.9	44.26 (44.34)	3.49 (3.60)

^a*In situ*: 1 mL 40% ethanol (v/v in *d*₈-thf), 10 mM [Rh], *L-L*/PEt₃/Rh = 1/2/1, ambient temperature, atmospheric pressure of nitrogen, 1 hour. ^b1 mL *d*₃-chloroform, ambient temperature, atmospheric pressure of nitrogen. ^cCoordination shift (Δδ = δ_{complex} - δ_C).

In the ³¹P{¹H} NMR spectrum, the complex is resolved as a sharp doublet at δ_p = 36.8-50.5 ppm. A singlet at δ_p ≈ -17.2 ppm is attributed to free triethylphosphine.¹⁵ The coordination shifts for [Rh(acac)(*L-L*)] (*L-L* = DIOP, CBM-DXP and BISBI) correspond to the formation of a seven-membered chelating ring,¹⁶ with magnitude approximately proportional to rigidity. In the corresponding solution IR spectra no ν_{CO} bands are observed at ~ 1980 cm⁻¹ or in the range 1760-1740 cm⁻¹, which confirms chelation of the diphosphine and acac respectively.¹⁷ The isolated complexes, obtained as red prisms, were subjected to microanalysis to verify composition.

Yellow crystals of [Rh(acac)(DIOP)] suitable for single crystal X-ray diffraction analysis were obtained by slow evaporation of acetone from a concentrated solution. The molecular structure and selected bond angles and distances are presented (Figure 3, Table 3). The empirical formula is given as [C_{37.5}H₄₂O_{4.5}P₂Rh] because a molecule of acetone co-crystallises per two molecules of the complex. The rhodium has a slightly distorted square planar coordination sphere and the rhodium-DIOP unit has C₂-symmetry. Bond angles (*e.g.* P-Rh-P = 95.5°) and distances (*e.g.* Rh-P = 2.18 Å and Rh-O = 2.07 Å) correspond well with those of other [Rh(acac)(PR₃)₂] complexes and do not merit further comment.¹⁸

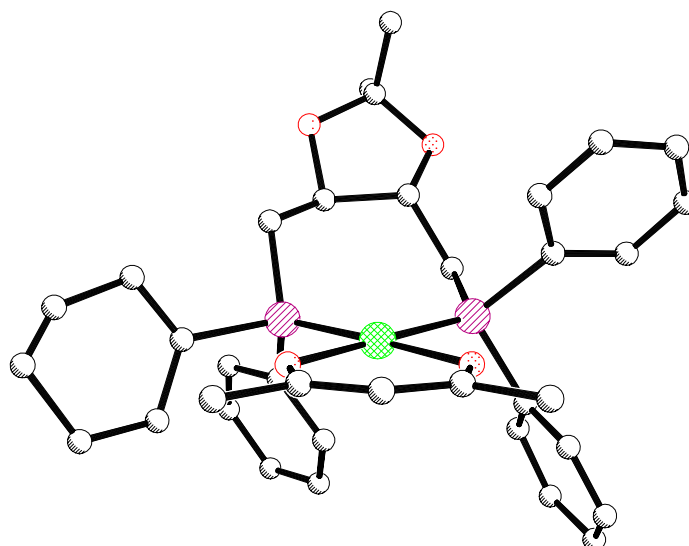


Figure 3. ORTEP drawing of [Rh(acac)(DIOP)] with ellipsoids at 50 % probability level. Hydrogen atoms are omitted for clarity.

Table 3: Selected bond distances (Å) and bond angles (°) for [Rh(acac)(DIOP)], (ESD).

bond distance		bond angle	
Rh-P(1)	2.188(2)	P(1)-Rh-P(6)	95.4(19)
Rh-P(6)	2.194(17)	P(1)-Rh-O(35)	89.2(15)
Rh-O(35)	2.044(5)	P(1)-Rh-O(37)	176.6(15)
Rh-O(37)	2.079(5)	P(6)-Rh-O(35)	175.2(15)
		P(6)-Rh-O(37)	87.9(14)
		O(35)-Rh-O(37)	87.4(19)
P(1)-C(2)	1.848(8)		
C(2)-C(3)	1.450(9)	Rh-P(1)-C(2)	118.9(3)
P(6)-C(5)	1.812(7)		
C(4)-C(5)	1.540(10)	Rh-P(6)-C(5)	122.4(2)
C(3)-C(4)	1.549(10)		

The complexation reaction of neat triethylphosphine was followed by solution IR spectroscopy and indicates the formation of [Rh(acac)(CO)(PEt₃)] by a ν_{CO} absorption band at 1981 cm⁻¹ due to the terminal CO moiety. Displacement of the second CO auxiliary could not be achieved, even after purging the solution with nitrogen. Indeed, reports of analogous rhodium-trialkylphosphine complexes are rare.¹⁹

The precursors [Rh(CO)₂Cl]₂ and [RhCl₃·3H₂O] reacted smoothly with the diphosphine to afford the sparingly soluble *trans*-bridged [Rh(CO)(μ-*L-L*)Cl]₂ dimer, leaving free triethylphosphine

in solution (Table 4). The $^{31}\text{P}\{^1\text{H}\}$ NMR spectra show a broad doublet at $\delta_{\text{P}} = 78.6\text{-}82.4$ ppm, the *trans* square planar coordination of the phosphorus nuclei demonstrated by their unique environment. In the corresponding solution IR spectra, the ν_{CO} band at $1953\text{-}1977$ cm^{-1} is characteristic of a terminal CO auxiliary *trans* to chloride.²⁰ As expected, the magnitude of this band depends upon the electronegativity of the diphosphine. A weak $\nu_{\text{Rh-Cl}}$ band at $319\text{-}335$ cm^{-1} is also observed. The spectral data is in excellent agreement with that reported for the $[\text{Rh}(\text{CO})(\mu\text{-DPPE})\text{Cl}]_2$ dimer,²¹ which would suggest a similar structure is taken up by these new complexes. In the molecular structure of $[\text{Rh}(\text{CO})(\mu\text{-dppe})\text{Cl}]_2$ each rhodium nucleus sits in a symmetrical, quasi-octahedral environment and is as Rh(III).²² Conductivity measurements confirm that only the dinuclear species was present in solution, with no ionic dissociation of $[\text{Rh}(\mu\text{-L-L})(\text{CO})\text{Cl}]_2$ to $[\text{Rh}(\text{L-L})_2]^+[\text{Rh}(\text{CO})_2\text{Cl}_2]^-$.

Table 4: Spectroscopic and physical data for solutions of $[\text{Rh}(\text{CO})(\text{L-L})\text{Cl}]_n$.

precursor	<i>L-L</i>	<i>n</i>	$^{31}\text{P}\{^1\text{H}\}$ NMR		IR (cm^{-1})		A_{M}^c ($\Omega^{-1}\text{cm}^2\text{mol}^{-1}$)
			δ (ppm)	$^1J_{\text{Rh-P}}$ (Hz)	ν_{CO}	$\nu_{\text{Rh-Cl}}$	
$[\text{Rh}(\text{CO})_2\text{Cl}]_2^a$, $\text{RhCl}_3 \cdot 3\text{H}_2\text{O}^{bi}$	XANTPHOS	2	d. 80.5	129	1963 (s)	335 (w)	1.81
	DIOP	2	d. 79.4	124	1953 (s)	319 (w)	1.68
	CBM-DXP	2	d. 78.5	121	1977(s)	324 (w)	1.53
	BISBI	2	d. 79.1	125	1959 (s)	317 (w)	2.05
	PEt ₃	1	d. 25.1	116	1958 (s)	301 (w)	
$\text{RhCl}_3 \cdot 3\text{H}_2\text{O}^{bii}$	CBM-DXP	1	dd. 45.1 dd. 68.4	124 153	2003 (s)	341 (w)	

^aConditions: 1mL 40% ethanol (v/v in d_8 -thf), 10 mM [Rh], *L-L*/PEt₃/Rh = 1/2/1, ambient temperature, atmospheric pressure of nitrogen. ^{bi}Conditions: 1mL 50% ethanol (v/v in d_8 -thf), 20 mM [Rh] with *L-L*/PEt₃/Rh = 1/1/2, ambient temperature, atmospheric pressure of nitrogen, 1.5 hours. ^{bii}0.3 hours, $^2J_{\text{P-P}} = 35$ Hz. ^cConductivity in ~ 0.25 mM [Rh] ethanol solution.

Observation of the square planar $[\text{Rh}(\text{CO})(\text{L-L})\text{Cl}]$ species was not expected because natural bite angle constraints of the diphosphine should result in formation of the energetically unstable *cis* geometry.^{20b} Surprisingly then, the formation of *cis*- $[\text{Rh}(\text{CO})(\text{CBM-DXP})\text{Cl}]$ is evidenced by two doublet of doublets in the $^{31}\text{P}\{^1\text{H}\}$ NMR spectrum (Figure 4a). It seems that the 3, 5-dimethylphenyl substituents on phosphorus provide sufficient site isolation to retard dimeric association. The resonance at $\delta_{\text{P}} = 45.1$ ppm is ascribed to the phosphorus nucleus *trans* to CO, and that at $\delta_{\text{P}} = 68.4$ ppm is ascribed to the phosphorus nucleus *trans* to chloride. The pattern is qualitatively similar to that observed for *cis*- $[\text{Rh}(\text{CO})(\text{DPPE})\text{Cl}]$,²¹ but a smaller rhodium-phosphorus coupling is suggestive of shorter rhodium-phosphorus bond lengths. This is consistent with the lower electronegativity of CBM-DXP. The solution IR spectrum shows a ν_{CO} band at 2003 cm^{-1} which is characteristic of a terminal CO *trans* to phosphorus (Figure 4b). Complexation of $[\text{Rh}(\text{CO})_2\text{Cl}]_2$ with only

triethylphosphine gave *trans*-[Rh(CO)(PEt₃)₂Cl], its spectral data in good agreement with that in the literature.²³

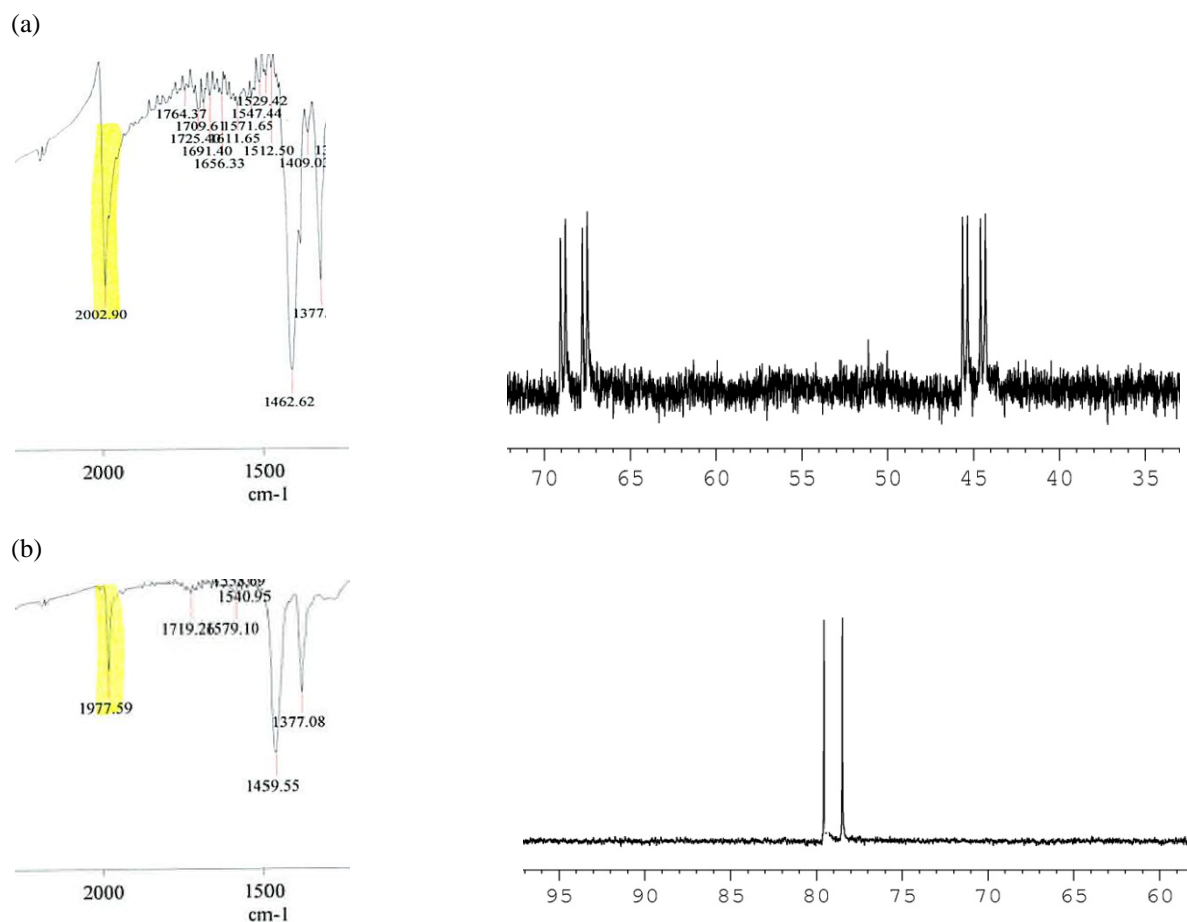


Figure 4. Solution IR and NMR spectra of [Rh(CO)(CBM-DXP)Cl]_n in 33% ethanol/*d*₈-thf:

(a) *cis*-[Rh(CO)(CMB-DXP)Cl], (b) *trans*-[Rh(CO)(μ-CMB-DXP)Cl]₂.

Complexes under syngas. When competing concentrations of a diphosphine and triethylphosphine are present in solution with a rhodium precursor under *syngas*, the catalyst resting state could potentially exist as an equilibrium ensemble of the *bis*-phosphine-modified rhodium-hydride-dicarbonyl complex, the carbonyl-bridged rhodium dimer and the *tris*-phosphine-modified rhodium-hydride-carbonyl complex. *In situ* formation of rhodium complexes from [Rh(acac)(CO)₂] in *d*₄-methanol was therefore investigated by high pressure NMR spectroscopy (Figure 5). Comparison with the reference system indicates almost exclusive formation of [RhH(CO)₂(XANTPHOS)], together with free triethylphosphine. After 15 minutes at 40°C, the complex is characterised by an apparent triplet of doublets at δ_H = -8.9 ppm in the ¹H NMR spectrum, with ¹J_{H-Rh} = 6.6 Hz and ²J_{P-H} = 14.7 Hz, and a doublet at δ_P = 20.7 ppm in the ³¹P{¹H} NMR spectrum, with ¹J_{Rh-P} = 124 Hz. It is worth noting the broad resonance at δ_P ≈ 9 ppm in the ³¹P{¹H} NMR spectrum, which suggests that

formation of the carbonyl-bridged rhodium dimer is inhibited. Line-shape analyses of the $^{31}\text{P}\{^1\text{H}\}$ NMR spectra over the temperature range -5 to 100°C gives no evidence for exchange between the XANTPHOS-chelated rhodium complex and free triethylphosphine (Figure 6).²⁴

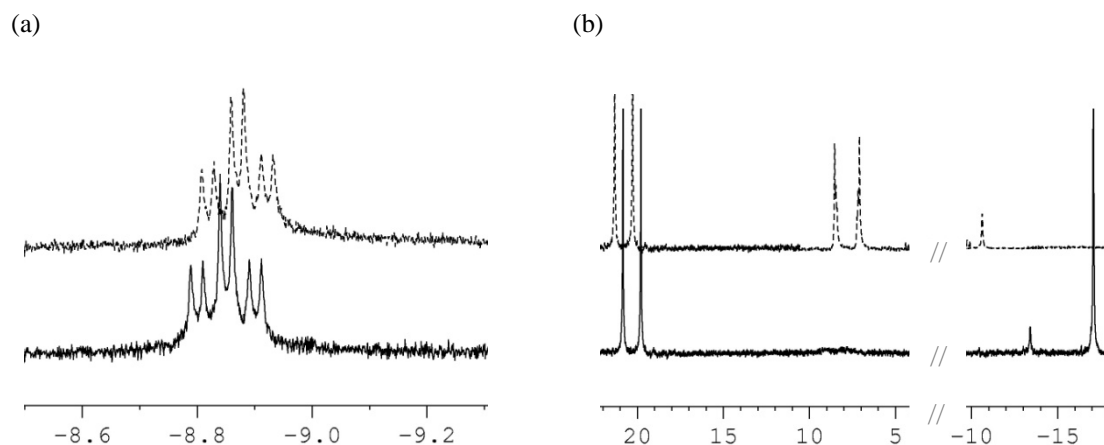


Figure 5. HP-NMR spectra of $[\text{Rh}(\text{CO})_2(\text{XANTPHOS})]/\text{PEt}_3$ (solid) and reference (perforated) at 45°C : (a) ^1H NMR spectrum, (b) $^{31}\text{P}\{^1\text{H}\}$ NMR spectrum.

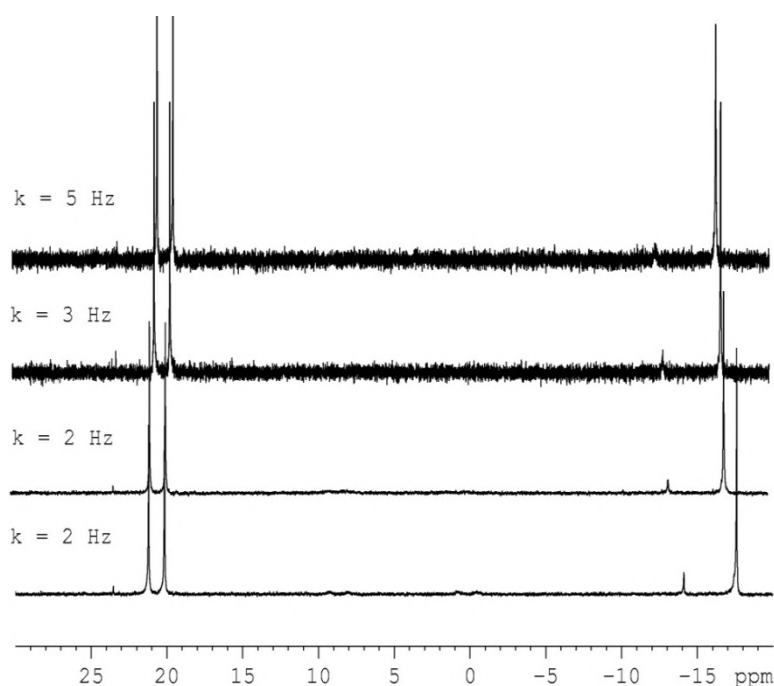


Figure 6. ^{31}P NMR spectra of $[\text{Rh}(\text{CO})_2(\text{XANTPHOS})]/\text{PEt}_3$ (-5 to 100°C) and calculated exchange rates.

The apparent influence of triethylphosphine on the solution concentration of $[\text{Rh}(\text{CO})(\text{XANTPHOS})(\mu\text{-CO})_2]$ was then investigated by high pressure IR spectroscopy (Table 5). A solution of $[\text{Rh}(\text{acac})(\text{XANTPHOS})]$ in methanol was pressurised with $\text{CO}/\text{H}_2 = 1$. In the reference spectrum the terminal and bridging ν_{CO} bands from the carbonyl-bridged rhodium dimer are observed

at 1985 cm^{-1} and 1723 cm^{-1} respectively, together with ν_{CO} bands at 2037 cm^{-1} (ν_1), 1990 cm^{-1} (ν_2), 1983 cm^{-1} (ν_3) and 1948 cm^{-1} (ν_4) that can be assigned to the geometric isomers of $[\text{RhH}(\text{CO})_2(\text{XANTPHOS})]$. The strong terminal ν_{CO} band from $[\text{Rh}(\text{CO})(\text{XANTPHOS})(\mu\text{-CO})]_2$ somewhat masks the ν_2 and ν_3 bands. Depressurising and repressurising with $\text{CO}/\text{D}_2 = 1$ allowed distinction between *ee*- $[\text{RhH}(\text{CO})_2(\text{XANTPHOS})]$ and *ea*- $[\text{RhH}(\text{CO})_2(\text{XANTPHOS})]$.²⁵ The ν_1 and ν_3 bands shift to a lower frequency upon hydride/deuteride exchange and are therefore assigned to the CO moieties of the *ee* complexes, with the unshifted ν_2 and ν_4 bands assigned to those of the *ea* isomer.

Table 5: HP-IR data for $[\text{RhH}(\text{CO})_2(\text{XANTPHOS})]$ and $[\text{Rh}(\text{CO})(\text{XANTPHOS})(\mu\text{-CO})]_2$ in methanol.^a

complex	ν_{CO} (cm^{-1})	
	CO/H_2	CO/D_2
<i>ee</i> - $[\text{RhH}(\text{CO})_2(\text{XANTPHOS})]$	2037 (<i>sym</i>), 1983 (<i>anti</i>)	2020 (<i>sym</i>), 1966 (<i>anti</i>)
<i>ea</i> - $[\text{RhH}(\text{CO})_2(\text{XANTPHOS})]$	1990 (<i>sym</i>), 1944 (<i>anti</i>)	1990 (<i>sym</i>), 1943 (<i>anti</i>)
$[\text{Rh}(\text{CO})(\text{XANTPHOS})(\mu\text{-CO})]_2$	1984, 1723 (μ)	1985, 1723 (μ)

^aConditions: 10 mL methanol, 5 mM $[\text{Rh}]$, $\text{XANTPHOS}/\text{Rh} = 2$, 40°C, 40 bar $\text{CO}/(\text{D}_2$ or $\text{H}_2) = 1$.

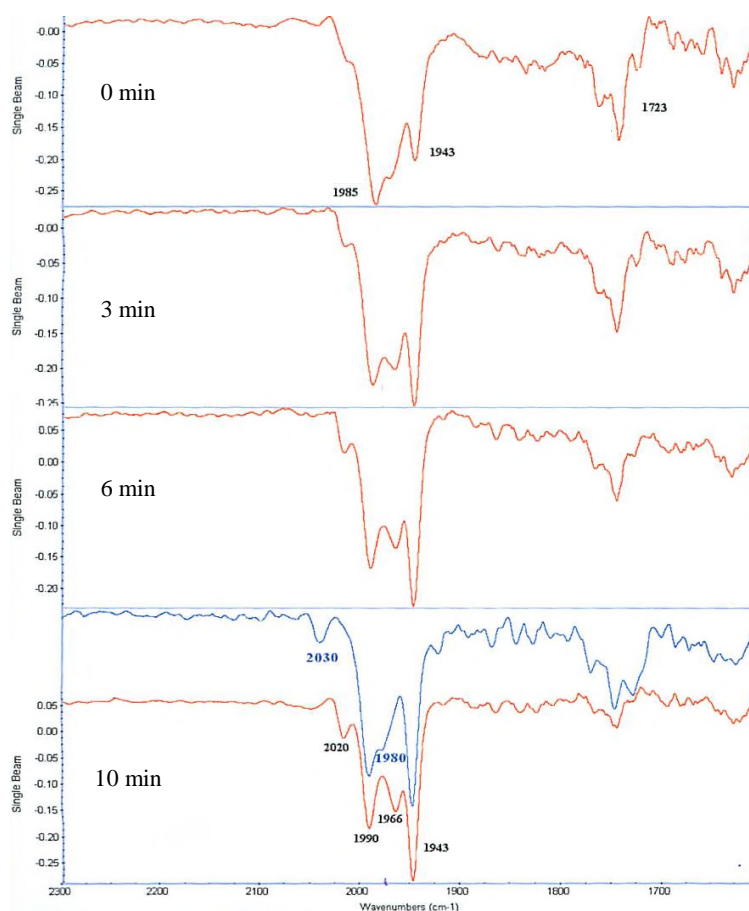


Figure 7. HP-IR spectra of the XANTPHOS/ PEt_3 / $[\text{Rh}(\text{acac})(\text{CO})_2]$ system in time.

Twenty minutes after enriching the catalyst solution in 25.8 mM triethylphosphine the terminal ν_{CO} band from the dimer is no longer discernable (Figure 7). This suggests that the free phosphine has a deleterious effect on bimetallic association. The *anti*-symmetric ν_{CO} bands from the $[\text{RhD}(\text{CO})_2(\text{XANTPHOS})]$ complexes intensify simultaneously, and the corresponding symmetric ν_{CO} bands become resolved at 2020 cm^{-1} and 1990 cm^{-1} for the *ee* and *ea* geometries respectively.

4.4 Catalysis

The selectivity of catalytic systems formed upon increasing the concentration of triethylphosphine in a solution of diphosphine and rhodium precursor was assessed (Table 6). The catalytic solutions were prepared *in situ* from $[\text{Rh}(\text{acac})(\text{CO})_2]$, and incubated for a period of 20 minutes to under 30 bar $\text{CO}/\text{H}_2 = 1$ at 120°C to allow formation of the active species.

Regioselectivity. As the catalyst solutions become enriched in up to 16 mM triethylphosphine, its cone angle enabling coordination as a third phosphine,²⁶ the selectivity for linear products diminishes only slightly from that observed for the reference systems. The resident state of rhodium is almost certainly $[\text{RhH}(\text{CO})_2(\text{L-L})]$, because CO dissociation from the *tris*-phosphine complex would be controversial. Although equilibrium between *bis*-phosphine and *tris*-phosphine rhodium species during subsequent allyl alcohol coordination and hydride migration is not precluded, the regioselective enhancement typically associated with a mixed ligand effect is not observed.^{3a, 3b, 4} Even a competitive excess of triethylphosphine, defined as $\text{L-L}/\text{PEt}_3/\text{Rh} = 2/ > 2/2$, is seemingly ineffective at promoting the association equilibrium, which implies that only the diphosphine is coordinated to rhodium at the instant regioselectivity is determined.

Further enrichment in triethylphosphine leads to a higher decline in regioselectivity for the diol fraction, but no significant deviation of this parameter is observed for the hydroxyaldehyde fraction. The involvement of a triethylphosphine-modified rhodium catalyst, which independently effects diol formation with regioselectivity in the range 1.8 ($\text{PEt}_3/\text{Rh} = 1.25$) to 2.4 ($\text{PEt}_3/\text{Rh} = 2.5$),^{2b, 2d} is thus intimated. However such a system also exhibits lower activity and so, regardless of concentration in the solution, its contribution to the observed regioselectivity effectively remains low.

The slightly enhanced regioselectivity noted for the diol fraction is almost certainly due to a small degree of sequential hydrogenation, because steric demands make 4-hydroxybutanal more susceptible to this transformation than 2-methyl-3-hydroxypropanal.

Chemoselectivity. Interestingly, selectivity to the C_3 -products derived from the isomerisation of and the hydrogenation of allyl alcohol remains relatively unaffected by the catalyst stoichiometry.

Table 6: Product profile for hydroxymethylation of allyl alcohol with diphosphine/PEt₃/Rh systems in ethanol.^a

		allyl alcohol-based selectivity (mol%)											C=O ^b	C-OH ^c	C ₃ ^d	
		1-propanal	1-propanol	2-methyl-propanal	methacrolein	2-methyl-propanol	2, 3- dihydrofuran	2-ethoxyfuran	crotonaldehyde	2-methyl-pentnal	2-methyl-1,3-propanediol	1, 4- butanediol	γ-butyrolactone	(l/b)	(l/b)	
	[PEt ₃] (mM)															
XANTPHOS	0	9	1	2	13	0	10	54	11	0	0	0	0	89 (5.1)	0	11
	0.5	8	0	0	14	1	6	62	6	1	0	0	0	89 (5.1)	1 (b)	10
	4	6	1	2	11	2	7	52	5	1	0	10	2	89 (5.2)	2 (0.2)	9
	10	0	4	3	0	9	3	12	0	3	2	56	5	18 (4.9)	72 (5.3)	10
	16	1	3	2	0	11	3	6	1	3	1	59	6	12 (4.9)	78 (5.2)	10
	24	1	5	2	0	18	0	12	0	3	1	49	7	13 (4.8)	75 (2.9)	12
	32	0	4	3	0	21	0	14	1	4	2	40	9	16 (4.7)	72 (2.4)	12
DIOP	0	2	0	2	11	2	15	63	4	0	0	1	0	96 (6.3)	3 (0.5)	2
	4	1	0	5	6	2	13	56	2	0	0	15	0	81 (6.3)	17 (6.5)	2
	10	1	0	3	0	9	7	11	0	0	1	61	7	20 (6.3)	78 (6.5)	1
	16	1	1	2	0	10	5	8	0	0	1	67	5	15 (6.3)	83 (6.5)	2
	24	0	1	2	0	15	3	8	3	0	1	61	5	17 (6.2)	82 (4.3)	2
CBM-DXP	32	1	1	3	0	17	0	12	5	0	2	52	8	19 (6.2)	79 (3.7)	2
	0	3	0	1	5	0	27	57	7	0	0	0	0	97 (13.2)	0	3
	4	2	1	5	1	1	31	45	3	1	0	8	1	85 (13.1)	10 (14.3)	5
	10	1	1	2	0	4	13	11	2	1	1	58	6	28 (13.1)	68 (14.3)	4
	16	0	2	1	0	5	7	12	1	1	0	66	5	20 (13.1)	76 (14.3)	4
BISBI	24	0	0	1	0	7	7	15	2	2	1	58	6	24 (13.0)	72 (10.3)	4
	32	0	2	2	0	7	5	17	3	1	1	56	6	26 (12.9)	70 (9.2)	4
	0	9	1	1	14	0	13	49	5	4	0	0	0	82 (4.5)	0	18
	4	7	2	2	13	0	10	52	4	4	0	3	0	80 (4.5)	3 (4.7)	17
	10	4	4	4	1	10	4	15	0	4	1	49	0	24 (4.5)	60 (4.6)	16
	16	4	6	3	0	11	5	9	0	4	1	49	5	17 (4.5)	65 (4.5)	18
	24	4	7	3	1	20	3	13	1	3	2	38	3	20 (4.4)	63 (4.4)	17
	32	6	5	4	0	23	3	15	2	3	1	31	4	23 (4.4)	60 (4.4)	17

^aConditions: 4 mL ethanol, 8 mM [Rh], diphosphine/Rh = 2, Rh/allyl alcohol = 1/185, 120°C, 40 bar CO/H₂ = 1, 4 hours. ^bHydroxylaldehyde derivatives. ^cDiol derivatives. ^dProducts of isomerisation and hydrogenation.

It is worth mentioning that 2-methylpentenal becomes a significant product in this distribution at higher concentrations of triethylphosphine. One explanation is that free triethylphosphine behaves as the base which is necessary to initiate the aldol condensation of 1-propanal.

The reference catalysts yield predominantly hydroxyaldehyde fractions. Composite assays of these are complicated by the thermal sensitivity of 4-hydroxybutanal and 2-methyl-3-hydroxypropanal. The linear isomer undergoes extensive degradation to 2-furanol, which is stabilised *via* dehydration to the vinyl cyclic ether or *via* alcoholysis with the solvent, and dehydration to crotonaldehyde, stabilised by α , β -conjugation. The branched isomer dehydrates smoothly to methacrolein, which is found to undergo oligomerisation over longer reaction periods.

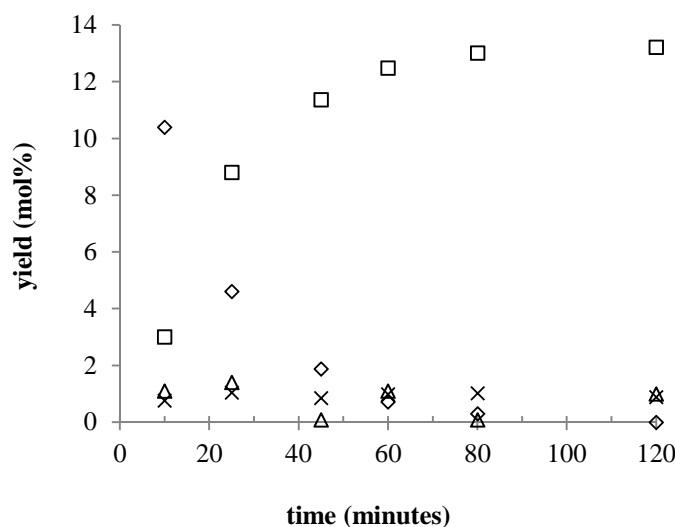


Figure 8. Conversion-time profile (*b* isomer only) for allyl alcohol hydroxymethylation with the DIOP/PEt₃/Rh system:

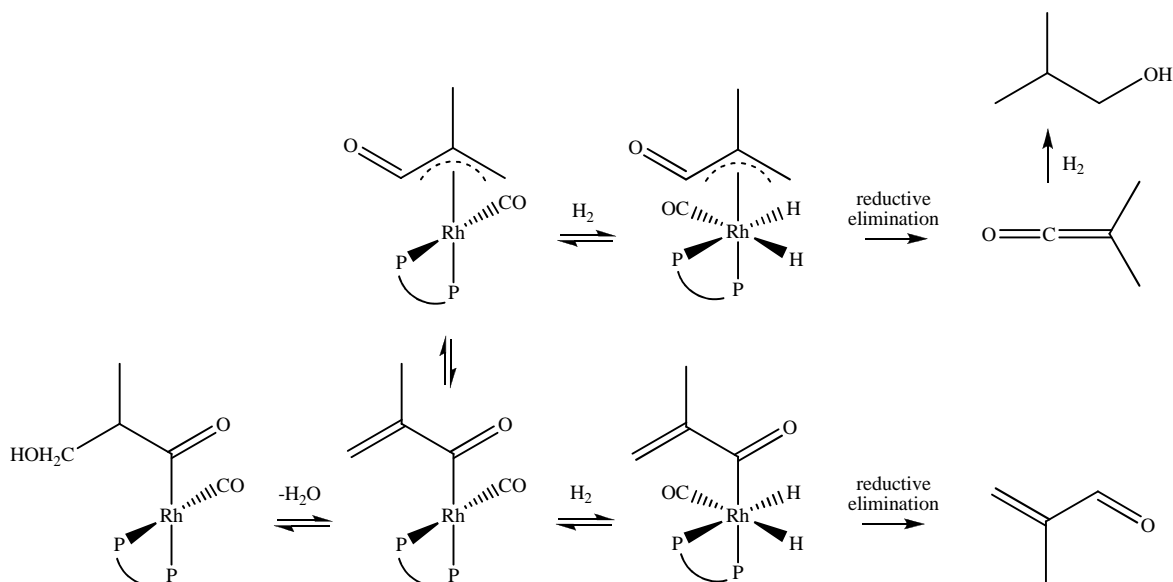
(□) 2-methylpropanol, (◇) 2-methylpropanal, (Δ) methacrolein, (×) 2-methylpropane-1, 3-diol.

(Conditions: 4 mL ethanol, 8 mM [Rh], DIOP/PEt₃/Rh = 2/2/1,

Rh/allyl alcohol = 1/185, 120°C, 40 bar CO/H₂ = 1)

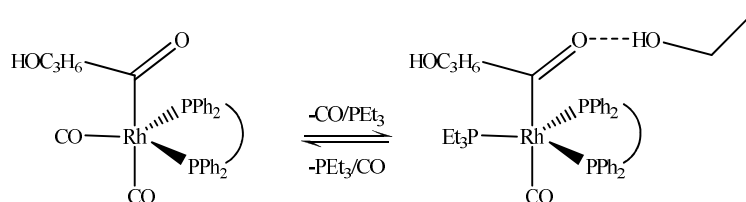
As the catalyst solutions are enriched in up to 16 mM triethylphosphine, 1, 4-butanediol and 2-methylpropanol formation is promoted at the expense of the hydroxyaldehyde fraction. By monitoring the recovered product mixture as a function of time it is demonstrated that 2-methylpropanol is formed *via* 2-methylpropanal, with an expected positive dependence on the concentration of triethylphosphine, and that the latter is not the product of selective methacrolein hydrogenation (Figure 8). An alternative possibility for 2-methylpropanol formation is *via* conjugation-driven dehydration of the rhodium=methylpropendiol-carbonyl intermediate.^{2b, 2d} Certainly this mechanism would account for the observation that *anti*-Markovnikoff hydride migration gave 1, 4-butanediol selectively, since dehydration of the rhodium=butenediol-carbonyl intermediate does not result in conjugated double bonds. It can be ascertained that the dehydration does not occur in the rhodium-

methylhydroxypropanoyl-dicarbonyl complex, although this would also give a conjugated system, since this route should also give a quantitative yield of methacrolein (Scheme 1). Non-intermediacy of the hydroxyaldehydes is further demonstrated by the resistance of 2-ethoxyfuran to the tandem hydrolysis-hydrogenation necessary for 1, 4-butanediol formation, unless in the presence of a weak base such as alumina or kieselgel



Scheme 1. Product pathways from dehydration of the rhodium-methylhydroxypropanoyl-dicarbonyl complex.

The stoichiometry at the point of inversion, defined as $L-L/PEt_3/Rh = 1/2/1$, suggests that a *tris*-phosphine rhodium intermediate exists at the instant where chemoselectivity is determined. Despite no evidence for triethylphosphine coordination in the regioselective determinant, in a broader approach equilibration between the *bis*-phosphine and *tris*phosphine modified rhodium-acyl-dicarbonyl complexes could be of consideration (Scheme 2).



Scheme 2. Equilibration of chelated rhodium-acyl complexes in the presence of triethylphosphine.

The displacement of a strong π -acceptor CO auxiliary by a strong σ -donor auxiliary should render the acyl oxygen electronegative, allowing protonation by ethanol as the pivotal step in domino hydroxymethylation. Reversible CO dissociation from the rhodium-octyl-dicarbonyl complex has

previously been observed at 5°C.¹ A selection of experiments was therefore repeated over a range of carbon monoxide partial pressures, maintaining a constant hydrogen partial pressure and 40 bar total pressure by addition of argon (Figure 9). The enhanced chemoselectivity at reduced carbon monoxide partial pressure reflects more facile CO displacement by triethylphosphine. The correlation is rendered non-linear however by increasingly competitive allyl alcohol hydrogenation in range 5-15 bar. Furthermore, 2-methylpropanal becomes a significant product at the expense of 2-methylpropanol when carbon monoxide partial pressure drops below 8 bar. If the hydrogenation catalyst exists predominantly as a *tris*-phosphine-modified rhodium-hydride, then steric hindrance would prevent hydrogenation of this branched product.

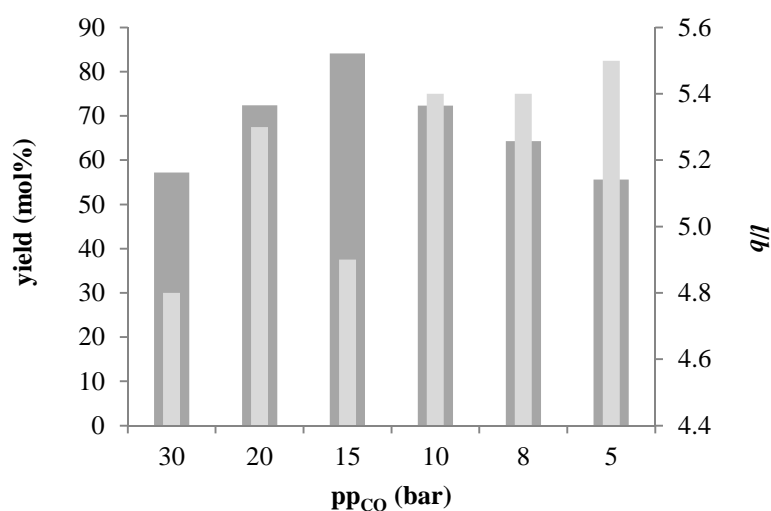


Figure 9. Hydroxymethylation activity of XANTPHOS/PEt₃/Rh system for allyl alcohol as a function of carbon monoxide partial pressure: V(■) yield (diols), (■) I/b.
(Conditions: 4 mL ethanol, 8 mM [Rh], XANTPHOS/PEt₃/Rh = 2/2/1,
Rh/allyl alcohol = 1/185, 120°C, 40 bar CO/H₂ = 1)

For catalyst solutions that are equimolar with respect to triethylphosphine a perfect linear correlation between chemoselectivity and flexibility of the diphosphine is established, typically $r^2 > 0.98$ (Figure 10). Rigidity of the chelate scaffold appears to be an important requisite for enhanced hydroxymethylation activity. One explanation may be that triethylphosphine can enforce the η^1 -dissociation of a more flexible diphosphine, effectively maintaining a *bis*-phosphine-modified rhodium-acyl-dicarbonyl intermediate. This would also account for the observed accentuation at higher triethylphosphine concentrations. For all the sequences investigated, optimum conversion of allyl alcohol to 1, 4-butanediol is observed when the catalyst stoichiometry approximates *L-L*/PEt₃/Rh = 2/2/1.

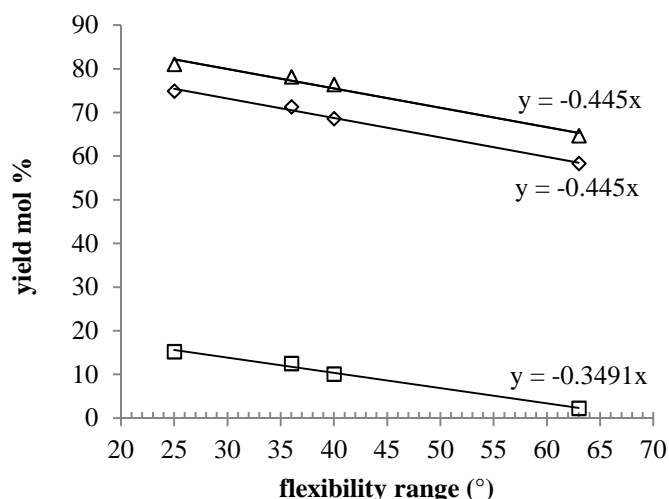


Figure 10. Hydroxymethylation activity of *L-L*/PEt₃/Rh systems for allyl alcohol as a function of *L-L* flexibility range: (□) *L-L*/PEt₃/Rh = 2/0.5/1, (◇) *L-L*/PEt₃/Rh = 2/1.25/1, (Δ) *L-L*/PEt₃/Rh = 2/2/1.

When the concentration of triethylphosphine exceeds that of the diphosphine, unexpected regression of chemoselectivity is observed. In this region of excess the deprotonation of ethanol by free triethylphosphine could be responsible.^{27a} In order to evaluate this a base solution of *L-L*/PEt₃/Rh = 2/2/1 in ethanol was enriched in 8 mM *N, N*-dimethylbenzylamine, which has a comparable acidity constant to triethylphosphine,^{27b} and then applied for catalysis. The product mixtures were assayed against those obtained using the base solution enriched in 8 mM triethylphosphine (Table 7).

Table 7: Hydroxymethylation of allyl alcohol with basified *L-L*/PEt₃/Rh systems in ethanol.^a

<i>L-L</i>	base ^b	allyl alcohol-based selectivity (mol%)			
		C=O ^c (<i>l/b</i>)	-OH ^d (<i>l/b</i>)	iso.	hyd.
XANTPHOS	triethylphosphine	13 (4.8)	75 (2.9)	9	3
	dimethylbenzylamine	13 (4.9)	77 (5.2)	8	2
DIOP	triethylphosphine	17 (6.2)	82 (4.3)	1	0
	dimethylbenzylamine	16 (6.2)	81 (6.4)	2	1
BISBI	triethylphosphine	20 (4.4)	63 (2.2)	15	2
	dimethylbenzylamine	20 (4.6)	63 (4.5)	14	3

^aConditions: 4 mL ethanol, 8 mM [Rh], *L-L*/PEt₃/Rh = 2/2/1, Rh/allyl alcohol = 1/185, 120°C, 40 bar CO/H₂ = 1, 3 hours. ^b8 mM [base]. ^cHydroxyaldehyde derivatives. ^dDiol derivatives.

Comparable inhibition of chemoselectivity is observed with these systems, confirming the role of free triethylphosphine as a proton sponge. The corresponding decline in linear selectivity for systems enriched in triethylphosphine is not observed in the test systems however, and suggests the emerging activity of a triethylphosphine-modified rhodium catalyst in the former case. It must be noted that amine-modified rhodium catalysts have been successfully applied in hydroxymethylation catalysis,²⁸

so some modification of the active catalyst in the presence of *N,N*-dimethylbenzylamine should be of consideration.

Catalyst decomposition. A dramatic colour change was observed upon recovering each sequence of catalyst solutions (Figure 11). Filtration through a thin silica pad revealed the dispersion of a fine metallic black powder in the medium of darker samples, suggesting some decomposition of the homogeneous catalyst.

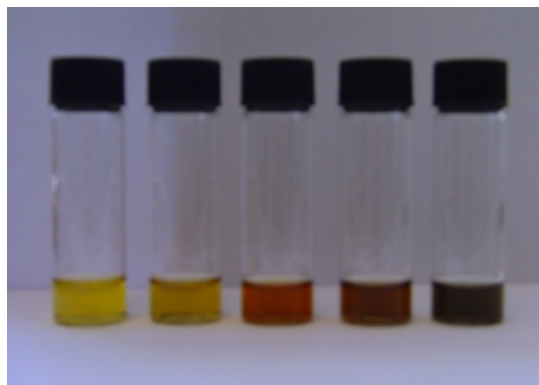


Figure 11. Example of a recovered catalyst sequence.

Metallic rhodium thus formed could be responsible effecting auto-tandem hydroxymethylation, so 0.2 gram atom elemental mercury per gram atom rhodium was introduced into the autoclave before re-application of the *L-L*/PEt₃/Rh system in catalysis. Any colloidal rhodium should amalgamate with the mercury and not be available as a heterogeneous hydrogenation catalyst. On analysis, 11 mol% hydroxyaldehyde, with *l/b* = 4.7, and 76 mol% diol, with *l/b* = 5.1, are recovered for the XANTPHOS/PEt₃/Rh system; 15 mol% hydroxyaldehyde, with *l/b* = 6.2, and 82 mol% diol, with *l/b* = 6.0, are recovered for the DIOP/PEt₃/Rh system; 21 mol% hydroxyaldehyde, with *l/b* = 13.4, and 75 mol% diol, with *l/b* = 13.7, are recovered for the CBM-DXP/PEt₃/Rh system; 17 mol% hydroxyaldehyde, with *l/b* = 3.9, and 64 mol% diol, with *l/b* = 4.2, are recovered for the BISBI/PEt₃/Rh system. The similarity of these product distributions with those identified for reactions without mercury present indicates homogeneity of the reaction. Ions of lead, mercury and bismuth should also inhibit heterogeneous hydrogenation as they are reducible by metallic rhodium.²⁹ Addition of 0.2 g atom lead distearate per gram atom rhodium does not appear to root an influence on hydroxymethylation activity.³⁰

Monitoring the post-filtration solution concentration of rhodium in time by icp-oes has shown that formation of the colloidal species only starts to occur on a significant scale upon complete substrate conversion (Figure 12).³¹ The deposition of a rhodium mirror below the solution level was observed in the last three runs. The exact role of triethylphosphine in destabilising the catalyst remains unclear.

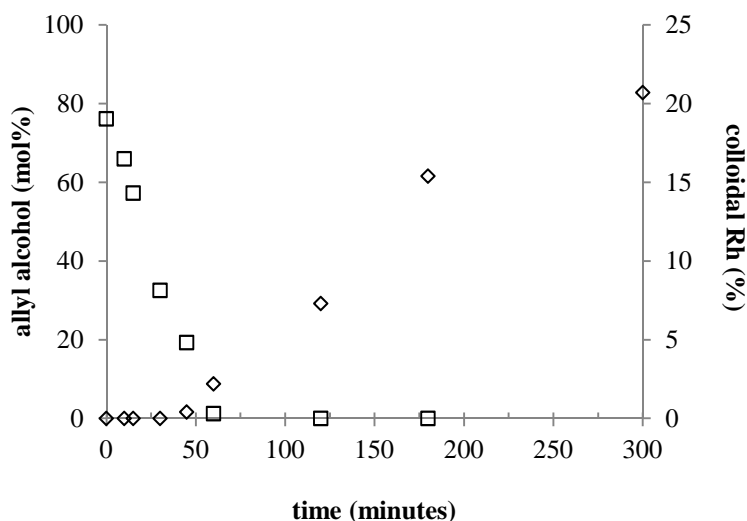


Figure 12. Decomposition of BISBI/PEt₃/Rh systems in hydroxymethylation of allyl alcohol in time:

(□) allyl alcohol, (◇) colloidal Rh.^a

(Conditions: 4 mL ethanol, 8 mM [Rh], BISBI/PEt₃/Rh = 2/2/1,

Rh/allyl alcohol = 1/185, 120°C, 40 bar CO/H₂ = 1)

Medium effect. The possibility for fine-tuning the specific hydroxymethylation activity of these catalyst systems through a medium effect was investigated (Table 8). Solvent polarity is defined here as the overall solvation capability and as such it cannot be quantitatively described by the physical parameters of the idealised electrostatic model. Instead, the solvatochromatic dye Nile Red is used as a polarity indicator (Figure 13).³²

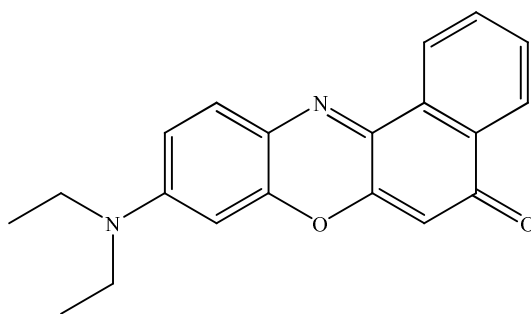


Figure 13. Nile Red dye.

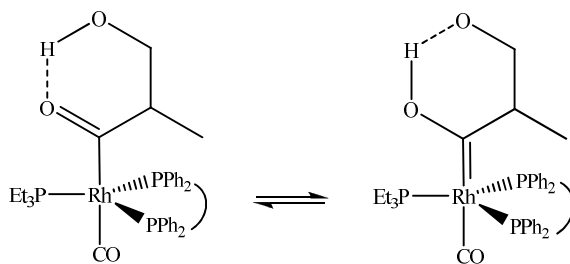
An empirical scale was constructed from the molar transition energies of the chromophore in solution, measured as $\lambda_{\text{max}}^{\text{abs}}$ by UV-vis spectrometry. A bathochromic shift of $\lambda_{\text{max}}^{\text{abs}}$ is observed with increasing solvent polarity, which means that solvation stabilises the Franck-Condon excited state relative to the equilibrium ground state of Nile Red.³³

Table 8: Hydroxymethylation of allyl alcohol with DIOP/PEt₃/Rh system in organic media.^a

	E_{NR} (kJ mol ⁻¹) ^b	2 hours		15 hours	
		C=O ^c (l/b)	-OH ^d (l/b)	C=O (l/b)	-OH (l/b)
methanol	217.7	17 (6.3)	79 (6.6)	15 (6.4)	81 (6.5)
ethanol	219.3	16 (6.4)	84 (6.4)	12 (6.3)	85 (6.4)
t-butanol	223.8	23 (6.1)	68 (6.9)	2 (0.4)	92 (6.3)
t-amyl alcohol	224.4	25 (6.8)	72 (6.9)	3 (0.1)	94 (6.4)
thf	235.2	86 (7.3)	9 (0)	20 (5.3)	73 (6.8)
hexane	246.6	90 (7.4)	4 (0)	45 (4.8)	48 (7.6)

^aConditions: 4 mL solvent, 8 mM [Rh], DIOP/PEt₃/Rh = 2/2/1, Rh/allyl alcohol = 1/185, 120°C, 40 bar CO/H₂ = 1, 3 hours. ^bMolar transition energy (kJ mol⁻¹) calculated from $E_{NR} = (hcNA/\lambda_{max}^{abs}) \times 10^6$. ^cYield of hydroxyaldehyde derivatives (mol%). ^dYield of diol derivatives (mol%).

In aprotic media, complete conversion of allyl alcohol is effected within 2 hours. Primarily hydroxyaldehyde derivatives are formed, presumably *via* the formal hydroformylation mechanism, with 2-methylpropanol as the only recognised diol derivative. This apparent anomaly could be the result of intramolecular protonation of the acyl moiety in the rhodium-methylhydroxypropionyl-carbonyl intermediate *via* a six-membered heterocycle, prompted by the steric requirements of the methyl group (Figure 14). For the linear isomer this would involve an energetically less-favoured seven-membered heterocycle.

**Figure 14.** Proposed intramolecular protonation in the rhodium-methylhydroxypropionyl-carbonyl complex.

Significant sequential hydrogenation is observed over a prolonged reaction time in thf, which has higher polarity than hexane. Activity for hydroxymethylation remains much less than when a protic medium is employed however, because at a low concentration of proton source the domino pathway becomes less important, although presumably allyl alcohol and hydroxyaldehyde products could also function as such. The regioselectivity of each fraction is primarily governed by the conversion of hydroxyaldehydes to diols, as hydrogenation of the linear isomer is preferential. Significant chemoselectivity, defined as > 30% of the product mixture, is observed after 2 hours in protic media. The regioselectivity of the diol fractions is not found to be significantly higher than that

of the corresponding hydroxyaldehyde fractions. Interestingly, 2-methyl-1, 3-propanediol becomes a significant product at the expense of 2-methylpropanol in tertiary alcoholic media. This is of interest because Lyondell-Basell has recently shown the potential for 2-methyl-1, 3-propanediol application in unsaturated polyester resin formulations,³⁴ so it remains the preferred branched product.

4.5 Deuterium Labelling Studies

Mechanism of 1-hexene deuteriohydroxymethylation. The selective formation of 1-heptanol and 2-methylhexanol *via* the auto-tandem hydroxymethylation of 1-hexene can be elegantly demonstrated by a corresponding labelling pattern in 1-heptanol recovered from 1-hexene deuteriohydroxymethylation and 1-heptanol recovered from 1-heptanal deuteration.³⁵ In order to establish whether this is the present pathway for 1-heptanol formation, labelling reactions using combinations of either CO/D₂ = 1 or CO/H₂ = 1 in the gas phase and ethanol-OD or ethanol-OH in the solvent phase were conducted. Catalyst solutions were prepared *in situ* from [Rh(acac)(CO)₂], using XANTPHOS/PEt₃/Rh = 2/2/1, under 40 bar CO/D₂ = 1 at 120°C. Following fractional distillation, the product and solvent fractions were examined by ¹³C{¹H} NMR and ¹H NMR spectroscopy respectively (Table 9).

Only 1-heptanol is recovered from 1-hexene deuteriohydroxymethylation in ethanol-OH. H/DO-CD₂-CH₂-CHD-C₄H₉ and H/DO-CHD-CH₂-CHD-C₄H₉ are observed as the major and minor isotopomers respectively (Figure 15). The main C₁ signal is split into a quintet by coupling to two deuterium nuclei, $J_{C-D} = 21.3$ Hz. The observed distortion is due to the underlying minor C₁ resonance which is resolved as a triplet, $J_{C-D} = 21.5$ Hz. The corresponding α -shifts average ~ 0.40 ppm per deuterium. The incorporation of hydrogen at C₁ may be due to hydrogen impurity in carbon monoxide and traces of hydrogen have previously been detected in carbon monoxide cylinders of the type used for these experiments. However, the selectivity of incorporation suggests that exchange of deuterium in one of the cationic rhodium intermediates with hydrogen from ethanol is a more credible source. Solvent ethanol-OH has undergone 22% conversion to ethanol-OD, compared with only 6% exchange observed in the absence of 1-hexene. Deuterium incorporation in the hydroxyl site of initially formed product could not be quantitatively determined due to the hydrogen-deuterium exchange equilibrium established in this site. Upon exchange with D₂O, a β -shift of 0.27 ppm is observed for the C₁ signal. The C₃ signal of both products is split into a triplet by coupling to a single deuterium nucleus, $J_{C-D} = 19.3$ Hz, which confirms the absence of hydrogen in the gas phase. The corresponding α -shifts are 0.37 ppm. The main C₂ signal experiences an upfield shift of 0.32 ppm, equivalent to three β -shifts due to the deuterium nuclei on vicinal carbons. The minor C₂ signal appears ~ 0.10 ppm downfield of this. A β -shift of 0.08 ppm is also observed for the C₄-resonances. By integration of the C₂ signals it is established that 86% of 1-heptanol was dideuterated in the C₁ site.

Table 9: Deuteriohydroxymethylation of 1-hexene with XANTPHOS/PEt₃/Rh in ethanol^a – ¹³C{¹H} NMR C₇-product analysis.^a

	1/ppm	J _{C-D} /Hz	2/ppm	I	3/ppm	J _{C-D} /Hz	4/ppm	5/ppm	6/ppm	7/ppm	solvent exchange
1-hexene +CO/D ₂ , ethanol-OH											22%
H/DO-CD ₂ -CH ₂ -CHD-C ₄ H ₉	61.88	m. 21.3	32.48	86	25.55	t. 19.3	29.27	31.85	22.63	14.09	
H/DO-CHD-CH ₂ -CHD-C ₄ H ₉	62.09	t. 21.5	35.57	14	25.55	t. 19.3	29.27	31.85	22.63	14.09	
1-heptanal +CO/D ₂ , ethanol-OH											84%
H/DO-CH ₂ -CH ₂ -CH ₂ -C ₄ H ₉	62.49		32.82	59	25.91		29.40	31.99	22.86	14.12	
H/DO-CHD-CH ₂ -CH ₂ -C ₄ H ₉	62.11	t. 21.5	32.75	41	25.91		29.40	31.99	22.86	14.12	
1-heptanal +CO/H ₂ , ethanol-OD											76%
H/DO-CH ₂ -CH ₂ -CH ₂ -C ₄ H ₉	62.51		32.83	45	25.92		29.40	32.00	22.86	14.12	
H/DO-CHD-CH ₂ -CH ₂ -C ₄ H ₉	62.10		32.76	55	25.92		29.40	32.00	22.86	14.12	
1-heptanal +CO/D ₂ , ethanol-OD											6%
H/DO-CHD-CH ₂ -CH ₂ -C ₄ H ₉	62.09	t. 21.5	32.75		25.91		29.38	32.00	22.86	14.11	

^aConditions: 4 mL ethanol, 8 mM [Rh], XANTPHOS/PEt₃/Rh = 2/2/1, Rh/1-hexene = 1/200, 120°C, 40 bar CO/(D₂ or H₂) = 1, 3 hours.

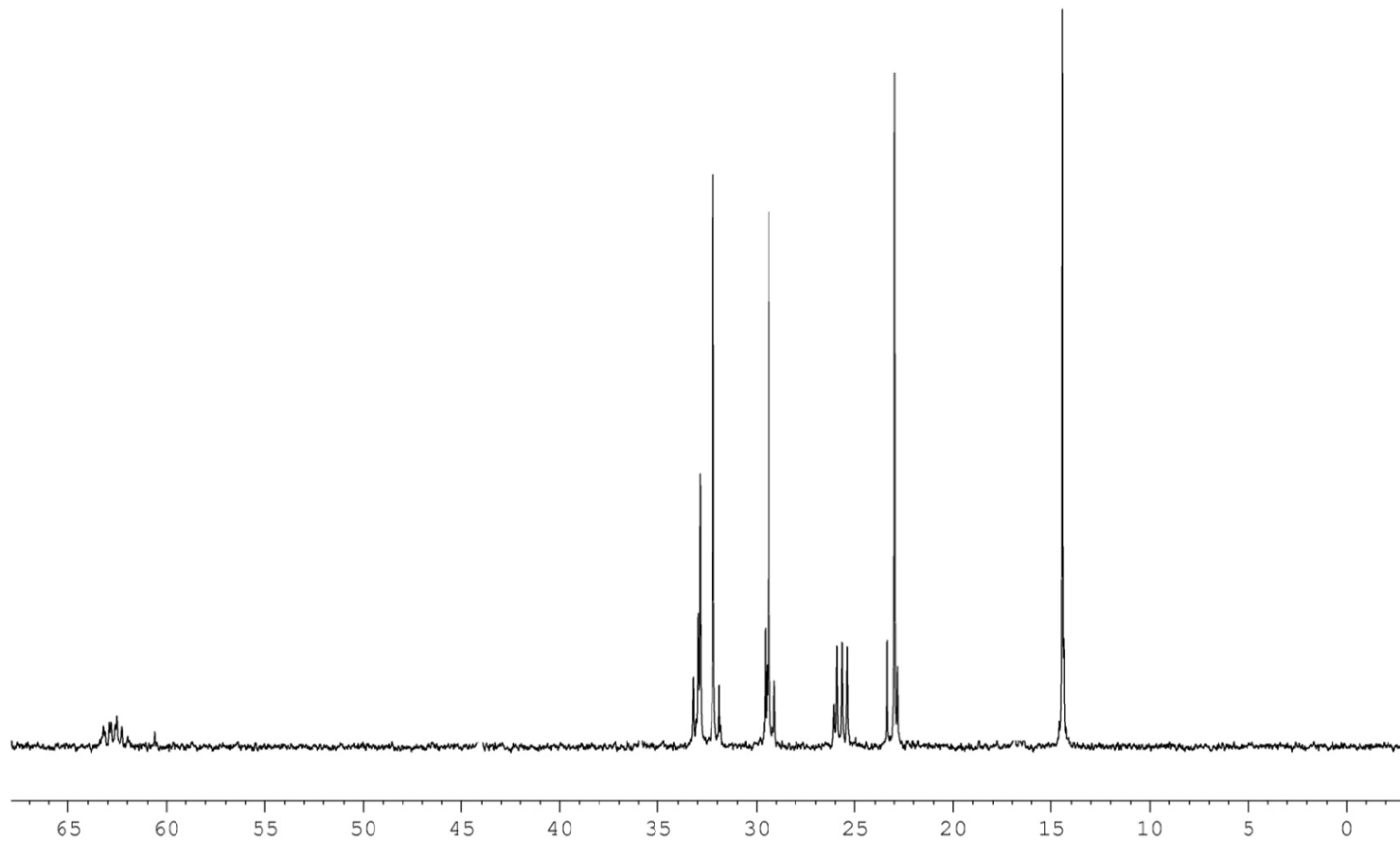


Figure 15. Deuteriohydroxymethylation of 1-hexene in ethanol- $^{13}\text{C}\{^1\text{H}\}$ nmr spectrum of product fraction.

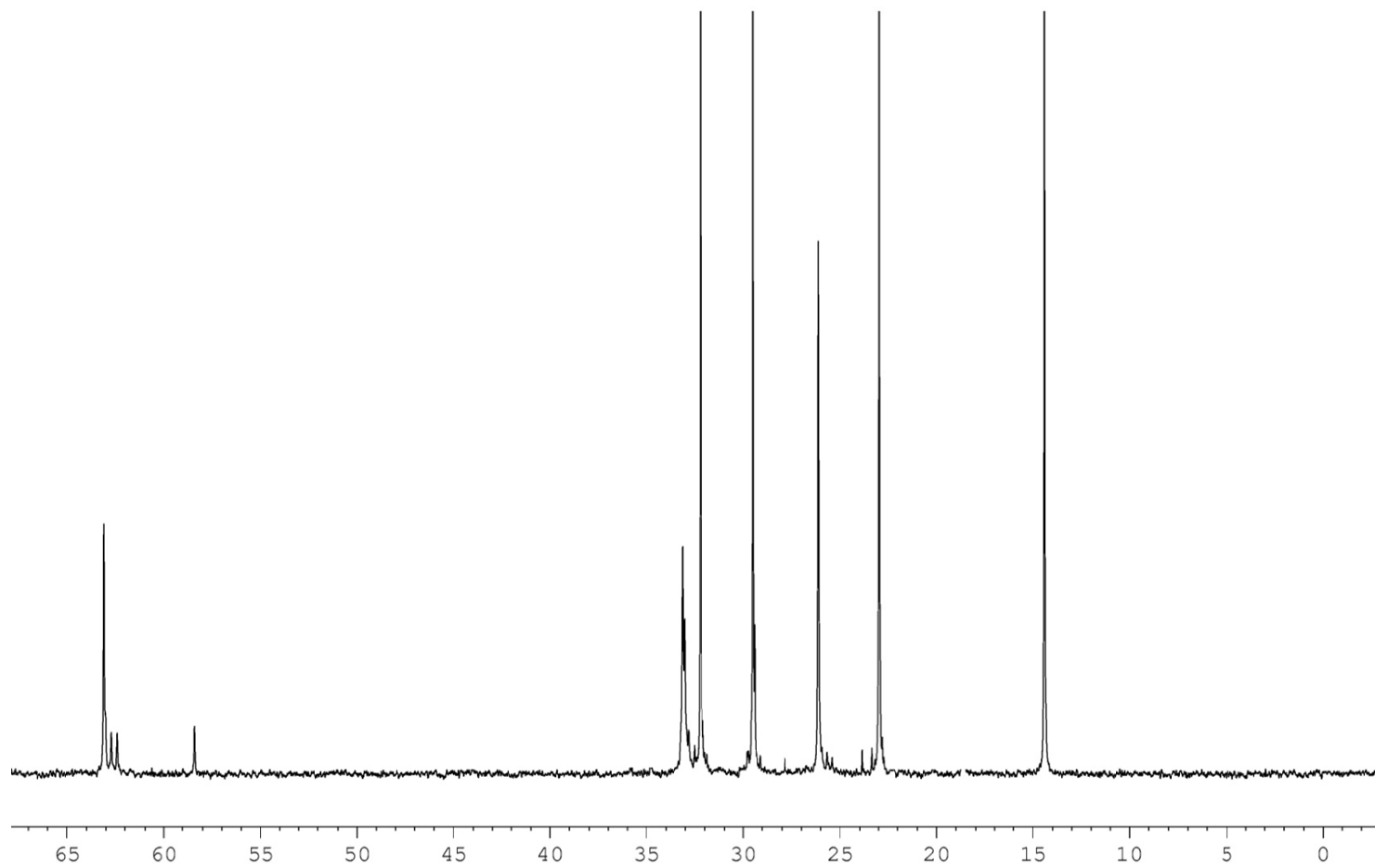
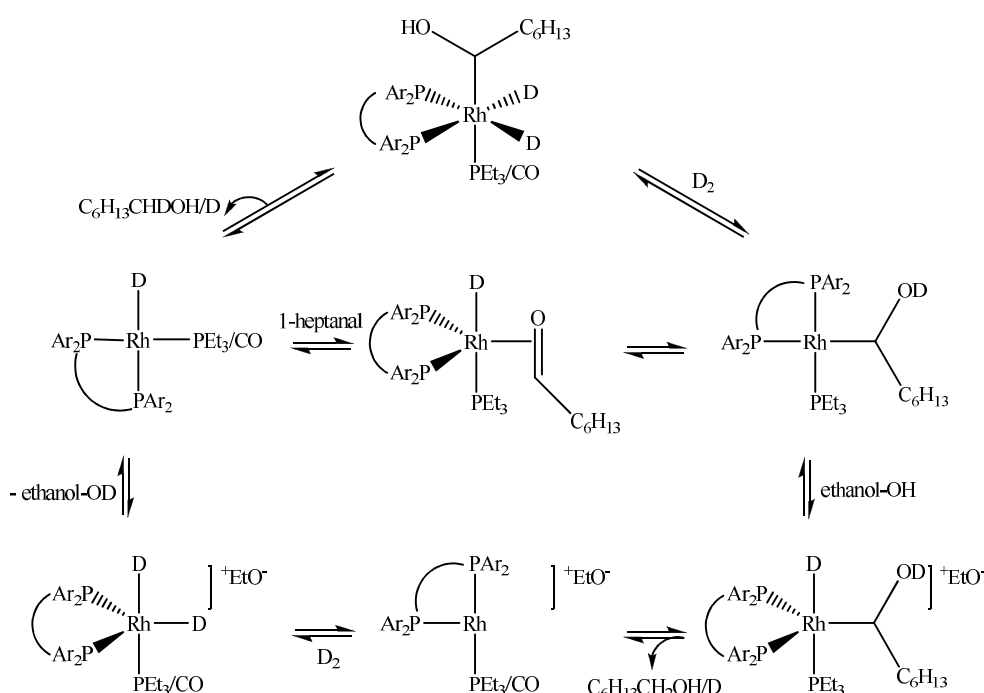


Figure 16. Deuteration of 1-heptanal in ethanol-OH- $^{13}\text{C}\{^1\text{H}\}$ nmr spectrum of product fraction.

1-Heptanol is recovered as H/DO-CHD-CH₂-CH₂-C₄H₉ and H/DO-CH₂-CH₂-CH₂-C₄H₉ from the deuteration of 1-heptanal in ethanol-OH (Figure 16). The C₁ signal of the monodeuterated product is resolved as a triplet, $J_{C-D} = 21.5$ Hz. An α -shift of 0.36 ppm and β -shift of 0.07 ppm are observed for C₁ and C₂ respectively. Resonances from non-deuterated 1-heptanol appear at the expected frequencies. Ethanol-OH appears to be the source of the hydrogen incorporated at C₁, since 84% exchange to ethanol-OD is observed in the solvent fraction. Integration of the C₂ signals shows that 59% of 1-heptanol has no deuterium incorporated in the C₁ position. Therefore if 1-hexene deuteriohydroxymethylation proceeds *via* a auto-tandem scheme, ~ 60% of 1-heptanol should be recovered with one deuterium in the C₁ site. Since only 14% is observed as this isotopomer, it can be concluded that 1-heptanol is reductively eliminated as a primary reaction product.

Mechanism of 1-heptanal deuteration. At this point it is prudent to rationalise the labelling pattern in the deuteration products of 1-heptanal (Scheme 3).



Scheme 3. Proposed mechanism for the deuteration of 1-heptanal with *L-L*/PEt₃/Rh systems in ethanol.

Since deuteration *via* the rhodium-heptoxy-carbonyl species necessitates deuterium incorporation in the C₁ position, the mechanism almost certainly proceeds *via* the rhodium-hydroxyheptyl-carbonyl complex. This requires low oxophilicity of rhodium,³⁶ implicating the possibility that a *tris*-phosphine complex is present at the point of deuteride migration. Since protonation equilibria are often rapidly established, formation of the precursor for H/DO-CH₂-CH₂-CH₂-C₄H₉ elimination should compete

effectively with the oxidative addition of D_2 , which generates the precursor for H/DO-CHD-CH₂-CH₂-C₄H₉ elimination.^{2a, 2c}

The role of the solvent as the hydride source is confirmed upon 1-heptanal hydrogenation in ethanol-OD which gives a different composite mixture of the isotomers (Figure 17).

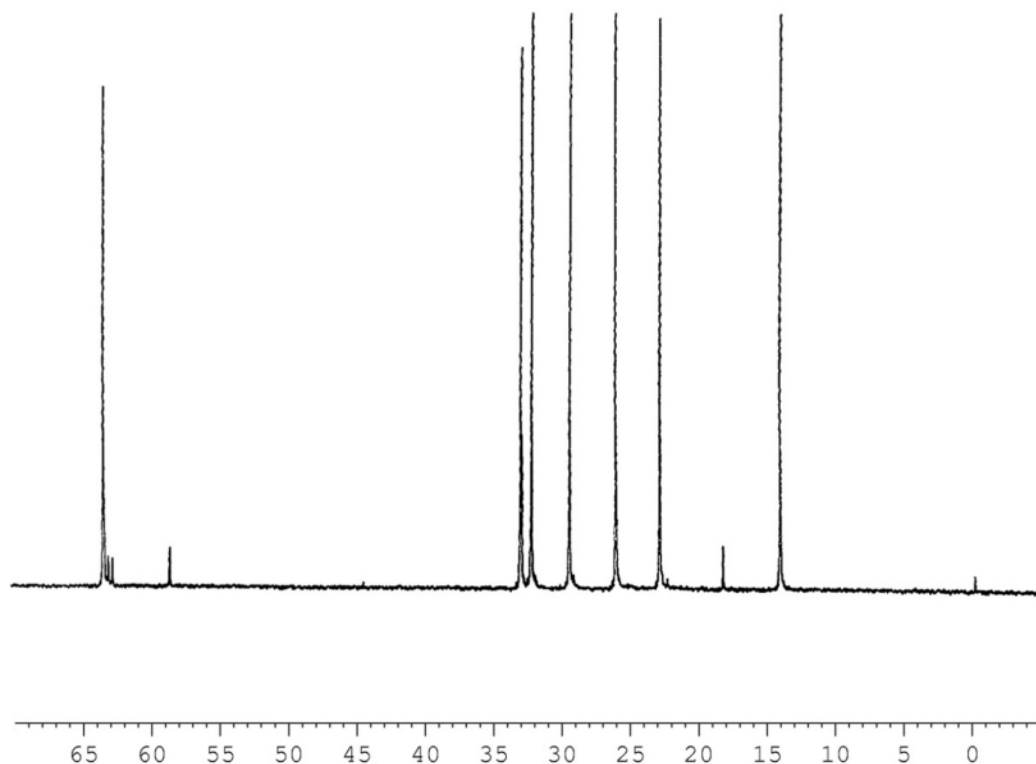


Figure 17. Hydrogenation of 1-heptanal in ethanol-OD- $^{13}C\{^1H\}$ NMR spectrum of product fraction.

By integration of the C₂ signals it is shown that 55% of 1-heptanol has deuterium incorporated in the C₁ position. Analysis of the solvent fraction reveals that 76% deuterium exchange had occurred in the hydroxyl position, with no indication of deuterium incorporation in any other sites. Exclusively H/DO-CHD-CH₂-CH₂-C₄H₉ is formed upon 1-heptanal deuteration in ethanol-OD, thus only the isotopic nucleus in the hydroxyl position of the solvent is involved.

4.6 Conclusions

As demonstrated explicitly in hydroxymethylation catalysis, the introduction of a primary trialkylphosphine to a solution of rhodium precursor and diphosphine can significantly affect specific activity (Figure 18). Using the *L-L*/PEt₃/Rh system in a protic medium, diol products were recovered in ~ 50 mol% yield as the PEt₃/Rh molar ratio approached 1. Heterogeneous hydrogenation does not appear to be taking place, and deuterium labelling studies implicated that catalysis proceeds *via* the domino scheme. There is evidence for the involvement of a *tris*-phosphine-modified rhodium-acyl-

carbonyl complex, but *in situ* complexation with various rhodium salts afforded exclusively diphosphine-modified species, with free triethylphosphine in solution. In terms of regioselectivity, the absence of a mixed ligand effect indicated that only the chelate was coordinated to rhodium at the instant this was determined. As the concentration of PEt_3 exceeds that of the diphosphine, competitive activity of triethylphosphine-modified rhodium species is presumed to account for reduced linear selectivity. In the absence of allyl alcohol, free triethylphosphine had a seemingly deleterious effect on the solution stability of $[\text{Rh}(\text{CO})(\text{L-L})(\mu\text{-CO})]_2$ and the active catalyst.

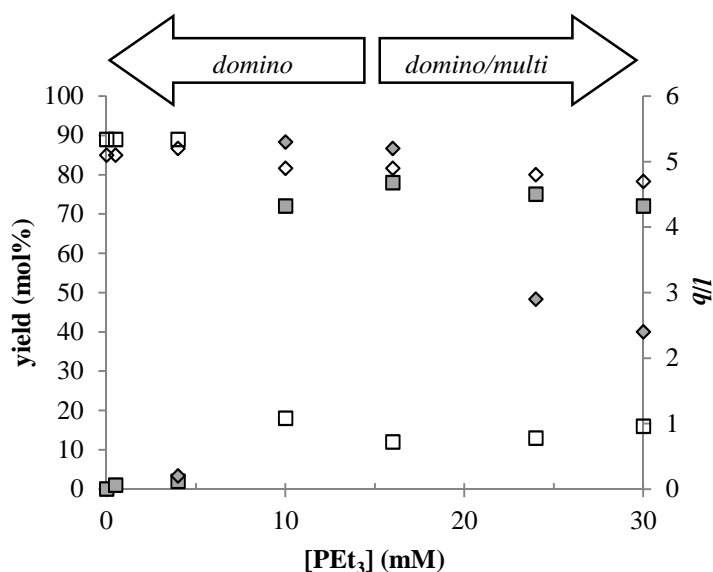


Figure 19. Hydroxymethylation activity of XANTPHOS/ PEt_3 /Rh system for allyl alcohol as a function of triethylphosphine concentration (□) hydroxyaldehyde yield, (■) diol yield, (◇, ◆) *l/b*.

(Conditions: 4 mL ethanol, 8 mM [Rh], XANTPHOS/Rh = 2/1, Rh/allyl alcohol = 1/185, 120°C, 40 bar $\text{CO}/\text{H}_2 = 1$)

It would be of interest to establish a repertoire of promoters based upon their ability to generate an enabling concentration of the activated rhodium-acyl-carbonyl. For example, under specified operating conditions is it better to employ a high concentration of mildly acidic promoter or a low concentration of strongly acid promoter.

4.7 Experimental Section

Materials. Chemicals were purchased from Lancaster Synthesis, Sigma-Aldrich and Strem. All operations were performed under N_2 (passed through column of dichromate adsorbed on silica) in a glove box or using standard Schlenk and catheter tubing techniques. All glassware was flame-dried under vacuum. Toluene, hexane and thf were distilled from sodium benzophenone ketyl, absolute ethanol was distilled from magnesium ethoxide, methanol was distilled from calcium methoxide,

acetone, *tert*-butanol and *tert*-amyl alcohol were distilled from calcium hydride, all under N₂ onto activated Linde 4 Å molecular sieves. All solvents were degassed prior to use by fpt cycles. XANTPHOS,¹³ DIOP³⁷ and BISBI³⁸ were prepared according to the literature procedures; CBM-DXP was provided by Lyondell-Basell.

Analytical techniques. NMR spectra were recorded on Bruker Avance 300 and Bruker Avance II 400 spectrometers with tetramethylsilane (¹H, ¹³C) and 85% H₃PO₄ (³¹P) as external references. Solution IR spectra were recorded on a Nicolet Avatar 360 FT-IR spectrometer. UV-*vis* absorption spectra were recorded on a Hewlett-Packard 8453 UV-*vis* spectrophotometer. Gas chromatography was performed on a Hewlett-Packard 6890 chromatograph fitted with a 30 m BP10™ column (carrier gas 3.2 psi He, flame-ionisation detector). Elemental analyses were done using a Perkin-Elmer 240C CHNS/O microanalyser. ICP-MS analyses were performed on an Iris Advantage analyser. Conductivity was measured in ~ 0.25 mM ethanol solution with a Metrohm E518 conductimeter.

Theoretical studies. The natural bite angles of the chelates were determined by semi-empirical calculations. Initial Rh-(*L-L*) conformations were determined by the PM3(tm) method as implemented in the SPARTAN 5. 1. 1 SGI software, with the rhodium-phosphorus bond length fixed at 2.315 Å. The geometries were optimised by eigenvector following as implemented in the GAUSSIAN 98 program, with a termination criterion of rms gradient < 0.001 kJ mol⁻¹ Å⁻¹. The flexibility range was estimated from a plot of Rh-(*L-L*) potential energy as a function of the bite angle.

Synthesis of complexes from [Rh(acac)(CO)₂]. A solution of the diphosphine (0.01 mmol) and 2.9 µL triethylphosphine (0.02 mmol) in ethanol (1 mL, 40% volume by volume in *d*₈-thf) was added to 2.5 mg [Rh(acac)(CO)₂] (0.01 mmol) held in an NMR tube at 30°C under N₂. After 1 hour the red solution was analysed by ³¹P{¹H} NMR spectroscopy. Evaporating the solvent afforded red prisms, which were washed with hexane (2×0.4 mL).

Synthesis of complexes from [Rh(CO)₂Cl]₂. A solution of the diphosphine (0.01 mmol) and 2.9 µL triethylphosphine (0.02 mmol) in ethanol (1 mL, 40% volume by volume in *d*₈-thf) was added to 3.9 mg [Rh(CO)₂Cl]₂ (0.01 mmol) held in an NMR tube at 30°C under N₂. When carbon monoxide evolution was no longer discernable, the yellow solution was analysed by ³¹P{¹H} NMR spectroscopy and by solution IR spectroscopy.

Synthesis of complexes from [RhCl₃·3H₂O]. A solution 0.1180 g [RhCl₃·3H₂O] (0.45 mmol) in ethanol (8 mL) was added dropwise to a refluxing solution of the diphosphine (0.45 mmol) and 131.3 µL triethylphosphine (0.90 mmol) in ethanol (15 mL) at 80°C under N₂. After 30 minutes, 2

mL 40% formaldehyde (weight by volume in water) was slowly injected and the mixture was allowed to stir for another 2 hours. An aliquot of the yellow solution (0.5 mL) was withdrawn for analysis by $^{31}\text{P}\{^1\text{H}\}$ NMR spectroscopy and by solution IR spectroscopy.

Crystal structure determination of [Rh(acac)(DIOP)]. Suitable crystals were grown by method of slow-cooling an acetone solution. $[\text{C}_{37.5}\text{H}_{42}\text{O}_{4.5}\text{P}_2\text{Rh}]$, $M_r = 729.56$. A red prism-shaped crystal (0.14 mm \times 0.10 mm \times 0.10 mm) was fixed to a glass capillary and transferred into the N_2 stream on a Rigaku Mercury/MM007 RA diffractometer with rotating anode. The measure crystal was monoclinic, space group $P2_1$ with $a = 10.6780(7)$ Å, $b = 17.6957(10)$ Å, $c = 20.2971(12)$ Å, $\alpha = 90.000^\circ$, $\beta = 92.298(10)^\circ$, $\gamma = 90.000^\circ$, $V = 3832.1(4)$ Å³, $Z = 4$, $D_x = 1.2965$ g cm⁻³, $F(000) = 1512$, $\mu(\text{MoK}\alpha) = 0.565$ mm⁻¹. 19222 reflections were measured, 9540 of which were independent, $R_{int} = 0.0595$ ($1.91^\circ < \theta < 23.19^\circ$, $T = 93(2)$ K, MoK α radiation, graphite monochromator, $\lambda = 0.605382$ Å, ϕ scan and ω scans with κ offset, distance crystal to detector 50 mm, absorption correction by SADABS). The structure was solved by the heavy atom method and refined by the full-matrix least-squares against F^2 method in SHELLXTL.³⁹ Refinement converged at $wR2 = 0.1273$, $\text{GooF} = 0.938$ and $-0.869 < \Delta\rho < 0.862$ e Å⁻³.

High pressure NMR. The 10 mm sapphire NMR cell was primed with a solution of 5.0 mg [Rh(acac)(CO)₂] (0.02 mmol), 11.6 mg XANTPHOS (0.02 mmol) and 5.8 μL triethylphosphine (0.04 mmol) in d_4 -methanol (1.5 mL) under N_2 . The cell was purged thrice with 10 bar $\text{CO}/\text{H}_2 = 1$ and then pressurised to 40 bar. NMR spectra at different temperatures were recorded. Line-shape analyses was performed using the $d\text{NMR}$ option in the TOPSPINTM software provided by Bruker BioSpin.

High pressure IR. The HP-IR cell was primed with a solution of 7.0 mg [Rh(acac)(CO)₂] (0.05 mmol) and 28.9 mg XANTPHOS (0.05 mmol) in methanol (10 mL) under N_2 . The cell was purged twice with 10 bar $\text{CO}/\text{H}_2 = 1$ and then pressurised to 40 bar. The IR spectrum at 40°C was recorded. Hydride-deuterium exchange was performed by cooling the cell to 25°C, depressurising and purging the solution thrice with 5 bar D_2 . Hereafter the autoclave was pressurised with 20 bar D_2 and 20 bar carbon monoxide. The IR spectrum at 40°C was recorded, a solution of 14.6 μL PEt_3 (0.10 mmol) in methanol (1 mL) was injected and another IR spectrum recorded after 20 minutes. The reference spectrum of methanol under 40 bar $\text{CO}/(\text{D}_2/\text{H}_2) = 1$ at 40°C was subtracted from the experimental spectrum.

Catalysis. Syngas was purchased from BOC (**Caution!** Carbon monoxide is extremely poisonous and accidents may be lethal. A sensitive personal detector was carried and all experiments were performed in a well ventilated fume-hood fitted with a detector, maintaining the concentration of carbon monoxide below the mac value at all times). Hydroxymethylation reactions were carried out

on the CAT rig with stirrer speed set at 800 rpm. In a typical experiment a solution of the diphosphine (0.08 mmol) and triethylphosphine (0.00-0.16 mmol) in ethanol (3 mL) was added to 10.4 mg [Rh(acac)(CO)₂] (0.04 mmol). The resulting solution was sonicated over 10 minutes and transferred into the autoclave under CO/H₂ = 1; any residues were transferred with a further aliquot of ethanol (1 mL). The solution was incubated for 20 minutes at 120°C and 30 bar CO/H₂ = 1. After 1 mL allyl alcohol (14.70 mmol, azeotropically dried with toluene and distilled) was injected the pressure was adjusted to 40 bar, and the reaction was run to completion. The autoclave was then cooled and depressurised. 50 µL diglyme was added as internal standard to a 1 mL aliquot of the product solution, and the sample was analysed by GC. The experiments were performed at least in duplo.

For experiments with a proton sponge, 5.94 µL *N, N*-dimethylbenzylamine (0.04 mmol) was added to a pre-catalyst solution of 10.4 mg [Rh(acac)(CO)₂] (0.04 mmol), diphosphine (0.08 mmol) and 11.6 µL triethylphosphine (0.08 mmol) in ethanol (4 mL). For testing of reaction homogeneity the autoclave was charged with 1 mL mercury and purged thrice with CO/H₂ = 1 before a solution of 10.4 mg [Rh(acac)(CO)₂] (0.04 mmol), diphosphine (0.08 mmol) and 11.6 µL triethylphosphine (0.08 mmol) in ethanol (4 mL) was introduced. For investigating catalyst decomposition, a solution of 10.4 mg [Rh(acac)(CO)₂] (0.04 mmol), 44.5 mg BISBI (0.08 mmol) and 11.6 µL triethylphosphine (0.08 mmol) in ethanol (4 mL) was applied in catalysis for an appointed reaction time. After filtration through a 2 mm × 4.5 mm pad of silica the product mixture was subjected to ICP-MS analysis. Conversion was calculated from the pressure change using $\Delta P = \Delta c \cdot R \cdot T$. Experiments at variable carbon monoxide partial pressures were performed in a Hastelloy autoclave. The autoclave was primed with a solution of 10.4 mg [Rh(acac)(CO)₂] (0.04 mmol), 46.4 mg XANTPHOS (0.08 mmol), 11.6 µL triethylphosphine (0.08 mmol) and 1 mL allyl alcohol (14.70 mmol) in ethanol (4 mL) under carbon monoxide, then pressurised as appointed. After 20 bar H₂ was introduced, the total pressure was adjusted with argon to 40 bar, and the autoclave heated to 120°C. After 4 hours the autoclave was cooled and depressurised.

Polarity measurements. The absorption maximum of Nile Red was determined by transmission UV-*vis* spectroscopy of a 1.89 mM solution, and related to the molar transition energy by $E_{NR} = (hcNA/\lambda_{\max}^{\text{abs}}) \times 10^6$.

Deuterium labelling. Carbon monoxide was purchased from BOC and D₂ was purchased from Cambridge Isotope Laboratories. Labelling reactions were performed in a Hastelloy autoclave. In a typical experiment a solution of 10.4 mg [Rh(acac)(CO)₂] (0.04 mmol), 46.4 mg XANTPHOS (0.08 mmol) and 11.6 µL triethylphosphine (0.08 mmol) in ethanol (4 mL) was sonicated over 10 minutes and transferred into the autoclave under carbon monoxide, together with 1 mL substrate. The autoclave was pressurised with 20 bar D₂ and 20 bar carbon monoxide, and then heated to 120°C. After 3 hours the autoclave was cooled and depressurised. The product mixture was fractionally

distilled off the catalyst. The C₇-fraction was analysed qualitatively by ¹³C{¹H} NMR spectroscopy and quantitatively by ¹³C{¹H, ²H} NMR spectroscopy and the solvent fraction was analysed by ¹H NMR spectroscopy.

References and Notes

- (1) van Leeuwen, P. W. N. M.; Claver, C. *Rhodium Catalysed Hydroformylation*. James, B. R.; Ugo, R. (Eds). Kluwer Academic: Dordrecht, 2000.
- (2) (a) MacDougall, J. K.; Simpson, M. C.; Green, M. J.; Cole-Hamilton, D. J. *J. Chem. Soc., Dalton Trans.* **1996**, 1161. (b) Simpson, M. C.; Currie, A. W. S.; Andersen, J.-A. M.; Cole-Hamilton, D. J.; Green, M. J. *J. Chem. Soc., Dalton Trans.* **1996**, 1793. (c) MacDougall, J. K. *PhD Thesis*, University of St. Andrews, 1991. Chapter 2. (d) Simpson, M. C. *PhD Thesis*, University of St. Andrews, 1994. Chapter 2. (e) Cheliatsidou, P. *PhD Thesis*, University of St. Andrews, 2005. Chapter 3.
- (3) (a) Hughes, O. R.; Unruh, J. D. *J. Mol. Catal.* **1981**, *12*, 71. (b) Hughes, O. R.; Young, D. A. *J. Am. Chem. Soc.* **1993**, *115*, 2066. (c) Casey, C. P.; Petrovich, L. M. *J. Am. Chem. Soc.* **1995**, *117*, 6007. (d) Maki, K.; Kujita, T.; Marumo, K. *Jap. Kokai*. 6.279.344, 1996. (e) Maki, K.; Kujita, T.; Marumo, K. *Jap. Kokai*. 6.279.345, 1996. (f) Dubner, W. S.; Shum, W. P. *US Pat.* 6.225.509, 2001.
- (4) Diéguez, M.; Pereira, M. M.; Madeu-Bultó, A. M.; Claver, C.; Bayón, J. C. *J. Mol. Catal. A* **1999**, *143*, 111.
- (5) (a) Kollár, L.; Kégl, T.; Bakos, J. *J. Organomet. Chem.* 1993, 453, 155. (b) Kollár, L.; Szalontai, G. *J. Organomet. Chem.* **1991**, *421*, 341.
- (6) Yoshiyuki, T.; Tomohiko, I. *Jap. Kokai*. 6.312.612, 2006.
- (7) Guram, A. S.; Briggs, J. R.; Packett, D. L.; Olson, K. D.; Eisenschmid, T. C.; Tjaden, E. B. *US Pat.* 6.172.269, 2001.
- (8) (a) Reetz, M. T.; Li, X. *Angew. Chem. Int. Ed.* **2005**, *44*, 2962. (b) Reetz, M. T.; Sell, T.; Meiswinkel, A.; Mehler, G. *Angew. Chem. Int. Ed.* **2003**, *42*, 790. (c) Duursma, A.; Hoen, R.; Schuppan, J.; Hulst, R.; Minnaard, A. J.; Feringa, B. L. *Org. Lett.* **2003**, *5*, 3111. (d) Peña, D.; Minnaard, A. J.; Boogers, J. A. F.; de Vries, A. H. M.; de Vries, J. G.; Feringa, B. L. *Org. Biomol. Chem.* **2003**, *1*, 1087.
- (9) Defined as the range of bite angles accessible within ≤ 3 kJ mol⁻¹ excess strain from the natural bite angle. van Leeuwen, P. W. N. M.; Kamer, P. C. J.; Reek, J. N. H.; Dierkes, P. *Chem. Rev.* **2000**, *100*, 2741.
- (10) SPARTAN 5. 1. 1 SGI. Wavefunction Inc., Irvine CA, 2005.
- (11) (a) DIOP, Rh-P = 2.306 Å, 2.342 Å. Ball, R. G.; James, B. R.; Mahajan, D.; Trotter, J. *Inorg. Chem.* **1981**, *20*, 254. Ball, R. G.; Trotter, J. *Inorg. Chem.* **1981**, *20*, 261. (b) BISBI, Rh-P = 2.318 Å, 2.318 Å. Casey, C. P.; Whiteker, G. T.; Melville, M. G.; Petrovich, L. M.; Gavney, J. A.; Powell, D. R. *J. Am. Chem. Soc.* **1992**, *114*, 5535. (c) NIXANTPHOS, Rh-P = 2.3288 Å, 2.3408 Å. BENZOANTPHOS, Rh-P = 2.3616 Å, 2.3408 Å. van der Veen, L. A.; Keeven, P. H.; Schoemaker, G. C.; Reek, J. N. H.; Kamer, P. C. J.; van Leeuwen, P. W. N. M.; Lutz, M.; Spek, A. L. *Organometallics* **2000**, *19*, 872.

- (12) GAUSSIAN 98, Revision A.9. Gaussian Inc., Pittsburg PA, 1998.
- (13) Kranenburg, M.; van der Burgt, Y. E. M.; Kamer, P. C. J.; van Leeuwen, P. W. N. M.; Goubitz, K.; Fraanje, J. *Organometallics* **1995**, *14*, 3081.
- (14) Casey, C. P.; Whiteker, G. T. *Isr. J. Chem.* **1990**, *30*, 299.
- (15) $^{31}\text{P}\{^1\text{H}\}$ NMR (CDCl_3 , 121.5 MHz): δ -18.1. *Organophosphorus Chemistry*. Allen, D. W.; Tebby, J. C. (Eds). RSC: Cambridge, 1999.
- (16) Kadyrov, R.; Börner, A.; Selke, R. *Eur. J. Inorg. Chem.* **1999**, 705.
- (17) AcacH, IR (0.1 M solution in toluene): $\nu_{\text{CO}} = 1759 \text{ cm}^{-1}$, 1740 cm^{-1} .
- (18) For examples see: (a) $[\text{Rh}(\text{hfacac})(\text{DPPE})]$, $[\text{Rh}(\text{hfacac})(\text{DPPP})]$. Angermund, K.; Baumann, A.; Dinjus, E.; Fornika, R.; Gorls, H.; Kessler, M.; Kruger, M.; Leitner, W. *Chem. Eur. J.* **1997**, *3*, 755. (b) $[\text{Rh}(\text{hfacac})(\text{DPPB})]$. Fornika, R.; Gorls, H.; Seemann, B.; Leitner, W. *J. Chem. Soc., Chem. Commun.* **1995**, *18*, 1929. (c) $[\text{Rh}(\text{acac})(\text{PCy}_3)_2]$. Esteruelas, M. A.; Lahoz, F. J.; Onate, E.; Oro, L. A.; Rodriguez, L.; Steinert, P.; Werner, H. *Organometallics* **1996**, *15*, 3436.
- (19) Simanko, W.; Mereiter, K.; Schmid, R.; Kirchner, K.; Trzeciak, A. M.; Ziolkowski, J. J. *J. Organomet. Chem.* **2000**, *602*, 59.
- (20) (a) Chan, A. S. C.; Shieh, H. -S.; Hill, J. R. *J. Organomet. Chem.* **1985**, *279*, 171. (b) Dyer, G.; Wharf, R. M.; Hill, W. E. *Inorg. Chim. Acta* **1987**, *137*. (c) James, B. R.; Mahajan, D.; Rettig, S. J.; Williams, G. M. *Organometallics* **1983**, *2*, 1452.
- (21) $^{31}\text{P}\{^1\text{H}\}$ NMR (CD_2Cl_2 , 120.0 Hz): δ 63.4 ppm, $^1J_{\text{Rh-P}} = 124 \text{ Hz}$, IR (KBr): $\nu_{\text{CO}} = 2010 \text{ cm}^{-1}$. Sanger, A. R. *J. Chem. Soc., Chem. Commun.* **1975**, 893.
- (22) Ball, G. E.; Cullen, W. W.; Fryzuk, M. D.; James, B. R.; Rettig, S. J. *Organometallics* **1991**, *10*, 2767.
- (23) (a) Gregorio, G.; Pregaglia, G.; Ugo, R. *Inorg. Chim. Acta* **1969**, *89*. (b) Rankin, J.; Poole, A. D.; Benyei, A. C.; Cole-Hamilton, D. J. *Chem. Commun.* **1997**, 1835.
- (24) The resonance transitions retain their line-width which means there is no decrease in transverse relaxation time, $\hbar_0 = (\pi T_2)^{-1}$.
- (25) For review see: Vaska, L. *J. Am. Chem. Soc.* **1966**, *88*, 4100.
- (26) $\theta = 132^\circ \pm 4^\circ$. Tolman, C. *J. Am. Chem. Soc.* **1970**, *92*, 2956.
- (27) (a) $\text{p}K_{\text{a}}(\text{MeOH}/\text{H}_2\text{O}) = 9.11$. (b) $\text{p}K_{\text{a}}(\text{MeOH}/\text{H}_2\text{O}) = 9.08$. Streuli, C. A. *Anal. Chem.* **1960**, *32*, 985.
- (28) (a) Mizoroki, T.; Kioka, M.; Suzuki, M.; Sakatani, Sh.; Okumura, A.; Maruya, K. *Bull. Chem. Soc. Jpn.* **1984**, *577*. (b) Imai, T. *US Pat.* 4.219.684, 1979. (c) Imai, T. *US Pat.* 4.438.287, 1984.
- (29) Aldridge, C. L.; Jonassen, H. B. *Nature* **1960**, *188*, 404.
- (30) $\text{Pb} \rightarrow \text{Pb}^{2+} + 2\text{e}$, $E^\circ = -0.13 \text{ V}$. $\text{Rh} \rightarrow \text{Rh}^{3+} + 3\text{e}$, $E^\circ = -0.80 \text{ V}$. Sternberg, H. W.; Wender, I.; Orchin, M. *Anal. Chem.* **1952**, *24*, 174.
- (31) Colloidal Rh (%) = $\{(8 \text{ mM} - [\text{Rh}]_{\text{detected}})/8 \text{ mM}\} \times 100\%$.
- (32) For comprehensive review see: Reichardt, C. *Chem. Rev.* **1994**, *94*, 2319.
- (33) (a) *Molecular Interactions and Electronic Spectra*. Mataga, N.; Kubota, T. (Eds). Dekker: New York, 1970. (b) Nicol, M. F. *Appl. Spectrosc. Rev.* **1974**, *8*, 183. (c) *Sol'vatokhromiya- Problemy i Metody*. Bakhshiev, N. G.; Libov, V. S.; Mazurenko, Y. T.; Amelichev, V. A.; Sajdov, G. V.; Gorodyskii, V. A. (Eds). Izdatel'stvo Leningradskovo Universiteta: Leningrad, 1989.

- (34) *MPDiol® Glycol: High Production Volume Chemical Challenge Program*. CAS RN 2163-42-0. Lyondell-Basell, 2004.
- (35) Chapter 2, p. 44.
- (36) Bryndza, H. E.; Tam, W. *Chem. Rev.* **1988**, *88*, 1163 and references therein.
- (37) Townsend, J. M.; Blount, J. F.; Sun, R. C.; Zawoiski, S.; Valentine, J. D. *J. Org. Chem.* **1980**, *45*, 2995.
- (38) Devon, T. J.; Phillips, G. W.; Puckette, T. A.; Stavinoha, J. L.; Vanderbilt, J. J. *US Pat.* 4.694.109.
- (39) SHELLXTL, Version 6.10. Sheldrick, G. M. Bruker AXS, Madison WI, 2004.

-Chapter 5-

Hydroxymethylation Catalysis Mediated by the Rhodium Complexes of Self-Assembling Heterodimers Based on DNA Base-Pairs

Abstract. Heterodimers of 2-*N*-pivaloylaminopyridine phosphines and isoquinolyl phosphines have been screened as diphosphine ligands for the rhodium-catalysed hydroxymethylation of allyl alcohol. The intramolecular hydrogen-bonding network is not resistant to erosion, but under appropriate operative conditions highly selective catalysts were afforded. In a typical example, for complexes of the type $[\text{RhH}(\text{CO})_2(\text{PAPP/IQP})]$ ($\text{PAPP} = 6\text{-(diphenylphosphino)-2-pivaloylaminopyridine/IQP} = 3\text{-(diphenylphosphino)isoquinolin-1(2H)-one}$ (**22a**), $3\text{-(diethylphosphino)isoquinolin-1-(2H)-one}$ (**22b**), $3\text{-(dicyclohexyl)isoquinolin-1-(2H)-one}$ (**22c**) and $3\text{-(bis(3, 5-dimethylphenyl)isoquinolin-1-(2H)-one}$ (**22d**)), linear selectivity increased in the order **22b** < **22a** < **22c** < **22d**. Activity for hydroxymethylation was found to be proportional to the acidity constant of the heterodimer, increasing in the order **22a** < **22d** < **22b** < **22c**. Overall, complexes based on the assembly of a dicyclohexylphosphine platform and a *bis*(3, 5-dimethylphenyl)phosphine platform proved most desirable, effecting up to 73 mol% selectivity to 1, 4-butanediol.

5.1 Introduction

A beneficial chelate effect on hydroformylation catalysis is well established, but conventional synthetic routes to diphosphine ligands are laborious. The supramolecular concept is based on generating diphosphines *via* the assembly of two easily accessible monophosphines with a complimentary binding motif. There is potential for an extensive catalyst tuning strategy suited to a combinatorial methodology and high throughput experimentation.¹

Dynamic metal-ligand interactions offer one approach to supramolecular design,² and these binding motifs are principally represented by axial coordination of a nitrogen-donor to the metal centre of a metalloporphyrin. This approach has been applied for the construction of coordination polymers and molecular squares,³ and the interactions are found to be stable under conditions relevant to catalysis.⁴ By the templation of zinc(II) salphen on pyridylphosphines, Kleij *et al.* have illustrated that the coordination geometry of the encapsulated assembly is determined by the configuration of the latter.⁵ Thus, sterically demanding tri(*m*-pyridyl)phosphine-based supramolecular structures were found to be mono-coordinated in several transition metal complexes. Conversely, the rhodium(I) complexes of tri(*p*-pyridyl)phosphine-based supramolecular structures displayed behaviour typical of chelated rhodium(I) species in the hydroformylation of 1-octene. The activity of these catalysts appeared to be regulated by the substitution pattern of the *meso*-phenyl functionalities. This coordinative pattern was later advanced by Reek *et al.* to create a library based on phosphite-modified zinc(II) porphyrins and nitrogen-containing phosphines, popularly termed SUPRAPhos.⁶ The chelation behaviour of these assemblies in rhodium(I) species was confirmed both by high pressure NMR spectroscopy and complexation studies. The catalytic parameters of these complexes in the hydroformylation of styrene were shown to be highly dependent upon the structural units, but in all cases chelation was maintained under the operating conditions.

Alternatively, supramolecular architectures can be realised *via* hydrogen-bonding. Breit *et al.* developed a 6-(diphenylphosphino)-2-pyridone platform which assembles with its tautomer in the presence of transition metal salt.⁷ The rhodium(I) complex was found to be an active and selective catalyst for the hydroformylation of terminal alkenes functionalised with bromide, acetate, ester, ketone, carbamate, salicylate or hydroxyl. However, cleavage of the hydrogen-bonding network was noted in the presence of protic additives. Duckmanton *et al.* and Reek *et al.* independently introduced monophosphines with a urea appendage,⁸ thereby establishing a self-complementary hydrogen-bonding motif. Anion sequestration into the *bis*urea binding pocket was found to direct a well-defined *trans*-chelation of the homodimers in their transition metal complexes, and the hydrogen-bonding network in these has been observed both in solution and in solid state. In the hydroformylation of 1-octene, the rhodium(I) complexes of these anion-templated homodimers were found to be relatively inactive, with regioselectivity of the order obtained with [Rh(acac)(CO)(PPh₃)] under analogous

conditions. The interaction between methylated cyclodextrins, used as inverse phase transfer reagents in aqueous biphasic hydroformylation,⁹ and sulfonated phosphine ligands has been extensively explored.¹⁰ In the case of TPPTS and flexible diphosphines, the formation of an inclusion complex causes η^1 -dissociation of the ligand from the rhodium species with a corresponding decline in linear selectivity. Interestingly, the opposite effect is observed in the case of rigid diphosphines.

The synthesis of asymmetric diphosphines has remained challenging. In this context Reetz and Feringa have shown the viability of a simple mixture of two monophosphines and a late transition metal, in which the heterocombination and two homocombinations exist simultaneously.¹¹ Self-association of platforms with different phosphorus donors generates a similar statistical mixture, but catalyst optimisation is only feasible when the heterodimer is more active and selective than either of the homodimeric species. Furthermore, a well-defined heteroleptic assembly is essential for the demarcation of catalyst structure impact on activity and selectivity.^{7a}

The DNA base pairing of adenine and thymine exemplifies well-defined complementary heterodimer assembly. Watson and Crick identified that the physical basis relies on inherent fixation of adenine as the lactim tautomer and thymine as the lactam tautomer.¹² Breit *et al.* have created a model template to emulate these properties (Figure 1).¹³

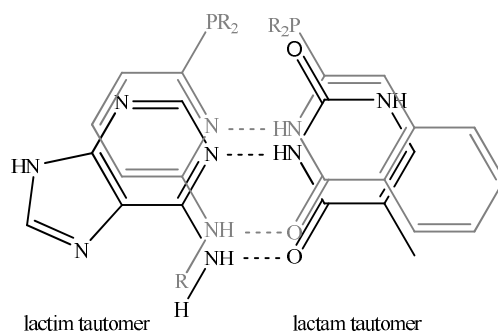


Figure 1. Heterodimerisation: (—) adenine-thymine base pair,
(—) aminopyridine-isoquinolone platforms.

Coordination of the diarylphosphine-modified platforms with $[\text{Pt}(\text{cod})\text{Cl}_2]$ in an aprotic solution led exclusively to the heteroleptic *cis*-complex, and the construction of a hydrogen-bonding network evocative of DNA base pairing was confirmed by single crystal X-ray crystallography. The catalyst library was screened for the hydroformylation of 1-octene. The heteroleptic complexes exhibited excellent activity and significantly enhanced regioselectivity relative to their homoleptic analogues. An analogous chiral library was screened with equal success for the asymmetric hydrogenation of acetamido-acrylate, methyl- α -acetyl-amino cinnamate and dimethylitaconate.

As an extension of their original work Breit *et al.* have developed a template based on new heterocyclic platforms, namely 2-*N*-pivaloyl aminothiazolylphosphine and azaindolylphosphine.¹⁴

Catalysts with outstanding activity and regioselectivity were identified for the hydroformylation of 1-hexene, even when catalysis was performed in a protic medium such as methanol. Stronger hydrogen-bonding upon incorporation of a five-membered heterocycle was held accountable for the improved rigidity of this heterodimer. Their findings have motivated our research into the application of this approach for the hydroxymethylation of allyl alcohol.

In this chapter, dimerisation of the 2-*N*-pivaloylaminopyridylphosphine platforms **1-4** and isoquinolyphosphine platforms **5-8** (Figure 2) was investigated by ^1H NMR titration in solution and by complexation with different rhodium precursors. The chelation mode of a selected heterodimer in its rhodium-hydride-dicarbonyl complex was elucidated by high pressure NMR spectroscopy. The optimum parameters for the hydroxymethylation of allyl alcohol were established and the performance of the heteroleptic rhodium(I) complexes is discussed in terms of steric and electronic requisites.

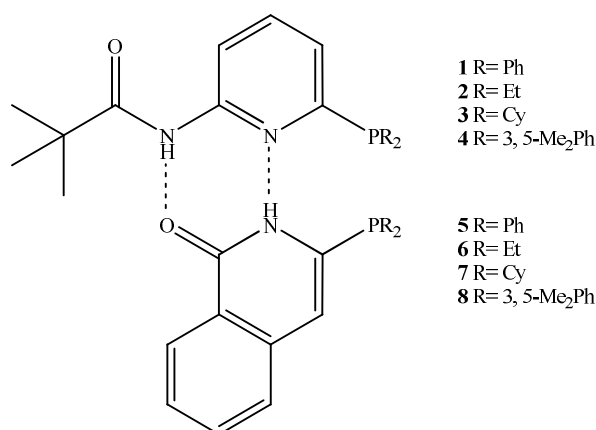
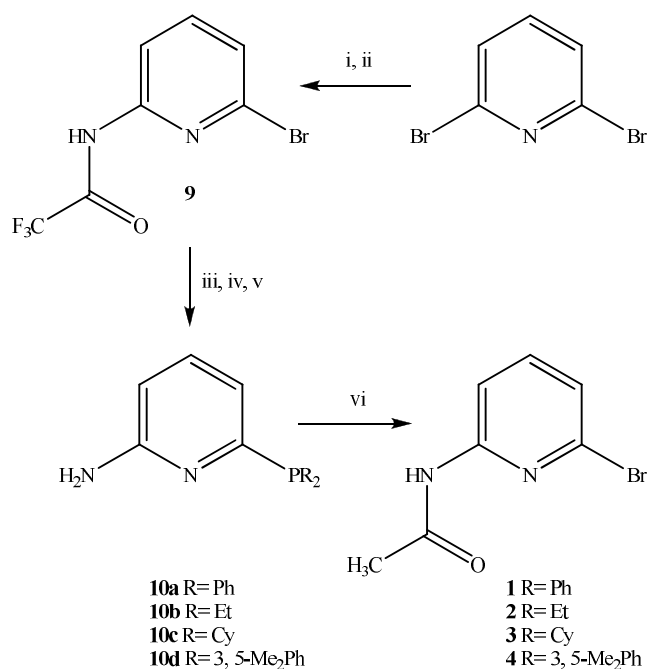


Figure 2. 2-*N*-pivaloylaminopyridylphosphines **1-4** and isoquinolyphosphines **5-8**.

5.2 Synthesis

2-*N*-Pivaloylaminopyridinyl phosphines. The retro-synthetic route towards **1-4** is illustrated (Scheme 1). 2-Bromo-6-aminopyridine is accessed from commercially available 2, 6-dibromopyridine by its reaction with 1.1 equivalents sodium amide, generated *in situ* from metallic sodium, ferric nitrate and liquid ammonia. Protection of the amine with 3 equivalents trifluoroacetic acid anhydride in triethylamine gives 2-bromo-6-*N*-trifluoroacetylaminopyridine (**9**) as yellow oil in 82% yield after flash chromatography. Clean lithium/bromide exchange is achieved by the addition of 2 equivalents *n*-BuLi, as verified by the ^1H NMR spectrum of a D₂O quenched sample. The lithiated 6-*N*-trifluoroacetylaminopyridine is trapped with a small excess of diarylchlorophosphine or dialkylchlorophosphine, causing a colour change from bright to pale yellow. Direct deprotection of the amine function is accomplished by stirring with 10 equivalents potassium carbonate in methanol.

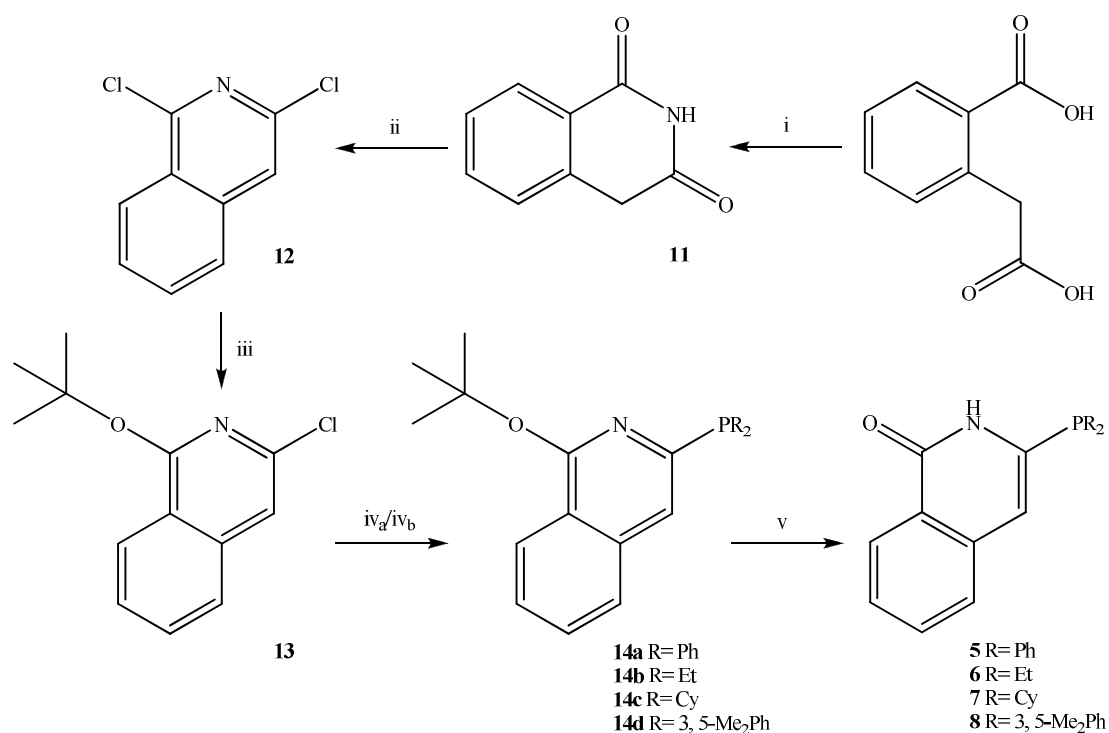


Scheme 1. Synthesis of 2-*N*-pivaloylaminopyridinyl phosphines **1-4**:

(i) Na/Fe(NO)₃·9H₂O/liquid NH₃, -80°C, (ii) TFAH/NEt₃, 0°C→ambient T, CH₂Cl₂, (iii) *n*-BuLi, -100°C, THF, (iv) ClPR₂, -80°C→ambient T, (v) K₂CO₃, 60°C, MeOH, (vi) (CH₃)₃COCl/NEt₃, 0°C→ambient T, CH₂Cl₂.

Purification is effected by flash chromatography to give ~ 85% of 6-(diarylphosphino)-2-aminopyridine (**10a**, **10d**) or ~ 49% of 6-(dialkylphosphino)-2-aminopyridine (**10b**, **10c**) as opaque residue. The pivaloate group is introduced upon reaction of **10a-10d** with 1.5 equivalents pivaloylchloride in the presence of triethylamine. Thus obtained are 61% of **1** as white foam, 59% of **3** as pale yellow foam and 65% of **4** as white foam, following flash chromatography. A hexane solution of **2** is percolated through a column of deactivated silica to give the pure product as viscous yellow oil in 53% yield.

Isoquinolonyl phosphines. The retro-synthetic approach to **5-8** is shown (Scheme 2). Homophthalimide (**11**) is generated from commercially available homophthalic acid *via* distillation of a 1, 2-dichlorobenzene solution of its ammonium salt. A crystallisation from aqueous acetic acid gives 91% **11** as powdery white solid. This method gave a considerably cleaner product than direct heating of the ammonium salt.¹⁵ The chlorodehydroxylation of **11** with neat PhPOCl₂ and a crystallisation from absolute ethanol gives 1, 3-dichloroisoquinoline (**12**) as a white powder in 88% yield.¹⁶ The use of a Fischer Porter bottle was necessary if using POCl₃, since the reaction only proceeds at 145°C which is considerably above the reflux temperature of this reagent. The utility of less-volatile PCl₅ was diminished by a tendency also to function as an oxidative chlorodehydroxylating agent. A simple nucleophilic substitution with 1.2 equivalents freshly sublimed potassium-*tert*-butoxide furnishes



Scheme 2. Synthesis of isoquinolonyl phosphines **5-8**:

- (i) 28% NH₄OH, 80°C at 5 mmHg, dichlorobenzene, (ii) PhPOCl₂, 160°C, neat,
 (iii) *t*-BuOK, 90°C, toluene, (iv_a) *n*-BuLi, -100°C, THF then ClP(alkyl)₂, -80°C→ambient T
 (iv_b) Na/P(aryl)₃/liquid NH₃, -78°C→ambient T, THF, (v) HCO₂H/H₂O, ambient T.

1-*tert*-butoxy-3-chloroisoquinoline (**13**), recovered as clear oil in 89% yield after bulb-to-bulb distillation of the crude residue. Clean lithium/chloride exchange with 1 equivalent *n*-BuLi is noted from the ¹H NMR spectrum of a D₂O quenched sample of the bright yellow solution. The lithiated 1-*tert*-butoxyisoquinoline is smoothly quenched with 1 equivalent dialkylchlorophosphine. Crude 1-*tert*-butoxy-3-(diethylphosphino)-isoquinoline (**14b**) is obtained in 77% yield, but all attempts at purification are met with decomposition. The crude residue of 1-*tert*-butoxy-3-dicyclohexylphosphino-isoquinoline (**14c**) is recrystallised from absolute ethanol to yield the product as white solid in 59% yield. The 1-*tert*-butoxy-3-(diarylphosphino)-isoquinolines (**14a**, **14d**) are derived by *in situ* reaction of 1-*tert*-butoxy-3-chloroisoquinoline with sodium and the triarylphosphine in liquid ammonia. Recrystallisation from methanol gives ~ 70% **14a** and **14b**. Aqueous dilution of a concentrated formic acid solution of **14a-14d** leads to instantaneous precipitation of **5-8**. A second crop of **5**, **7** and **8** is available upon crystallising the aqueous formic acid residue from acetone. The high purity crops yield 70% of **5**, 73% of **7** and 66% of **8** as white flakes. The crude residue of **6** is extracted with *n*-pentane/petroleum ether and decanted from the sludge to give the pure product as viscous pale yellow oil in 53% yield.

5.3 Heterodimerisation and Rhodium Chemistry in Solution

Heterodimerisation. The association behaviour of the complementary platforms was investigated by ^1H NMR titrations in solution.¹⁷ This technique provides several independent signals for evaluation and the observed chemical shift change also imparts conformational information about the supramolecular structure, which is difficult to extract from UV-*vis* titration and calorimetric data.¹⁸ Hydrogen bonding induces protons to shift upfield and the extent of association is here evaluated in terms of the chemical shift difference observed for the pivaloyl amide proton and the quinolyl amide proton.

The heterodimeric configurations of **1/7** and **4/5** were validated using the method of continuous variation. For each system the mole fraction of the isoquinolyl phosphine was incrementally varied in the range 0-1, while maintaining an absolute concentration of 1 mM. The derived Job plots are highly symmetrical with maxima at $mr = 0.5$, which corresponds to a 1/1 stoichiometry in solution (Figure 3).

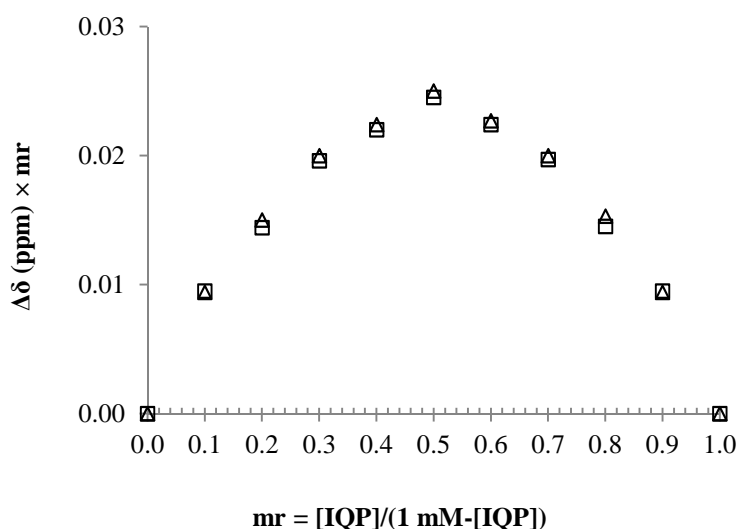


Figure 3. Continuous variation plot derived from ^1H NMR titration data: (□) **1/7**, (Δ) **4/5**.

The associations of **1/7** and **4/5** were examined by classical titration, with the concentration of the 2-*N*-pivaloylaminopyridyl phosphine fixed at 5 mM and the concentration of the isoquinolyl phosphine incrementally amplified (Figure 4). The association constant (K_a) was calculated by fitting the experimental data to the 1/1 association model (Equation 1) using the nonlinear least-squares fit method in ORIGIN,¹² which operates the Levenberg-Marquardt algorithm.²⁰

$$\Delta\delta = \frac{\delta_A - \delta_1}{2} \left\{ \frac{[IQP]t}{[PAPP]t} + 1 + \frac{1}{K_a[PAPP]t} \pm \sqrt{\left(\frac{[IQP]t}{[PAPP]t} + 1 + \frac{1}{K_a[PAPP]t} \right)^2 - 4 \frac{[IQP]t}{[PAPP]t}} \right\} \quad (\text{Equation 1})$$

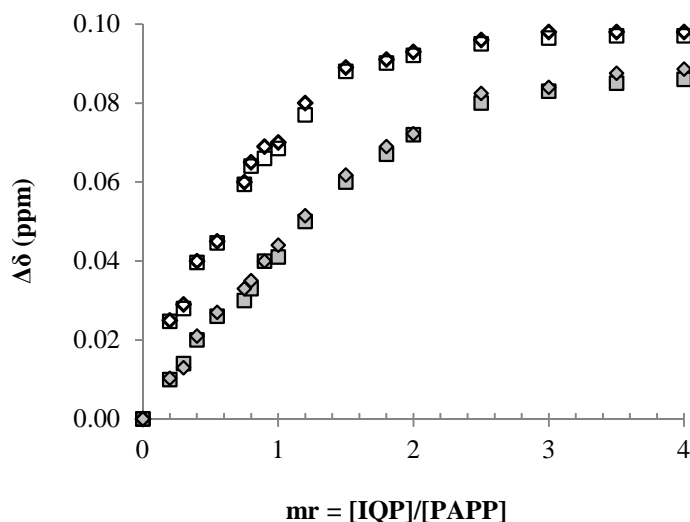


Figure 4. Titration curves:

(□) 1/7 in benzene, (◇) 4/5 in benzene, (■) 1/7 in methanol, (◆) 4/5 in methanol.

In either medium, the association constants for both heterodimers are comparable (Table 1). The small discrepancy is possibly the result of additional π -stacking interactions between the aryl functionalities on **4** and **5**. Some interference of a free hydroxyl moiety with the hydrogen-bonding network is manifested as slightly lower constants for association in methanol. Nevertheless, application in protic media is not exempt because the Weber- Person-Deranleau criteria, which state that $K_a > 1 \times 10^3$ M for accurate determination, are still met.²¹ The association constant for **4/5** assembly in benzene is enhanced fourteen-fold in the presence of a rhodium salt, corresponding to a 6.41 kJ M^{-1} difference in binding free energy. The rhodium coordination sphere can thus be regarded as a templation arena.

Table 1: Constants for the association of 2-*N*-pivaloylaminopyridyl phosphine and isoquinolyl phosphine in solution.^a

<i>PAPP/IQP</i>	K_a^b		$-\Delta G^{oc}$
	benzene	methanol	
1/7	1.09	1.04	17.04
4/5	1.11	1.07	17.08
4/5 + [RhH(CO)(PPh₃)₃]	15.38		23.49

^aConditions: 0.4 mL solvent, 5 mM [*PAPP*], 25°C, atmospheric pressure of argon. ^bAssociation constant ($\times 10^3 \text{ M}^{-1}$). ^cFree binding energy in benzene (kJ M^{-1}) calculated from $\Delta G^\circ = -RT \ln K_a$.

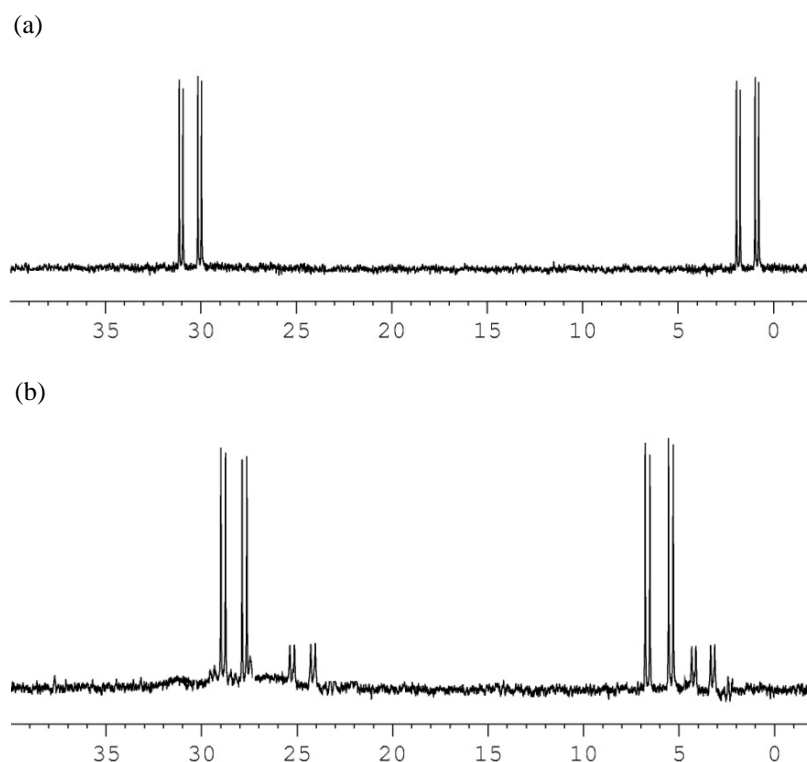
Rhodium(I) complexes under nitrogen. Transferability of the hetero-combinatorial association to a cationic rhodium centre was investigated, monitoring *in situ* complexation with $[\text{Rh}(\text{cod})_2][\text{BF}_4]$ by $^{31}\text{P}\{^1\text{H}\}$ NMR spectroscopy (Table 2).

Table 2: $^{31}\text{P}\{^1\text{H}\}$ NMR data for $[\text{Rh}(\text{X})(\text{PAPP}/\text{IQP})][\text{BF}_4]$ complexes in d_2 -dichloromethane.^a

<i>PAPP/IQP</i>	X	<i>PAPP</i>		<i>IQP</i>		
		δ (ppm)	$^1J_{\text{Rh-P}}$ (Hz)	δ (ppm)	$^1J_{\text{Rh-P}}$ (Hz)	$^2J_{\text{P-P}}$ (Hz)
1/6	cod	dd. 30.2	138	dd. 1.1	126	28
2/5	cod	dd. 1.1	126	dd. 30.7	138	28
3/8 – (92%)	phen	dd. 6.4	119	dd. 28.9	136	29
3/8 – (8%)	phen	dd. 4.2	118	dd. 24.9	134	26
4/7 – (89%)	phen	dd. 28.2	136	dd. 7.1	120	29
4/7 – (11%)	phen	dd. 24.4	135	dd. 5.6	118	26

^aConditions: 0.5 mL d_2 -dichloromethane, 50 mM [Rh], Rh/*PAPP/IQP*= 1/1/1, ambient temperature, atmospheric pressure of nitrogen, 2 hours.

Formation of the heteroleptic complexes $[\text{Rh}(\text{cod})(\mathbf{1/6})]\text{BF}_4$ and $[\text{Rh}(\text{cod})(\mathbf{2/5})][\text{BF}_4]$ is demonstrated by the resolution of two doublets of doublets (Figure 5a).

**Figure 5.** $^{31}\text{P}\{^1\text{H}\}$ NMR spectra of $[\text{Rh}(\text{PAPP}/\text{IQP})(\text{X})][\text{BF}_4]$:

(a) $[\text{Rh}(\text{cod})(\mathbf{2/5})][\text{BF}_4]$, (b) $[\text{Rh}(\text{phen})(\mathbf{3/8})][\text{BF}_4]$.

The unambiguous determination of rhodium-phosphorus coupling and phosphorus-phosphorus coupling for $[\text{Rh}(\text{cod})(\mathbf{3/8})][\text{BF}_4]$ and $[\text{Rh}(\text{cod})(\mathbf{4/7})][\text{BF}_4]$ is frustrated by extensive line-broadening, the consequence of an unresolved dynamic process. For these, a more defined complex was afforded upon replacing the cod auxiliary by addition of 1, 10-phenanthroline.^{22a} The heteroleptic

complexes $[\text{Rh}(\text{phen})(\mathbf{3}/\mathbf{8})][\text{BF}_4]$ and $[\text{Rh}(\text{phen})(\mathbf{4}/\mathbf{7})][\text{BF}_4]$ appear to exist as two ABX spin systems in a $\sim 9/1$ ratio (Figure 5b). One possibility for the formation of rotamers may be distorted square planar coordination geometry at rhodium,²² induced by two locking configurations of the rigid phosphorus substituents. An alternative explanation could be that supplementary axial chirality is induced by distortion of the hydrogen-bonding network in the chelate.^{13b}

Rhodium(I) complexes under syngas. The chelation geometry in $[\text{RhH}(\text{CO})_2(\mathbf{4}/\mathbf{6})]$ was elucidated by high pressure NMR spectroscopy. *In situ* formation of the complex from $[\text{Rh}(\text{acac})(\text{CO})_2]$ in d_8 -toluene is found to occur after 15 minutes at 45°C. The hydride resonance is observed as a doublet of doublet of doublets at $\delta_{\text{H}} = 9.36$ ppm in the ^1H NMR spectrum, with $^2J_{\text{P-H}} = 9.5$ and $^2J_{\text{P-H}} = 5.7$ Hz (Figure 6). These are typical of a *cis*-coupling between apical hydride and equatorial phosphine in a trigonal bipyramidal complex.²³ From the $^1\text{H}\{^{31}\text{P}\}$ NMR spectrum, $^1J_{\text{Rh-H}} = 3.8$ Hz is determined. The relatively small magnitude indicates that the dynamic equilibrium favours *ee* chelation.²⁴ Two broad doublets are observed in the corresponding $^{31}\text{P}\{^1\text{H}\}$ NMR spectrum. Due to the extensive line broadening rhodium-phosphorus coupling and phosphorus-phosphorus coupling cannot be identified.

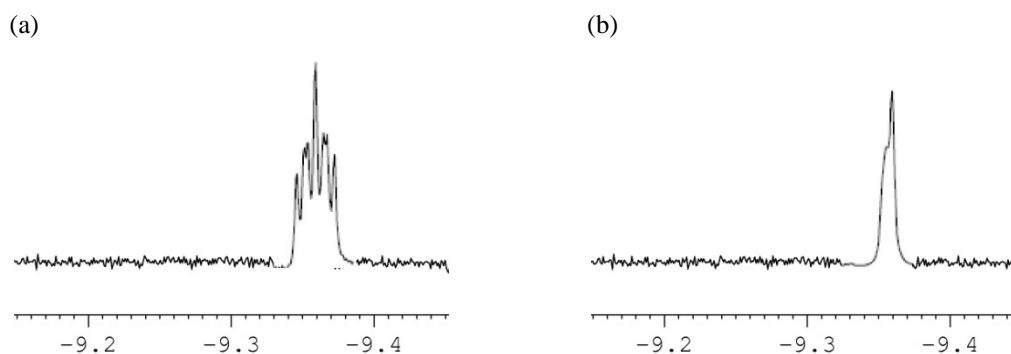


Figure 6. High pressure NMR spectra of $[\text{RhH}(\text{CO})_2(\mathbf{4}/\mathbf{6})]$ at 45°C:

(a) ^1H NMR spectrum (b) $^1\text{H}\{^{31}\text{P}\}$ NMR spectrum.

The Rossi and Hoffmann molecular orbital analysis of electronic site preference in penta-coordinate d^8 metal complexes suggests preference of π -acceptor auxiliaries for equatorial coordination and preference of σ -donor auxiliaries for axial coordination in order to prevent electronic destabilisation.²⁵ This electronic imposition on the chelation mode has been observed experimentally in the rhodium-hydride-dicarbonyl complexes of electronically asymmetric diphosphines.^{24d} The suspected *ee* geometry of $[\text{RhH}(\text{CO})_2(\mathbf{4}/\mathbf{6})]$ therefore suggests that the chelation mode for these systems is determined foremost by constraints of the associated platforms.

5.4 Heterodimeric Stability

In order to ensure that the heterodimer is operative in catalysis, intramolecular hydrogen-bond stability was evaluated in terms of linear selectivity observed in the hydroxymethylation of allyl alcohol. A strong chelate effect on this parameter is well established.²⁶ The complex $[\text{RhH}(\text{CO})_2(\mathbf{2}/\mathbf{6})]$ (**22f**) was prepared upon pressurising a solution of $[\text{Rh}(\mathbf{2}/\mathbf{6})(\text{acac})]$ with 40 bar $\text{CO}/\text{H}_2 = 1$ at the requisite temperature.

Temperature. Asymmetrically placed hydrogen bonds are recognised as being thermally sensitive with bond energies approximating -30 kJ mol^{-1} ,²⁷ so the thermal endurance of the heterodimeric structure was assessed by screening regioselectivity against reaction temperature (Figure 7). Approximate regioselectivity is maintained at $l/b \approx 6.3$ in the range 60 to 95°C. Above 100°C deterioration towards the regioselective range of the non-chelated reference system is noted, corresponding to a continuous erosion of the hydrogen-bonding network between **2** and **6**. The deposition of black mirror in the autoclave indicates catalyst decomposition at temperatures exceeding 140°C.

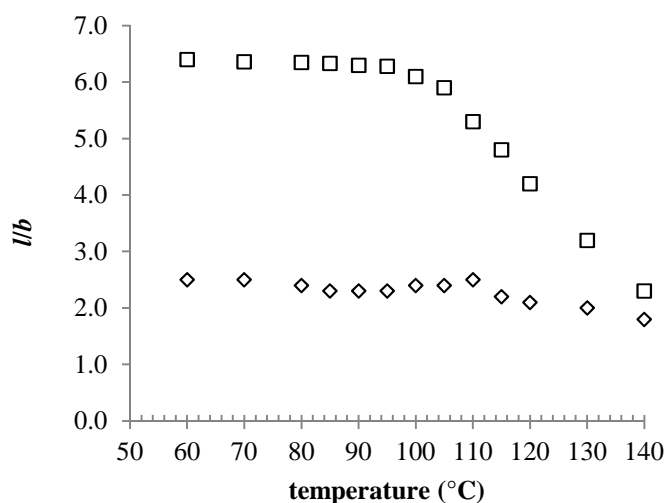


Figure 7. Temperature effect on regioselectivity in the hydroformylation of allyl alcohol: (□) **22f**, (◇) PPhEt_2 . (Conditions: 4.5 mL toluene, 8 mM $[\text{Rh}]$, $\mathbf{2}/\mathbf{6}/\text{Rh} = 2/2/1$, 40 bar $\text{CO}/\text{H}_2=1$, $\text{Rh}/\text{allyl alcohol} = 1/184$)

Rhodium/allyl alcohol molar ratio. The resilience of the heterodimer against disruption by the hydrogen-bonding capacity of the substrate was evaluated as a function of the Rh/S molar ratio (Figure 8). The regioselectivity remains apparently unaffected when this molar ratio is in the range 1/90 to 1/290. At higher values a deleterious effect on linear selectivity is observed, indicating

cleavage of the hydrogen-bonding network between **2** and **6**. Interestingly, the regioselectivity is affected to a smaller degree by high 10-decen-1-ol to rhodium molar ratios. This disparity is most likely attributable to a degree of catalyst poisoning by methacrolein in the former system,²⁸ which effectively reduces catalyst concentration. Such a suggestion is in concurrence with previous reports in which a high catalyst concentration was correlated with improved regioselectivity.²⁶ Additionally, more prominent dispersion forces in 10-decen-1-ol may negate its structural dissociation and possible interference with hydrogen-bonding in the heterodimer.

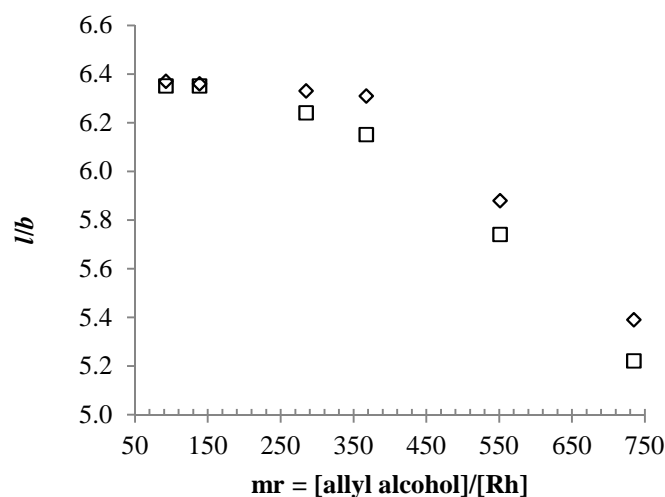


Figure 8. Rh/S molar ratio effect on the hydroformylation of homoallylic alcohols with **22f**:

(□) allyl alcohol, (◇) 10-decen-1-ol.^a

(Conditions: (5- $V_{\text{substrate}}$) mL toluene, 8 mM [Rh], **2/6**/Rh = 2/2/1, 90°C, 40 bar CO/H₂=1)

Reaction medium. Although hydroxymethylation can be optimised relative to hydroformylation by employing as the medium a linear alcohol, a free hydroxyl moiety was previously found to inhibit hydrogen-bonding in analogous heterodimers.^{13a} The possibility for fine-tuning catalyst selectivity through a solvent effect was therefore investigated (Table 3). The substituted di(*tert*-butyl)methanols were synthesised according to the literature procedures.²⁹ The relative polarity of each medium was estimated from the solvatochromatic shift of its Nile Red solution.³⁰

As expected, hydroxymethylation does not occur when catalysis is performed in toluene. A polar medium is necessary in order to activate the rhodium-bound acyl functionality, either for hydride transfer or protonation. Coordinating solvents such as alcohols may be capable of partaking in catalysis by coordination to rhodium, and the high linear selectivity observed in *iso*-propanol and *tert*-butanol could therefore be attributed to crowding in the catalyst coordination sphere which would enforce formation of the less sterically hindered linear rhodium-hydroxypropyl-carbonyl intermediate.

Table 3: Hydroxymethylation of allyl alcohol with **22f** in organic media.^a

	E_{NR} (kJ mol ⁻¹) ^b					diol fraction	
	200	210	220	230	240	yield (mol%)	<i>l/b</i>
methanol	217.7					55	4.6
ethanol	219.3					64	4.5
i-propanol	220.1					61	6.4
t-butanol	223.8					55	5.2
methyl di(<i>tert</i> -butyl) methanol	225.4					16	3.6
ethyl di(<i>tert</i> -butyl) methanol	225.9					25	3.9
toluene	242.1					3	1/0

^aConditions: 4 mL solvent, 8 mM [Rh], **2/6**/Rh = 2/2/1, 90°C, 40 bar CO/H₂ = 1, 4 hours. ^bMolar transition energy (kJ mol⁻¹) calculated from $E_{NR} = (hcNA/\lambda_{\max}^{\text{abs}}) \times 10^6$.

It is therefore surprising to observe adverse chemoselectivity when catalysis is performed in high substituted di(*tert*-butyl)methanols. One explanation could be that these do not form self-associated polymers higher than cyclic or open dimers, which are more liable to disrupt the hydrogen-bonding network in the heterodimer than polymeric associations of smaller homologues.

5.5 Catalysis

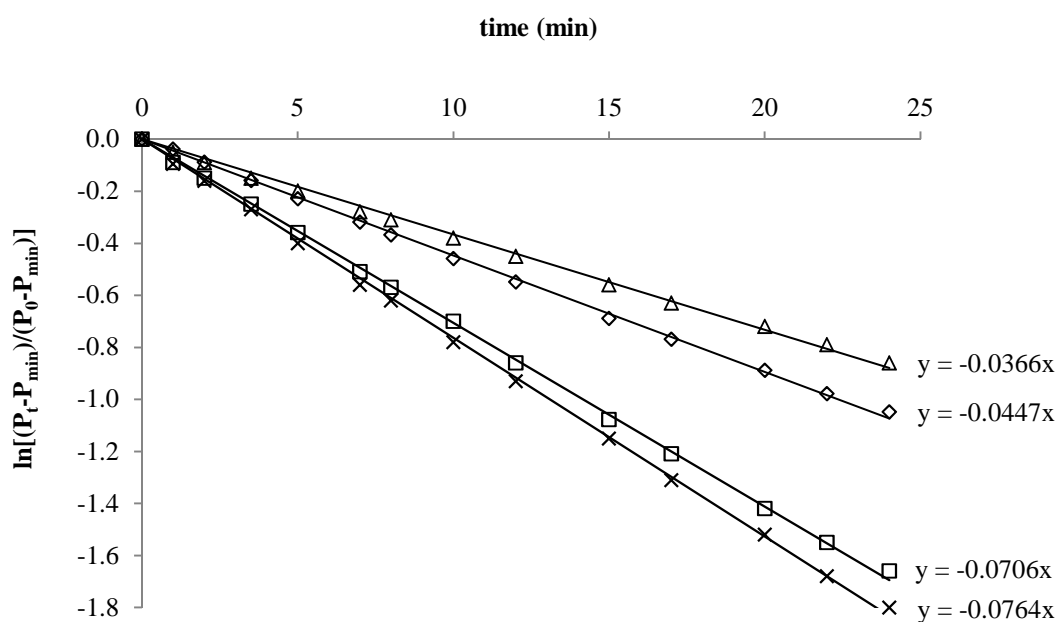
The performance of hetero-combinatorial catalysts derived from the matrix of **1-8** was assessed; the homo-combinatorial systems were used as *monodentate* prototypes to calibrate the data (Table 5). The complexes [Rh(acac)(*PAPP/IQP*)] (*PAPP* = **1-4**, *IQP* = **5-8**) were prepared and coordination was confirmed by ³¹P{¹H} NMR spectroscopy (Table 4). The corresponding trigonal bipyramidal species [RhH(CO)₂(*PAPP/IQP*)] (**22a-22p**) were generated upon pressurising with 40 bar CO/H₂=1 at 90°C in the presence of excess 2-*N*-pivaloylaminopyridyl phosphine and isoquinolyl phosphine. Generating the active complex in this manner avoids the complications associated with having several rhodium species present.³¹

A product mixture of linear aldehyde (2, 3-dihydrofuran, 2-furanol, 1-butanol), branched aldehyde (2-methylpropanal), linear alcohol (1, 4-butanediol, 3-butenol) and branched alcohol (2-methylpropanol) was recovered; only trace quantities of other isomers were observed. 1-Propanal and 1-propanol were recovered as the substrate isomerisation and substrate hydrogenation products respectively.³²

Table 4: $^{31}\text{P}\{^1\text{H}\}$ NMR data^a and selected ESI-MS data for $[\text{Rh}(\text{acac})(\text{PAPP}/\text{IQP})]$ complexes.

	precursor for	<i>PAPP</i>		<i>IQP</i>			M^+ -acac
		δ (ppm)	$^1J_{\text{Rh-P}}$ (Hz)	δ (ppm)	$^1J_{\text{Rh-P}}$ (Hz)	$^2J_{\text{P-P}}$ (Hz)	
1/5	22a	dd. 57.4	185	dd. 57.8	186	51	795.12
1/6	22b	dd. 58.4	185	dd. 28.8	174	50	
1/7	22c	dd. 58.1	184	dd. 35.3	189	49	
1/8	22d	dd. 57.6	185	dd. 56.8	184	51	
2/5	22e	dd. 28.6	179	dd. 58.4	186	50	698.16
2/6	22f	dd. 28.4	179	dd. 28.9	180	49	
2/7	22g	dd. 29.1	178	dd. 34.7	174	49	710.31
2/8	22h	dd. 28.5	179	dd. 56.7	184	50	
3/5	22i	dd. 33.4	174	dd. 58.9	185	49	806.25
3/6	22j	dd. 59.0	173	dd. 33.1	180	48	
3/7	22k	prepared <i>in situ</i> as precursor did not form cleanly					
3/8	22l	dd. 32.9	174	dd. 57.6	183	50	
4/5	22m	dd. 56.3	183	dd. 57.7	186	51	850.23
4/6	22n	dd. 56.6	182	dd. 28.6	179	50	
4/7	22o	dd. 56.9	181	dd. 34.9	174	49	864.32
4/8	22p	dd. 56.4	183	dd. 56.7	184	51	

^aConditions: 1.2 mL d_3 -chloroform, 8 mM [Rh], $\text{PAPP}/\text{IQP}/\text{Rh} = 1/1/1$, ambient temperature, atmospheric pressure of nitrogen.

**Figure 9.** Plot of $\ln[(P_t - P_{\text{min}})/(P_0 - P_{\text{min}})]$ in time for allyl alcohol hydroxymethylation with **22a-d**:

(\square) **22a**, (\diamond) **22b**, (Δ) **22c**, (\times) **22d**.

Table 5: Hydroxymethylation of allyl alcohol with **22a-22p** in *iso*-propanol.^a

catalyst	allyl alcohol-based selectivity (mol%)				k^d	tof ^e (h ⁻¹)
	C=O ^b (I/b)	-OH ^c (I/b)	iso.	hyd.		
Rh-1/1	83 (3.4)	2 (1/0)	10	5	8.9	400.5
Rh-2/2	9 (2.5)	71 (2.7)	14	6	8.4	377.9
Rh-3/3	59 (1.5)	5 (0.2)	30	6	7.3	328.4
Rh-4/4	96 (16.5)	0 (-)	3	1	9.7	436.6
Rh-5/5	86 (3.6)	1 (1/0)	8	5	9.2	414.2
Rh-6/6	10(2.9)	73 (3.0)	12	5	8.8	296.3
Rh-7/7	66 (1.7)	5 (0.4)	23	6	7.6	341.8
Rh-8/8	95 (16.8)	0 (-)	2	3	9.8	440.7
22a	95 (11.1)	0 (-)	3	2	5.4	243.1
22b	57 (10.2)	36 (10.6)	3	4	3.1	139.5
22c	30 (11.4)	63 (11.5)	5	2	2.8	126.0
22d	96 (18.7)	0 (-)	2	2	5.9	265.3
22e	61 (9.9)	34 (9.9)	3	2	3.2	143.7
22f	36 (6.4)	57 (5.1)	2	2	2.4	108.4
22g	13 (9.5)	80 (9.8)	5	2	1.6	72.1
22h	62 (16.2)	35 (16.3)	2	1	3.5	157.7
22i	35 (11.4)	64 (11.7)	1	1	2.9	130.3
22j	14 (9.2)	79 (9.7)	5	2	1.6	73.8
22k	72 (1.7)	4 (0.3)	19	5	7.1	319.6
22l	33 (18.8)	63 (19.1)	3	1	3.1	140.1
22m	97 (19.1)	0 (-)	2	1	5.9	265.2
22n	60 (16.0)	38 (16.1)	1	1	3.5	157.5
22o	35 (18.7)	61 (19.0)	1	3	2.9	132.3
22p	99 (23.1)	0 (-)	1	0	6.1	274.9

^aConditions: 4 mL *iso*-propanol, 8 mM [Rh], Rh/PAPP/IQP = 1/2/2, Rh/allyl alcohol = 1/185, 90°C, 40 bar CO/H₂ = 1. ^bHydroxyaldehyde derivatives. ^cDiol derivatives. ^dFirst order rate constant ($\times 10^{-4} \text{ s}^{-1}$) calculated as the gradient of a plot of $\ln(P_t/P_{t=0})$ in time. ^eTurnover frequency at 1 mol L⁻¹ allyl alcohol.

Activity. Initial reaction rates were determined from reaction profile plots of $\ln(P_t/P_{t=0})$ in time (Figure 9). The reactions are found to be first order with respect to allyl alcohol concentration. This is indicative of type I kinetics wherein the catalyst resting state is the rhodium-hydride-dicarbonyl complex and the rate-determining step is allyl alcohol coordination to the 16-electron rhodium-hydride-carbonyl species.

Compared with most traditional diphosphine-modified catalysts, these heteroleptic complexes display remarkably high activity. Enhanced activity may be attributable to the two-point hydrogen-

bonding motif which imparts no additional degrees of freedom to the platforms, with rotation of the binding motif around a parallel axis not affecting the relative positions of appended groups. Similar activating effects have been observed in hydroformylation with covalent diphosphine-modified catalysts.

Catalyst activity was monitored as a function of the phosphorus substitution pattern (Figure 10). The electronic requisite of each platform was determined as the amplitude of the phosphorus-selenium coupling constant in the corresponding selenide, readily obtained upon reaction of **1-8** with an excess of elemental selenium in d_3 -chloroform. The reliability of this method for assessing the σ -donor character of the phosphorus lone-pair orbital is established.³

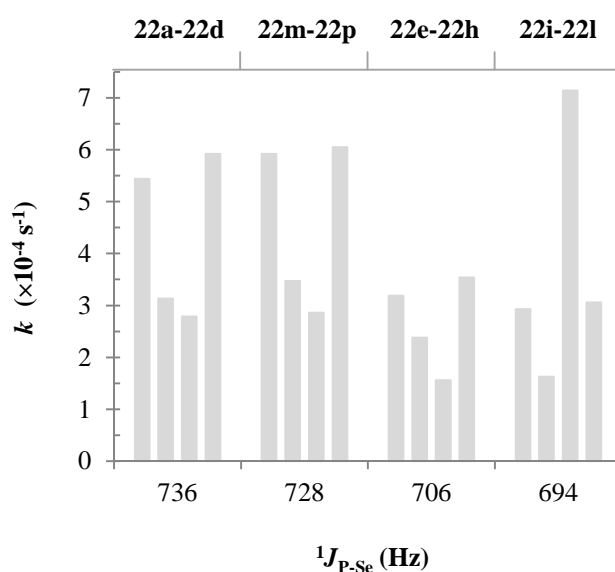


Figure 10. Activity of **22a-22p** in hydroxymethylation of allyl alcohol relative to J_{P-Se} of the selenated platforms.

Dialkyl-substitution on phosphorus is inhibitive to the activity of **22b-22c**, **22e-22h**, **22i-22l** (**22k** exclusive) and **22n-22o**. Superior σ -donor character leads to stronger rhodium-carbonyl π back-bonding which deters the rate-determining displacement of a carbon monoxide auxiliary from the rhodium-hydride-dicarbonyl resting state. Conversely, diaryl-substitution on phosphorus is beneficial, and enhances catalyst activity by a factor of 1.5 to 2.0. The correlation is rendered non-linear by the observation that **22h**, **22l** and **22n-22p** are more active than **22e**, **22i** and **22a-22c** respectively. As a phenyl-substituent and 3, 5- dimethylphenyl-substituent are not isosteric this enhanced activity is probably due to higher spatial demands promoting dissociation of a carbon monoxide auxiliary. Coordination chemistry established that the highly steric **3/7** assembly is a poor chelate for rhodium(I), and so preferential formation of the corresponding *mono*-phosphine complexes may be responsible for the high activity observed with **22k**.

Regioselectivity. The regioselectivity displayed by the heteroleptic catalysts is typically 3 times that of their homoleptic analogues, which confirms the presence of a chelate in the kinetically competent species. Furthermore, performance with regards to this parameter exceeds the level typically achieved with diphosphine-modified catalysts.³⁴ A possible explanation could be that charge distortion induced by the asymmetric chelate enables stabilisation of the rhodium-hydroxypropyl-carbonyl complex *via* a β -agostic interaction between the hydroxyl oxygen in the substrate and the rhodium centre, while rendering a similar interaction in the rhodium-methylhydroxyethyl-carbonyl unattractive by prospective formation of a four-membered heterocycle (Figure 11). The enhanced stability of the transient linear isomer could result in a higher concentration of this species or in a lower activation barrier for its formation.

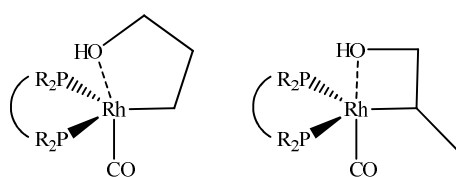


Figure 11. β -agostic oxygen-rhodium interaction in the rhodium-hydroxyalkyl-carbonyl regio-isomers.

The highest linear selectivity is attained with **22p**. Catalyst systems incorporating either component platform **4** or **8** also give a superior performance, with an approximate two-fold enhancement noted over those incorporating the diphenylphosphine-modified analogues. The rotational limitation of the *bis*-(3, 5-dimethylphenyl)phosphine moiety enforces the chiral configuration required for *anti*-Markovnikoff hydride migration.³⁵ The reduced regioselective performance of **22b**, **22e-22h**, **22j** and **22n** is collective consequence of small steric requirement and strong σ -donor capacity.²⁶ According to the Chatt-Dewar-Duncanson model of metal-alkene binding, strong σ -donor auxiliaries promote α -alkene coordination with the substituent oriented opposite to the hydride position of the equatorial plane.³⁶ Migration of the hydride to the terminal alkenic carbon is exasperated by extensive metal-alkene π -backbonding which introduces a high barrier to alkene rotation. Additionally, strong σ -donor ligands augment rhodium $^{\delta+}$ -hydride $^{\delta-}$ polarisation and facilitate nucleophilic interaction between the hydride and the terminal alkenic carbon, which bears a more positive fractional charge.³⁷ **22c**, **22g**, **22i-22j**, **22l** and **22o** afford comparable regioselectivity to **22b-22e**, **22i** and **22m**. This intimates that the steric requisite of the dicyclohexylphosphine moiety takes precedence over its electronic consideration, with hindrance created in the rhodium coordination sphere favouring formation of the less demanding linear rhodium-hydroxypropyl-carbonyl. The involvement of a *mono*-phosphine-modified regioselective determinant in hydroxymethylation with **22k** is corroborated by coincident regioselectivity when the homoleptic catalysts **Rh-3/3** and **Rh-7/7** are applied.

It is noteworthy that modification of the phosphorus moiety on the aminopyridine platform has the greater impact on catalyst performance, probably because the electronegative nature of the isoquinolone nucleus³⁸ delocalises the electronic influence of the phosphorus moiety. In light of earlier comment, such a consideration would also account for the higher regioselectivity of the homoleptic catalysts based on the isoquinolone platform.

A slightly higher regioselectivity noted for the diol fraction than for the hydroxyaldehyde fraction is almost certainly due to a small degree of sequential hydrogenation, because steric demands make 4-hydroxybutanal more susceptible to this transformation than 2-methyl-3-hydroxypropanal.

Chemoselectivity. The heteroleptic catalysts give low selectivity to the C₃-products derived from the isomerisation and hydrogenation of allyl alcohol. The relative inactivity for isomerisation may be due to the exclusive *ee* chelation mode adopted by the heterodimers in a trigonal bipyramidal geometry. The embraced rhodium centre could be sterically inaccessible to the hydroxyl hydrogen, or cannot sufficiently stabilise the intermediate hydrido η^3 -allyl configuration.³⁹

It is worth noting that for these asymmetric diphosphines, desirable chemoselective determination may be negated by a *trans* influence. There should be an electronic preference for formation of the new rhodium-hydroxybutanoyl/2-methylhydroxypropanoyl σ -bond *trans* to the weaker σ -donor platform. The most thermodynamically stable isomer is thus generated, with the CO auxillary coordinated *trans* to the stronger σ -donor platform.

The presence of at least one dialkylphosphine-substituted platform in the catalyst motif leads to significant chemoselectivity, defined as > 30 mol% of the recovered reaction products. The best results are accomplished with the highly basic **22g** and **22j**, which give ~ 80 mol% diols. Steric repulsion in **22k** directs formation of the *mono*-phosphine rhodium-hydroxybutanoyl/2-methylhydroxypropanoyl-carbonyl complexes, which would account for the exclusive recovery of hydroxyaldehydes in accordance with previous work using tri(*iso*-propyl)phosphine as the ligand.⁴⁰ **22a**, **22d**, **22m** and **22p** which are based exclusively on diarylphosphine-modified platforms yield < 2 mol% diols, almost certainly *via* sequential hydrogenation of the hydroxyaldehyde products.

Chemoselectivity was screened against the acidity constant of the heterodimer, defined as the sum of those of the composite platforms. An acidity scale of **1-8** was developed in acetonitrile, which has a sufficiently high dielectric constant to keep ion pairs dissociated.⁴¹ For each platform, the constant for equilibrium with a protonated nitrogen-donor base of known acidity in acetonitrile was measured by quantitative ¹H and ³¹P{¹H} NMR spectroscopy (Table 6).⁴² The *p*-trifluoromethylanilinium, anilinium and morpholinium tetrafluoroborate salts were synthesised according to the literature procedures.⁴³ The data is fitted with 4th order polynomial trend-lines (Figure 14).

Table 6: Thermodynamic data for phosphine/phosphonium salt equilibria of **1-8** in d_3 -acetonitrile.^a

	ligand (acid)		base		equilibration	[HL ⁺]		[NH ₂]/[NH ₃ ⁺]	K	pK	pK _a ^{MeCNb}
	δ _p (ppm)	RNH ₃ ⁺	pK _a ^{MeCN}	δ _p (ppm)		[HL ⁺]/[L]					
1	-11.4	CF ₃ -4-C ₆ H ₄ NH ₃ BF ₄	8.6 ^c		0.5-1.5 h	3.6	0.79	0.21	0.16	0.80	7.80
2	-19.1	C ₆ H ₅ NH ₃ BF ₄	10.6 ^d		1-1.5 h	-3.1	0.41	0.61	0.25	0.60	9.98
3	1.9	O(CH ₂ CH ₂) ₂ NH ₃ BF ₄	16.6 ^d		< 3 h	22.5	0.94	0.06(mbd)	0.06	1.22	15.38
4	-12.5	CF ₃ -4-C ₆ H ₄ NH ₃ BF ₄	8.6		1-1.5 h	2.4	0.78	0.23	0.18	0.74	7.86
5	-9.7	CF ₃ -4-C ₆ H ₄ NH ₃ BF ₄	8.6		< 1 h	4.9	0.85	0.15	0.13	0.89	7.71
6	-17.1	C ₆ H ₅ NH ₃ BF ₄	10.6		< 1.5 h	-2.3	0.35	0.65 (mbd)	0.23	0.64	9.96
7	1.0	O(CH ₂ CH ₂) ₂ NH ₃ BF ₄	16.6		2.5-3 h	22.1	0.92	0.08(mbd)	0.07	1.15	15.45
8	-9.6	CF ₃ -4-C ₆ H ₄ NH ₃ BF ₄	8.6		< 1.5 h	2.0	0.72	0.26	0.19	0.72	7.88

^aConditions: 1.0 mL d_3 -acetonitrile, 0.1 M [L], 0.1 M [RNH₃⁺], 25°C. ^bAcidity constant ($pK_a^{\text{MeCN}} = pK_a[\text{RNH}_3^+]^{\text{MeCN}} - pK^{\text{MeCN}}$). ^c44a in References and Notes. ^d44b in References and Notes.

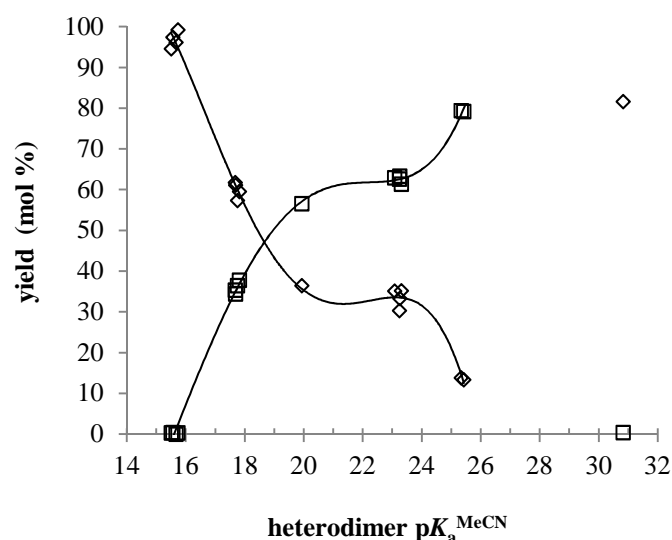


Figure 14. Chemoselectivity of **22a-22p** in hydroxymethylation of allyl alcohol relative to heterodimer $pK_a^{\text{MeCN}} = pK_a(\mathbf{1-4})^{\text{MeCN}} + pK_a(\mathbf{1-4})^{\text{MeCN}}$:
 (□) diol fraction, (◇) hydroxyaldehyde fraction.

Chemoselectivity displays a considerable dependence on the acidity constant when this is < 20 and > 24 (Figure 12). The transient plateau between these limits is indicative of a chemoselective desensitisation, which could originate from an enhanced *trans* influence because electronic distinction between the two platforms is highest when the acidity constant ≈ 23 . Extensive steric interaction in the coordination sphere of **22k** is probably responsible for the significant deviation observed when the acidity constant = 30.8.

5.6 Conclusions.

One of the most beneficial features of supramolecular catalysis is the potential for efficient catalyst screening. This has been applied successfully for general reactions, but reports for specific transformations are scarce. In this chapter heterodimers based on 2-*N*-pivaloylaminopyridyl phosphines and isoquinolyl phosphines were screened as diphosphine ligands for the rhodium-catalysed hydroxymethylation of allyl alcohol. Association behaviour in solution confirmed a 1/1 binding stoichiometry, with association constants in the range 1.04×10^3 to $1.11 \times 10^3 \text{ M}^{-1}$, depending on the medium. Heteroleptic species were formed upon complexation with neutral and cationic rhodium salts, and preferential *ee* geometry of the rhodium-hydride-dicarbonyl complex suggests that the chelation mode is predominantly imposed by the steric constraints of the hetero-combinatorial assembly.

Despite the sensitivity of the intramolecular hydrogen-bonding network to temperature and free hydroxyl functionalities, highly regioselective catalysts were afforded. Studies have indicated a

correlation between chemoselectivity and the heterodimer acidity constant, but when electronic distinction between the two platforms is high a *trans* influence renders this non-linear.

This research is intent on accomplishing linear-selective hydroxymethylation of allyl alcohol. Heterodimers constructed from a diethylphosphine-modified platform in association with a dicyclohexyl-modified platform gave highly chemoselective catalysts, with ~ 80 mol% diol derivatives recovered in $l/b \approx 9.8$. These structures combine strong σ -donor character with an intermediary steric requisite. The catalyst based on the *bis*(diethylphosphine)-heterodimer afforded reasonable chemoselectivity, but lower linear selectivity. Excessive steric repulsion in the *bis*(dicyclohexylphosphine)-heterodimer led to the formation of *mono*-phosphine catalysts, which performed poorly. Heterodimers constructed from a *bis*(3, 5-dimethylphenyl)phosphine platform in association with a dicyclohexyl platform gave highly regioselective catalysts but with some sacrifice of chemoselectivity, with ~ 62 mol% diol derivatives recovered in $l/b \approx 19.1$. These structures combine highly steric moieties with sufficient σ -donor character provided by the dicyclohexyl-modified platform.

While the current results are promising, optimised rigidity of the heterodimeric structure is necessary to economise batch catalysis in terms of substrate concentration and medium selection. Breit has recently shown that substitution of the six-membered 2-*N*-pivaloylaminopyridine skeleton for the 5-membered 2-*N*-pivaloylaminothiazole heterocycle led to a stronger hydrogen-bonding network. An alternative would be to introduce an electronegative moiety adjacent to a donor site, and to this end an investigation of the catalyst performance incited by 2-*N*-trifluoroacetylaminopyridine platforms would be of interest.

5.7 Experimental Section

Materials. Chemicals were purchased from Acros Organics, Sigma-Aldrich, AGS and Strem. Unless stated otherwise, all operations were performed under N_2 (passed through column of dichromate adsorbed on silica) in a glove box or using standard Schlenk and catheter tubing techniques. All glassware was flame-dried under vacuum. Diethyl ether, hexane and thf were distilled from sodium benzophenone ketyl, dichloromethane was distilled from calcium hydride, ethyl acetate was twice distilled from P_2O_5 , *iso*-propanol was distilled from sodium, all under N_2 onto activated Linde 4 Å molecular sieves. HPLC-grade toluene, pentane and cyclohexane were dispensed from argon-flushed La Roche A-2/Engelhard Q-5 drying columns. All solvents were degassed prior to use by fpt cycles. $MgSO_4$, Celite and Kieselgel (60 SiO_2) were activated in a tube furnace at 250°C for 3 hours. 2-Amino-6-bromopyridine,⁴⁵ *bis*(3, 5-dimethylphenyl)chlorophosphine⁴⁶ and *tris*(3, 5-dimethylphenyl)phosphine⁴⁶ were prepared according to the literature procedures.

Analytical techniques. NMR spectra were recorded on Bruker Avance 300 and Bruker Avance II 400 spectrometers with tetramethylsilane (^1H , ^{13}C), 85% H_3PO_4 (^{31}P) and CFCl_3 (^{19}F) as external references. Gas chromatography was performed on a Hewlett-Packard 6890 chromatograph fitted with a 30 m BP10TM column (carrier gas 3.2 mL min^{-1} He, flame-ionisation detector). Elemental analyses were done using a Perkin-Elmer 240C CHNS/O microanalyser. Melting point ranges were determined using an MPA1000 OptiMelt analyser.

6-Bromo-2-N-trifluoroacetylaminopyridine (9). 10.8 mL triethylamine (78.00 mmol, distilled from KOH) was slowly added to a solution of 10.9 mL trifluoroacetic acid anhydride (78.00 mmol) in dichloromethane (6 mL) at 0°C , and after 5 minutes 4.5000 g 2-amino-6-bromopyridine (25.95 mmol) was introduced in one portion. The solution was stirred at ambient temperature, the conversion being monitored by GC-MS. The reaction was then quenched by addition of saturated NaHCO_3 solution (45 mL), and the aqueous phase was extracted with ethyl acetate ($4 \times 35\text{ mL}$). The combined extracts were dried over MgSO_4 and concentrated *in vacuo*. The dark yellow residue was purified by flash chromatography (Kieselgel, cyclohexane/ethyl acetate = 5/1), yielding 5.7356 g (82 %) of yellow oil. $R_f = 0.43$ (cyclohexane/ethyl acetate = 5/1). ^1H NMR (CDCl_3 , 300.1 MHz): δ 8.63 (br s, 1H), 8.08 (dd, $J = 7.9$ and 1.3 Hz , 1H), 7.69 (t, $J = 7.8\text{ Hz}$, 1H), 7.34 (dd, $J = 7.8$ and 1.4 Hz , 1H). $^{13}\text{C}\{^1\text{H}\}$ NMR (CDCl_3 , 75.5 MHz): δ 155.2 (q, $^2J_{\text{F-C}} = 37.4\text{ Hz}$), 150.1 (s), 143.9 (s), 140.6 (s), 125.3 (s), 115.3 (q, $^1J_{\text{F-C}} = 286.4\text{ Hz}$), 113.5 (s). $^{19}\text{F}\{^1\text{H}\}$ NMR (CDCl_3 , 282.2 MHz): 76.08. *Anal.* Calculated for $\text{C}_7\text{H}_4\text{BrN}_2\text{OF}_3$: C, 31.25; H, 1.50; N, 10.41. Found: C, 31.11; H, 1.37; N, 10.34.

6-(Diphenylphosphino)-2-aminopyridine (10a). Over 10 min, 2.9 mL of a 1.6 M solution of *n*-BuLi (4.67 mmol) in hexanes was added to a solution of 0.6267 g **9** (2.33 mmol) in thf (15 mL) at -100°C . After stirring at constant temperature for 90 min a solution of 433 μL diphenylchlorophosphine (2.47 mmol) in thf (4 mL) was introduced dropwise. Following another 90 min at -100°C , the yellow solution was slowly warmed to 35°C and stirred 12 hours before approximately 50 μL H_2O ($\sim 2.80\text{ mmol}$) was added. Solvents were then removed *in vacuo* and dichloromethane (9 mL) was added to the residue. The resulting suspension was filtered through a silica pad and *in vacuo* concentration of the filtrate gave cream foam. $^{31}\text{P}\{^1\text{H}\}$ NMR (CD_2Cl_2 , 121.4 MHz): $\delta - 3.1$.

Direct deprotection was accomplished *in situ* by adding a suspension of 3.2040 g K_2CO_3 (22.12 mmol) in methanol (20 mL), and stirring gently at 60°C for 4 hours. After diluting with saturated NaHCO_3 solution (14 mL), the aqueous phase was extracted with ethyl acetate ($3 \times 25\text{ mL}$) and the combined extracts were percolated through a column of $\text{MgSO}_4\text{-zsm-5}$. The filtrate was concentrated *in vacuo* and the off-white solid purified by flash chromatography (Kieselgel, hexane/ethyl acetate = 1/1), yielding 0.5632 g (87 %) of white solid. $R_f = 0.46$ (hexane/ethyl acetate = 1). ^1H NMR (CDCl_3 , 300.1 MHz): δ 7.59 (dt, $J = 7.6\text{ Hz}$, $^4J_{\text{P-H}} = 8.0\text{ Hz}$, 1H), 7.42 (m, 6H), 7.33 (m, 4H), 7.03 (dd, $J = 7.5$

and 1.2 Hz, 1H), 6.19 (fine split d, $J = 7.5$ Hz, 1H), 4.74 (br s, 2H). $^{13}\text{C}\{^1\text{H}\}$ NMR (CDCl_3 , 75.5 MHz): δ 163.9 (d, $^1J_{\text{P-C}} = 9.2$ Hz), 157.4 (d, $^2J_{\text{P-C}} = 14.8$ Hz), 147.1 (s), 138.3 (d, $^3J_{\text{P-C}} = 1.5$ Hz), 136.2 (d, $^1J_{\text{P-C}} = 20.6$ Hz), 134.9 (d, $^2J_{\text{P-C}} = 10.2$ Hz), 129.3, 128.7 (d, $^3J_{\text{P-C}} = 2.2$ Hz), 108.6 (s). $^{31}\text{P}\{^1\text{H}\}$ NMR (CDCl_3 , 121.4 MHz): $\delta - 12.3$. *Anal.* Calculated for $\text{C}_{17}\text{H}_{15}\text{N}_2\text{P}$: C, 73.36; H, 5.43; N, 10.07. Found: C, 73.55; H, 5.44; N, 9.98.

6-(Diethylphosphino)-2-aminopyridine (10b). Preparation of **10b** was performed by a similar procedure to that employed for the preparation of **10a**. Starting from 0.6100 g **9** (2.27 mmol), 2.8 mL of a 1.6 M solution of *n*-BuLi (4.55 mmol) in hexanes, 293 μL diethylchlorophosphine (2.41 mmol) and 49 μL H_2O (~ 2.7 mmol) yielded the protected product as yellow foam. $^{31}\text{P}\{^1\text{H}\}$ NMR (CD_2Cl_2 , 121.4 MHz): $\delta - 13.4$.

Direct deprotection using 3.1237 g K_2CO_3 (21.57 mmol) in methanol (20 mL) and purification by percolating through a short column of triethylamine-deactivated silica at -5°C yielded 0.2192 g (53 %) of opaque residue. ^1H NMR (CDCl_3 , 300.1 MHz): δ 7.55 (dt, $J = 7.5$ Hz, $^4J_{\text{P-H}} = 8.0$ Hz, 1H), 7.06 (dd, $J = 7.5$, 1.3 Hz, 1H), 6.19 (fine split d, $J = 7.5$ Hz, 1H), 4.91 (br s, 2H), 1.74 (dq, $J = 8.1$ Hz, $^2J_{\text{P-H}} = 13.7$ Hz, 4H), 1.10 (td, $J = 8.1$ Hz, $^3J_{\text{P-H}} = 0.8$ Hz, 6H). $^{13}\text{C}\{^1\text{H}\}$ NMR (CDCl_3 , 75.5 MHz): δ 159.5 (d, $^1J_{\text{P-C}} = 8.8$ Hz), 148.1 (d, $^2J_{\text{P-C}} = 14.0$ Hz), 145.6 (s), 137.7 (d, $^3J_{\text{P-C}} = 1.5$ Hz), 107.8 (s), 23.4 (d, $^1J_{\text{P-C}} = 24.8$ Hz), 8.8 (d, $^2J_{\text{P-C}} = 10.6$ Hz). $^{31}\text{P}\{^1\text{H}\}$ NMR (CDCl_3 , 121.4 MHz): $\delta - 16.9$. *Anal.* Calculated for $\text{C}_9\text{H}_{15}\text{N}_2\text{PS}$: C, 50.45; H, 7.06; N, 13.07; S, 14.96. Found: C, 50.63; H, 6.94; N, 13.19; S, 14.93.

6-(Dicyclohexylphosphino)-2-aminopyridine (10c). Preparation of **10c** was performed by a similar procedure to that employed for the preparation of **10a**. Starting from 0.6237 g **9** (2.32 mmol), 2.9 mL of a 1.6 M solution of *n*-BuLi (4.64 mmol) in hexanes, 543 μL dicyclohexylchlorophosphine (2.41 mmol) and 50 μL H_2O (~ 2.80 mmol) yielded the protected product as white flakes. $^{31}\text{P}\{^1\text{H}\}$ NMR (CD_2Cl_2 , 121.4 MHz): $\delta 1.2$.

Direct deprotection using 3.1885 g K_2CO_3 (22.02 mmol) in methanol (20 mL) yielded 0.3301 g (49 %) of white solid. $R_f = 0.58$ (hexane/ethyl acetate = 1/2). ^1H NMR (CDCl_3 , 300.1 MHz): δ 7.39 (dt, $J = 7.5$ Hz, $^4J_{\text{P-H}} = 8.2$ Hz, 1H), 6.86 (dd, $J = 7.5$, 1.4 Hz, 1H), 6.44 (fine split d, $J = 7.5$ Hz, 1H), 4.48 (br s, 2H), 1.63-1.42 (m, 20H), 1.40-1.26 (m, 2H). $^{13}\text{C}\{^1\text{H}\}$ NMR (CDCl_3 , 75.5 MHz): δ 158.4 (d, $^1J_{\text{P-C}} = 8.0$ Hz), 148.3 (d, $^2J_{\text{P-C}} = 13.7$ Hz), 146.2 (s), 138.5 (d, $^3J_{\text{P-C}} = 1.5$ Hz), 107.2 (s), 29.4-28.8 (m). $^{31}\text{P}\{^1\text{H}\}$ NMR (CDCl_3 , 121.4 MHz): $\delta -0.7$. *Anal.* Calculated for $\text{C}_{17}\text{H}_{27}\text{N}_2\text{P}$: C, 70.31; H, 9.37; N, 9.65. Found: C, 70.36; H, 9.25; N, 9.66.

6-(Bis(3, 5-dimethylphenyl)phosphino)-2-aminopyridine (10d). Preparation of **10d** was performed by a similar procedure to that employed for the preparation of **10a**. Starting from 0.6200 g **9** (2.31 mmol), 2.9 mL of a 1.6 M solution of *n*-BuLi (4.62 mmol) in hexanes, 501 μL

dicyclohexylchlorophosphine (2.45 mmol) and 50 μL H_2O (~ 2.80 mmol) yielded the protected product as cream foam. $^{31}\text{P}\{^1\text{H}\}$ NMR (CD_2Cl_2 , 121.4 MHz): δ -3.6.

Direct deprotection using 3.1747 g K_2CO_3 (21.92 mmol) in methanol (20 mL) yielded 0.6489 (84 %) of white solid. $R_f = 0.53$ (hexane/ethyl acetate = 1). ^1H NMR (C_6D_6 , 300.1 MHz): δ 7.64 (dt, $J = 7.4$ Hz, $^4J_{\text{P-H}} = 8.0$ Hz, 1H), 7.39 (t, $J = 1.4$ Hz, 2H), 7.03 (fine split m, 2H), 7.00 (dd, $J = 7.4$, 1.2 Hz, 1H), 6.56 (fine split t, $J = 7.4$ Hz, 1H), 3.99 (br s, 2H), 2.29 (s, 6H). $^{13}\text{C}\{^1\text{H}\}$ NMR (C_6D_6 , 75.5 MHz): δ 163.6 (d, $^1J_{\text{P-C}} = 9.2$ Hz), 157.4 (d, $^2J_{\text{P-C}} = 14.8$ Hz), 146.8 (s), 138.6 (d, $^3J_{\text{P-C}} = 2.6$ Hz), 138.3 (d, $^3J_{\text{P-C}} = 1.5$ Hz), 130.9, 128.6 (d, $^1J_{\text{P-C}} = 21.2$ Hz), 127.3 (d, $^2J_{\text{P-C}} = 10.5$ Hz), 108.9 (s), 21.7 (s). $^{31}\text{P}\{^1\text{H}\}$ NMR (C_6D_6 , 121.4 MHz): δ -12.9. *Anal.* Calculated for $\text{C}_{21}\text{H}_{23}\text{N}_2\text{P}$: C, 75.43; H, 6.93; N, 8.38. Found: C, 75.33; H, 7.05; N, 8.41.

6-(Diphenylphosphino)-2-pivaloylaminopyridine (1). To a solution of 0.1804 g **10a** (0.65 mmol) in dichloromethane (45 mL) at 0°C , 172 μL triethylamine (1.24 mmol, distilled from KOH) and 120 μL pivaloyl chloride (0.99 mmol) were added consecutively. The solution was slowly warmed to ambient temperature, stirred for 40 hours and reduced to half volume *in vacuo*. The remaining suspension was stirred with approximately 0.2500 g activated charcoal and then filtered through a Celite pad. The filtrate was concentrated *in vacuo* and the white residue was purified by column chromatography (Kieselgel, cyclohexane/ethyl acetate = 8/1), yielding 0.1437g (61 %) of white foam. $R_f = 0.65$ (cyclohexane/ethyl acetate = 8/1). ^1H NMR (C_6D_6 , 300.1 MHz): δ 8.49 (dd, $J = 7.4$, 1.2 Hz, 1H), 8.21 (dt, $J = 7.5$ Hz, $^4J_{\text{P-H}} = 8.0$ Hz, 1H), 7.95 (br s, 1H), 7.45 (m, 6H), 7.41 (m, 4H), 7.12 (fine split d, $J = 7.4$ Hz, 1H), 1.28 (s, 9H). $^{13}\text{C}\{^1\text{H}\}$ NMR (C_6D_6 , 75.5 MHz): δ 176.6 (s), 163.5 (d, $^1J_{\text{P-C}} = 6.2$ Hz), 152.8 (d, $^2J_{\text{P-C}} = 14.5$ Hz), 146.1 (s), 138.5 (d, $^3J_{\text{P-C}} = 1.2$ Hz), 136.2 (d, $^1J_{\text{P-C}} = 19.5$ Hz), 134.9 (d, $^2J_{\text{P-C}} = 9.2$ Hz), 129.3, 128.7 (d, $^3J_{\text{P-C}} = 1.5$ Hz), 115.6 (s), 38.9 (s, weak), 28.4 (s). $^{31}\text{P}\{^1\text{H}\}$ NMR (C_6D_6 , 121.4 MHz): δ -11.7. *Anal.* Calculated for $\text{C}_{22}\text{H}_{23}\text{N}_2\text{PO}$: C, 72.91; H, 6.40; N, 7.73. Found: C, 72.79; H, 6.45; N, 7.79.

6-(Diethylphosphino)-2-pivaloylaminopyridine (2). Preparation of **2** was performed by a similar procedure to that employed for the preparation of **1**. Starting from 0.1514 g **10b** (0.83 mmol), 219 μL triethylamine (1.58 mmol) and 153 μL pivaloyl chloride (1.25 mmol) gave a yellow residue. Purification of its hexane solution by percolating through a short column of triethylamine-deactivated silica at -5°C yielded 0.1194 g (54 %) of viscous yellow oil. ^1H NMR (C_6D_6 , 300.1 MHz): δ 8.52 (dd, $J = 7.5$, 1.4 Hz, 1H), 8.13 (br s, 1H), 7.92 (td, $J = 7.5$, $^4J_{\text{P-H}} = 8.0$ Hz, 1H), 7.04 (fine split d, $J = 7.5$ Hz, 1H), 1.69 (dq, $J = 8.1$ Hz, $^1J_{\text{P-H}} = 13.7$ Hz, 8H), 1.28 (s, 9H), 1.07 (td, $J = 8.1$ Hz, $^2J_{\text{P-H}} = 0.8$ Hz, 12H). $^{13}\text{C}\{^1\text{H}\}$ NMR (C_6D_6 , 75.5 MHz): δ 176.5 (s), 159.8 (d, $^1J_{\text{P-C}} = 5.5$ Hz), 147.4 (d, $^2J_{\text{P-C}} = 13.6$ Hz), 145.9 (s), 137.5 (d, $^3J_{\text{P-C}} = 1.2$ Hz), 115.6 (s), 38.9 (s, weak), 28.4 (s), 23.2 (d, $^1J_{\text{P-C}} = 22.7$ Hz), 8.8 (d, $^2J_{\text{P-C}} = 9.8$ Hz). $^{31}\text{P}\{^1\text{H}\}$ NMR (C_6D_6 , 121.4 MHz): δ -18.7. *Anal.* Calculated for $\text{C}_{14}\text{H}_{23}\text{N}_2\text{POS}$: C, 56.36; H, 7.77; N, 9.39; S, 10.74. Found: C, 55.99; H, 7.84; N, 9.37; S, 10.81.

6-(Dicyclohexylphosphino)-2-pivaloylaminopyridine (3). Preparation of **3** was performed by a similar procedure to that employed for the preparation of **1**. Starting from 0.2014 g **10c** (0.69 mmol), 179 μ L triethylamine (1.32 mmol) and 128 μ L pivaloyl chloride (1.04 mmol) yielded 0.1525 g (59 %) of pale yellow foam. $R_f = 0.74$ (hexane/ethyl acetate = 1/3). ^1H NMR (CDCl_3 , 300.1 MHz): δ 8.50 (dd, $J = 7.5, 1.4$ Hz, 1H), 8.15 (br s, 1H), 7.82 (dt, $J = 7.5$ Hz, $^4J_{\text{P-H}} = 8.2$ Hz, 1H), 7.13 (fine split d, $J = 7.5$ Hz, 1H), 1.59-1.38 (m, 20H), 1.36-1.25 (m, 2H), 1.26 (s, 9H). $^{13}\text{C}\{^1\text{H}\}$ NMR (CDCl_3 , 75.5 MHz): δ 176.5 (s), 158.4 (d, $^1J_{\text{P-C}} = 5.3$ Hz), 146.5 (d, $^2J_{\text{P-C}} = 11.8$ Hz), 145.0 (s), 137.7 (d, $^3J_{\text{P-C}} = 1.2$ Hz), 114.8 (s), 39.2 (s, weak), 31.1-28.8 (m), 28.6 (s). $^{31}\text{P}\{^1\text{H}\}$ NMR (CDCl_3 , 121.4 MHz): δ 1.5. *Anal.* Calculated for $\text{C}_{22}\text{H}_{35}\text{N}_2\text{PO}$: C, 70.56; H, 9.42; N, 7.48. Found: C, 70.69; H, 9.40; N, 7.43.

6-(Bis(3, 5-dimethylphenyl)phosphino)-2-pivaloylaminopyridine (4). Preparation of **4** was performed by a similar procedure to that employed for the preparation of **1**. Starting from 0.1935 g **10c** (0.58 mmol), 152 μ L triethylamine (1.10 mmol) and 107 μ L pivaloyl chloride (0.87 mmol) yielded 0.1578 g (65 %) of white foam. $R_f = 0.71$ (cyclohexane/ethyl acetate = 6/1). ^1H NMR (C_7D_8 , 300.1 MHz): δ 8.48 (dd, $J = 7.5, 1.2$ Hz, 1H), 8.17 (dt, $J = 7.5$ Hz, $^4J_{\text{P-H}} = 8.0$ Hz, 1H), 7.98 (br s, 1H), 7.39 (apparent t, $J = 1.4$ Hz, 2H), 7.16 (fine split t, $J = 7.4$ Hz, 1H), 7.03 (fine split m, 2H), 2.31 (s, 6H) 1.28 (s, 9H). $^{13}\text{C}\{^1\text{H}\}$ NMR (C_7D_8 , 75.5 MHz): δ 176.6 (s), 163.1 (d, $^1J_{\text{P-C}} = 6.0$ Hz), 152.6 (d, $^2J_{\text{P-C}} = 14.2$ Hz), 147.3 (s), 138.6 (d, $^3J_{\text{P-C}} = 1.2$ Hz), 138.3 (s), 130.9 (s), 128.2 (d, $^1J_{\text{P-C}} = 19.8$ Hz), 127.3 (d, $^2J_{\text{P-C}} = 10.0$ Hz), 115.9 (s), 39.3 (s, weak), 28.3 (s). $^{31}\text{P}\{^1\text{H}\}$ NMR (C_7D_8 , 121.4 MHz): δ -12.4. *Anal.* Calculated for $\text{C}_{26}\text{H}_{31}\text{N}_2\text{PO}$: C, 74.62; H, 7.47; N, 6.69. Found: C, 74.55; H, 7.42; N, 6.75.

Homophthalimide (11). This procedure does not require an inert atmosphere. From a solution of 8.2300 g homophthalic acid (45.68 mmol) in 15 mL 28 % ammonium hydroxide solution (~ 0.38 mol), H_2O and ammonia were distilled off under reduced pressure (80°C and 5 mmHg) until the yellow ammonium salt solidified. To this, *o*-dichlorobenzene (20 mL) was introduced and subsequently distilled off (200°C and 760 mmHg). The orange residue was cooled to ambient temperature and precipitation of the imide was induced by addition of cold methanol (15 mL). After 24 hours the suspension was filtered and the yellow solid was washed with methanol (3 \times 15 mL). The product was purified by a recrystallisation from 45% acetic acid solution, yielding 6.6992 g (91 %) of white needles after drying over P_2O_5 *in vacuo*. Mpr. 232-234°C. ^1H NMR (CDCl_3 , 300.1 MHz): δ 10.12 (s, 1H), 7.88 (dd, $J = 7.5$ and 1.3 Hz, 1H), 7.58-7.55 (m, 2H), 7.18 (td, $J = 7.5, 1.2$ Hz, 1H), 3.42 (s). $^{13}\text{C}\{^1\text{H}\}$ NMR (CDCl_3 , 75.5 MHz): δ 170.6 (s), 160.3 (s), 135.9 (s) 135.5 (s), 133.0 (s), 130.4 (s), 127.9 (s), 126.1 (s), 38.3 (s). *Anal.* Calculated for $\text{C}_9\text{H}_7\text{NO}_2$: C, 67.07; H, 4.38; N, 8.69. Found: C, 66.95; H, 4.36; N, 8.65.

1, 3-Dichloroisoquinoline (12). In a neat reaction, 4.1550 g homophthalimide (25.78 mmol) and 9.1 mL phenylphosphonic dichloride (64.45 mmol) were stirred together at 160°C for

approximately 3 hours until evolution of HCl was no longer discernable by litmus. The deep red solution was cooled to 0°C and excess phenylphosphonic dichloride was hydrolysed by the addition of cold H₂O (50 mL, ~ 30 mL per 8 g reagent used). The aqueous mixture was extracted with diethyl ether (4×30 mL). The combined extracts were treated with 5% KOH solution (20 mL), neutralised with H₂O, and then dried over MgSO₄. The solution was concentrated *in vacuo* and the white residue was crystallised from absolute ethanol, yielding 5.1057 g (88%) of white powder after drying over P₂O₅ *in vacuo*. Mpr. 119-123°C. ¹H NMR (C₆D₆, 300.1 MHz): δ 8.47 (dd, *J* = 7.6, 2.0 Hz, 1H), 7.84 (s, 1H), 7.72 (td, *J* = 7.6, 2.0 Hz, 1H), 7.61-7.58 (m, 2H). ¹³C{¹H} NMR (C₆D₆, 75.5 MHz): δ 151.3 (s), 144.9 (s), 139.2 (s, v. weak), 134.5 (s), 128.4 (s), 126.7 (s), 126.4 (s), 125.6 (s), 120.0 (s). *Anal.* Calculated for C₉H₅NCl₂: C, 54.58; H, 2.54; N, 7.07. Found: C, 54.68; H, 2.56; N, 7.00.

1-tert-Butoxy-3-chloroisoquinoline (13). To a solution of 3.1922 g 1, 3-dichloroisoquinoline (16.12 mmol) in toluene (40 mL), 2.1706 g potassium-*tert*-butoxide (19.34 mmol, freshly sublimed at 160°C and 2 mmHg) was added in one portion. The solution was maintained at 90°C under gentle reflux, the conversion being monitored by GC-MS. The yellow suspension was cooled to ambient temperature, and filtered through a silica pad. The filtrate was concentrated *in vacuo* and the residual yellow liquid was purified by bulb-to-bulb distillation (210°C, 10⁻¹ mmHg), yielding 3.3817 g (89%) of clear oil. ¹H NMR (C₆D₆, 300.1 MHz): δ 8.42 (dd, *J* = 7.8, 2.2 Hz, 1H), 7.62 (dt, *J* = 7.8, 2.2 Hz, 1H), 7.54 (td, *J* = 7.8 and 2.2 Hz, 1H), 7.45 (m, 2H), 1.39 (s, 9H). ¹³C{¹H} NMR (C₆D₆, 75.5 MHz): δ 162.5 (s), 144.7 (s), 138.1 (s, weak), 131.7 (s), 126.5 (s), 126.2 (s), 124.1 (s), 117.9 (s), 112.8 (s), 86.4 (s, weak), 27.7 (s). *Anal.* Calculated for C₁₃H₁₄NOCl: C, 66.24; H, 5.99; N, 5.94. Found: C, 66.13; H, 6.08; N, 5.94.

1-tert-Butoxy-3-(diphenylphosphino)isoquinoline (14a). Over 5 minutes, 0.5500 g elemental sodium (23.91 mmol) was added to liquid ammonia (~ 40 mL) at -78°C. To the dark blue solution was introduced 3.0819 g triphenylphosphine (11.75 mmol), and after 2 hours a solution of 2.7622 g **13** (11.75 mmol) in thf (6 mL). The solution was slowly warmed to ambient temperature and the ammonia was evaporated over 16 hours. The residue was quenched with H₂O (30 mL), extracted with diethyl ether (3 × 25 mL) and the combined extracts were percolated through a column of MgSO₄-zsm-5. The filtrate was concentrated *in vacuo* and the opaque residue was purified by a recrystallisation from methanol, yielding 2.9891 g (66%) of white solid after drying *in vacuo* at 50°C. ¹H NMR (C₆D₆, 300.1 MHz): δ 8.42 (dd, *J* = 7.8 and 2.2 Hz, 1H), 7.62 (dt, *J* = 7.8, 2.2 Hz, 1H), 7.52 (td, *J* = 7.8, 2.2 Hz, 1H), 7.49-7.42 (m, 5H), 7.23-7.11 (m, 6H), 6.99 (dd, *J* = 2.2 Hz, ³*J*_{P-H} = 7.2 Hz, 1H), 1.41 (s, 9H). ¹³C{¹H} NMR (C₆D₆, 75.5 MHz): δ 164.1 (d, ¹*J*_{P-C} = 9.7 Hz), 160.5 (s), 138.0 (d, ³*J*_{P-C} = 5.8 Hz, 4000 scans), 137.6 (d, ¹*J*_{P-C} = 11.7 Hz), 134.7 (d, ²*J*_{P-C} = 18.9 Hz), 132.1 (s), 128.9 (s), 128.7 (d, ³*J*_{P-C} = 7.2 Hz), 126.6 (s), 126.3 (s), 124.1 (s), 121.5 (d, ²*J*_{P-C} = 24.7 Hz), 118.9 (s), 83.3 (s), 28.5 (s). ³¹P{¹H} NMR (C₆D₆, 121.4 MHz): δ -3.4.

1-tert-Butoxy-3-(diethylphosphino)isoquinoline (14b). 2.7 mL of a 1.6 M solution of *n*-BuLi (4.28 mmol) in hexanes was added dropwise to a solution of 1.0050 g **13** (4.28 mmol) in thf (35 mL) at -100°C. After stirring at constant temperature for 30 min a solution of 521 µL diethylchlorophosphine (4.28 mmol) was introduced. The yellow solution was slowly warmed to 25°C and stirred 5 hours before quenching with H₂O (200 µL). After solvents were removed *in vacuo*, the residue was treated with saturated ammonium chloride solution (30 mL) and extracted with dichloromethane (3×30 mL). The combined extracts were dried over MgSO₄ and concentrated *in vacuo*, yielding 0.9536 g (77%) of viscous yellow oil. ¹H NMR (CDCl₃, 300.1 MHz): δ 8.44 (dd, *J* = 7.8 and 2.0 Hz, 1H), 7.65 (dt, *J* = 7.8, 2.0 Hz, 1H), 7.52 (td, *J* = 7.8, 2.2 Hz, 1H), 7.45 (td, *J* = 7.8, 2.0 Hz, 1H), 7.04 (dd, *J* = 2.0 Hz, ³*J*_{P-H} = 6.9 Hz, 1H), 1.71 (dq, *J* = 8.5 Hz, ²*J*_{P-H} = 14.2 Hz, 8H), 1.41 (s, 9H), 0.99 (t, *J* = 8.5 Hz, 12H). ¹³C{¹H} NMR (CD₂Cl₂, 75.5 MHz): δ 161.4 (s), 159.7 (d, ¹*J*_{P-C} = 9.2 Hz), 136.8 (d, ³*J*_{P-C} = 4.8 Hz, 4000 scans), 130.6 (s), 126.3 (s), 126.2 (s), 124.1 (s), 118.8 (s), 114.4 (d, ²*J*_{P-C} = 21.9 Hz), 83.1 (s), 28.5 (s), 20.1 (d, ¹*J*_{P-C} = 23.2 Hz), 8.8 (d, ²*J*_{P-C} = 10.4 Hz). ³¹P{¹H} NMR (CD₂Cl₂, 121.4 MHz): δ -8.9.

1-tert-Butoxy-3-(dicyclohexylphosphino)isoquinoline (14c). Preparation of **14c** was performed by a similar procedure to that employed for the preparation of **14b**. Starting from 1.0200 g **13** (3.53 mmol), 2.2 mL of a 1.6 M solution of *n*-BuLi (3.53 mmol) in hexanes, 779 µL dicyclohexylchlorophosphine (3.53 mmol) and a recrystallisation from absolute ethanol yielded 0.8279 g (59%) of off-white solid after drying *in vacuo* at 50°C. ¹H NMR (CDCl₃, 300.1 MHz): δ 8.42 (dd, *J* = 7.8 and 1.8 Hz, 1H), 7.66 (dt, *J* = 7.8, 1.8 Hz, 1H), 7.53 (td, *J* = 7.8, 2.2 Hz, 1H), 7.47 (td, *J* = 7.8, 1.8 Hz, 1H), 7.01 (dd, *J* = 1.8 Hz, ³*J*_{P-H} = 6.4 Hz, 1H), 1.6-1.43 (m, 16H), 1.41 (s, 9H), 1.32 (m, 4H). ¹³C{¹H} NMR (CDCl₃, 75.5 MHz): δ 161.2 (s), 158.8 (d, ¹*J*_{P-C} = 5.5 Hz), 136.8 (d, ³*J*_{P-C} = 1.2 Hz, 4000 scans), 130.6 (s), 126.4 (s), 126.0 (s), 124.1 (s), 118.6 (s), 113.7 (d, ¹*J*_{P-C} = 13.7 Hz), 83.4 (s), 34.0 (d, ²*J*_{P-C} = 18.6 Hz), 30.8-28.6 (m), 28.3 (s), 26.7 (s). ³¹P{¹H} NMR (CDCl₃, 121.4 MHz): δ 4.3.

1-tert-Butoxy-3-(bis(3, 5-dimethylphenyl)phosphino)isoquinoline (14d). Preparation of **14d** was performed by a similar procedure to that employed for the preparation of **14a**. Starting from 0.2820 g elemental sodium (12.26 mmol), 2.0858 g *tris*(3, 5-dimethylphenyl)phosphine (6.03 mmol) and 1.4164 g **13** (6.03 mmol) yielded 1.9436 g (73%) of white solid. ¹H NMR (C₇D₈, 300.1 MHz): δ 8.43 (dd, *J* = 7.8 and 2.2 Hz, 1H), 7.62 (dt, *J* = 7.8, 2.2 Hz, 1H), 7.54 (td, *J* = 7.8, 2.2 Hz, 1H), 7.46 (td, *J* = 7.8, 2.2 Hz, 1H), 7.34 (t, *J* = 1.8 Hz, 2H), 7.07 (dd, *J* = 2.2 Hz, ³*J*_{P-H} = 7.0 Hz, 1H), 7.01 (m, 4H), 2.35 (s, 12H), 1.41 (s, 9H). ¹³C{¹H} NMR (C₇D₈, 75.5 MHz): ¹³C{¹H} NMR (C₆D₆, 75.5 MHz): δ 162.9 (d, ¹*J*_{P-C} = 9.5 Hz), 160.5 (s), 138.3 (s), 137.4 (d, ³*J*_{P-C} = 5.3 Hz, 3000 scans), 132.3 (s), 130.9 (s), 132.2 (d, ¹*J*_{P-C} = 10.5 Hz), 127.4 (d, ²*J*_{P-C} = 17.8 Hz), 126.6 (s), 126.1 (s), 124.1 (s), 118.9 (s), 117.6 (d, ²*J*_{P-C} = 22.0 Hz), 83.3 (s), 28.5 (s). ³¹P{¹H} NMR (C₇D₈, 121.4 MHz): δ -4.2.

3-(Diphenylphosphino)isoquinolin-1(2H)-one (5). 1.500 g **14a** (3.89 mmol) was dissolved in neat concentrated formic acid (15 mL), and the solution was stirred at ambient temperature for 1 hour. Precipitation of the isoquinolone was induced by dilution with H₂O (25 mL), and the suspension was filtered through a glass frit. The white flakes were washed with 70% formic acid solution (3 × 5 mL). The combined aqueous formic acid filtrates were reduced *in vacuo*, and the opaque residue was crystallised from acetone. The combined crops yielded 0.8968 g (70%) of white flakes after drying *in vacuo* at 80°C. ¹H NMR (CDCl₃, 300.1 MHz): δ 9.29 (s, 1H), 7.65-7.45 (m, 14H), 7.03 (d, ³J_{P-H} = 22.3 Hz, 1H), 2.34 (s, 12H). ¹³C{¹H} NMR (CDCl₃, 75.5 MHz): δ 162.9 (s), 145.3 (d, ¹J_{P-C} = 4.4 Hz), 138.5 (d, ³J_{P-C} = 2.9 Hz), 136.4 (d, ¹J_{P-C} = 18.6 Hz), 132.4 (d, ²J_{P-C} = 10.2 Hz), 132.4 (s), 130.1 (s), 129.3 (d, ³J_{P-C} = 7.3 Hz), 128.2 (s), 127.9 (s), 126.8 (s), 126.3 (s), 109.1 (d, ²J_{P-C} = 16.0 Hz). ³¹P{¹H} NMR (C₆D₆, 121.4 MHz): δ -9.3. *Anal.* Calculated for C₂₁H₁₆NPO: C, 76.59; H, 4.90; N, 4.25. Found: C, 76.47; H, 4.94; N, 4.27.

3-(Diethylphosphino)isoquinolin-1(2H)-one (6). Preparation of **6** was performed by a similar procedure to that employed for the preparation of **5**. Starting from 0.7500 g **14b** (2.59 mmol) and neat concentrated formic acid (10 mL) gave a yellow residue, to which *n*-pentane/petroleum ether = 2/1 (5 mL) was added. The mixture was sonicated over 5-10 minutes and the solution was transferred from the insoluble paste by syringe and concentrated *in vacuo*, yielding 0.3972 g (53%) of viscous pale yellow oil. ¹H NMR (C₆D₆, 300.1 MHz): δ 9.15 (s, 1H), 7.63-7.51 (m, 4H), 6.37 (d, ³J_{P-H} = 21.0 Hz, 1H), 1.48 (dq, *J* = 8.2 Hz, ²J_{P-H} = 14.8 Hz, 8H), 0.97 (td, *J* = 8.2 Hz, ³J_{P-H} = 0.5 Hz, 12H). ¹³C{¹H} NMR (C₆D₆, 75.5 MHz): δ 155.9 (s), 142.5 (d, ¹J_{P-C} = 4.0 Hz), 138.4 (d, ³J_{P-C} = 2.2 Hz), 132.0 (s), 128.2 (s), 127.9 (s), 126.5 (s), 127.7 (s), 108.3 (d, ²J_{P-C} = 15.2 Hz), 18.4 (d, ¹J_{P-C} = 24.2 Hz), 9.11 (d, ²J_{P-C} = 11.5 Hz). ³¹P{¹H} NMR (C₆D₆, 121.4 MHz): δ -17.4. *Anal.* Calculated for C₁₃H₁₆NPOS: C, 58.85; H, 6.08; N, 5.28; S, 12.09. Found: C, 58.71; H, 6.21; N, 5.05; S, 11.84.

3-(Dicyclohexylphosphino)isoquinolin-1(2H)-one (7). Preparation of **7** was performed by a similar procedure to that employed for the preparation of **5**. Starting from 1.0137 g **14c** (2.55 mmol) and neat concentrated formic acid (10 mL) yielded 0.6356 g (73%) of off-white powder. ¹H NMR (C₆D₆, 300.1 MHz): δ 9.26 (s, 1H), 7.65-7.45 (m, 4H), 6.33 (d, ³J_{P-H} = 20.7 Hz, 1H), 1.6-1.43 (m, 16H), 1.32 (m, 4 H). ¹³C{¹H} NMR (C₆D₆, 75.5 MHz): δ 155.7 (s), 142.1 (d, ¹J_{P-C} = 3.8 Hz), 138.3 (d, ³J_{P-C} = 1.8 Hz), 132.1 (s), 128.4 (s), 128.1 (s), 127.5 (s), 126.8 (s), 107.5 (d, ²J_{P-C} = 13.7 Hz), 30.8-28.6 (m), 26.7 (s). ³¹P{¹H} NMR (C₆D₆, 121.4 MHz): δ 0.8. *Anal.* Calculated for C₂₁H₂₈NPO: C, 73.87; H, 8.27; N, 4.10. Found: C, 74.12; H, 8.35; N, 4.19.

3-(Bis(3, 5-dimethylphenyl)phosphino)isoquinolin-1(2H)-one (8). Preparation of **8** was performed by a similar procedure to that employed for the preparation of **5**. Starting from 0.9614 g **14d** (2.18 mmol) and neat concentrated formic acid (9 mL) yielded 0.5546 g (66%) of white flakes.

^1H NMR (CDCl_3 , 300.1 MHz): δ 9.25 (s, 1H), 7.66-7.52 (m, 4H), 7.35 (t, $J = 1.9$ Hz, 2H), 7.06 (m, 4H), 7.02 (d, $^3J_{\text{P-H}} = 21.6$ Hz, 1H), 2.34 (s, 12H). $^{13}\text{C}\{^1\text{H}\}$ NMR (CDCl_3 , 75.5 MHz): δ 162.8 (s), 144.9 (d, $^1J_{\text{P-C}} = 4.2$ Hz), 138.7 (d, $^3J_{\text{P-C}} = 2.5$ Hz), 138.4 (s), 132.4 (s), 132.0 (d, $^1J_{\text{P-C}} = 9.8$ Hz), 130.9 (s), 127.4 (d, $^2J_{\text{P-C}} = 17.0$ Hz), 128.3 (s), 128.0 (s), 126.8 (s), 126.3 (s), 108.6 (d, $^2J_{\text{P-C}} = 14.5$ Hz), 21.9 (s). $^{31}\text{P}\{^1\text{H}\}$ NMR (C_7D_8 , 121.4 MHz): δ -9.8. *Anal.* Calculated for $\text{C}_{25}\text{H}_{24}\text{NPO}$: C, 77.90; H, 6.28; N, 3.63. Found: C, 77.85; H, 6.17; N, 3.62.

Method of continuous variation. For a particular hetero-combinatorial assembly, a series of 11 samples was prepared. Within each series, the mole fraction of the isoquinolinyl phosphine was incrementally increased from 0 to 1 while maintaining an absolute concentration of 1 mM in d_6 -benzene (1.5 mL). Each equilibrium was established in a 5 mm NMR tube at 25°C under N_2 . The ^1H NMR spectrum was recorded at 25°C. Chemical shift was given on the δ scale (ppm) and referenced to an external sample of tms ($\delta = 0.00$). The chemical shift changes of the pivaloyl amide proton and of the quinolyl amide proton were then plotted as a function of the isoquinolinyl phosphine molar ratio.

Determination of association constants. For a particular hetero-combinatorial assembly, the concentration of the 2-*N*-pivaloylaminopyridyl phosphine was fixed at 5 mM in d_6 -benzene (1.5 mL) and the concentration of the isoquinolinyl phosphine was incrementally increased to give molar ratios in the range 0.2-4.0. Each equilibrium was established in a 5 mm NMR tube at 25°C under N_2 . The ^1H NMR spectrum was recorded at 25°C. Chemical shift was given on the δ scale (ppm) and referenced to an external sample of tms ($\delta = 0.00$). Assuming a 1/1 association mechanism, the observed chemical shifts of the pivaloyl amide proton and of the quinolyl amide proton are described by the equation

$$\Delta\delta = \frac{\delta_A - \delta_1}{2} \left\{ \frac{[\text{IQP}]t}{[\text{PAPP}]t} + 1 + \frac{1}{K_a[\text{PAPP}]t} \pm \sqrt{\left(\frac{[\text{IQP}]t}{[\text{PAPP}]t} + 1 + \frac{1}{K_a[\text{PAPP}]t} \right)^2 - 4 \frac{[\text{IQP}]t}{[\text{PAPP}]t}} \right\}$$

in which K_a is the association constant and $[]_t$ denotes total concentration. K_a was thus solved using the nonlinear least-square fit method in ORIGIN. The association of **4** and **5** was additionally evaluated in the presence of 5.1 mg $[\text{Rh}(\text{CO})(\text{PPh}_3)_3\text{H}]$ (7.5×10^{-3} mmol), introduced at the start of the titration.

Duplicate titrations were performed in d_4 -methanol (1.5 mL).

Synthesis of complexes from $[\text{Rh}(\text{cod})_2][\text{BF}_4]$. A solution of the 2-*N*-pivaloylaminopyridyl (0.02 mmol) and the isoquinolinyl phosphine (0.02 mmol) in d_2 -dichloromethane (1 mL) was added slowly to a solution of 8.1 mg $[\text{Rh}(\text{cod})_2][\text{BF}_4]$ (0.02 mmol) in d_2 -dichloromethane (1 mL) held in an NMR tube at 32°C under N_2 . After 1 hour the clear solution was analysed by $^{31}\text{P}\{^1\text{H}\}$ NMR spectroscopy. In order to afford sharper line width, the cod auxiliary in the complexes of **3/8** and **4/7**

was subsequently replaced by addition of 4.5 mg 1, 10-phenanthroline (0.025 mmol). In each case, $^{31}\text{P}\{^1\text{H}\}$ NMR spectroscopy of the red solution proved formation of the defined complex.

High pressure NMR. In a typical experiment the 10 mm sapphire NMR cell was primed with a solution of 5.0 mg $[\text{Rh}(\text{acac})(\text{CO})_2]$ (0.02 mmol), 9.2 mg **4** (0.02 mmol) and 5.1 mg **6** (0.02 mmol) in d_8 -toluene (1.5 mL) under N_2 . The cell was purged thrice with $\text{CO}/\text{H}_2 = 1$ and then pressurised to 40 bar. NMR spectra were recorded at 45°C.

Synthesis of complexes from $[\text{Rh}(\text{acac})(\text{CO})_2]$. A solution of the 2-*N*-pivaloylaminopyridyl (0.10 mmol) and the isoquinolinylyl phosphine (0.10 mmol) in toluene (5 mL) was added dropwise to a solution of 25.9 mg $[\text{Rh}(\text{acac})(\text{CO})_2]$ (0.10 mmol) in toluene (3.5 mL) under N_2 . The red solution was slowly warmed to 45°C, stirred for 2 hours and reduced to third volume *in vacuo*. Precipitation of the complex was induced by dropwise addition of cold *n*-pentane and the suspension was filtered through a glass frit. The red prisms were washed with *n*-pentane/acetone = 4/1 (4×2 mL) and then dried over P_2O_5 *in vacuo*.

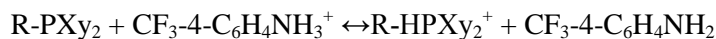
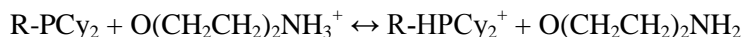
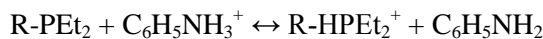
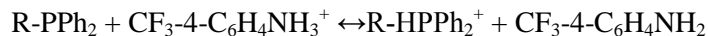
Catalysis. Syngas was purchased from BOC (**Caution!** Carbon monoxide is extremely poisonous and accidents may be lethal. A sensitive personal detector was carried and all experiments were performed in a well ventilated fume-hood fitted with a detector, maintaining the concentration of carbon monoxide below the mac value at all times). Reactions were carried out on the CAT rig with stirrer speed set at 800 rpm. In a typical experiment, a solution of the 2-*N*-pivaloylaminopyridyl (0.04 mmol) and the isoquinolinylyl phosphine (0.04 mmol) in *iso*-propanol (3 mL) was added to the corresponding $[\text{Rh}(\text{acac})(\text{PAPP-IQP})]$ (0.04 mmol). The resulting solution was sonicated over 10 minutes and transferred into the autoclave under $\text{CO}/\text{H}_2 = 1$; any residues were transferred with a further aliquot of *iso*-propanol (1 mL). The solution was incubated for 10 minutes under 30 bar $\text{CO}/\text{H}_2 = 1$ at 90°C. After 1 mL allyl alcohol (14.70 mmol, azeotropically dried with toluene and distilled) was injected the pressure was adjusted to 40 bar, and the reaction was run to completion. The autoclave was then cooled and depressurised. 50 μL diglyme was added as internal standard to a 1 mL aliquot of the product solution, and the sample was analysed by gc. The experiments were performed in duplo.

Polarity measurements. The absorption maximum of Nile Red was determined by transmission UV-*vis* spectroscopy of a 1.89 mM solution, and related to the molar transition energy by $E_{\text{NR}} = (hcNA/\lambda_{\text{max}}^{\text{abs}}) \times 10^6$.

Preparation of phosphorus-selenides. A solution of 15.8 mg elemental selenium (0.2 mmol) was added dropwise to a refluxing solution of the phosphine (0.04 mmol) in d_3 -chloroform (1.5 mL)

held in an NMR tube at 25°C under N₂. After 20 minutes the solution was analysed by ³¹P{¹H} NMR spectroscopy.

Determination of acidity constants. The constants for the equilibria



were studied. A solution of **1-8** (0.10 mmol) and the appropriate protonated nitrogen base (0.10 mmol) was prepared in *d*₃-acetonitrile (1 mL). Each equilibrium was established in a 5 mm NMR tube at 25°C under N₂. After an equilibration period, the ¹H and ³¹P{¹H} NMR spectra were recorded at 25°C. Chemical shift was given on the δ scale (ppm) and referenced to an internal capillary of P(OMe)₃ in *d*₆-benzene (δ = 3.51, 137.7). The equilibrium constant was calculated from the ratios [RNH₂]/[RNH₃⁺] and [HL⁺]/[L] were determined from the ¹H and ³¹P{¹H} NMR spectra respectively, and related to the acidity constant by

$$\text{pKa} = \text{pK}_a^{\text{MeCN}}[\text{RNH}_3^+] - \text{pK}^{\text{MeCN}}.$$

References and Notes

- (1) (a) Stambuli, J. P.; Stauffer, S. R.; Shaughnessy, K. H.; Hartwig, J. F. *J. Am. Chem. Soc.* **2001**, *123*, 2677. (b) Harris, R. F.; Natio, A. A. J.; Copeland, G. T.; Miller, S. J. *J. Am. Chem. Soc.* **2000**, *122*, 11270. (c) Reetz, M. T. *Angew. Chem. Int. Ed.* **2002**, *41*, 1335. (d) de Vries, J. G.; de Vries, A. H. M. *Eur. J. Org. Chem.* **2003**, 799.
- (2) For reviews see: (a) Wilkinson, M. J.; van Leeuwen, P. W. N. M.; Reek, J. N. H. *Org. Biomol. Chem.* **2005**, *3*, 2371. (b) Reyes, S. J.; Burgess, K. *Chem. Soc. Rev.* **2006**, *35*, 416. (c) Kleij, A. W.; Reek, J. N. H. *Chem. Eur. J.* **2006**, *12*, 4218.
- (3) (a) Coordination polymers. Anderson, H. L.; Hunter, C. A.; Sanders, J. K. M. *J. Chem. Soc., Chem. Commun.* **1989**, 226. (b) molecular squares. Stang, P. J.; Fan, J.; Olenyuk, B. *Chem. Commun.* **1997**, 1453.
- (4) (a) Slagt, V. F.; Reek, J. N. H.; Kamer, P. C. J.; van Leeuwen, P. W. N. M. *Angew. Chem. Int. Ed.* **2001**, *40*, 4271. (b) Slagt, V. F.; Kamer, P. J. C.; van Leeuwen, P. W. N. M.; Reek, J. N. H. *J. Am. Chem. Soc.* **2004**, *126*, 1526.
- (5) (a) Kleij, A. W.; Lutz, M.; Spek, A. L.; van Leeuwen, P. W. N. M.; Reek, J. N. H. *Chem. Commun.* **2005**, 3661. (b) Kleij, A. W.; Kuil, M.; Tooke, D. M.; Spek, A. L.; Reek, J. N. H. *Inorg. Chem.* **2005**, *44*, 7696.
- (6) Reek, J. N. H.; Röder, M.; Goudriaan, E.; Kamer, P. C. J.; van Leeuwen, P. W. N. M.; Slagt, V. F. *J. Organomet. Chem.* **2005**, *690*, 4505.
- (7) (a) Breit, B.; Seiche, W. *J. Am. Chem. Soc.* **2003**, *125*, 6608. (b) Birkholz, M. –N.; Dubrovina, N. V.; Jiao, H.; Michalik, D.; Holz, J.; Paciello, R.; Breit, B.; Börner, A. *Chem. Eur. J.* **2007**, *13*, 5896.

- (8) (a) Duckmanton, P. A.; Blake, A. J.; Love, J. B. *Inorg. Chem.* **2005**, *44*, 7709. (b) Knight, L. K.; Freixa, Z.; van Leeuwen, P. W. N. M.; Reek, J. N. H. *Organometallics* **2006**, *25*, 954. (c) Sandee, A. J.; van der Burg, A. M.; Reek, J. N. H. *Chem. Commun.* **2007**, 864.
- (9) Anderson, J. R.; Campi, E. M.; Jackson, W. R. *Catal. Lett.* 1991, *9*, 55.
- (10) (a) Monflier, E.; Tilloy, S.; Méliet, C.; Mortreux, A.; Fourmentin, S.; Landy, D.; Surpateanu, G. *New J. Chem.* **1999**, *23*, 469. (b) Monflier, E.; Bricout, H.; Hapiot, F.; Tilloy, S.; Aghmiz, A.; Masdeu-Bultó, A. M. *Adv. Synth. Catal.* **2004**, *346*, 425. (c) Tilloy, S.; Crowyn, G.; Monflier, E.; van Leeuwen, P. W. N. M.; Reek, J. N. H. *New J. Chem.* **2006**, *30*, 377.
- (11) (a) Reetz, M. T.; Li, X. *Angew. Chem. Int. Ed.* **2005**, *44*, 2962. (b) Reetz, M. T.; Sell, T.; Meiswinkel, A.; Mehler, G. *Angew. Chem. Int. Ed.* **2003**, *42*, 790. (c) Duursma, A.; Hoen, R.; Schuppan, J.; Hulst, R.; Minnaard, A. J.; Feringa, B. L. *Org. Lett.* **2003**, *5*, 3111. (c) Peña, D.; Minnaard, A. J.; Boogers, J. A. F.; de Vries, A. H. M.; de Vries, J. G.; Feringa, B. L. *Org. Biomol. Chem.* **2003**, *1*, 1087.
- (12) (a) Watson, J. D.; Crick, F. H. C. *Nature* **1953**, *171*, 964. (b) Sanger, W. *Principles of Nucleic Acid Structure*. Springer-Verlag: New York, 1984.
- (13) (a) Breit, B.; Seiche, W. *Angew. Chem. Int. Ed.* **2005**, *44*, 1640. (b) Weis, M.; Waloch, C.; Seiche, W.; Breit, B. *J. Am. Chem. Soc.* **2006**, *128*, 4188.
- (14) Waloch, C.; Wieland, J.; Keller, M.; Breit, B. *Angew. Chem. Int. Ed.* **2007**, *46*, 3037.
- (15) Harriman, B. R.; Shelton, R. S.; van Campen, M.G.; Warren, M.R. *J. Am. Chem. Soc.* **1945**, *67*, 1481.
- (16) Robison, M. M. *J. Am. Chem. Soc.* **1958**, *80*, 5481.
- (17) For comprehensive review see: (a) Connors, K. A. *Binding Constants*. Wiley: New York, 1987. (b) Otwinowski, Z.; Minor, W. *Methods in Enzymology* **1997**, *276*, 307.
- (18) Schneider, H. J.; Kramer, R.; Simova, S.; Schneider, U. *J. Am. Chem. Soc.* **1998**, *110*, 6442.
- (19) ORIGIN-08. OriginLab, Northampton, MA.
- (20) Chen, J. S.; Shirts, R. B. *J. Phys. Chem.* **1985**, *89*, 1643.
- (21) (a) Weber, G.; Anderson, S. R. *Biochemistry* **1965**, *4*, 1942. (b) Person, W. B. *J. Am. Chem. Soc.* **1965**, *87*, 167. (c) Deranleau, D. A. *J. Am. Chem. Soc.* **1969**, *91*, 4044.
- (22) (a) $[\text{Rh}(\text{phen})_2]^+$ has a distorted square planar geometry. Caldaran, H.; de Armond, M. K.; Hanck, K. W.; Sahini, V. E. *J. Am. Chem. Soc.* **1976**, *98*, 4455. (b) $[\text{Rh}(\text{PMe}_3)_4]^+$ has a tetrahedral geometry. Jones, R. A. *J. Chem. Soc., Dalton Trans.* **1979**, 489.
- (23) Damoense, L.; Datt, M.; Green, M.; Steenkamp, C. *Coord. Chem. Rev.* **2004**, *248*, 2393.
- (24) $^1J_{\text{Rh-H}} < 2$ Hz routinely observed for *ee* chelates. (a) Casey, C. P.; Whiteker, G. T.; Melville M. G.; Petrovich, L. M.; Gavney, J. A.; Powell, D. R. *J. Am. Chem. Soc.* **1992**, *114*, 5535. (b) Kranenburg, M.; van der Burgt, Y. E. M.; Kamer, P. C. J.; van Leeuwen, P. W. N. M.; *Organometallics* **1995**, *14*, 3081. (c) van der Veen, L. A.; Boele, M. D. K.; Bregman, F. R.; Kamer, P. C. J.; van Leeuwen, P. W. N. M.; Goubitz, K.; Fraanje, J.; Schenk, H.; Bo, C. *J. Am. Chem. Soc.* **1998**, *120*, 11616. (d) Casey, C. P.; Paulsen, E. L.; Beuttenmueller, E. W.; Proft, B. R.; Petrovich, L. M.; Matter, B. A.; Powell, D. R. *J. Am. Chem. Soc.* **1997**, *119*, 11817. (e) Nettekoven, U.; Kamer, P. C. J.; Widhalm, M.; van Leeuwen, P. W. N. M. *Organometallics* **2000**, *19*, 4596.
- (25) Rossi, A. R.; Hoffmann, R. *Inorg. Chem.* **1975**, *14*, 365.

- (26) van Leeuwen, P. W. N. M.; Claver, C. *Rhodium Catalysed Hydroformylation*. James, B. R.; Ugo, R. (Eds). Kluwer Academic: Dordrecht, 2000.
- (27) Desiraju, G. R.; Steiner, T. *The Weak Hydrogen Bond in Structural Chemistry and Biology*. Oxford University Press: Oxford, 1999.
- (28) Chapter 2, p. 44.
- (29) Lomas, J. S. *J. Phys. Org. Chem.* **2005**, *18*, 1001.
- (30) Chapter 4, p. 123.
- (31) Preutt, R. L.; Smith, J. A. *J. Org. Chem.* **1969**, *34*, 327.
- (32) A2.2, p. 180.
- (33) (a) Allen, D. A.; Taylor, B. F. *J. Chem. Soc., Dalton Trans.* **1982**, 51. (b) Holz, J.; Zayas, O.; Jiao, H.; Baumann, W.; Spannenberg, A.; Monsees, A.; Riermeier, T. H.; Almena, J.; Kadyrov, R.; Börner, A. *Chem. Eur. J.* **2006**, *12*, 5001.
- (34) (a) DIOP, *l/b* = 7.4. White, D. F. S. *PhD Thesis*, University of St. Andrews, 2001. Chapter 2. (b) XANTPHOS, *l/b* = 4.5; ^tBu-XANTPHOS, *l/b* = 6.2. White, D. F. S. *PhD Thesis*, University of St. Andrews, 2001. Chapter 4.
- (35) Chapter 3, p. 76.
- (36) (a) Dewar, M. *Bull. Soc. Chim. Fr.* **1951**, *18*, 79. (b) Chatt, J.; Duncanson, L. M. *J. Chem. Soc.* **1953**, 2939. (c) Chatt, J.; Duncanson, L. M.; Venanzi, L. M. *J. Chem. Soc.* **1955**, 4456.
- (37) da Silva, A. C.; de Oliveira, K. C. B.; Gusevskaya, E. V.; dos Santos, E. N. *J. Mol. Catal. A* **2002**, *179*, 133.
- (38) Wilhelmsson, L. M.; Holmén, A.; Lincoln, P.; Nielsen, P. E.; Nordén, B. *J. Am. Chem. Soc.* **2001**, *123*, 2434.
- (39) Chapter 2, p. 53.
- (40) (a) Cheliatsidou, P.; White, D. F. S.; Slawin, A. M. Z.; Cole-Hamilton, D. J. *Dalton Trans.* **2008**, 2389. (b) Cheliatsidou, P.; White, D. F. S.; Cole-Hamilton, D. J. *Dalton Trans.* **2004**, 2425.
- (41) *K* = 36.0. *Handbook of Chemistry and Physics*. Lide, D. R. (Ed). CRC Press: Boca Raton, 2000.
- (42) Where the molar ratio could not be determined directly due to poor resolution in the ¹H NMR spectrum, the equilibrium concentrations of [RNH₂] and [RNH₃⁺] were assumed to be equal to those of [HL⁺] and [L] respectively on the basis of mass-balance arguments.
- (43) (a) CF₃-4- C₆H₄NH₃BF₄, C₆H₅NH₃BF₄. Naudin, E.; Gouérec, P.; Bélanger, D. *J. Electroanal. Chem.* **1998**, *459*, 1. (b) O(CH₂CH₂)₂NH₃BF₄. Nuttall, R. H.; Sharp, D. W. A.; Waddington, T. C. *J. Chem. Soc.* **1960**, 4965.
- (44) (a) Abdur-Rashid, K.; Fong, T. P.; Greaves, B.; Gusev, D. G.; Hinman, J. G.; Landau, S. E.; Lough, A. J.; Morris, R. H. *J. Am. Chem. Soc.* **2000**, *122*, 9155. (b) Coetzee, J. F.; Padmanabhan, G. R. *J. Am. Chem. Soc.* **1965**, *87*, 5005.
- (45) (a) den Hertog, H. J.; Wibaut, J. P. *Recl. Trav. Chim. Pays* **1932**, *51*, 381. (b) den Hertog, H. J. Jouwersma, C. *Ibid.* **1936**, *55*, 122.
- (46) Chapter 3, p. 97.

Summary

Hydroxymethylation catalysis provides a valuable strategy for the high volume production of alcohols from α -alkenes. Generally this involves a hydroformylation-hydrogenation sequence, but the capacity to optimise selectivity for each transformation is limited. Condensation reactions between aldehyde products and alcohol products frustrate process economics. By an alternative scheme, all relevant bond-forming reactions occur in a single mechanism. This thesis describes several approaches to catalyst development and the application of derived systems for the hydroxymethylation of allyl alcohol. A review of auto-tandem hydroxymethylation and domino hydroxymethylation is presented in Chapter 1.

In Chapter 2 the synthesis of *bis*-(diethylphosphine) ligands based on a modular series of chiral alicyclic scaffolds is described. High pressure NMR studies have shown that the catalytically active complex $[\text{RhH}(\text{CO})_2(\text{L-L})]$ adopts preferentially *ea* geometry, with $[\text{Rh}(\text{CO})(\text{L-L})(\mu\text{-CO})]_2$ as the primary competing species. Catalyst performance can be correlated with the flexibility of the chelating ring; this favoured a high monomer/dimer ratio which enhances activity, but could not rigidify the configuration of the diethylphosphine groups which inhibits linear selectivity. Deuterium labelling studies were suggestive of a domino hydroxymethylation scheme. From the rhodium-hydroxyalkyl-hydride-carbonyl cation, a reductive elimination furnishes the diol derivatives and a β -hydride abstraction furnishes the hydroxyaldehyde derivatives. Up to 53 mol% selectivity to 1, 4-butanediol was attained. The catalysts could be recycled *via* biphasic separation, however poisoning by methacrolein caused a decline of activity upon reuse of the solution.

An investigation of enhanced specific activity *via* the *meta*-effect is the subject of Chapter 3. The effect of systematic *meta*-substitution in triphenylphosphine upon physicochemical properties was investigated by IR spectroscopy and electrochemistry, both of which showed no significant structural impact on the uncoordinated triarylphosphine. Variable temperature ^1H NMR studies however revealed a change in the solution dynamics of the corresponding Vaska complex. The activation barrier to phosphorus-(*ipso*)carbon rotation increases as a function of *meta*-substitution, with rotation of substituted aryl rings past each other being more strained. This should create a well-defined coordination sphere around rhodium, and is proposed to account for the high linear selectivity

observed in the hydroformylation of allylic alcohols with $[\text{RhH}(\text{CO})\{(3, 5\text{-Me}_2\text{Ph})\text{P}\}_3]$. Linear-selectivity reached 96 mol%. Catalyst recycling was executed *via* biphasic separation, retaining on over twelve cycles an average of ~ 94 % efficiency. The kinetics of allyl alcohol hydroformylation with $[\text{RhH}(\text{CO})\{(3, 5\text{-Me}_2\text{Ph})\text{P}\}_3]$ was found to be well represented by the model

$$\text{rate} = \frac{k[\text{CO}][\text{H}_2]^{1.5}[\text{Rh}]^{1.4}[\text{allyl alcohol}]}{(1 + K_1[\text{CO}])(1 + K_2[\text{allyl alcohol}])}$$

A detailed analysis of how substrate-specific the influence of the *meta*-effect remains to be performed.

In Chapter 4 domino hydroxymethylation by multi-component *L-L*/PEt₃/Rh systems is described. The regioselective performance of a diphosphine rhodium catalyst in hydroformylation was translated for hydroxymethylation upon introduction of triethylphosphine at a *L-L*/PEt₃ molar ratio ≥ 1 . The highest observed selectivity to 1, 4-butanediol was 66 mol%. Competitive activity of triethylphosphine-modified rhodium species presumably accounts for the reduced linear selectivity observed when *L-L*/PEt₃ molar ratio < 1 . Despite aggravated catalyst decomposition at higher triethylphosphine concentrations, heterogeneous hydrogenation does not appear to take place. Deuterium labelling studies also discount a sequential homogeneous hydrogenation. There is evidence for the activation of a *tris*-phosphine-modified rhodium-acyl-carbonyl complex, but such a species could not be isolated from complexation reactions with a variety of precursors. It would be of interest to determine alternative promoters and to establish whether it is preferential to employ a high concentration of mildly acidic species or a low concentration of highly acidic species.

The self-assembly of DNA base pair analogues 2-*N*-pivaloylaminopyridyl phosphine and isoquinolyl phosphine, each modified with diphenylphosphine, diethylphosphine, dicyclohexylphosphine and *bis*(3, 5-dimethylphenyl)phosphine, is described in Chapter 5. In the presence of a rhodium precursor, exclusive formation of the heteroleptic complex was observed. Although the intramolecular hydrogen-bonding network is sensitive to temperature and free hydroxyl functionalities, highly regioselective catalysts were generally afforded under the appropriate operating conditions. Only the catalyst based on the *bis*(dicyclohexylphosphine)-heterodimer performed poorly, presumably due to the formation of *mono*-phosphine complexes. High chemoselectivity was correlated with the heterodimer acidity constant, however this is rendered non-linear by a *trans* influence when electronic distinction between the platforms is high. Overall, complexes based on the assembly of a dicyclohexylphosphine platform and a *bis*(3, 5-dimethylphenyl)phosphine platform were found to be optimal; up to 73 mol% selectivity to 1, 4-butanediol was reached.

It has been demonstrated in this thesis that in order to effect linear-selective domino hydroxymethylation of allyl alcohol, two distinct transition state structures must be optimised. High regioselectivity demands an asymmetric rhodium-hydride-dicarbonyl complex, which can be

generated by an asymmetric chelate or by rigidifying the configuration of the substituents on phosphorus. Interestingly, chelation geometry in this transition state has little impact on this parameter. It has been shown that domino hydroxymethylation is activated by an electron-rich rhodium-acyl-dicarbonyl. The state of electron density on rhodium can be controlled by the substitution pattern on the phosphorus donors, but can also be changed by the inclusion of a suitable promoter. The chelation geometry in this transition state is more significant; placing the acyl functionality *trans* to a phosphorus donor concentrates the electronic effect in the rhodium-alkyldiol-hydride-carbonyl cation to such an extent as to impede hydride migration and reductive elimination of the diol, favouring β -hydride abstraction and reductive elimination of the hydroxyaldehyde.

Appendices

A 1. High Pressure Equipment

A 1.1 High Pressure Spectroscopy

An understanding of how the auxiliaries govern the coordination chemistry of a rhodium complex in solution is of fundamental importance in hydroformylation catalysis, as it allows tuning for a specific transformation. Since the early 1970s, high pressure spectroscopic techniques have been developed to facilitate the observation of rhodium species in solution under catalytic conditions. High pressure NMR and high pressure IR spectroscopy are the most extensively applied today.

High pressure NMR cell. The 10 mm outer diameter \times 8 mm inner diameter \times 88 mm depth sapphire tube was purchased from Saphikon (Milford, NH) and the titanium alloy pressure valve was constructed at the SoCW (St. Andrews). The cell is pressurised *via* a spiral $\frac{1}{8}$ inch ss316 high pressure connector. The assembly has been tested up to 80 bar at 100°C. The spinner was designed to give the cell a low centre of gravity, allowing air flow adjustment in the spectrometer. Spectra are recorded on a Bruker Advance 300 spectrometer fitted with a 10 mm txo probe.

High pressure IR cell. The cylindrical internal reflectance cell comprises a 35 mL internal volume autoclave modified with a 45° conically angled cir crystal. The autoclave was purchased from Parr Instruments (Moline, IL) and is fitted with a six-blade rotor, thermocouple pocket, pressure valve and individually pressurised injection reservoir. Pressure connections are made with $\frac{1}{4}$ inch ss316 high-pressure tubing. The system has been tested up to 120 bar at 150°C. The polished cylindrical windows are made of zinc selenide with an optical diameter of 10 mm and transparency up to 700 cm^{-1} , as supplied by Spectra-Tech (Shelton, CT). Spectra are recorded on a Nicolet Avatar 460 FT-IR spectrometer with a cooled HgCdTe detector.

A 1.2 Catalysis

CAT rig. Kinetic measurements were performed on the catalyst evaluation and optimisation rig, constructed at SoCW (St. Andrews). Each component is isolatable by valves from Swagelok (Solon, OH). The autoclave, injection port and ballast vessel were supplied by Baskerville (Manchester). The autoclave is fitted with a three-blade rotor, thermocouple pocket and pressure

valve. The ballast vessel is also fitted with a pressure valve, which allows the components to be pressurised independently of each other *via* ¼ inch ss316 high-pressure tubing from the source. The pressure of each component is monitored by a designated rdp E308 pressure transducer. As feed gas becomes depleted during catalysis, the mass flow controller maintains the autoclave under constant pressure by a feed stream from the ballast vessel. The mass flow controller was purchased from Bronkhorst High-Tech (Ruurlo). Kinetics is measured as the pressure change in time, with data collected from PICOMONITOR ADC16 hardware *via* a com port. PICOLOG (Version 5.04.2) is used to monitor and log the relevant pressure data.

Hastelloy autoclave. The glass-lined Hastelloy autoclave is modified with a magnetic rotor, thermocouple pocket, pressure valve and injection port. The system is pressurised *via* ¼ inch ss316 high-pressure tubing from the source. The limitations must be noted. Firstly, the diffusion of feed gas across the gas-liquid interface is an important consideration in terms of reaction kinetics and inadequate rotary turbulence may lead to a mass transport limitation. Secondly, condensation of the reaction between the autoclave and the glass liner compromised quantification. On isolation of the product mixture for analysis this condensate was added to the bulk recovered from the glass liner, but inevitably small amounts were lost. Thus the products are effectively concentrated, which in some cases led to an apparent > 100% conversion.

A 2. Catalytic Product Analyses

A 2.1 Qualification and Quantification

GC-MS. Qualitative analyses were performed on a Hewlett-Packard 6890 equipped with a Hewlett-Packard 5973 mass selective detector. The product solution was injected directly. The gas chromatograph is interfaced with AGILENT CHEMSTATION (Version B. 04.01) and NIST 08 MS LIBRARY (Version ASCII) for analysis.

Method parameters:

sample volume	0.1 µL
column	Supelco™ mdn-35, 30 m × 0.25 mm
carrier gas	helium
flow rate	2.5 mL min ⁻¹
split ratio	100:1
injector temperature	200°C
detector temperature	250°C

temperature program:

initial 30°C/5 min/ramp 25°C min⁻¹/200°C/ hold 5 min

GC-FID. Quantitative analyses were performed on a Hewlett-Packard 6890 by the method of internal standards. For each of 1-propanal, 1-propanol, 2-methylpropanal, methacrolein, 2-methylpropanol, 2, 3-dihydrofuran, 2-ethoxyfuranol, crotonaldehyde, 2-methylpentenal, 2-methyl-1, 3-propanediol, 1, 4-butanediol and γ -butyrolactone, a series of standard solutions was made up in ethanol. A 1 mL aliquot of each solution was treated with 50 μ L diglyme, and this sample was injected as detailed. The gas chromatograph is interfaced with AGILENT CHEMSTATION (Version B. 04.01) for analysis. The stored base-line from a blank sample is subtracted from the chromatogram to overcome any drift, although this assumes reproducibility.

Method parameters:

sample volume	0.1 μ L
column	BP10™, 30 m \times 0.32 mm
carrier gas	N ₂
flow rate	3.2 mL min ⁻¹
split ratio	50:1
injector temperature	150°C
fid temperature	200°C

temperature program:

initial 40°C/5 min/ramp 16°C min⁻¹/200°C/ hold 5 min

Product solutions were analogously standardised and analysed. The calibration graph for each component was used to calculate its concentration in the product solution. The calibration graphs are available in the electronic appendix.

A different GC method was developed for the analyses in Chapter 3.6.

Method parameters:

sample volume	0.1 μ L
column	BP10™, 30 m \times 0.32 mm
carrier gas	N ₂
flow rate	2.0 mL min ⁻¹
split ratio	100:1
injector temperature	150°C
fid temperature	200°C

temperature program:

initial 80°C/7 min/ramp 20°C min⁻¹/180°C/ hold 15 min

product	R_t	classification	formation mechanism
1-propanal	6.81	iso.	isomersiation of allyl alcohol
1-propanol	7.08	hyd. (~ 60 %), iso. (~40 %)	hydrogenation of allyl alcohol, hydrogenation of 1-propanal
2-methylpropanal	7.41	C=O, <i>b</i>	C=C hydrogenation of methacrolein
methacrolein	10.30	C=O, <i>b</i>	dehydration of 2-methyl-3-hydroxypropanal
2-methylpropanol	10.65	C-OH, <i>b</i>	branched hydroxymethylation product
2, 3-dihydrofuran	18.42	C=O, <i>l</i>	dehydration of 2-furanol
2-ethoxyfuran	21.36	C=O, <i>l</i>	alcoholysis of 2-furanol with ethanol
2-furanol	21.85	C=O, <i>l</i>	intramolecular lactol formatin of 4-hydroxybutanal
1-butanol	22.39	C-OH, <i>l</i>	dehydration of rhodium-hydroxybutanol fragment with reductive elimination
crotonaldehyde	23.11	C=O, <i>l</i>	dehydration of 4-hydroxybutanal with C=C migration
2-methylpentenal	23.87	iso.	aldol addition of 1-propanal
2-methyl-3-hydroxypropanal	24.06	C=O, <i>b</i>	branched hydroformylation product
4-hydroxybutanal	25.77	C=O, <i>l</i>	linear hydroformylation product
2-methyl-1, 3-propanediol	27.73	C-OH, <i>b</i>	branched hydroxymethylation product
1, 4-butandeiol	29.89	C-OH, <i>l</i>	linear hydroxymethylation product
γ -butyrolactone	30.14	C=O, <i>l</i>	intramolecular lactol formation in rhodium-hydroxybutanyl, oxidation of 2-furanol

Acknowledgements

Completion of this thesis has proved once again that perseverance will triumph, and so it is with nostalgic pleasure that I now reflect on four exuberant years. One wanders into the land of platitude in saying that no work is the product of only one-person's effort, but it is true all the same. My gratitude is owed to the raft of people whose support and encouragement have been crucial, especially at less congenial times. Thanks, heartfelt and enduring, to everyone, but some names deserve a particular mention here.

My supervisors, I would like to thank you both for giving me this wonderful research opportunity. Dear David, despite an inhumanly hectic agenda you always made time to discuss my work with a seemingly boundless stream of ideas and a much appreciated infectious enthusiasm. The most elegant and erudite of academics; without you it would not have been as much fun, let alone possible. Dan, for the refreshing ideas and the introductory insight into industrial chemistry I am greatly indebted.

Over this last year my writing area bore some resemblance to Miss Havisham's apartments. Much of the data clutter I provided myself, but as much was gratefully harvested by certain members of staff. Alex Slawin, I am grateful for the excellent crystallography facility. From the technical department I want to thank in particular Sylvia Williamson for microanalyses and ICP-MS measurements, Melanja Smith for her assistance during high pressure NMR experiments and Sneh Arjen for her assistance during electrochemical measurements.

I also want to thank those colleagues I have worked alongside with for their help with my activities in, around and away from the fumehood. Peter, when I began catalysis I soon realised how indispensable your practical expertise in this area was. Simon, *vous m'avez enseigné que la vie est trop courte pour s'inquiéter*. Nick, *je ne pouvais pas imaginer un voisin plus divertissant*. Jan, *het was leuk om weer eens Nederlands te kunnen praten met iemand en om in de zomer maanden een rondje te gaan golfen na een dag in het lab*. Jacorien, Jenny and Lynzi, you were always ready to join in a frustration vent when needed. Mark, Gavin, Lucas, Gong, Uli and Bianca, with great pleasure we shared the occasionally limited space of lab 464.

It is a pleasure to thank the friends who have provided necessary relaxation and diversions. Sahrah, in difficult times your friendship was so important. Your sharp sense of humour brightened many an ominous day, and I thank you for all the high-spirited times we have had together. Karen, Ann and Brian, for the hours of amusing conversation and moral support during the last year I am grateful. Lorna, Sumi, Neil and Peter, thank you for your friendship and the generous sprinklings of heartening words.

I am also greatly indebted to my family who have encouraged my academic pursuits from the very beginning . Liefste oma, tijdens mijn promotie periode heb ik steeds minder tijd voor je gehad maar daar had je altijd alle begrip voor. Papa, ik ben supertrots dat je als leek op dit vakgebied mensen kon vertellen waarmee ik al die jaren bezig was, al dan met golf analogie. Mama, de laatste jaren zijn voor jouw moeilijk geweest en toch bleef je me met een lach aanmoedigen. Mijn lieve, kleine en slimme zusje Elien, dank je voor de onvoorwaardelijke steun tijdens de afgelopen jaren.

To end I would like to thank my best friend and life partner for his inexorable patience during this last trying year. Colin, you have supported me and kept me sane, and I could not have done this without you.